CHAPTER 6

THE SENSORLESS CONTROLLER DESIGN FOR OF THE SYMMETRICAL TRIPLE-STAR IPM

6.1 Introduction

In this chapter a controller is designed for the symmetrical triple star IPM machine. The controller is designed using two different models of the machine. The first model is the average model which includes the coupling terms of the machine. The drive is designed using minimum copper loss strategy. The generated controller has some complexity due to the coupling between the different axis of the model. To remove the complexity of the drive, it is designed again using the decoupled model that was presented in the chapter 4. The controller also uses minimum copper loss strategy and has a sensorless position estimator to estimate the rotor angle. The rotor angle estimator is operating on the fifth sequence of the stationary reference frame of the machine. The proper signal processing method for extracting the rotor position from the high frequency currents is presented in this chapter which is the main contribution of this chapter. The designed controller is implemented on the full order coupled model of the machine (presented in chapter 3) and the simulation results are presented for several speed profiles. Finally, the controller and the positon observer are discretized and translated to C++ language. The generated code is used to program a DSP and the simulation results were verified by the experimental results.

6.2 Controller Design Using Average Model

The speed controller of the triple-star symmetrical machine can be designed based on the average model of the machine that was presented in the chapter 4. The converter of the controller is shown in the Figure 6.1. From this figure, the converter has three isolated sets of three phase loads with three isolated neutral points (n_1, n_2, n_3). As it can be seen from the Figure 6.1, each set has three phases (ABC). And the sets, share the same DC link.

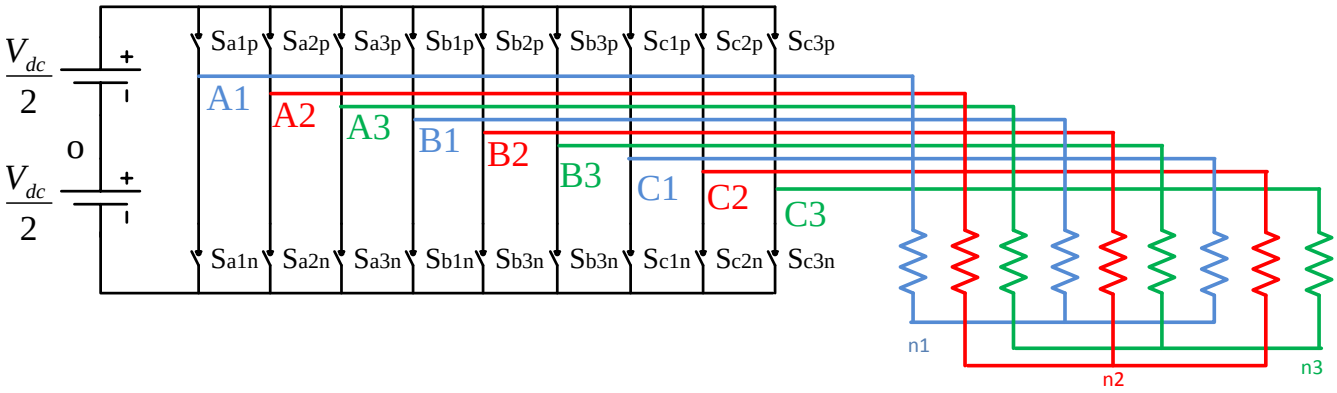

Figure 6.1: The triple-star inverter.

In Figure 6.1 'S_{xip}' defines the switching function of the top switch of leg 'x' of the converter number 'i' and 'S_{xin}' defines the switching function of the bottom switch of leg 'x' of the converter number 'i'. The switches of each leg of the inverter are complementary therefore for each set the switching functions can be expressed as:

$$\begin{aligned} S_{a1p} + S_{a1n} &= 1 \\ S_{b1p} + S_{b1n} &= 1 \\ S_{c1p} + S_{c1n} &= 1 \end{aligned} \tag{6.1}$$

$$\begin{aligned} S_{a2p} + S_{a2n} &= 1 \\ S_{b2p} + S_{b2n} &= 1 \\ S_{c2p} + S_{c2n} &= 1 \end{aligned} \tag{6.2}$$

$$S_{a3p} + S_{a3n} = 1$$
$$S_{b3p} + S_{b3n} = 1 \quad (6.3)$$
$$S_{c3p} + S_{c3n} = 1$$

The phase voltage for each of the inverter legs can be expressed as:

$$V_{A1O} = \frac{V_{dc}}{2}(S_{a1p} - S_{a1n})$$
$$V_{B1O} = \frac{V_{dc}}{2}(S_{b1p} - S_{b1n}) \quad (6.4)$$
$$V_{C1O} = \frac{V_{dc}}{2}(S_{c1p} - S_{c1n})$$

$$V_{A2O} = \frac{V_{dc}}{2}(S_{a2p} - S_{a2n})$$
$$V_{B2O} = \frac{V_{dc}}{2}(S_{b2p} - S_{b2n}) \quad (6.5)$$
$$V_{C2O} = \frac{V_{dc}}{2}(S_{c2p} - S_{c2n})$$

$$V_{A3O} = \frac{V_{dc}}{2}(S_{a3p} - S_{a3n})$$
$$V_{B3O} = \frac{V_{dc}}{2}(S_{b3p} - S_{b3n}) \quad (6.6)$$
$$V_{C3O} = \frac{V_{dc}}{2}(S_{c3p} - S_{c3n})$$

Where V_{dc}=200 (Volts) and switching frequency is 6 (kHz). From the equations (6.1) to (6.3) the switching function of the bottom switch of each leg of the converter (leg 'x') can be expressed as:

$$S_{xn} = 1 - S_{xp} \quad (6.7)$$

By substituting the equation (6.7), the voltage equations can be rewritten as equations (6.8) to (6.9).

$$
\begin{aligned}
V_{A1O} &= \frac{V_{dc}}{2}(2S_{a1p}-1)\\
V_{B1O} &= \frac{V_{dc}}{2}(2S_{b1p}-1)\\
V_{C1O} &= \frac{V_{dc}}{2}(2S_{c1p}-1)
\end{aligned}
\tag{6.8}
$$

$$
\begin{aligned}
V_{A2O} &= \frac{V_{dc}}{2}(2S_{a2p}-1)\\
V_{B2O} &= \frac{V_{dc}}{2}(2S_{b2p}-1)\\
V_{C2O} &= \frac{V_{dc}}{2}(2S_{c2p}-1)
\end{aligned}
\tag{6.9}
$$

$$
\begin{aligned}
V_{A3O} &= \frac{V_{dc}}{2}(2S_{a3p}-1)\\
V_{B3O} &= \frac{V_{dc}}{2}(2S_{b3p}-1)\\
V_{C3O} &= \frac{V_{dc}}{2}(2S_{c3p}-1)
\end{aligned}
\tag{6.10}
$$

The voltages can be transformed to an arbitrary reference frame using the equation (6.11).

$$
\begin{bmatrix} V_{q1}\\ V_{d1}\\ V_{O1}\\ V_{q2}\\ V_{d2}\\ V_{O2}\\ V_{q3}\\ V_{d3}\\ V_{O3} \end{bmatrix} = T_r(\theta_{arb}) \begin{bmatrix} \frac{V_{dc}}{2}(2S_{a1p}-1)\\ \frac{V_{dc}}{2}(2S_{b1p}-1)\\ \frac{V_{dc}}{2}(2S_{c1p}-1)\\ \frac{V_{dc}}{2}(2S_{a2p}-1)\\ \frac{V_{dc}}{2}(2S_{b2p}-1)\\ \frac{V_{dc}}{2}(2S_{c2p}-1)\\ \frac{V_{dc}}{2}(2S_{a3p}-1)\\ \frac{V_{dc}}{2}(2S_{b3p}-1)\\ \frac{V_{dc}}{2}(2S_{c3p}-1) \end{bmatrix}
\tag{6.11}
$$

The switching function of each switch can be written as equation (6.12) [168].

$$S_{xip} = \frac{M_{xip}}{2} + \frac{1}{2}, \quad M_{xip} = \frac{2V_{xi}}{V_{dc}} \tag{6.12}$$

Where: M_{xip} Represents the modulation index of top switch of leg 'x' of set number 'i' and 'V_{xi}' is the reference voltage of the phase 'x' of the set 'i' and 'V_{dc}' is the DC link voltage.

$$\begin{bmatrix} V_{q1} \\ V_{d1} \\ V_{O1} \\ V_{q2} \\ V_{d2} \\ V_{O2} \\ V_{q3} \\ V_{d3} \\ V_{O3} \end{bmatrix} = \frac{V_{dc}}{2} \begin{bmatrix} M_{q1} \\ M_{d1} \\ M_{O1} \\ M_{q2} \\ M_{d2} \\ M_{O2} \\ M_{q3} \\ M_{d3} \\ M_{O3} \end{bmatrix}, \begin{bmatrix} M_{q1} \\ M_{d1} \\ M_{O1} \\ M_{q2} \\ M_{d2} \\ M_{O2} \\ M_{q3} \\ M_{d3} \\ M_{O3} \end{bmatrix} = \frac{2T_r(\theta_{arb})}{V_{dc}} \begin{bmatrix} V_{a1p} \\ V_{b1p} \\ V_{c1p} \\ V_{a2p} \\ V_{b2p} \\ V_{c2p} \\ V_{a3p} \\ V_{b3p} \\ V_{c3p} \end{bmatrix} \tag{6.13}$$

Where 'M_x' is the modulation index of switch 'x'. By substituting the switching function from equation (6.12) in to the equation (6.11), the transformed voltages can be generated. The equation (6.13) can be used to generate the modulation indexes for the converter in the arbitrary reference frame (using the given voltages) according to equation (6.14).

$$\begin{bmatrix} M_{a1} \\ M_{b1} \\ M_{c1} \\ M_{a2} \\ M_{b2} \\ M_{c2} \\ M_{a3} \\ M_{b3} \\ M_{c3} \end{bmatrix} = T^{-1}{}_{arb}(\theta_{arb}) \begin{bmatrix} M_{q1} \\ M_{d1} \\ M_{O1} \\ M_{q2} \\ M_{d2} \\ M_{O2} \\ M_{q3} \\ M_{d3} \\ M_{O3} \end{bmatrix} = \frac{2T^{-1}{}_{arb}(\theta_{arb})}{V_{dc}} \begin{bmatrix} V_{q1} \\ V_{d1} \\ V_{O1} \\ V_{q2} \\ V_{d2} \\ V_{O2} \\ V_{q3} \\ V_{d3} \\ V_{O3} \end{bmatrix} \tag{6.14}$$

Where: '$T_{arb}(\theta_{arb})$' is the transformation matrix to arbitrary reference frame, presented in equation (6.15).

$$T_{arb}(\theta_{arb}) = \frac{2}{3}\begin{pmatrix} C(\theta_{arb}+\beta) & C(\theta_{arb}+\beta-\psi) & C(\theta_{arb}+\beta+\psi) & 0 & 0 & 0 & 0 & 0 & 0 \\ S(\theta_{arb}+\beta) & S(\theta_{arb}+\beta-\psi) & S(\theta_{arb}+\beta+\psi) & 0 & 0 & 0 & 0 & 0 & 0 \\ \frac{1}{2} & \frac{1}{2} & \frac{1}{2} & 0 & 0 & 0 & 0 & 0 & 0 \\ 0 & 0 & 0 & C(\theta_{arb}) & C(\theta_{arb}-\psi) & C(\theta_{arb}+\psi) & 0 & 0 & 0 \\ 0 & 0 & 0 & S(\theta_{arb}) & S(\theta_{arb}-\psi) & S(\theta_{arb}+\psi) & 0 & 0 & 0 \\ 0 & 0 & 0 & \frac{1}{2} & \frac{1}{2} & \frac{1}{2} & 0 & 0 & 0 \\ 0 & 0 & 0 & 0 & 0 & 0 & C(\theta_{arb}+\beta-\psi) & C(\theta_{arb}-\beta-\psi) & C(\theta_{arb}-\beta+\psi) \\ 0 & 0 & 0 & 0 & 0 & 0 & S(\theta_{arb}+\beta-\psi) & S(\theta_{arb}-\beta-\psi) & S(\theta_{arb}-\beta+\psi) \\ 0 & 0 & 0 & 0 & 0 & 0 & \frac{1}{2} & \frac{1}{2} & \frac{1}{2} \end{pmatrix} \quad (6.15)$$

$\theta_{arb} = reference \quad frame\ angle, \beta = \frac{2\pi}{9},\ \psi = \frac{2\pi}{3}, C = \cos, S = \sin$

The controller of the machine is designed based on the machine model generated in the chapter 4. The controller is implemented to the full order coupled model that was generated in the section 3.3. The average model of the machine is repeated here in equation (6.16). From Table 4.2 the self and mutual inductances in the q or d axis are equal. To have a simpler model and analysis the q and d axis inductances are shown by L_q and L_d respectively.

$$\begin{bmatrix} V_{q1} \\ V_{d1} \\ V_{q2} \\ V_{d2} \\ V_{q3} \\ V_{d3} \end{bmatrix} = r_s \begin{bmatrix} i_{q1} \\ i_{d1} \\ i_{q2} \\ i_{d2} \\ i_{q3} \\ i_{d3} \end{bmatrix} + \omega_r \begin{bmatrix} 0 & 1 & 0 & 0 & 0 & 0 \\ -1 & 0 & 0 & 0 & 0 & 0 \\ 0 & 0 & 0 & 1 & 0 & 0 \\ 0 & 0 & -1 & 0 & 0 & 0 \\ 0 & 0 & 0 & 0 & 0 & 1 \\ 0 & 0 & 0 & 0 & -1 & 0 \end{bmatrix} \left(\begin{bmatrix} L_q & 0 & L_q & 0 & L_q & 0 \\ 0 & L_d & 0 & L_d & 0 & L_d \\ L_q & 0 & L_q & 0 & L_q & 0 \\ 0 & L_d & 0 & L_d & 0 & L_d \\ L_q & 0 & L_q & 0 & L_q & 0 \\ 0 & L_d & 0 & L_d & 0 & L_d \end{bmatrix} \begin{bmatrix} i_{q1} \\ i_{d1} \\ i_{q2} \\ i_{d2} \\ i_{q3} \\ i_{d3} \end{bmatrix} + \begin{bmatrix} 0 \\ \lambda_{pmd1} \\ 0 \\ \lambda_{pmd2} \\ 0 \\ \lambda_{pmd3} \end{bmatrix} \right)$$

$$+ p \left(\begin{bmatrix} L_q & 0 & L_q & 0 & L_q & 0 \\ 0 & L_d & 0 & L_d & 0 & L_d \\ L_q & 0 & L_q & 0 & L_q & 0 \\ 0 & L_d & 0 & L_d & 0 & L_d \\ L_q & 0 & L_q & 0 & L_q & 0 \\ 0 & L_d & 0 & L_d & 0 & L_d \end{bmatrix} \begin{bmatrix} i_{q1} \\ i_{d1} \\ i_{q2} \\ i_{d2} \\ i_{q3} \\ i_{d3} \end{bmatrix} + \begin{bmatrix} \lambda_{pmq1} \\ \lambda_{pmd1} \\ \lambda_{pmq2} \\ \lambda_{pmd2} \\ \lambda_{pmq3} \\ \lambda_{pmd3} \end{bmatrix} \right) \tag{6.16}$$

$$T_e = \frac{3}{2}\frac{P}{2} \begin{bmatrix} (L_d - L_q) i_{d1} i_{q1} + (L_d - L_q) i_{q1} i_{d2} + (L_d - L_q) i_{q1} i_{d3} + (L_d - L_q) i_{q2} i_{d1} + \\ (L_d - L_q) i_{q3} i_{d1} + (L_d - L_q) i_{q2} i_{d3} + (L_d - L_q) i_{d2} i_{q2} + (L_d - L_q) i_{q3} i_{d2} + \\ (L_d - L_q) i_{d3} i_{q3} + \lambda_{pmd1}\, i_{q1} + \lambda_{pmd2}\, i_{q2} + \lambda_{pmd3}\, i_{q3} - \lambda_{pmq1}\, i_{d1} - \lambda_{pmq2}\, i_{d2} - \\ \lambda_{pmq3} i_{d3} \end{bmatrix}$$

For simpler analysis the sum of the current of the machines can be considered as 'i_q' and 'i_d'.

$$i_{q1} = \alpha_1 i_q \;\; i_{q2} = \alpha_2 i_q \;\; i_{q3} = \alpha_3 i_q$$
$$i_{d1} = \beta_1 i_d \;\; i_{d2} = \beta_2 i_d \;\; i_{d3} = \beta_3 i_d$$

$$\begin{aligned} i_q &= \alpha_1 i_q + \alpha_2 i_q + \alpha_3 i_q, \quad 1 = \alpha_1 + \alpha_2 + \alpha_3 \\ i_d &= \beta_1 i_d + \beta_2 i_d + \beta_3 i_d, \quad 1 = \beta_1 + \beta_2 + \beta_3 \end{aligned} \tag{6.17}$$

Using equation (6.17), the electromagnetic torque could be presented as:

$$T_e = T_{e1} + T_{e2} + T_{e3} = \frac{3}{2}\frac{P}{2}\begin{bmatrix} (L_d - L_q)\alpha_1 \beta_1 i_d i_q + (L_d - L_q)\alpha_1 \beta_2 i_q i_d + \\ (L_d - L_q)\alpha_1 \beta_3 i_q i_d + (L_d - L_q)\alpha_2 \beta_1 i_q i_d + \\ (L_d - L_q)\alpha_3 \beta_1 i_q i_d + (L_d - L_q)\alpha_2 \beta_3 i_q i_d + \\ (L_d - L_q)\alpha_2 \beta_2 i_d i_q + (L_d - L_q)\alpha_3 \beta_2 i_q i_d + \\ (L_d - L_q)\alpha_3 \beta_3 i_d i_q + \lambda_{pmd1}\alpha_1 i_q + \lambda_{pmd2}\alpha_2 i_q + \\ \lambda_{pmd3}\alpha_3 i_q - \lambda_{pmq1}\beta_1 i_d - \lambda_{pmq2}\beta_2 i_d - \\ \lambda_{pmq3}\beta_3 i_d \end{bmatrix} \tag{6.18}$$

The current regulator is operating under minimum copper loss strategy. The total copper loss of the machine can be defined as:

$$P_c = \frac{3}{2} r_s \left({i_{q1}}^2 + {i_{d1}}^2 + {i_{q2}}^2 + {i_{d2}}^2 + {i_{q3}}^2 + {i_{d3}}^2 \right) \tag{6.19}$$

Substituting the currents from equation (6.16) into the equation (6.19) results in:

$$P_c = \frac{3}{2} r_s \left(\alpha_1^2 {i_q}^2 + \beta_1^2 {i_d}^2 + \alpha_2^2 {i_q}^2 + \beta_2^2 {i_d}^2 + \alpha_3^2 {i_q}^2 + \beta_3^2 {i_d}^2 \right) \tag{6.20}$$

The total electromagnetic torque has to be equal to the load torque therefore the load constraint can be defined as:

$$T_L - T_{e1} - T_{e2} - T_{e3} = J\left(\frac{2}{P}\right) p\omega_r = \sigma_\omega \tag{6.21}$$

Using the Lagrange method to obtain the minimum value of the copper loss with the electromagnetic torque as a constraint, the Lagrange optimization function can be presented as:

$$L = \frac{3}{2} r_s \left(\alpha_1^{\,2} i_q^{\,2} + \beta_1^{\,2} i_d^{\,2} + \alpha_2^{\,2} i_q^{\,2} + \beta_2^{\,2} i_d^{\,2} + \alpha_3^{\,2} i_q^{\,2} + \beta_3^{\,2} i_d^{\,2} \right) - \lambda \left(T_L - T_{e1} - T_{e2} - T_{e3} - \sigma_\omega \right) \quad (6.22)$$

Where ' λ ' is the Lagrange multiplier. By solving the equations (6.23) to (6.31) (coming from Lagrange derivations) simultaneously, the optimum point of the copper loss can be obtained.

$$\frac{F}{\partial \alpha_1} = 3 r_s \left(\alpha_1 i_q^{\,2} \right) - \lambda \left(-\frac{3}{2}\frac{P}{2} \left[\left(L_d - L_q \right) \beta_1 i_d i_q + \left(L_d - L_q \right) \beta_2 i_q i_d + \left(L_d - L_q \right) \beta_3 i_q i_d + \lambda_{pmd1} i_q \right] \right) = 0 \quad (6.23)$$

$$\frac{F}{\partial \alpha_2} = 3 r_s \left(\alpha_2 i_q^{\,2} \right) - \lambda \left(-\frac{3}{2}\frac{P}{2} \left[\left(L_d - L_q \right) \beta_1 i_d i_q + \left(L_d - L_q \right) \beta_2 i_q i_d + \left(L_d - L_q \right) \beta_3 i_q i_d + \lambda_{pmd2} i_q \right] \right) = 0 \quad (6.24)$$

$$\frac{F}{\partial \alpha_3} = 3 r_s \left(\alpha_3 i_q^{\,2} \right) - \lambda \left(-\frac{3}{2}\frac{P}{2} \left[\left(L_d - L_q \right) \beta_1 i_d i_q + \left(L_d - L_q \right) \beta_2 i_q i_d + \left(L_d - L_q \right) \beta_3 i_q i_d + \lambda_{pmd3} i_q \right] \right) = 0 \quad (6.25)$$

$$\frac{F}{\partial \beta_1} = 3 r_s \left(\beta_1 i_d^{\,2} \right) - \lambda \left(-\frac{3}{2}\frac{P}{2} \left[\left(L_d - L_q \right) \alpha_1 i_d i_q + \left(L_d - L_q \right) \alpha_2 i_q i_d + \left(L_d - L_q \right) \alpha_3 i_q i_d - \lambda_{pmq1} i_d \right] \right) = 0 \quad (6.26)$$

$$\frac{F}{\partial \beta_2} = 3 r_s \left(\beta_2 i_d^{\,2} \right) - \lambda \left(-\frac{3}{2}\frac{P}{2} \left[\left(L_d - L_q \right) \alpha_1 i_d i_q + \left(L_d - L_q \right) \alpha_2 i_q i_d + \left(L_d - L_q \right) \alpha_3 i_q i_d - \lambda_{pmq2} i_d \right] \right) = 0 \quad (6.27)$$

$$\frac{F}{\partial \beta_3} = 3 r_s \left(\beta_3 i_d^{\,2} \right) - \lambda \left(-\frac{3}{2}\frac{P}{2} \left[\left(L_d - L_q \right) \alpha_1 i_d i_q + \left(L_d - L_q \right) \alpha_2 i_q i_d + \left(L_d - L_q \right) \alpha_3 i_q i_d - \lambda_{pmq3} i_d \right] \right) = 0 \quad (6.28)$$

$$\frac{F}{\partial i_q} = 3 r_s \left(\alpha_1^{\,2} i_q + \alpha_2^{\,2} i_q + \alpha_3^{\,2} i_q \right) - \lambda \left(-\frac{3}{2}\frac{P}{2} \begin{bmatrix} \left(L_d - L_q \right) \alpha_1 \beta_1 i_d + \left(L_d - L_q \right) \alpha_1 \beta_2 i_d + \\ \left(L_d - L_q \right) \alpha_1 \beta_3 i_d + \left(L_d - L_q \right) \alpha_2 \beta_1 i_d + \\ \left(L_d - L_q \right) \alpha_3 \beta_1 i_d + \left(L_d - L_q \right) \alpha_2 \beta_3 i_d + \\ \left(L_d - L_q \right) \alpha_2 \beta_2 i_d + \left(L_d - L_q \right) \alpha_3 \beta_2 i_d + \\ \left(L_d - L_q \right) \alpha_3 \beta_3 i_d + \lambda_{pmd1} \alpha_1 + \lambda_{pmd2} \alpha_2 + \lambda_{pmd3} \alpha_3 \end{bmatrix} \right) = 0 \quad (6.29)$$

$$\frac{F}{\partial i_d} = 3r_s\left(\beta_1{}^2 i_d + \beta_2{}^2 i_d + \beta_3{}^2 i_d\right) - \lambda\left(-\frac{3}{2}\frac{P}{2}\begin{bmatrix}\left(L_d - L_q\right)\alpha_1\beta_1 i_q + \left(L_d - L_q\right)\alpha_1\beta_2 i_q + \\ \left(L_d - L_q\right)\alpha_1\beta_3 i_q + \left(L_d - L_q\right)\alpha_2\beta_1 i_q + \\ \left(L_d - L_q\right)\alpha_3\beta_1 i_q + \left(L_d - L_q\right)\alpha_2\beta_3 i_q + \\ \left(L_d - L_q\right)\alpha_2\beta_2 i_q + \left(L_d - L_q\right)\alpha_3\beta_2 i_q + \\ \left(L_d - L_q\right)\alpha_3\beta_3 i_q - \lambda_{pmq1}\beta_1 - \lambda_{pmq2}\beta_2 - \lambda_{pmq3}\beta_3\end{bmatrix}\right) = 0 \quad (6.30)$$

$$\frac{F}{\partial\lambda} = \left(T_L - \frac{3}{2}\frac{P}{2}\begin{bmatrix}\left(L_d - L_q\right)\alpha_1\beta_1 i_d i_q + \left(L_d - L_q\right)\alpha_1\beta_2 i_q i_d + \left(L_d - L_q\right)\alpha_1\beta_3 i_q i_d + \\ \left(L_d - L_q\right)\alpha_2\beta_1 i_q i_d + \left(L_d - L_q\right)\alpha_3\beta_1 i_q i_d + \left(L_d - L_q\right)\alpha_2\beta_3 i_q i_d + \\ \left(L_d - L_q\right)\alpha_2\beta_2 i_d i_q + \left(L_d - L_q\right)\alpha_3\beta_2 i_q i_d + \left(L_d - L_q\right)\alpha_3\beta_3 i_d i_q + \\ \lambda_{pmd1}\alpha_1 i_q + \lambda_{pmd2}\alpha_2 i_q + \lambda_{pmd3}\alpha_3 i_q - \lambda_{pmq1}\beta_1 i_d - \lambda_{pmq2}\beta_2 i_d \\ -\lambda_{pmq3}\beta_3 i_d\end{bmatrix}\right) \quad (6.31)$$

The ‘ α_1 ’, ‘ α_2 ’ and ‘ α_3 ’ can be determined from equations (6.23) to (6.25) as:

$$\alpha_1 = \frac{\lambda\left(-\frac{3}{2}\frac{P}{2}\left[\left(L_d - L_q\right)\beta_1 i_d + \left(L_d - L_q\right)\beta_2 i_q + \left(L_d - L_q\right)\beta_3 i_q + \lambda_{pmd1}\right]\right)}{3r_s\, i_q} \quad (6.32)$$

$$\alpha_2 = \frac{\lambda\left(-\frac{3}{2}\frac{P}{2}\left[\left(L_d - L_q\right)\beta_1 i_d + \left(L_d - L_q\right)\beta_2 i_d + \left(L_d - L_q\right)\beta_3 i_d + \lambda_{pmd1}\right]\right)}{3r_s i_q} \quad (6.33)$$

$$\alpha_3 = \frac{\lambda\left(-\frac{3}{2}\frac{P}{2}\left[\left(L_d - L_q\right)\beta_1 i_d + \left(L_d - L_q\right)\beta_2 i_q + \left(L_d - L_q\right)\beta_3 i_d + \lambda_{pmd1}\right]\right)}{3r_s\, i_q} \quad (6.34)$$

Equations (6.32) to (6.34) result in:

$$\alpha_1 = \alpha_2 = \alpha_3 = \frac{1}{3} \quad (6.35)$$

Also the ‘ β_1 ’, ‘ β_2 ’ and ‘ β_3 ’ can be determined from equations (6.26) to (6.28) as:

$$\beta_1 = \frac{\lambda\left(-\frac{3}{2}\frac{P}{2}\left[\left(L_d - L_q\right)\alpha_1 i_q + \left(L_d - L_q\right)\alpha_2 i_q + \left(L_d - L_q\right)\alpha_3 i_q - \lambda_{pmq1}\right]\right)}{3r_s\, i_d} \tag{6.36}$$

$$\beta_2 = \frac{\lambda\left(-\frac{3}{2}\frac{P}{2}\left[\left(L_d - L_q\right)\alpha_1 i_q + \left(L_d - L_q\right)\alpha_2 i_q + \left(L_d - L_q\right)\alpha_3 i_q - \lambda_{pmq1}\right]\right)}{3r_s\, i_d} \tag{6.37}$$

$$\beta_3 = \frac{\lambda\left(-\frac{3}{2}\frac{P}{2}\left[\left(L_d - L_q\right)\alpha_1 i_q + \left(L_d - L_q\right)\alpha_2 i_q + \left(L_d - L_q\right)\alpha_3 i_q - \lambda_{pmq1}\right]\right)}{3r_s\, i_d} \tag{6.38}$$

Equations (6.36) to (6.38) result in:

$$\beta_1 = \beta_2 = \beta_3 = \frac{1}{3} \tag{6.39}$$

Substituting the above values for β_i, α_i into the equations (6.29) to (6.31) results in:

$$\frac{F}{\partial i_q} = \frac{1}{3} r_s\left(i_q + i_q + i_q\right) - \lambda\left(-\frac{3}{2}\frac{P}{2}\begin{bmatrix} \frac{1}{9}\left(L_d - L_q\right)i_d + \frac{1}{9}\left(L_d - L_q\right)i_d + \frac{1}{9}\left(L_d - L_q\right)i_d + \\ \frac{1}{9}\left(L_d - L_q\right)i_d + \frac{1}{9}\left(L_d - L_q\right)i_d + \frac{1}{9}\left(L_d - L_q\right)i_d + \\ \frac{1}{9}\left(L_d - L_q\right)i_d + \frac{1}{9}\left(L_d - L_q\right)i_d + \frac{1}{9}\left(L_d - L_q\right)i_d + \\ \frac{1}{3}\lambda_{pmd1} + \frac{1}{3}\lambda_{pmd2} + \frac{1}{3}\lambda_{pmd3} \end{bmatrix}\right) = 0 \tag{6.40}$$

$$\Rightarrow r_s\left(i_q\right) = \lambda\left(-\frac{3}{2}\frac{P}{2}\left[\left(L_d - L_q\right)i_d + \frac{1}{3}\lambda_{pmd1} + \frac{1}{3}\lambda_{pmd2} + \frac{1}{3}\lambda_{pmd3}\right]\right)$$

$$\frac{F}{\partial i_d}=\frac{1}{3}r_s\left(i_d+i_d+i_d\right)-\lambda\left(-\frac{3}{2}\frac{P}{2}\begin{bmatrix}\frac{1}{9}\left(L_d-L_q\right)i_q+\frac{1}{9}\left(L_d-L_q\right)i_q+\frac{1}{9}\left(L_d-L_q\right)i_q+\\ \frac{1}{9}\left(L_d-L_q\right)i_q+\frac{1}{9}\left(L_d-L_q\right)i_q+\frac{1}{9}\left(L_d-L_q\right)i_q+\\ \frac{1}{9}\left(L_d-L_q\right)i_q+\frac{1}{9}\left(L_d-L_q\right)i_q+\\ \frac{1}{9}\left(L_d-L_q\right)i_q-\frac{1}{3}\lambda_{pmq1}-\frac{1}{3}\lambda_{pmq2}-\frac{1}{3}\lambda_{pmq3}\end{bmatrix}\right)=0 \qquad (6.41)$$

$$\Rightarrow r_s\left(i_d\right)=\lambda\left(-\frac{3}{2}\frac{P}{2}\left[\left(L_d-L_q\right)i_q-\frac{1}{3}\lambda_{pmq1}-\frac{1}{3}\lambda_{pmq2}-\frac{1}{3}\lambda_{pmq3}\right]\right)$$

$$\frac{F}{\partial\lambda}=\left(T_L-\sigma_\omega-\frac{3}{2}\frac{P}{2}\begin{bmatrix}\frac{1}{9}\left(L_d-L_q\right)i_di_q+\frac{1}{9}\left(L_d-L_q\right)i_qi_d+\frac{1}{9}\left(L_d-L_q\right)i_qi_d+\\ \frac{1}{9}\left(L_d-L_q\right)i_qi_d+\frac{1}{9}\left(L_d-L_q\right)i_qi_d+\frac{1}{9}\left(L_d-L_q\right)i_qi_d+\\ \frac{1}{9}\left(L_d-L_q\right)i_di_q+\frac{1}{9}\left(L_d-L_q\right)i_qi_d+\\ \frac{1}{9}\left(L_d-L_q\right)i_di_q+\frac{1}{3}\lambda_{pmd1}i_q+\frac{1}{3}\lambda_{pmd2}i_q+\frac{1}{3}\lambda_{pmd3}i_q-\\ \frac{1}{3}\lambda_{pmq1}i_d-\frac{1}{3}\lambda_{pmq2}i_d-\frac{1}{3}\lambda_{pmq3}i_d\end{bmatrix}\right)=0\Rightarrow \qquad (6.42)$$

$$i_q=\frac{T_L-\sigma_\omega}{\frac{3}{2}\frac{P}{2}\left[\left(L_d-L_q\right)i_d+\frac{1}{3}\lambda_{pmd1}+\frac{1}{3}\lambda_{pmd2}+\frac{1}{3}\lambda_{pmd3}-\frac{1}{3}\lambda_{pmq1}i_d-\frac{1}{3}\lambda_{pmq2}i_d-\frac{1}{3}\lambda_{pmq3}i_d\right]}$$

From the equations (6.40) and (6.41), ‘ λ ’ is calculated as equations (6.43) and (6.44).

$$\lambda=\frac{r_s\,i_d}{-\frac{3}{2}\frac{P}{2}\left[\left(L_d-L_q\right)i_q-\frac{1}{3}\lambda_{pmq1}-\frac{1}{3}\lambda_{pmq2}-\frac{1}{3}\lambda_{pmq3}\right]} \qquad (6.43)$$

$$\lambda = \frac{r_s\, i_q}{-\frac{3}{2}\frac{P}{2}\left[\left(L_d - L_q\right)i_d + \frac{1}{3}\lambda_{pmd1} + \frac{1}{3}\lambda_{pmd2} + \frac{1}{3}\lambda_{pmd3}\right]} \tag{6.44}$$

From equations (6.43) and (6.44) the relationship between the q and d currents can be presented as equation (6.45).

$$\frac{r_s\, i_d}{\frac{3}{2}\frac{P}{2}\left[\left(L_d - L_q\right)i_q - \frac{1}{3}\lambda_{pmq1} - \frac{1}{3}\lambda_{pmq2} - \frac{1}{3}\lambda_{pmq3}\right]} = \frac{r_s i_q}{\frac{3}{2}\frac{P}{2}\left[\left(L_d - L_q\right)i_d + \frac{1}{3}\lambda_{pmd1} + \frac{1}{3}\lambda_{pmd2} + \frac{1}{3}\lambda_{pmd3}\right]} \tag{6.45}$$

The final relationship between the q and d axis currents can be obtained using the following procedure:

$$\frac{i_d}{\left[\left(L_d - L_q\right)i_q - \frac{1}{3}\lambda_{pmq1} - \frac{1}{3}\lambda_{pmq2} - \frac{1}{3}\lambda_{pmq3}\right]} = \frac{i_q}{\left[\left(L_d - L_q\right)i_d + \frac{1}{3}\lambda_{pmd1} + \frac{1}{3}\lambda_{pmd2} + \frac{1}{3}\lambda_{pmd3}\right]} \tag{6.46}$$

The equation (6.46) can be represented as:

$$\left[\left(L_d - L_q\right)i_d{}^2 + \frac{i_d}{3}\lambda_{pmd1} + \frac{i_d}{3}\lambda_{pmd2} + \frac{i_d}{3}\lambda_{pmd3}\right] = \left[\left(L_d - L_q\right)i_q{}^2 - \frac{i_q}{3}\lambda_{pmq1} - \frac{i_q}{3}\lambda_{pmq2} - \frac{i_q}{3}\lambda_{pmq3}\right] \tag{6.47}$$

$$\Rightarrow \left(L_d - L_q\right)i_d{}^2 + \frac{i_d}{3}\left(\lambda_{pmd1} + \lambda_{pmd2} + \lambda_{pmd3}\right) - \left(L_d - L_q\right)i_q{}^2 + \frac{i_q}{3}\left(\lambda_{pmq1} + \lambda_{pmq2} + \lambda_{pmq3}\right) = 0$$

By dividing the both sides of equation (6.47) by '$\left(L_d - L_q\right)$' the final relationship between the q and d currents can be represented as:

$$i_d{}^2 + i_d \frac{\left(\lambda_{pmd1} + \lambda_{pmd2} + \lambda_{pmd3}\right)}{3\left(L_d - L_q\right)} - i_q{}^2 + i_q \frac{\left(\lambda_{pmq1} + \lambda_{pmq2} + \lambda_{pmq3}\right)}{3\left(L_d - L_q\right)} = 0 \tag{6.48}$$

The equation (6.48) is a quadratic equation in terms of 'i_d' and can be solved as equation (4.49).

$$i_d = -\frac{\left(\lambda_{pmd1} + \lambda_{pmd2} + \lambda_{pmd3}\right)}{6\left(L_d - L_q\right)} \pm \sqrt{\left(\frac{\left(\lambda_{pmd1} + \lambda_{pmd2} + \lambda_{pmd3}\right)}{6\left(L_d - L_q\right)}\right)^2 + \left(i_q{}^2 - i_q \frac{\left(\lambda_{pmq1} + \lambda_{pmq2} + \lambda_{pmq3}\right)}{3\left(L_d - L_q\right)}\right)} \quad (6.49)$$

The equation (6.48) is an ellipse and it is plotted in Figure 6.2. It should be noted that the flux linkages due to the permanent magnets in the q axis are zero.

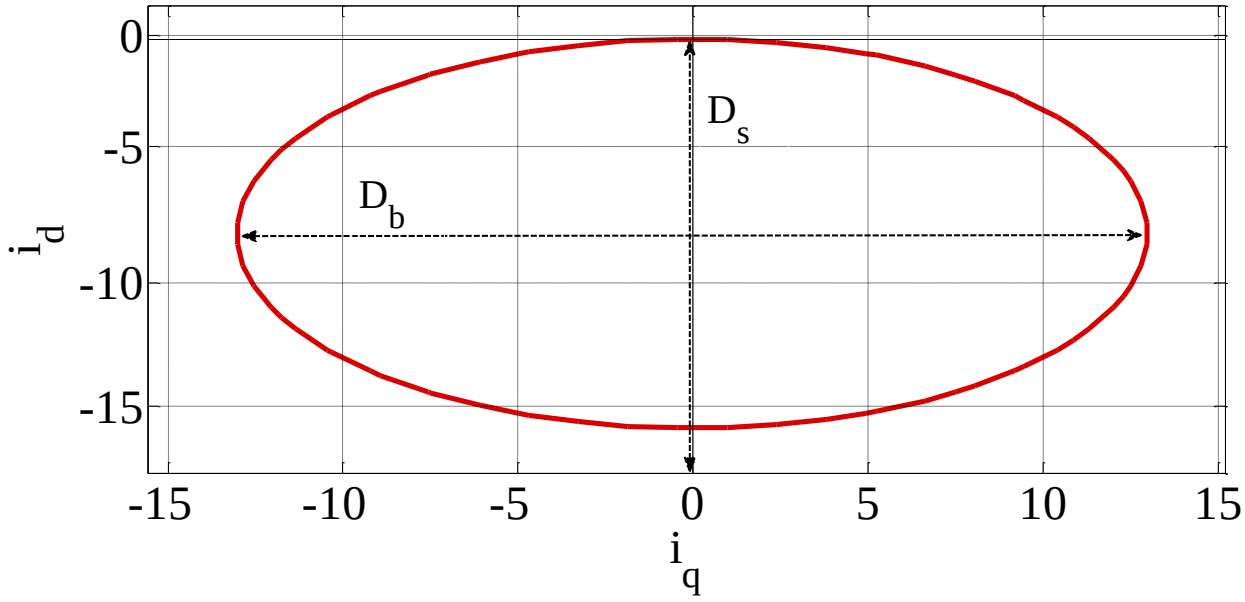

Figure 6.2: The plot of the ellipse in representing the q and d axis current relation.

The ellipse has two diameters. The expressions for the length of the bigger and smaller diameters and also the center of the ellipse are presented in equations (6.50), (6.51) and (6.52) respectively.

$$D_b = 2\sqrt{2}\,\frac{\left(\lambda_{pmd1} + \lambda_{pmd2} + \lambda_{pmd3}\right)}{3\left(L_d - L_q\right)} \quad (6.50)$$

$$D_s = \frac{\left(\lambda_{pmd1} + \lambda_{pmd2} + \lambda_{pmd3}\right)}{3\left(L_d - L_q\right)} \tag{6.51}$$

$$(i_q, i_d)_{cen} = \left(0, \frac{\left(\lambda_{pmd1} + \lambda_{pmd2} + \lambda_{pmd3}\right)}{6\left(L_d - L_q\right)} \right) \tag{6.52}$$

In equations (6.49) the q axis current is the input and the d axis current is the output. The q axis current itself also should be generated from equation (6.42). By defining A and B according to equation (6.53), and substituting them to equation (6.49) the d axis current can be expressed as (6.54).

$$A = \frac{\left(\lambda_{pmd1} + \lambda_{pmd2} + \lambda_{pmd3}\right)}{6\left(L_d - L_q\right)}, \quad B = \frac{\left(\lambda_{pmq1} + \lambda_{pmq2} + \lambda_{pmq3}\right)}{3\left(L_d - L_q\right)} \tag{6.53}$$

$$i_d = -A \pm \sqrt{\left(A\right)^2 + \left(i_q{}^2 - i_q B\right)} \tag{6.54}$$

Substituting the d axis current in to the equation (6.42), the q axis current can be generated as:

$$i_q = \frac{T_L - \sigma_\omega}{\frac{3}{2}\frac{P}{2}\left[\left(L_d - L_q\right)\left(-A \pm \sqrt{(A)^2 + \left(i_q{}^2 - i_q B\right)}\right) + \frac{1}{3}\left(\lambda_{pmd1} + \lambda_{pmd2} + \lambda_{pmd3}\right) - \frac{\left(-A \pm \sqrt{(A)^2 + \left(i_q{}^2 - i_q B\right)}\right)}{3}\left(\lambda_{pmq1} - \frac{1}{3}\lambda_{pmq2} - \frac{1}{3}\lambda_{pmq3}\right)\right]} \quad (6.55)$$

The equation (6.55) is equal to:

$$\left[\left(L_d - L_q\right)\left(-Ai_q \pm \sqrt{\left(Ai_q\right)^2 + \left(i_q{}^4 - i_q{}^3 B\right)}\right) + \frac{i_q}{3}\left(\lambda_{pmd1} + \lambda_{pmd2} + \lambda_{pmd3}\right) - \left(Ai_q \pm \sqrt{\left(Ai_q\right)^2 + \left(i_q{}^4 - i_q{}^3 B\right)}\right)\frac{\left(\lambda_{pmq1} - \frac{1}{3}\lambda_{pmq2} - \frac{1}{3}\lambda_{pmq3}\right)}{3}\right] \quad (6.56)$$

$$= \frac{4\left(T_L - \sigma_\omega\right)}{3P}$$

Since $\lambda_{pmqi}=0 \Rightarrow B=0$ equation (6.56) changes to:

$$-Ai_q \pm \sqrt{\left(Ai_q\right)^2+{i_q}^4}+\frac{i_q\left(\lambda_{pmd1}+\lambda_{pmd2}+\lambda_{pmd3}\right)}{3\left(L_d-L_q\right)}=\frac{4\left(T_L-\sigma_\omega\right)}{3P\left(L_d-L_q\right)} \Rightarrow$$

$$\pm \sqrt{\left(Ai_q\right)^2+{i_q}^4}=\frac{4\left(T_L-\sigma_\omega\right)}{3P\left(L_d-L_q\right)}+Ai_q-\frac{i_q\left(\lambda_{pmd1}+\lambda_{pmd2}+\lambda_{pmd3}\right)}{3\left(L_d-L_q\right)} \tag{6.57}$$

Squaring the both sides of equation (6.57) results in:

$$\left(Ai_q\right)^2+{i_q}^4=\left(\frac{4\left(T_L-\sigma_\omega\right)}{3P\left(L_d-L_q\right)}\right)^2+\left(Ai_q\right)^2+\left(\frac{i_q\left(\lambda_{pmd1}+\lambda_{pmd2}+\lambda_{pmd3}\right)}{3\left(L_d-L_q\right)}\right)^2+ \tag{6.58}$$

$$\frac{8Ai_q\left(T_L-\sigma_\omega\right)}{3P\left(L_d-L_q\right)}-\frac{2A{i_q}^2\left(\lambda_{pmd1}+\lambda_{pmd2}+\lambda_{pmd3}\right)}{3\left(L_d-L_q\right)}-\frac{i_q 8\left(T_L-\sigma_\omega\right)\left(\lambda_{pmd1}+\lambda_{pmd2}+\lambda_{pmd3}\right)}{9P\left(L_d-L_q\right)^2}$$

Substituting ‘A’ in equation (6.58) and simplifying it, results in:

$${i_q}^4+{i_q}^2\left(\frac{2A\left(\lambda_{pmd1}+\lambda_{pmd2}+\lambda_{pmd3}\right)}{3\left(L_d-L_q\right)}-\left(\frac{\left(\lambda_{pmd1}+\lambda_{pmd2}+\lambda_{pmd3}\right)}{3\left(L_d-L_q\right)}\right)^2\right)+ \tag{6.59}$$

$$i_q\left(\frac{8\left(T_L-\sigma_\omega\right)\left(\lambda_{pmd1}+\lambda_{pmd2}+\lambda_{pmd3}\right)}{9P\left(L_d-L_q\right)^2}-\frac{8A\left(T_L-\sigma_\omega\right)}{3P\left(L_d-L_q\right)}\right)=\left(\frac{4\left(T_L-\sigma_\omega\right)}{3P\left(L_d-L_q\right)}\right)^2$$

$${i_q}^4+i_q\left(\frac{4\left(T_L-\sigma_\omega\right)\left(\lambda_{pmd1}+\lambda_{pmd2}+\lambda_{pmd3}\right)}{9P\left(L_d-L_q\right)^2}\right)-\left(\frac{4\left(T_L-\sigma_\omega\right)}{3P\left(L_d-L_q\right)}\right)^2=0 \tag{6.60}$$

6.2.1 Speed Controller Design

Using the generated currents for q and d axis as the reference currents, control loops can be designed. The speed controller loop can be designed using the mechanical dynamic equation according to Figure 6.3. According to this figure the equation (6.61) can be presented for the speed controller loop.

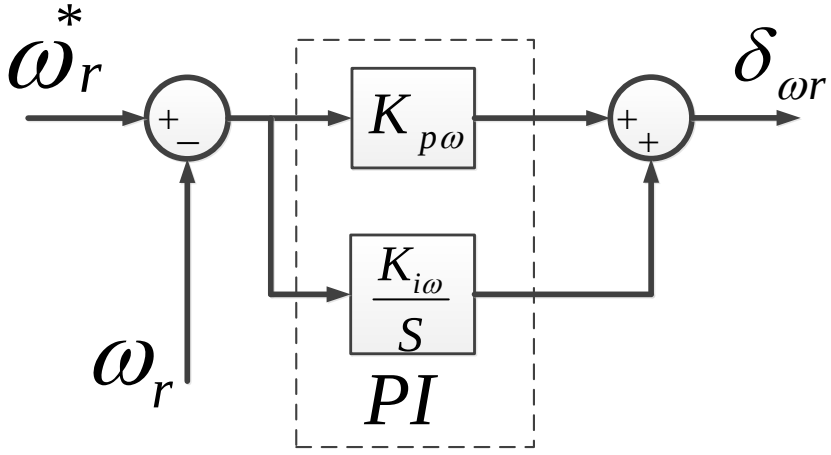

Figure 6.3: The speed controller loop.

$$p\omega_r = \sigma_\omega = \left(K_{p\omega} + \frac{K_{i\omega}}{p} \right)\left(\omega_r^* - \omega_r \right) \tag{6.61}$$

Where ' $K_{p\omega}$ ' and ' $K_{i\omega}$ ' are the proportional and the integral gains of the PI controller respectively.

From the equation (6.61) the transfer function between rotor speed and the reference speed is:

$$\frac{\omega_r}{\omega_r^*} = \frac{pK_{p\omega} + K_{i\omega}}{p^2 + K_{p\omega}p + K_{i\omega}} \tag{6.62}$$

By setting the denominator of the transfer function equal to the second order Butterworth polynomial the controller coefficients can be calculated [161].

$$S^2 + K_{p\omega}S + K_{i\omega} = p^2 + \sqrt{2}p\omega_o + \omega_o \tag{6.63}$$

The speed controller loop has to be at least 10 times faster than the desired rotor speed profile [157]. The final desired speed profile is a trapezoidal waveform that has the frequency of 0.05 (Hz). Therefore, the frequency of the speed controller loop has to be selected bigger than 0.5 (Hz). Setting $\omega_o = 7$ the correspondent relationship between the denominator of the transfer function and the Butterworth polynomial yields:

$$K_{p\omega} = \sqrt{2}\omega_o = 7\sqrt{2} \tag{6.64}$$

$$K_{i\omega} = \omega_o^2 = 49 \tag{6.65}$$

6.2.2 Current Regulators Design

Using the dynamic equations of the q and d axis voltages in the rotor reference frame, the current regulators for controlling the ' i_q ' and ' i_d ' can be designed. Equations (6.66) to (6.68) show the voltage equations for the machines in d and q axis of the rotor reference frame. It should be noted that the leakage inductance ' L_{ls} ' is added to the self-inductances of the machines.

$$\begin{aligned} V_{ds1} &= r_s i_{ds1} + p\left(\left(L_{ls} + L_d\right)i_{ds1} + L_d i_{ds2} + L_d i_{ds3} + \lambda_{pmd1}\right) + \omega_r\left(\left(L_{ls} + L_q\right)i_{qs1} + L_q i_{qs2} + L_q i_{qs3}\right) \\ V_{qs1} &= r_s i_{qs1} + p\left(\left(L_{ls} + L_q\right)i_{qs1} + L_q i_{qs2} + L_q i_{qs3}\right) - \omega_r\left(\left(L_{ls} + L_d\right)i_{ds1} + L_d i_{ds2} + L_d i_{ds3} + \lambda_{pmd1}\right) \end{aligned} \tag{6.66}$$

$$V_{ds2} = r_s i_{ds2} + p\left(L_d i_{ds1} + \left(L_{ls} + L_d\right) i_{ds2} + L_d i_{ds3} + \lambda_{pmd2}\right) + \omega_r \left(L_q i_{qs1} + \left(L_{ls} + L_q\right) i_{qs2} + L_q i_{qs3}\right)$$

$$V_{qs2} = r_s i_{qs2} + p\left(L_q i_{qs1} + \left(L_{ls} + L_q\right) i_{qs2} + L_q i_{qs3}\right) - \omega_r \left(L i_{ds1} + \left(L_{ls} + L_d\right) i_{ds2} + L_d i_{ds3} + \lambda_{pmd2}\right) \quad (6.67)$$

$$V_{ds3} = r_s i_{ds3} + p\left(L_d i_{ds1} + L_d i_{ds2} + \left(L_{ls} + L_d\right) i_{ds3} + \lambda_{pmd3}\right) + \omega_r \left(L_q i_{qs1} + L_q i_{qs2} + \left(L_{ls} + L_d\right) i_{qs3}\right)$$

$$V_{qs3} = r_s i_{qs3} + p\left(L_q i_{qs1} + L_q i_{qs2} + \left(L_{ls} + L_d\right) i_{qs3}\right) - \omega_r \left(L_d i_{ds1} + L_d i_{ds2} + \left(L_{ls} + L_d\right) i_{ds3} + \lambda_{pmd3}\right) \quad (6.68)$$

From the above equations the derivation of the flux linkages of *q* and *d* axis can be defined as equations (6.69) and (6.70).

$$\begin{bmatrix} p\lambda_{qs1} \\ p\lambda_{qs2} \\ p\lambda_{qs3} \end{bmatrix} = \begin{bmatrix} V_{qs1} - r_s i_{qs1} + \omega_r \left(\left(L_{ls} + L_d\right) i_{ds1} + L_d i_{ds2} + L_d i_{ds3} + \lambda_{pmd1}\right) \\ V_{qs2} - r_s i_{qs2} + \omega_r \left(L i_{ds1} + \left(L_{ls} + L_d\right) i_{ds2} + L_d i_{ds3} + \lambda_{pmd2}\right) \\ V_{qs3} - r_s i_{qs3} + \omega_r \left(L_d i_{ds1} + L_d i_{ds2} + \left(L_{ls} + L_d\right) i_{ds3} + \lambda_{pmd3}\right) \end{bmatrix} \quad (6.69)$$

$$\begin{bmatrix} p\lambda_{ds1} \\ p\lambda_{ds2} \\ p\lambda_{ds3} \end{bmatrix} = \begin{bmatrix} V_{ds1} - r_s i_{ds1} - \omega_r \left(\left(L_{ls} + L_q\right) i_{qs1} + L_q i_{qs2} + L_q i_{qs3}\right) \\ V_{ds2} - r_s i_{ds2} - \omega_r \left(L_q i_{qs1} + \left(L_{ls} + L_q\right) i_{qs2} + L_q i_{qs3}\right) \\ V_{ds3} - r_s i_{ds3} - \omega_r \left(L_q i_{qs1} + L_q i_{qs2} + \left(L_{ls} + L_d\right) i_{qs3}\right) \end{bmatrix} \quad (6.70)$$

By defining the derivatives of the flux linkages as 'δ_i' the equation for the flux linkages can be represented as:

$$\begin{bmatrix} L_{ls}+L_q & L_q & L_q \\ L_q & L_{ls}+L_q & L_q \\ L_q & L_q & L_{ls}+L_q \end{bmatrix}\begin{bmatrix} pi_{qs1} \\ pi_{qs2} \\ pi_{qs3} \end{bmatrix}=\begin{bmatrix} \delta_1 \\ \delta_2 \\ \delta_3 \end{bmatrix}=\begin{bmatrix} p\lambda_{qs1} \\ p\lambda_{qs2} \\ p\lambda_{qs3} \end{bmatrix} \tag{6.71}$$

From the equation (6.71) the derivations of the currents can be obtained as:

$$\begin{bmatrix} pi_{qs1} \\ pi_{qs2} \\ pi_{qs3} \end{bmatrix}=\begin{bmatrix} L_{ls}+L_q & L_q & L_q \\ L_q & L_{ls}+L_q & L_q \\ L_q & L_q & L_{ls}+L_q \end{bmatrix}^{-1}\begin{bmatrix} \delta_1 \\ \delta_2 \\ \delta_3 \end{bmatrix}=\frac{1}{{L_{ls}}^2+3L_qL_{ls}}\begin{bmatrix} L_{ls}+2L_q & -L_q & -L_q \\ -L_q & L_{ls}+2L_q & -L_q \\ -L_q & -L_q & L_{ls}+2L_q \end{bmatrix}\begin{bmatrix} \delta_1 \\ \delta_2 \\ \delta_3 \end{bmatrix} \tag{6.72}$$

Therefore, the derivatives of the currents can be separated as:

$$pi_{qs1}=\frac{1}{{L_{ls}}^2+3L_qL_{ls}}\left(\left(L_{ls}+L_q\right)p\lambda_{qs1}-L_qp\lambda_{qs2}-L_qp\lambda_{qs3}\right) \tag{6.73}$$

$$pi_{qs2}=\frac{1}{{L_{ls}}^2+3L_qL_{ls}}\left(-L_qp\lambda_{qs1}+\left(L_{ls}+L_q\right)p\lambda_{qs2}-L_qp\lambda_{qs3}\right) \tag{6.74}$$

$$pi_{qs3}=\frac{1}{{L_{ls}}^2+3L_qL_{ls}}\left(-L_qp\lambda_{qs1}-L_qp\lambda_{qs2}+\left(L_{ls}+L_q\right)p\lambda_{qs3}\right) \tag{6.75}$$

By substituting the derivatives of the flux linkages from equation (6.70) into the equations (6.73) to (6.75), they change to the equations (6.76) to (6.78).

$$pi_{qs1}=\frac{1}{{L_{ls}}^2+3L_qL_{ls}}\begin{pmatrix} \left(L_{ls}\right)\left(V_{qs1}-r_si_{qs1}+\omega_r\left(\left(L_{ls}+L_d\right)i_{ds1}+L_di_{ds2}+L_di_{ds3}+\lambda_{pmd1}\right)\right)+ \\ \left(L_q\right)\left(V_{qs1}-V_{qs2}-V_{qs3}\right)+\left(L_q\right)\left(-r_si_{qs1}+r_si_{qs2}+r_si_{qs3}\right) \\ \omega_r\left(L_q\right)\left(\left(\left(L_{ls}-L_d\right)i_{ds1}-\left(L_{ls}+L_d\right)i_{ds2}-\left(L_{ls}+L_d\right)i_{ds3}\right)\right)+ \\ \omega_r\left(L_q\right)\left(\lambda_{pmd1}-\lambda_{pmd2}-\lambda_{pmd3}\right) \end{pmatrix} \tag{6.76}$$

$$pi_{qs2}=\frac{1}{{L_{ls}}^2+3L_qL_{ls}}\begin{pmatrix} \left(L_{ls}\right)\left(V_{qs2}-r_si_{qs2}+\omega_r\left(Li_{ds1}+\left(L_{ls}+L_d\right)i_{ds2}+L_di_{ds3}+\lambda_{pmd2}\right)\right)+ \\ \left(L_q\right)\left(V_{qs2}-V_{qs1}-V_{qs3}\right)+\left(L_q\right)\left(-r_si_{qs2}+r_si_{qs1}+r_si_{qs3}\right)+ \\ \omega_r\left(L_q\right)\left(\left(L_{ls}-L_d\right)i_{ds2}-\left(L_{ls}+L_d\right)i_{ds1}-\left(L_{ls}+L_d\right)i_{ds3}\right)+ \\ \omega_r\left(L_q\right)\left(\lambda_{pmd2}-\lambda_{pmd1}-\lambda_{pmd3}\right) \end{pmatrix} \tag{6.77}$$

$$pi_{qs3}=\frac{1}{{L_{ls}}^2+3L_qL_{ls}}\begin{pmatrix}(L_{ls})(V_{qs3}-r_si_{qs3}+\omega_r(L_di_{ds1}+L_di_{ds2}+(L_{ls}+L_d)i_{ds3}+\lambda_{pmd3}))+\\(L_q)(V_{qs3}-V_{qs1}-V_{qs2})+(L_q)(r_si_{qs1}+r_si_{qs2}-r_si_{qs3})+\\\omega_r(L_q)((L_{ls}+L_d)i_{ds1})-\omega_r(L_q)((L_{ls}+L_d)i_{ds2})+\\\omega_r(L_q)((L_{ls}-L_d)i_{ds3})+(L_q)(\omega_r(\lambda_{pmd3}-\lambda_{pmd1}-\lambda_{pmd2}))\end{pmatrix} \tag{6.78}$$

The same method can be applied to the d axis currents. By defining the derivatives of the flux linkages as ' τ_i ' the equation (6.79) can be written.

$$\begin{bmatrix}L_{ls}+L_d & L_d & L_d\\ L_d & L_{ls}+L_d & L_d\\ L_d & L_d & L_{ls}+L_d\end{bmatrix}\begin{bmatrix}pi_{ds1}\\pi_{ds2}\\pi_{ds3}\end{bmatrix}=\begin{bmatrix}\tau_1\\\tau_2\\\tau_3\end{bmatrix}=\begin{bmatrix}p\lambda_{ds1}\\p\lambda_{ds2}\\p\lambda_{ds3}\end{bmatrix} \tag{6.79}$$

Using the equation (6.79) the derivations of the currents can be presented as equation (6.80).

$$\begin{bmatrix}pi_{ds1}\\pi_{ds2}\\pi_{ds3}\end{bmatrix}=\begin{bmatrix}L_{ls}+L_d & L_d & L_d\\ L_d & L_{ls}+L_d & L_d\\ L_d & L_d & L_{ls}+L_d\end{bmatrix}^{-1}\begin{bmatrix}\tau_1\\\tau_2\\\tau_3\end{bmatrix}\Rightarrow \tag{6.80}$$

$$\frac{1}{{L_{ls}}^2+3L_dL_{ls}}\begin{bmatrix}L_{ls}+2L_d & -L_d & -L_d\\ -L_d & L_{ls}+2L_d & -L_d\\ -L_d & -L_d & L_{ls}+2L_d\end{bmatrix}\begin{bmatrix}\tau_1\\\tau_2\\\tau_3\end{bmatrix}$$

From equation (6.80) the currents derivations can be presented as equation (6.81).

$$pi_{ds1}=\frac{1}{{L_{ls}}^2+3L_dL_{ls}}((L_{ls}+L_d)p\lambda_{ds1}-L_dp\lambda_{ds2}-L_dp\lambda_{ds3}) \tag{6.81}$$

$$pi_{ds2} = \frac{1}{L_{ls}{}^2 + 3L_d L_{ls}} \left(- L_d \, p\lambda_{ds1} + \left(L_{ls} + L_d \right) p\lambda_{ds2} - L_d \, p\lambda_{ds3} \right) \tag{6.82}$$

$$pi_{ds3} = \frac{1}{L_{ls}{}^2 + 3L_d L_{ls}} \left(- L_d \, p\lambda_{ds1} - L_d \, p\lambda_{ds2} + \left(L_{ls} + L_d \right) p\lambda_{ds3} \right) \tag{6.83}$$

By substituting the derivations of the flux linkages from equation (6.69) into the equations (6.81) to (6.83), they change to the equations (6.84) to (6.86).

$$pi_{ds1} = \frac{1}{L_{ls}{}^2 + 3L_d L_{ls}} \begin{pmatrix} \left(L_{ls} \right) \left(V_{ds1} - r_s i_{ds1} - \omega_r \left(\left(L_{ls} + L_q \right) i_{qs1} + L_q i_{qs2} + L_q i_{qs3} \right) \right) + \\ \left(L_d \right) \left(V_{ds1} - V_{ds2} - V_{ds3} \right) + \left(L_d \right) \left(- r_s i_{ds1} + r_s i_{ds2} + r_s i_{ds3} \right) - \\ \omega_r \left(L_d \right) \left(L_{ls} - L_q \right) i_{qs1} + \omega_r \left(L_d \right) \left(L_{ls} + L_q \right) i_{qs2} + \omega_r \left(L_d \right) \left(L_{ls} + L_d \right) i_{qs3} \end{pmatrix} \tag{6.84}$$

$$pi_{ds2} = \frac{1}{L_{ls}{}^2 + 3L_d L_{ls}} \begin{pmatrix} \left(L_{ls} \right) \left(V_{ds2} - r_s i_{ds2} - \omega_r \left(L_q i_{qs1} + \left(L_{ls} + L_q \right) i_{qs2} + L_q i_{qs3} \right) \right) + \\ \left(L_d \right) \left(V_{ds2} - V_{ds1} - V_{ds3} \right) + \left(L_d \right) \left(- r_s i_{ds2} + r_s i_{ds1} + r_s i_{ds3} \right) - \\ \omega_r \left(L_d \right) \left(\left(L_{ls} - L_q \right) i_{qs2} \right) + \omega_r \left(L_d \right) \left(\left(L_{ls} + L_q \right) i_{qs1} \right) + \omega_r \left(L_d \right) \left(\left(L_{ls} + L_d \right) i_{qs3} \right) \end{pmatrix} \tag{6.85}$$

$$pi_{ds3} = . \frac{1}{L_{ls}{}^2 + 3L_d L_{ls}} \begin{pmatrix} \left(L_{ls} \right) \left(V_{ds3} - r_s i_{ds3} - \omega_r \left(L_q i_{qs1} + L_q i_{qs2} + \left(L_{ls} + L_d \right) i_{qs3} \right) \right) + \\ \left(L_d \right) \left(V_{ds3} - V_{ds1} - V_{ds2} \right) + \left(L_d \right) \left(- r_s i_{ds3} + r_s i_{ds1} + r_s i_{ds2} \right) + \\ \omega_r \left(L_d \right) \left(\left(L_{ls} + L_q \right) i_{qs1} \right) + \omega_r \left(L_d \right) \left(\left(L_{ls} + L_q \right) i_{qs2} \right) - \omega_r \left(L_d \right) \left(\left(L_{ls} - L_d \right) i_{qs3} \right) \end{pmatrix} \tag{6.86}$$

Substituting the current derivations in the voltage equations of the machine, they change to the equations (6.87) to (6.92).

$$r_s i_{ds1} + \left(L_{ls} + L_d\right) p i_{ds1} = V_{ds1} - \frac{L_d}{L_{ls} + 3L_d}\left(V_{ds2} + V_{ds3} - r_s i_{ds2} - r_s i_{ds3} - \omega_r\left(2L_q i_{qs1} + \left(L_{ls} + 2L_q\right) i_{qs2} + \left(L_{ls} + 2L_d\right) i_{qs3}\right)\right)$$

$$- \frac{L_d}{{L_{ls}}^2 + 3L_d L_{ls}}\left(-2L_d V_{ds1} + 2r_s L_d i_{ds1} + 2\omega_r L_d L_q i_{qs2} + 2\omega_r L_{ls} L_d i_{qs1} + 2\omega_r {L^2}_q i_{qs1} + 2\omega_r {L^2}_d i_{qs3}\right) \tag{6.87}$$

$$- \omega_r\left(\left(L_{ls} + L_q\right) i_{qs1} + L_q i_{qs2} + L_q i_{qs3}\right)$$

$$r_s i_{qs1} + \left(L_{ls} + L_q\right) p i_{qs1} = V_{qs1} - \frac{L_q}{L_{ls} + 3L_q}\left(V_{qs2} + V_{qs3} - r_s i_{qs2} - r_s i_{qs3} + \omega_r\left(2L_d i_{ds1} + \left(L_{ls} + 2L_d\right) i_{ds2} + \left(L_{ls} + 2L_d\right) i_{ds3} + \lambda_{pmd2} + \lambda_{pmd3}\right)\right)$$

$$- \frac{L_q}{{L_{ls}}^2 + 3L_q L_{ls}}\left(-2L_q V_{qs1} + 2r_s L_q i_{qs1} + \omega_r L_q\left(-2L_d i_{ds2} - 2\left(L_{ls} + L_d\right) i_{ds1} - 2L_d i_{ds3}\right) - 2\omega_r L_q\left(\lambda_{pmd1}\right)\right) \tag{6.88}$$

$$+ \omega_r\left(\left(L_{ls} + L_d\right) i_{ds1} + L_d i_{ds2} + L_d i_{ds3} + \lambda_{pmd1}\right)$$

$$r_s i_{ds2} + \left(L_{ls} + L_d\right) p i_{ds2} = V_{ds2} - \frac{L_d}{{L_{ls}}^2 + 3L_d L_{ls}} \left(-2L_d V_{ds2} + 2L_d r_s i_{ds2} + 2\omega_r L_d L_q i_{qs1} + 2\omega_r \left(L_d\right)\left(L_{ls} + L_q\right) i_{qs2} + 2\omega_r L_d L_d i_{qs3}\right)$$

$$- \frac{L_d}{{L_{ls}}^2 + 3L_d L_{ls}} \left(\left(L_{ls}\right)\left(V_{ds1} + V_{ds3} - r_s i_{ds1} - r_s i_{ds3} - \omega_r \left(\left(L_{ls} + L_q\right) i_{qs1} + L_q i_{qs2} + L_q i_{qs3} + L_q i_{qs1} + L_q i_{qs2} + \left(L_{ls} + L_d\right) i_{qs3}\right)\right)\right) \tag{6.89}$$

$$- \omega_r \left(L_q i_{qs1} + \left(L_{ls} + L_q\right) i_{qs2} + L_q i_{qs3}\right)$$

$$r_s i_{qs2} + \left(L_{ls} + L_q\right) p i_{qs2} = V_{qs2} - \frac{L_q}{L_{ls} + 3L_q} \left(\left(V_{qs1} + V_{qs3} - r_s i_{qs1} - r_s i_{qs3} + \omega_r \left(\left(L_{ls} + 2L_d\right) i_{ds1} + 2L_d i_{ds2} + \left(L_{ls} + 2L_d\right) i_{ds3} + \lambda_{pmd1} + \lambda_{pmd3}\right)\right)\right)$$

$$- \frac{L_q}{{L_{ls}}^2 + 3L_q L_{ls}} \left(-2L_q V_{qs2} + 2L_q r_s i_{qs2} + \omega_r \left(L_q\right)\left(-2L_d i_{ds1} - 2\left(L_{ls} + L_d\right) i_{ds2} - 2L_d i_{ds3} +\right) - 2\omega_r L_q \lambda_{pmd2}\right) \tag{6.90}$$

$$+ \omega_r \left(L i_{ds1} + \left(L_{ls} + L_d\right) i_{ds2} + L_d i_{ds3} + \lambda_{pmd2}\right)$$

$$r_s i_{ds3} + p\left(L_{ls} + L_d\right) i_{ds3} = V_{ds3} - \frac{L_d}{L_{ls} + 3L_d}\left(\left(V_{ds1} + V_{ds2} - r_s i_{ds1} - r_s i_{ds2} - \omega_r\left(\left(L_{ls} + L_q\right) i_{qs1} + L_q i_{qs2} + L_q i_{qs3} + L_q i_{qs1} + \left(L_{ls} + L_q\right) i_{qs2} + L_q i_{qs3}\right)\right)\right)$$

$$- \frac{L_d}{{L_{ls}}^2 + 3L_d L_{ls}}\left(-2L_d V_{ds3} + 2L_d r_s i_{ds3} + 2\omega_r L_d L_q i_{qs1} + 2\omega_r L_d L_q i_{qs2} + 2\omega_r L_d\left(L_{ls} + L_d\right) i_{qs3}\right) \tag{6.91}$$

$$- \omega_r\left(L_q i_{qs1} + L_q i_{qs2} + \left(L_{ls} + L_d\right) i_{qs3}\right)$$

$$r_s i_{qs3} + p\left(L_{ls} + L_d\right) i_{qs3} = V_{qs3} - \frac{L_q}{L_{ls} + 3L_q}\left(\left(V_{qs1} + V_{qs2} - r_s i_{qs1} - r_s i_{qs2} + \omega_r\left(\left(L_{ls} + 2L_d\right) i_{ds1} + 2L_d i_{ds3} + \left(L_{ls} + 2L_d\right) i_{ds2} + \lambda_{pmd2} + \lambda_{pmd1}\right)\right)\right)$$

$$- \frac{L_q}{{L_{ls}}^2 + 3L_q L_{ls}}\left(-2L_q V_{qs3} + 2L_q r_s i_{qs3} + \omega_r L_q\left(-2L_d i_{ds1} - 2L_d i_{ds2} - 2\left(L_{ls} + L_d\right) i_{ds3}\right) - 2\omega_r L_q \lambda_{pmd3}\right) \tag{6.92}$$

$$+ \omega_r\left(L_d i_{ds1} + L_d i_{ds2} + \left(L_{ls} + L_d\right) i_{ds3} + \lambda_{pmd3}\right)$$

Now using the modified voltage equations, the current regulators can be designed as follows. For the machine 'j' (j =1,2 ,3), the *d* axis PI controller for current regulator is shown in Figure 6.4. According to this figure the equation for the current regulator can be presented as equation (6.93).

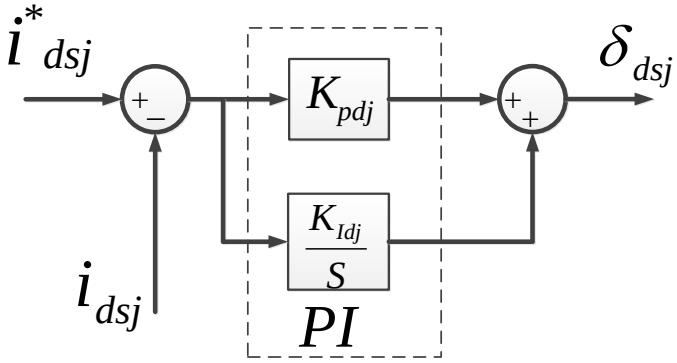

Figure 6.4: The d axis current regulator.

$$r_s i_{dsj} + (L_{ls} + L_d) p i_{dsj} = \delta_{dsj} = \left(K_{pdj} + \frac{K_{Idj}}{p} \right) \left(i_{dsj}^{\ *} - i_{dsj} \right) \tag{6.93}$$

From the above equation the transfer function can be presented as:

$$r_s i_{dsj} + (L_{ls} + L_d) p i_{dsj} + \left(K_{pdj} + \frac{K_{Idj}}{p} \right) (i_{dsj}) = \left(K_{pdj} + \frac{K_{Idj}}{p} \right) \left(i_{dsj}^{\ *} \right) \tag{6.94}$$

Finally, the transfer function between the reference and the feedback current of the d axis of the machine 'j' is:

$$\frac{i_{dsj}}{i_{dsj}^{\ *}} = \frac{\dfrac{\left(pK_{pdj} + K_{Idj} \right)}{\left(L_{ls} + L_d \right)}}{p^2 + p \dfrac{\left(r_s + K_{pdj} \right)}{\left(L_{ls} + L_d \right)} + \dfrac{K_{Idj}}{\left(L_{ls} + L_d \right)}} \tag{6.95}$$

The denominator of the equation (6.95) can be set equal to the second order Butterworth polynomial to obtain the controller gains for machine 'j' as K_{pdj} and K_{Idj}.

$$p^2 + p\frac{\left(r_s + K_{pdj}\right)}{\left(L_{ls} + L_d\right)} + \frac{K_{Idj}}{\left(L_{ls} + L_d\right)} = p^2 + \sqrt{2}p\omega_o + \omega_o{}^2 \tag{6.96}$$

From the above equation the controller coefficients can be calculated as:

$$\sqrt{2}\omega_o = \frac{\left(r_s + K_{pdj}\right)}{\left(L_{ls} + L_d\right)} \tag{6.97}$$

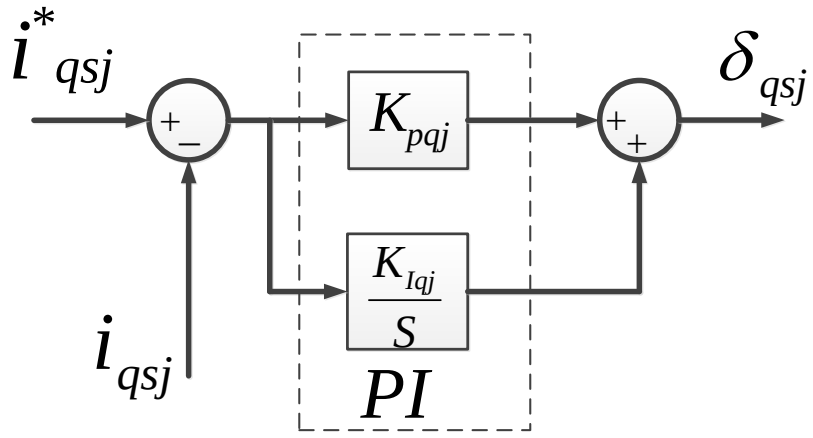

Figure 6.5: The q axis current regulator.

Table: 6.1: The machine parameters.

L_q	0.048(H)
L_d	0.0012 (H)
r_s	0.01 (Ohm)
L_{ls}	0.00001 (H)
λ_{pm}	0.2 (Wb)

The internal loops of a current controller have to be at least 10 times faster than the main loop [157]. Since the frequency of the speed controller loop is selected as 7 (rad/sec), the frequency of the current regulator has to be at least 70 (rad/sec). By substituting the machine parameters and selecting $\omega_o = 200 \quad (rad/\sec)$, the proportional and the integral coefficient of the current regulator can be calculated according to equation (6.98) and (6.99) respectively.

$$K_{pdj} = \sqrt{2}\omega_o\left(L_{ls} + L_d\right) - r_s = \sqrt{2} \times 200 \times 0.0012 - 0.01 = 0.3294 \tag{6.98}$$

$$\frac{K_{Idj}}{\left(L_{ls} + L_d\right)} = \omega_o{}^2 \rightarrow K_{id} = 48 \tag{6.99}$$

For the *q* axis current controller for machine *'j'* also the controller can be designed as:

$$r_s i_{qsj} + \left(L_{ls} + L_q\right) p i_{qsj} = \delta_{qsj} = \left(K_{pqj} + \frac{K_{Iqj}}{p}\right)\left(i_{qsj}{}^* - i_{qsj}\right) \tag{6.100}$$

From the above equation the transfer function can be presented as:

$$r_s i_{qsi} + \left(L_{ls} + L_d\right) p i_{qsi} + \left(K_{pqi} + \frac{K_{Iqi}}{p}\right)\left(i_{qsi}\right) = \left(K_{pqi} + \frac{K_{Iqi}}{p}\right)\left(i_{qsi}{}^*\right) \tag{6.101}$$

Finally, the transfer function is:

$$\frac{i_{qsj}}{i_{qsj}{}^*} = \frac{\dfrac{\left(pK_{pqj} + K_{Iqj}\right)}{\left(L_{ls} + L_q\right)}}{p^2 + p\dfrac{\left(r_s + K_{pqj}\right)}{\left(L_{ls} + L_q\right)} + \dfrac{K_{Idj}}{\left(L_{ls} + L_q\right)}} \tag{6.102}$$

The denominator of the equation (6.102) can be set equal to the second order Butterworth polynomial to obtain the K_{pqj} and K_{Iqj}. Using the machine parameters from chapter 3 the controller coefficients are calculated using equation (3.103).

$$p^2 + p\frac{\left(r_s + K_{pqj}\right)}{\left(L_{ls} + L_q\right)} + \frac{K_{Idj}}{\left(L_{ls} + L_q\right)} = p^2 + \sqrt{2}p\omega_o + \omega_o{}^2 \tag{6.103}$$

Again to have a faster internal controller the frequency of the current regulator should be at least 10 times bigger than the speed controller loop. Therefore, selecting $\omega_o = 200 \ \ (rad/\sec)$ results in:

$$\sqrt{2}\omega_o = \frac{\left(r_s + K_{pqj}\right)}{\left(L_{ls} + L_q\right)} \tag{6.104}$$

$$K_{pqj} = \sqrt{2}\omega_o\left(L_{ls} + L_q\right) - r_s = 0.73539 - 0.01 = 0.725397 \tag{6.105}$$

$$\frac{K_{Iqj}}{\left(L_{ls} + L_q\right)} = \omega_o{}^2 \rightarrow K_{iq} = 104 \tag{6.106}$$

From the controllers, the voltage of the q and d axis of the machines can be generated as:

$$V_{ds1} = \delta_{ds1} + \frac{L_d}{L_{ls} + 3L_d}\left(V_{ds2} + V_{ds3} - r_s i_{ds2} - r_s i_{ds3} - \omega_r\left(2L_q i_{qs1} + \left(L_{ls} + 2L_q\right)i_{qs2} + \left(L_{ls} + 2L_d\right)i_{qs3}\right)\right)$$

$$+ \frac{L_d}{L_{ls}^{\ 2} + 3L_d L_{ls}}\left(-2L_d V_{ds1} + 2r_s L_d i_{ds1} + 2\omega_r L_d L_q i_{qs2} + 2\omega_r L_{ls} L_d i_{qs1} + 2\omega_r L^2{}_q i_{qs1} + 2\omega_r L^2{}_d i_{qs3}\right) \quad (6.107)$$

$$+ \omega_r\left(\left(L_{ls} + L_q\right)i_{qs1} + L_q i_{qs2} + L_q i_{qs3}\right)$$

$$V_{qs1} =$$

$$\delta_{qs1} + \frac{L_q}{L_{ls} + 3L_q}\left(V_{qs2} + V_{qs3} - r_s i_{qs2} - r_s i_{qs3} + \omega_r\left(2L_d i_{ds1} + \left(L_{ls} + 2L_d\right)i_{ds2} + \left(L_{ls} + 2L_d\right)i_{ds3} + \lambda_{pmd2} + \lambda_{pmd3}\right)\right) \quad (6.108)$$

$$+ \frac{L_q}{L_{ls}^{\ 2} + 3L_q L_{ls}}\left(-2L_q V_{qs1} + 2r_s L_q i_{qs1} + \omega_r L_q\left(-2L_d i_{ds2} - 2\left(L_{ls} + L_d\right)i_{ds1} - 2L_d i_{ds3}\right) - 2\omega_r L_q\left(\lambda_{pmd1}\right)\right)$$

$$- \omega_r\left(\left(L_{ls} + L_d\right)i_{ds1} + L_d i_{ds2} + L_d i_{ds3} + \lambda_{pmd1}\right)$$

$$V_{ds2} =$$

$$\delta_{ds2} + \frac{L_d}{L_{ls}^{\ 2} + 3L_d L_{ls}}\left(-2L_d V_{ds2} + 2L_d r_s i_{ds2} + 2\omega_r L_d L_q i_{qs1} + 2\omega_r \left(L_d\right)\left(L_{ls} + L_q\right)i_{qs2} + 2\omega_r L_d L_d i_{qs3}\right) \tag{6.109}$$

$$+ \frac{L_d}{L_{ls}^{\ 2} + 3L_d L_{ls}}\left(\left(L_{ls}\right)\left(V_{ds1} + V_{ds3} - r_s i_{ds1} - r_s i_{ds3} - \omega_r\left(\left(L_{ls} + L_q\right)i_{qs1} + L_q i_{qs2} + L_q i_{qs3} + L_q i_{qs1} + L_q i_{qs2} + \left(L_{ls} + L_d\right)i_{qs3}\right)\right)\right)$$

$$+ \omega_r\left(L_q i_{qs1} + \left(L_{ls} + L_q\right)i_{qs2} + L_q i_{qs3}\right)$$

$$V_{qs2} =$$

$$\delta_{qs2} + \frac{L_q}{L_{ls} + 3L_q}\left(\left(V_{qs1} + V_{qs3} - r_s i_{qs1} - r_s i_{qs3} + \omega_r\left(\left(L_{ls} + 2L_d\right)i_{ds1} + 2L_d i_{ds2} + \left(L_{ls} + 2L_d\right)i_{ds3} + \lambda_{pmd1} + \lambda_{pmd3}\right)\right)\right) \tag{6.110}$$

$$+ \frac{L_q}{L_{ls}^{\ 2} + 3L_q L_{ls}}\left(-2L_q V_{qs2} + 2L_q r_s i_{qs2} + \omega_r\left(L_q\right)\left(-2L_d i_{ds1} - 2\left(L_{ls} + L_d\right)i_{ds2} - 2L_d i_{ds3} +\right) - 2\omega_r L_q \lambda_{pmd2}\right)$$

$$- \omega_r\left(L i_{ds1} + \left(L_{ls} + L_d\right)i_{ds2} + L_d i_{ds3} + \lambda_{pmd2}\right)$$

$$V_{ds3} =$$

$$\delta_{ds3} + \frac{L_d}{L_{ls} + 3L_d}\left(\left(V_{ds1} + V_{ds2} - r_s i_{ds1} - r_s i_{ds2} - \omega_r\left(\left(L_{ls} + L_q\right)i_{qs1} + L_q i_{qs2} + L_q i_{qs3} + L_q i_{qs1} + \left(L_{ls} + L_q\right)i_{qs2} + L_q i_{qs3}\right)\right)\right) \tag{6.111}$$

$$+ \frac{L_d}{{L_{ls}}^2 + 3L_d L_{ls}}\left(-2L_d V_{ds3} + 2L_d r_s i_{ds3} + 2\omega_r L_d L_q i_{qs1} + 2\omega_r L_d L_q i_{qs2} + 2\omega_r L_d\left(L_{ls} + L_d\right)i_{qs3}\right)$$

$$+ \omega_r\left(L_q i_{qs1} + L_q i_{qs2} + \left(L_{ls} + L_d\right)i_{qs3}\right)$$

$$V_{qs3} =$$

$$\delta_{qs3} + \frac{L_q}{L_{ls} + 3L_q}\left(\left(V_{qs1} + V_{qs2} - r_s i_{qs1} - r_s i_{qs2} + \omega_r\left(\left(L_{ls} + 2L_d\right)i_{ds1} + 2L_d i_{ds3} + \left(L_{ls} + 2L_d\right)i_{ds2} + \lambda_{pmd2} + \lambda_{pmd1}\right)\right)\right)$$

(6.112)

$$+ \frac{L_q}{{L_{ls}}^2 + 3L_q L_{ls}}\left(-2L_q V_{qs3} + 2L_q r_s i_{qs3} + \omega_r L_q\left(-2L_d i_{ds1} - 2L_d i_{ds2} - 2\left(L_{ls} + L_d\right)i_{ds3}\right) - 2\omega_r L_q \lambda_{pmd3}\right)$$

$$- \omega_r\left(L_d i_{ds1} + L_d i_{ds2} + \left(L_{ls} + L_d\right)i_{ds3} + \lambda_{pmd3}\right)$$

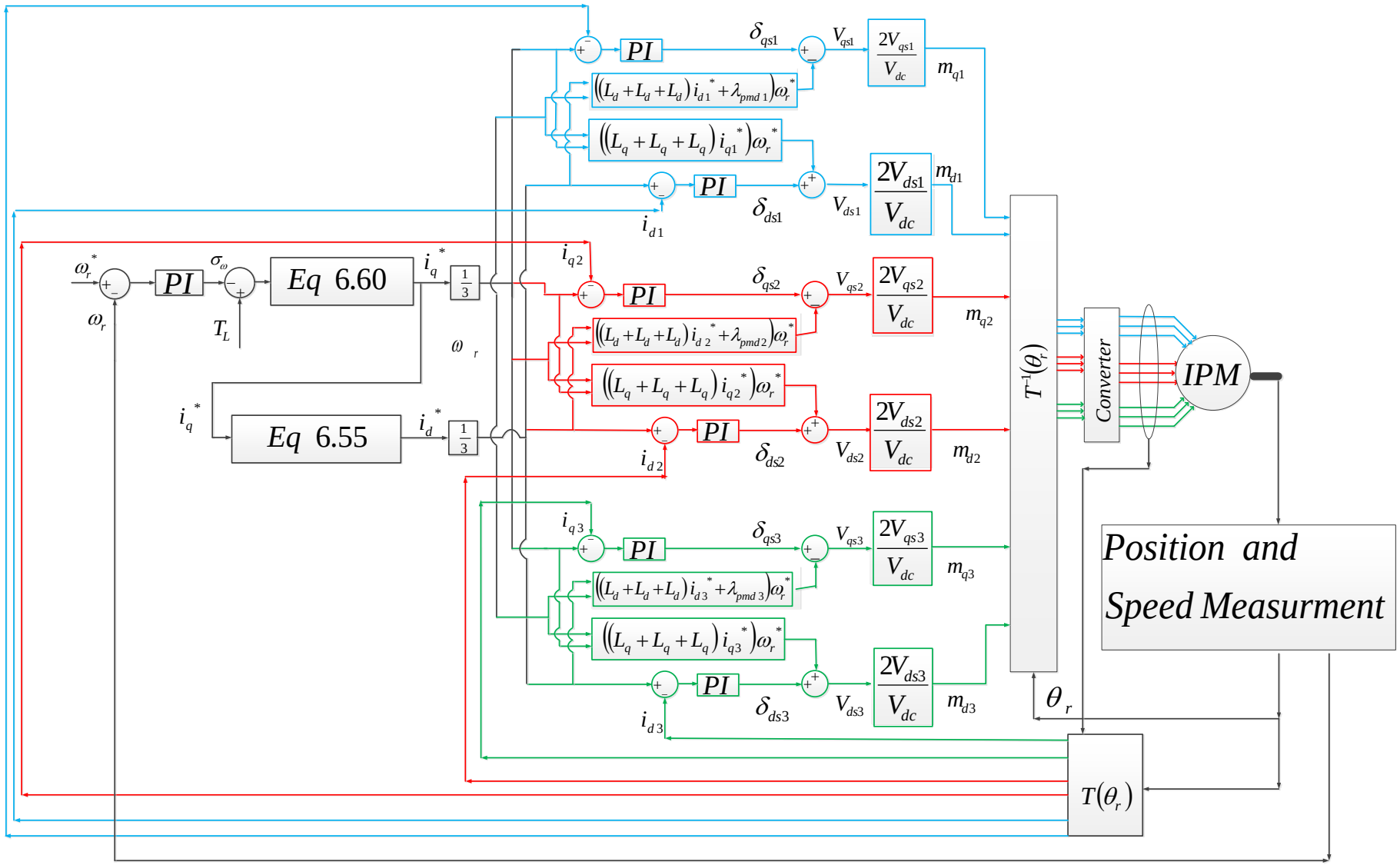

Figure 6.6: The symmetrical triple-star controller.

The designed controller is simulated with the full order coupled model of the machine generated in chapter 3. The following figures show some of the simulation results for a trapezoidal speed reference. Figure 6.7 shows the reference and the rotor speed. It can be seen that the controller can track the reference speed precisely. The reference and the feedback current for the d and q axis of each machine are shown in the Figures 6.8 and 6.9 respectively. The current regulators finally generate the voltages in the q and d axis of the rotor reference frame to regulate their currents. Figure 6.10 shows the q and d axis voltages of each machine in the rotor reference frame. The flux linkages and the electromagnetic torques of the machines are shown in the Figures 6.11 and 6.12 respectively.

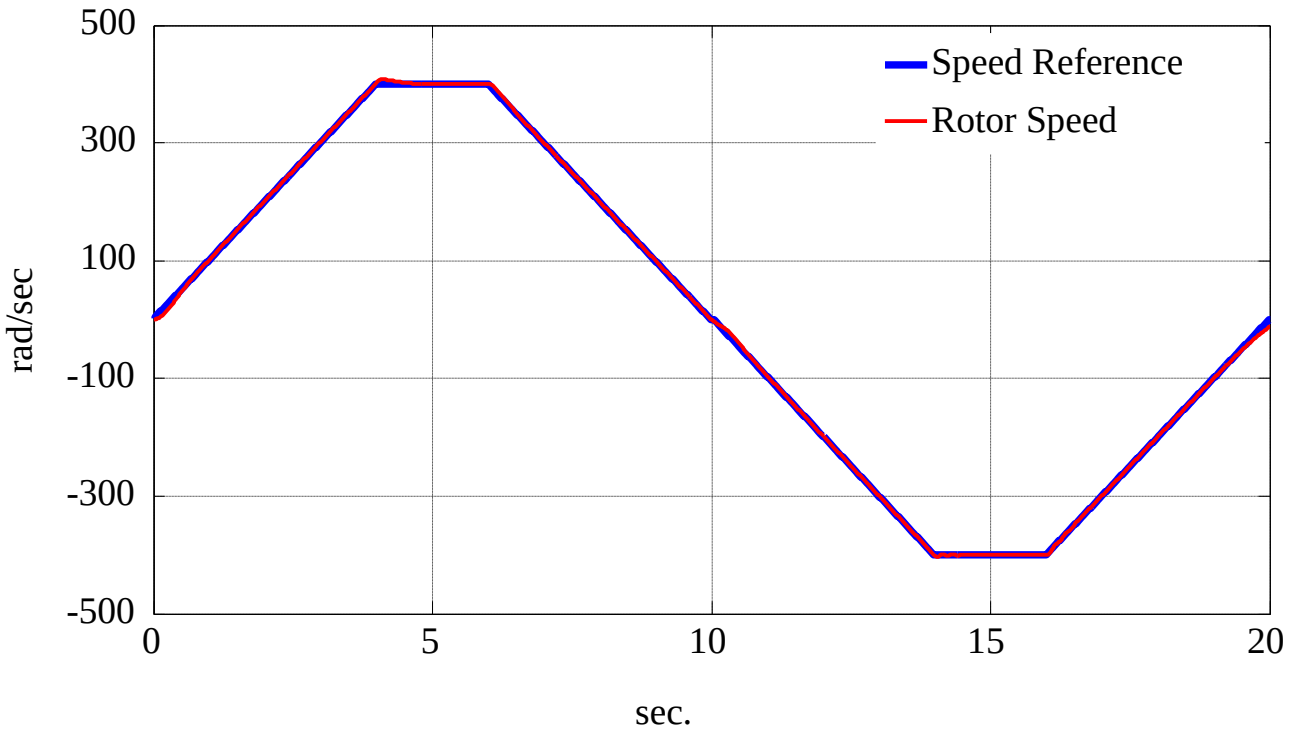

Figure 6.7: The speed reference and the rotor speed.

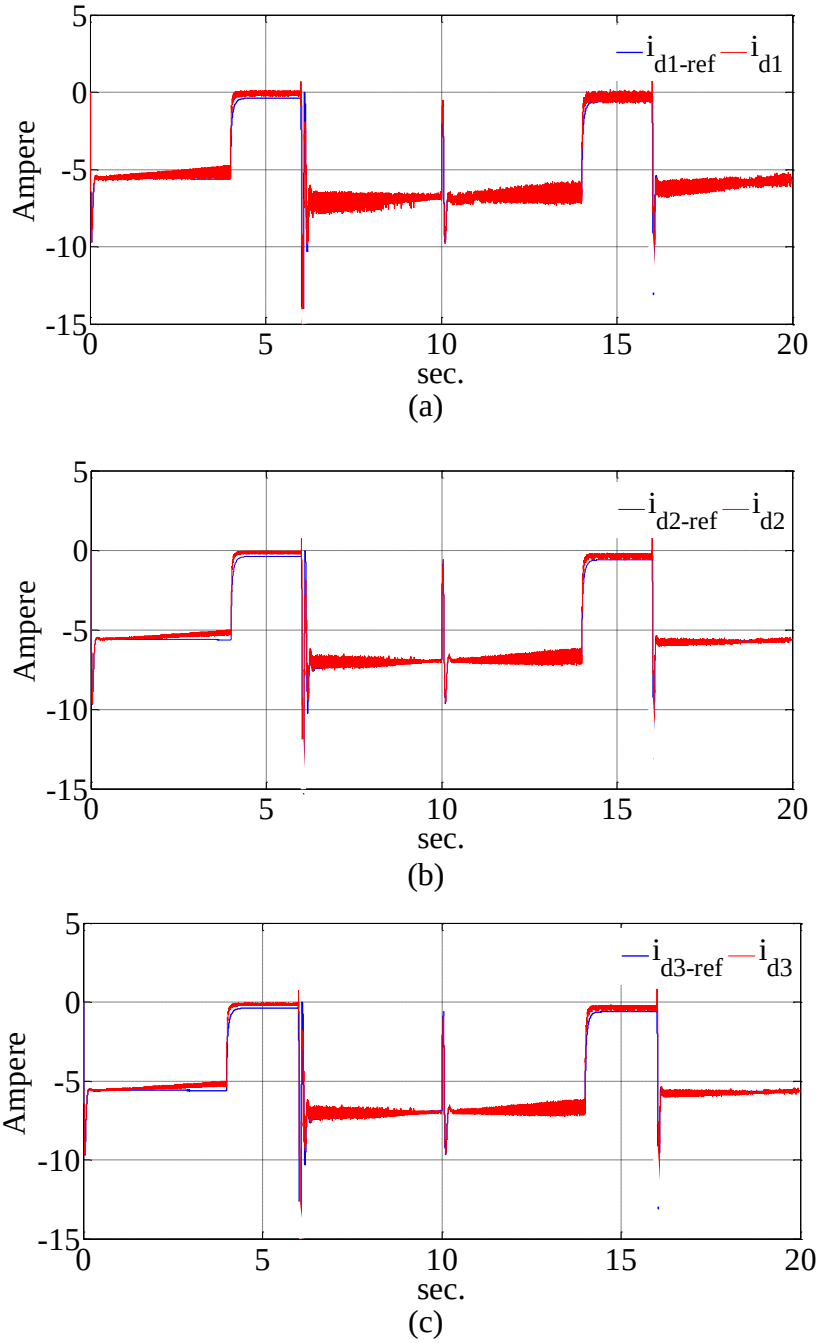

Figure 6.8: The d axis reference and the feedback current for, (a) Machine '1', (b) Machine '2', (C) Machine '3'.

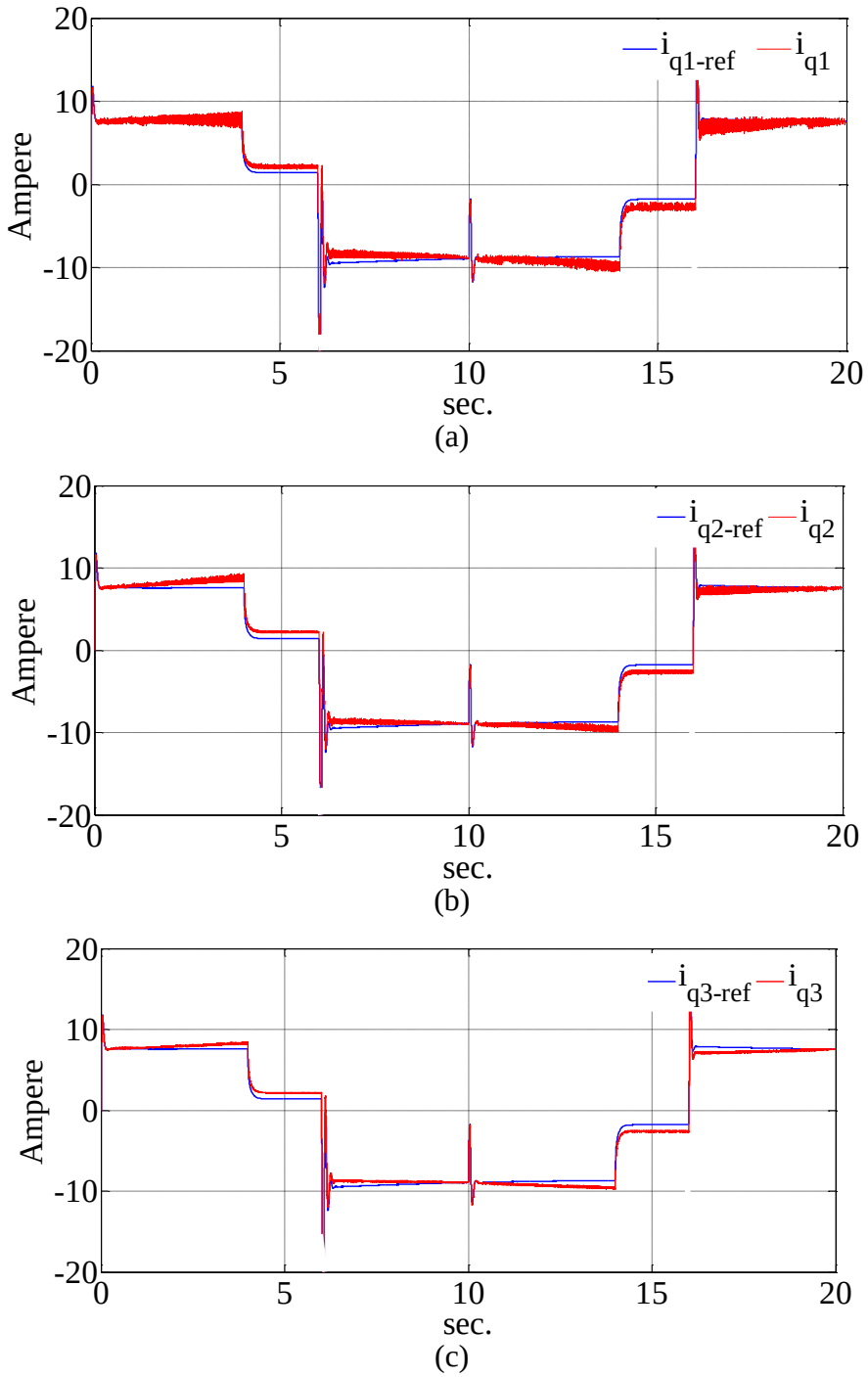

Figure 6.9: The q axis reference and the feedback current for, (a) Machine '1', (b) Machine '2', (c) Machine '3'.

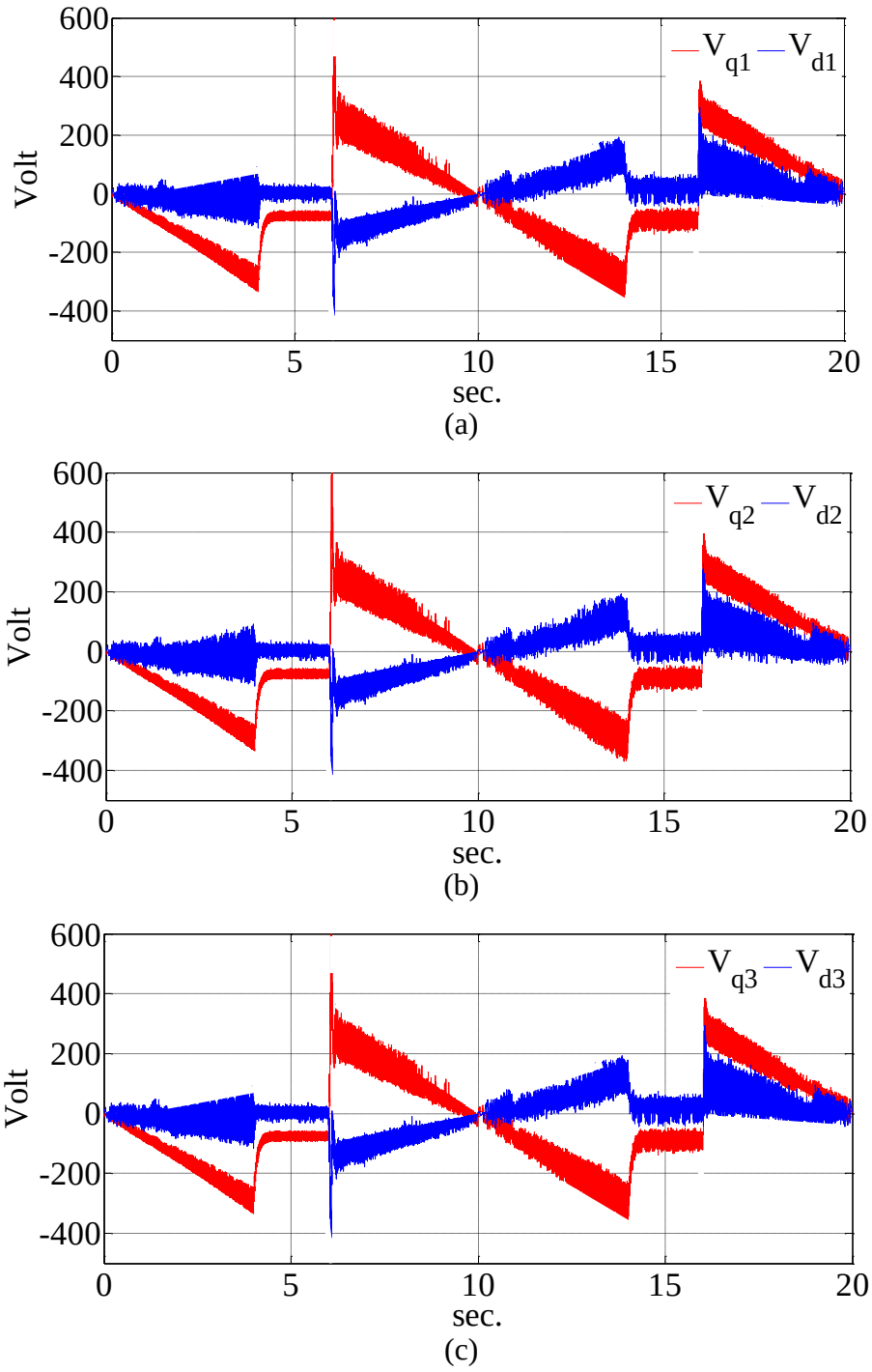

Figure 6.10: The q and d axis voltages for, (a) Machine '1', (b) Machine '2', (C) Machine '3'.

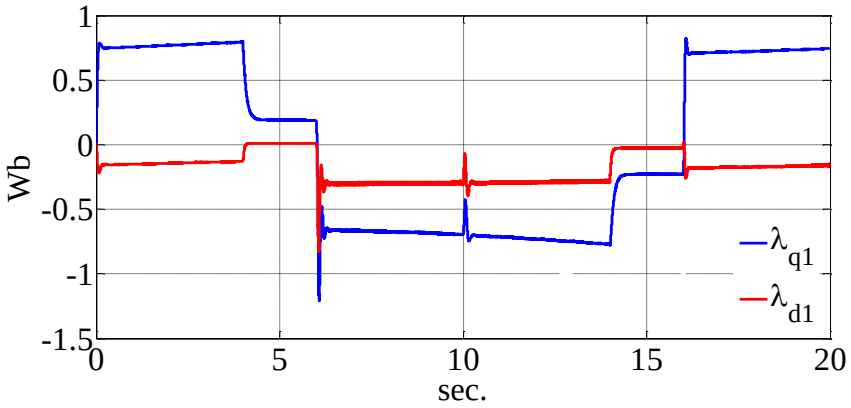

(a)

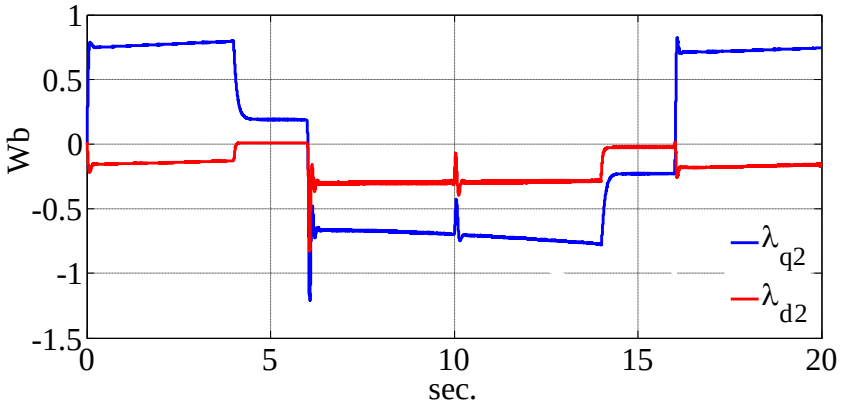

(b)

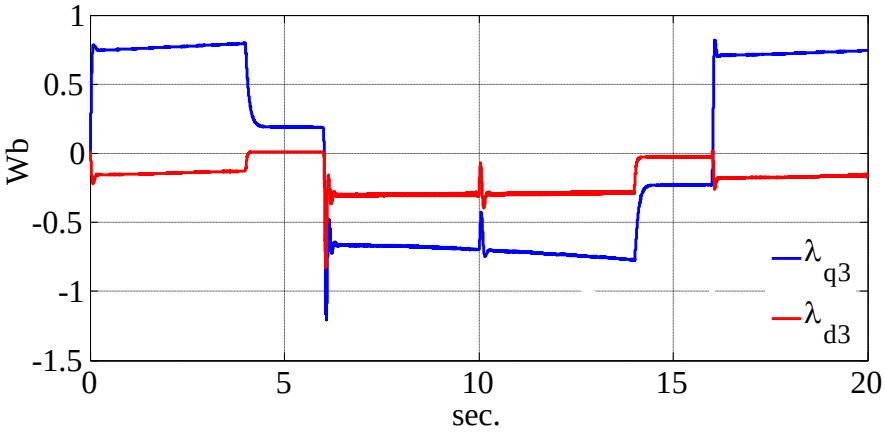

(c)

Figure 6.11: The q and d flux linkages for, (a) Machine ‘1’, (b) Machine ‘2’,(c) Machine ‘3’.

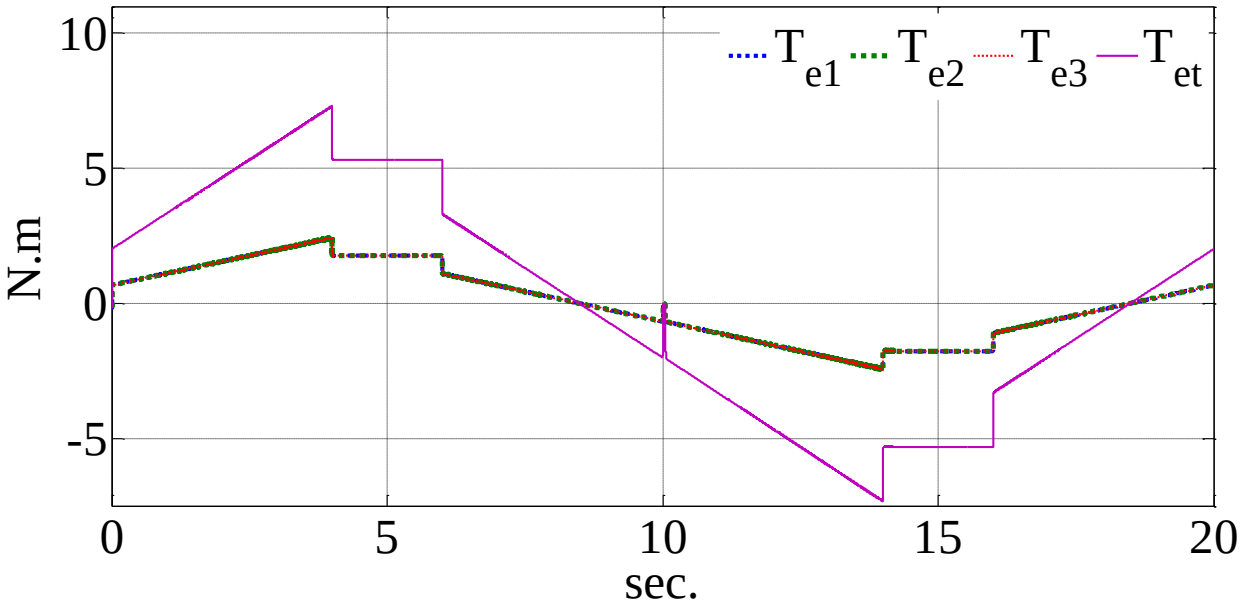

Figure 6.12: The electromagnetic torque of each machine and total.

6.3 Controller Design Using the Decoupled Model

From equations (6.107) to (6.112) it is clear that, because of the coupling between the machines 1, 2 and 3 the controllers have complicated forms that make them difficult to be implemented in DSP. To make the controller simpler, the decoupled model, generated in the chapter 4 (presented in equation 4.133), can be used. The machine model is repeated in equations (6.113) and (6.114).

$$\begin{bmatrix} V_{q1n} \\ V_{d1n} \\ V_{q2n} \\ V_{d2n} \\ V_{q3n} \\ V_{d3n} \end{bmatrix} = r_s \begin{bmatrix} i_{q1n} \\ i_{d1n} \\ i_{q2n} \\ i_{d2n} \\ i_{q3n} \\ i_{d3n} \end{bmatrix} + \omega_{rn} \left(\begin{bmatrix} L_{ls}+3L_{md} & 0 & 0 & 0 & 0 & 0 \\ 0 & L_{ls}+3L_{mq} & 0 & 0 & 0 & 0 \\ 0 & 0 & L_{ls} & 0 & 0 & 0 \\ 0 & 0 & 0 & L_{ls} & 0 & 0 \\ 0 & 0 & 0 & 0 & L_{ls} & 0 \\ 0 & 0 & 0 & 0 & 0 & L_{ls} \end{bmatrix} \begin{bmatrix} i_{q1n} \\ i_{d1n} \\ i_{q2n} \\ i_{d2n} \\ i_{q3n} \\ i_{d3n} \end{bmatrix} + \begin{bmatrix} 0 \\ -\lambda_{pm} \\ 0 \\ 0 \\ 0 \\ 0 \end{bmatrix} \right)$$

$$+ \begin{bmatrix} L_{ls}+3L_{md} & 0 & 0 & 0 & 0 & 0 \\ 0 & L_{ls}+3L_{mq} & 0 & 0 & 0 & 0 \\ 0 & 0 & L_{ls} & 0 & 0 & 0 \\ 0 & 0 & 0 & L_{ls} & 0 & 0 \\ 0 & 0 & 0 & 0 & L_{ls} & 0 \\ 0 & 0 & 0 & 0 & 0 & L_{ls} \end{bmatrix} \begin{bmatrix} pi_{q1n} \\ pi_{d1n} \\ pi_{q2n} \\ pi_{d2n} \\ pi_{q3n} \\ pi_{d3n} \end{bmatrix}, \omega_{rn} = \omega_r \begin{bmatrix} 0 & -1 & 0 & 0 & 0 & 0 \\ 1 & 0 & 0 & 0 & 0 & 0 \\ 0 & 0 & 0 & 1 & 0 & 0 \\ 0 & 0 & -1 & 0 & 0 & 0 \\ 0 & 0 & 0 & 0 & 0 & 1 \\ 0 & 0 & 0 & 0 & -1 & 0 \end{bmatrix} \quad (6.113)$$

$$T_e = \frac{3P}{4}\left(3\left(L_{md} - L_{mq}\right) i_{d1n} i_{q1n} + \lambda_{pm} i_{q1n}\right) \quad (6.114)$$

The current regulator is designed based on the minimum copper loss strategy. The total copper loss is defined in the equation (6.115).

$$P_{loss} = \frac{3}{2}\sum_{i=1}^{3} r_s \left(i^2_{qin} + i^2_{din}\right) = \frac{3}{2} r_s \left(i^2_{q1n} + i^2_{d1n} + i^2_{q2n} + i^2_{d2n} + i^2_{q3n} + i^2_{d3n}\right) \quad (6.115)$$

The goal of the optimization is to minimize the copper loss while the machine still supplies the load torque. Therefore, the constraint of the optimization is:

$$T_L = \frac{3P}{4}\left(3\left(L_{md} - L_{mq}\right) i_{d1n} i_{q1n} + \lambda_{pm} i_{q1n}\right) \quad (6.116)$$

By defining ‘λ’ as the Lagrange multiplier, the Lagrange function can be defined as equation (6.117) [133].

$$L=\frac{3}{2}r_s\left(i^2_{q1n}+i^2_{d1n}+i^2_{q2n}+i^2_{d2n}+i^2_{q3n}+i^2_{d3n}\right)+$$

$$\lambda\left(T_L-\frac{3P}{4}\left(3\left(L_{md}-L_{mq}\right)i_{d1n}i_{q1n}+\lambda_{pm}i_{q1n}\right)\right) \tag{6.117}$$

To obtain the different parameters at the optimum point, equations (6.118) to (6.124) (Lagrange derivations) need to be solved simultaneously:

$$\frac{dL}{di_{q1n}}=2r_s\left(i_{q1n}\right)-\lambda\frac{3P}{4}\left(3\left(L_{md}-L_{mq}\right)i_{d1n}+\lambda_{pm}\right)=0\Rightarrow$$

$$\lambda=\frac{8r_si_{q1n}}{3P\left(3\left(L_{md}-L_{mq}\right)i_{d1n}+\lambda_{pm}\right)} \tag{6.118}$$

$$\frac{dL}{di_{d1n}}=2r_s\left(i_{d1n}\right)-\lambda\frac{3P}{4}\left(3\left(L_{md}-L_{mq}\right)i_{q1n}\right)=0\Rightarrow\lambda=\frac{8r_si_{d1n}}{9P\left(L_{md}-L_{mq}\right)i_{q1n}} \tag{6.119}$$

$$\frac{dL}{di_\lambda}=T_L-\frac{3P}{4}\left(3\left(L_{md}-L_{mq}\right)i_{d1n}i_{q1n}+\lambda_{pm}i_{q1n}\right)=0 \tag{6.120}$$

$$\frac{dL}{di_{q2n}}=2r_s\left(i_{q2n}\right)=0\Rightarrow i_{q2n}=0 \tag{6.121}$$

$$\frac{dL}{di_{d2n}}=2r_s\left(i_{d2n}\right)=0\Rightarrow i_{d2n}=0 \tag{6.122}$$

$$\frac{dL}{di_{q3n}} = 2r_s\left(i_{q3n}\right) = 0 \Rightarrow i_{q3n} = 0 \tag{6.123}$$

$$\frac{dL}{di_{d3n}} = 2r_s\left(i_{d3n}\right) = 0 \Rightarrow i_{d3n} = 0 \tag{6.124}$$

The equations (6.118) and (6.119) lead to equation (6.125).

$$\frac{8r_s i_{d1n}}{9P\left(L_{md} - L_{mq}\right)i_{q1n}} = \frac{8r_s i_{q1n}}{3P\left(3\left(L_{md} - L_{mq}\right)i_{d1n} + \lambda_{pm}\right)} \Rightarrow$$

$$\frac{i_{d1n}}{3\left(L_{md} - L_{mq}\right)i_{q1n}} = \frac{i_{q1n}}{\left(3\left(L_{md} - L_{mq}\right)i_{d1n} + \lambda_{pm}\right)} \tag{6.125}$$

From equation (6.125) the relationship between d and q currents can be derived as:

$$i^2_{d1n} + \frac{\lambda_{pm} i_{d1n}}{3\left(L_{md} - L_{mq}\right)} - i^2_{q1n} = 0 \Rightarrow$$

$$i_{d1n} = -\frac{\lambda_{pm}}{6\left(L_{md} - L_{mq}\right)} \pm \sqrt{\left(\frac{\lambda_{pm}}{6\left(L_{md} - L_{mq}\right)}\right)^2 + i^2_{q1n}} \tag{6.126}$$

The equation (6.126) represents an ellipse. Using MATLAB/EZ plots, the ellipse is plotted as Figure 6.13. The bigger and the smaller diameters and also the central point of the ellipse are represented in equations (6.127) to (6.129) respectively. It should be noted that, since the

transformation to decoupled reference frame does not change the machine characteristics, the ellipses of Figures 6.13 and 6.2 are identical.

$$D_b = 2\sqrt{2}\,\frac{\lambda_{pm}}{3\left(L_{md} - L_{mq}\right)} \tag{6.127}$$

$$D_s = \frac{\lambda_{pm}}{3\left(L_{md} - L_{mq}\right)} \tag{6.128}$$

$$(i_{qn}, i_{dn}) = \left(0,\ \frac{\lambda_{pm}}{6\left(L_{md} - L_{mq}\right)}\right) \tag{6.129}$$

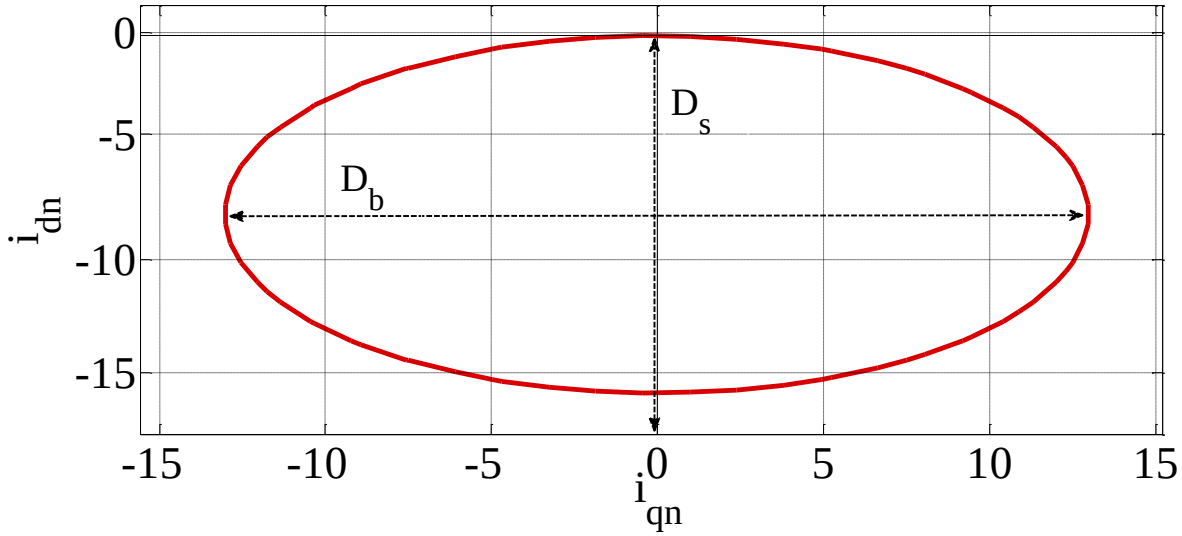

Figure 6.13: The plot of the ellipse representing the q_{1n} and d_{1n} axis current relation.

6.3.1 Speed Controller Design

The speed controller loop also can be designed based on the Figure 6.3 and mechanical dynamic equation of the rotor presented equation (6.130).

$$T_e = J\left(\frac{2}{P}\right)p\omega_r + T_L \Rightarrow T_e - T_L = J\left(\frac{2}{P}\right)p\omega_r = K_{\omega r}(S)\left(\omega_r^{*} - \omega_r\right) = \delta_{\omega_r} \tag{6.130}$$

From the equation (6.130) the transfer function between the reference and rotor speed can be expressed as equation (6.131).

$$p\omega_r = \sigma_\omega = \left(K_{p\omega} + \frac{K_{i\omega}}{p}\right)\left(\omega_r^{*} - \omega_r\right) \tag{6.131}$$

Where: '$K_{p\omega}$' and '$K_{i\omega}$' are the proportional and the integral gains of the PI controller respectively. From the equation (6.131), the transfer function of between rotor speed and the reference speed is:

$$\frac{\omega_r}{\omega_r^{*}} = \frac{pK_{p\omega} + K_{i\omega}}{p^2 + K_{p\omega}p + K_{i\omega}} \tag{6.132}$$

The coefficients of this controller are calculated in the section 6.2.1. Also using the equations (6.126) and (6.130) the reference for the q axis current can be obtained as equation (6.133).

$$\begin{cases} \dfrac{3P}{4}\left(3\left(L_{md} - L_{mq}\right)i_{d1n}i_{q1n} + \lambda_{pm}i_{q1n}\right) = \delta_{\omega_r} - T_L \\ i_{d1n} = -\dfrac{\lambda_{pm}}{6\left(L_{md} - L_{mq}\right)} \pm \sqrt{\left(\dfrac{\lambda_{pm}}{6\left(L_{md} - L_{mq}\right)}\right)^2 + i^2{}_{q1n}} \end{cases} \Rightarrow \tag{6.133}$$

$$9\left(L_{md} - L_{mq}\right)^2 i^4{}_{q1n} + \frac{4\lambda_{pm}i_{q1n}\left(\delta_{\omega_r} - T_L\right)}{3P} = \left(\frac{4\left(\delta_{\omega_r} - T_L\right)}{3P}\right)^2$$

In this equation the q axis current can be calculated from the load torque and ' δ_{ω_r} '. The reference current of q axis can be substituted in the equation (6.126) to obtain the d axis reference. After obtaining the reference signals for q and d axis currents the current regulators can be designed.

6.3.2 Current Regulator Design

The current regulators can be designed based on the dynamic equations of the q_{1n} and d_{1n} voltages that are presented in equation (6.113). Based on the equation (6.113) the 'i_{d1n}' controller can be designed according to the equation (6.134).

$$V_{d1n} = r_s i_{d1n} + \omega_r \left(\left(L_{ls} + 3L_{md} \right) i_{q1n} \right) + p\left(L_{ls} + 3L_{mq} \right) i_{d1n} \tag{6.134}$$

$$r_s i_{d1n} + p\left(L_{ls} + 3L_{mq} \right) i_{d1n} = V_{d1n} - \omega_r \left(\left(L_{ls} + 3L_{md} \right) i_{q1n} \right) = \delta_{d1n} = K_{d1}\left(i_{d1n}^{\ *} - i_{d1n} \right) \tag{6.135}$$

The current regulator loop is shown in Figure 6.14. By selecting the PI controller for the d axis, according to this figure, the transfer function of the reference and the actual current can be derived as equation (6.136).

$$r_s i_{d1n} + p\left(L_{ls} + 3L_{mq} \right) i_{d1n} + \left(K_{Pd1} + \frac{K_{Id1}}{p} \right) i_{d1n} = \left(K_{Pd1} + \frac{K_{Id1}}{p} \right) \left(i_{d1n}^{\ *} \right) \Rightarrow$$

$$\frac{i_{d1n}}{i_{d1n}^{\ *}} = \frac{\dfrac{\left(pK_{Pd1} + K_{Id1} \right)}{\left(L_{ls} + 3L_{mq} \right)}}{p^2 + p\dfrac{\left(r_s + K_{Pd1} \right)}{\left(L_{ls} + 3L_{mq} \right)} + \dfrac{K_{Id1}}{\left(L_{ls} + 3L_{mq} \right)}} \tag{6.136}$$

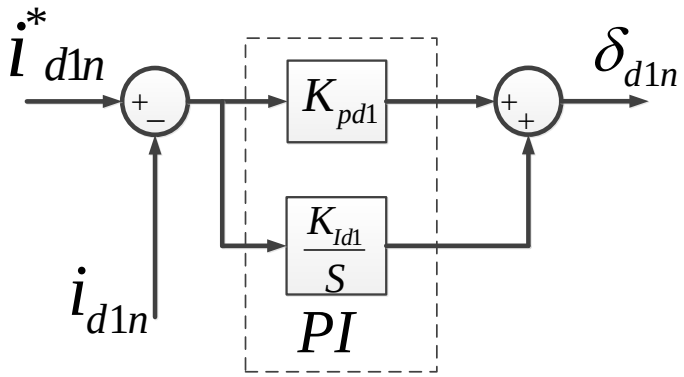

Figure 6.14: The d_{1n} axis current regulator.

Where: 'K_{Pd1}' and 'K_{Id1}' are the proportional and the integral coefficients of the PI controller. By setting the denominator of the transfer function of equation (6.136) equal to the second order Butterworth polynomial, the controller coefficients can be calculated as:

$$p^2 + p\frac{(r_s + K_{Pd1})}{(L_{ls} + 3L_{mq})} + \frac{K_{Id1}}{(L_{ls} + 3L_{mq})} = p^2 + \sqrt{2}p\omega_o + \omega_o{}^2 \tag{6.137}$$

Again to have a faster internal controller, the frequency of the current regulator should be at least 10 times bigger than the speed controller loop. Therefore, selecting $\omega_o = 200 \quad (rad/\sec)$ results in:

$$\sqrt{2}\omega_o = \frac{(r_s + K_{Pd1})}{(L_{ls} + 3L_{mq})} \tag{6.138}$$

$$K_{Pd1} = \sqrt{2}\omega_o(L_{ls} + 3L_{mq}) - r_s = 2.1548 - 0.01 = 2.1448 \tag{6.139}$$

$$\frac{K_{Id1}}{(L_{ls} + 3L_{mq})} = \omega_o{}^2 \rightarrow K_{iq} = 312 \tag{6.140}$$

And finally, the voltage of the d axis voltage can be generated as equation (6.141). In this equation the term 'δ_{d1n}' is the output of the PI operating on the d axis current controller.

$$V_{d1n} = \delta_{d1n} + \omega_r \left(L_{ls} + 3L_{md}\right) i_{q1n} \tag{6.141}$$

Similarly, the controller for the 'i_{q1n}' current can be designed using the dynamic voltage equation of the same axis. The current regulator loop is shown in the Figure 6.15.

$$V_{q1n} = r_s i_{q1n} + \omega_r \left(-\left(L_{ls} + 3L_{mq}\right) i_{d1n} + \lambda_{pm}\right) + p\left(L_{ls} + 3L_{md}\right) i_{q1n} \tag{6.142}$$

$$r_s i_{q1n} + p\left(L_{ls} + 3L_{md}\right) i_{q1n} = V_{q1n} + \omega_r \left(-\left(L_{ls} + 3L_{mq}\right) i_{d1n} + \lambda_{pm}\right) = \delta_{q1n} = K_{q1}\left(i_{q1n}{}^{*} - i_{q1n}\right) \tag{6.143}$$

Then by selecting the PI controller for the q axis, the transfer function of the reference and the actual current can be derived as equation (6.144).

$$r_s i_{q1n} + p\left(L_{ls} + 3L_{md}\right) i_{q1n} + \left(K_{Pq1} + \frac{K_{Iq1}}{p}\right) i_{q1n} = \left(K_{Pq1} + \frac{K_{Iq1}}{p}\right) i_{q1n}{}^{*} \Rightarrow$$

$$\frac{i_{q1n}}{i_{q1n}{}^{*}} = \frac{\dfrac{\left(pK_{Pq1} + K_{Iq1}\right)}{\left(L_{ls} + 3L_{md}\right)}}{p^2 + p\dfrac{\left(r_s + K_{Pq1}\right)}{\left(L_{ls} + 3L_{md}\right)} + \dfrac{K_{Iq1}}{\left(L_{ls} + 3L_{md}\right)}} \tag{6.144}$$

Where: 'K_{Pq1}' and 'K_{Iq1}' are the proportional and the integral coefficients of the PI controller. By setting the denominator of the transfer function of equation (6.144) equal to the second order Butterworth polynomial, the controller coefficients can be calculated as equation (6.145).

$$p^2 + p\frac{\left(r_{se} + K_{Pq1}\right)}{\left(L_{ls} + 3L_{md}\right)} + \frac{K_{Iq1}}{\left(L_{ls} + 3L_{md}\right)} = p^2 + \sqrt{2}p\omega_o + {\omega_o}^2 \tag{6.145}$$

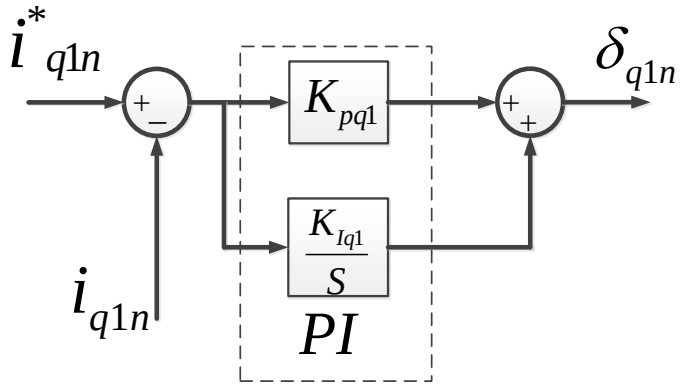

Figure 6.15: The q_{1n} axis current regulator.

Again to have a faster internal controller, the frequency of the current regulator should be at least 10 times bigger than the speed controller loop. Therefore, selecting $\omega_o = 200 \quad (rad/\sec)$ results in:

$$\sqrt{2}\omega_o = \frac{\left(r_{se} + K_{Pq1}\right)}{\left(L_{ls} + 3L_{md}\right)} \tag{6.146}$$

$$K_{Pq1} = \sqrt{2}\omega_o\left(L_{ls} + 3L_{md}\right) - r_s = \sqrt{2} \times 200 \times 0.048 - 0.01 = 0.915 \tag{6.147}$$

$$\frac{K_{Iq1}}{\left(L_{ls} + 3L_{md}\right)} = {\omega_o}^2 \rightarrow K_{Iq1} = 100 \tag{6.148}$$

And finally the voltage of the q axis voltage can be generated as equation (6.149). In this equation the term 'δ_{q1n}' is the output of the PI operating on the q axis current controller.

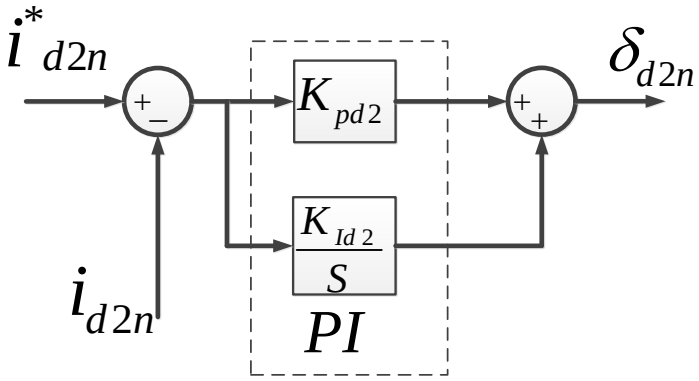

Figure 6.16: The d_{2n} axis current regulator.

$$V_{q1n} = \delta_{q1n} - \omega_r\left(-\left(L_{ls} + 3L_{mq}\right)i_{d1n} + \lambda_{pm}\right) \tag{6.149}$$

Since the rest of the axis are not torque producers, they have simpler controllers. Based on the equation (6.113) the equation governing the 'd_{2n}' axis voltage is:

$$V_{d2n} = r_s i_{d2n} - \omega_r L_{ls} i_{q2n} + pL_{ls} i_{d2n} \tag{6.150}$$

From the equation (6.150) and based on the Figure 6.16 the controller can be designed as:

$$r_s i_{d2n} + pL_{ls} i_{d2n} = V_{d2n} + \omega_r L_{ls} i_{q2n} = \delta_{d2n} = \left(K_{pd2} + \frac{K_{Id2}}{p}\right)\left(i_{d2n}{}^* - i_{d2n}\right) \tag{6.151}$$

Where: 'K_{Pd2}' and 'K_{Id2}' are the proportional and the integral coefficients of the PI controller. The transfer function of the controller can be derived as:

$$\frac{i_{d2n}}{i_{d2n}{}^*} = \frac{\dfrac{\left(pK_{Pd2} + K_{Id2}\right)}{L_{ls}}}{p^2 + p\dfrac{\left(r_s + K_{Pd2}\right)}{L_{ls}} + \dfrac{K_{Id2}}{L_{ls}}} \tag{6.152}$$

By setting the denominator of the transfer function of equation (6.152) equal to the second order Butterworth polynomial, the controller coefficients can be calculated.

$$p^2 + p\frac{(r_s + K_{Pd2})}{L_{ls}} + \frac{K_{Id2}}{L_{ls}} = p^2 + \sqrt{2}p\omega_o + {\omega_o}^2 \tag{6.153}$$

Again to have a faster internal controller, the frequency of the current regulator should be at least 10 times bigger than the speed controller loop. Therefore, selecting $\omega_o = 200 \quad (rad/\sec)$ results in:

$$\sqrt{2}\omega_o = \frac{(r_s + K_{Pd2})}{L_{ls}} \tag{6.154}$$

$$K_{Pq2} = \sqrt{2}\omega_o(L_{ls}) - r_s = \sqrt{2} \times 200 \times 0.01 - 0.01 = 5.62 \tag{6.155}$$

$$\frac{K_{Id2}}{(L_{ls})} = {\omega_o}^2 \rightarrow K_{Id2} = 400 \tag{6.156}$$

And finally, the voltage of the d axis voltage can be generated as equation (6.157). In this equation the term ' δ_{d2n} ' is the output of the PI operating on the d axis current controller.

$$V_{d2n} = \delta_{d2n} - \omega_r L_{ls} i_{q2n} \tag{6.157}$$

Using the same procedure, the controller for q axis current also can be designed. Based on the equation (6.113), the equation governing the ' q_{2n} ' axis voltage is:

$$V_{q2n} = r_s i_{q2n} + \omega_r L_{ls} i_{d2n} + pL_{ls} i_{q2n} \tag{6.158}$$

From the equation (6.158), the controller can be designed as Figure 6.17 and equation (6.159).

$$r_s i_{q2n} + pL_{ls} i_{q2n} = V_{q2n} - \omega_r L_{ls} i_{d2n} = \delta_{q2n} = \left(K_{pq2} + \frac{K_{Iq2}}{p} \right) \left(i_{q2n}{}^{*} - i_{q2n} \right) \quad (6.159)$$

Where: 'K_{Pq2}' and 'K_{Iq2}' are the proportional and the integral coefficients of the PI controller. Using equation (6.159), the transfer function of the controller can be derived as:

$$\frac{i_{q2n}}{i_{q2n}{}^{*}} = \frac{\frac{\left(pK_{Pq2} + K_{Iq2} \right)}{L_{ls}}}{p^2 + p\frac{\left(r_s + K_{Pq2} \right)}{L_{ls}} + \frac{K_{Iq2}}{L_{ls}}} \quad (6.160)$$

By setting the denominator of the transfer function of equation (6.160) equal to the second order Butterworth polynomial, the controller coefficients can be calculated.

$$p^2 + p\frac{\left(r_s + K_{Pq2} \right)}{L_{ls}} + \frac{K_{Iq2}}{L_{ls}} = p^2 + \sqrt{2} p\omega_o + \omega_o{}^2 \quad (6.161)$$

Again to have a faster internal controller the frequency of the current regulator should be at least 10 times bigger than the speed controller loop. Therefore, selecting $\omega_o = 200 \ \ (rad/\sec)$ results in:

$$\sqrt{2}\omega_o = \frac{\left(r_s + K_{Pq2} \right)}{L_{ls}} \quad (6.162)$$

$$K_{Pq2} = \sqrt{2}\omega_o \left(L_{ls} \right) - r_s = \sqrt{2} \times 200 \times 0.01 - 0.01 = 5.62 \quad (6.163)$$

$$\frac{K_{Iq2}}{\left(L_{ls} \right)} = \omega_o{}^2 \rightarrow K_{Iq2} = 400 \quad (6.164)$$

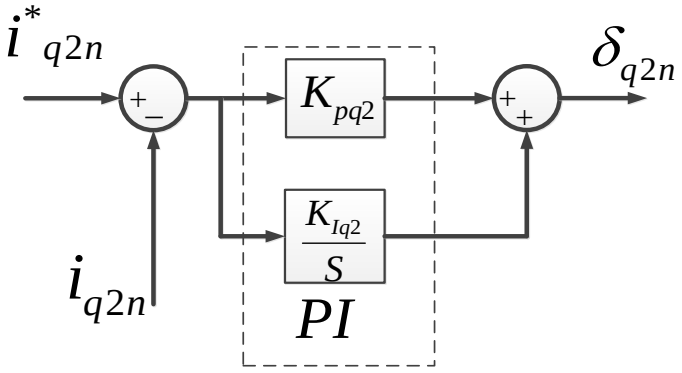

Figure 6.17: The q_{2n} axis current regulator.

And finally, the voltage of the q axis voltage can be generated as equation (6.165). In this equation the term 'δ_{q2n}' is the output of the PI operating on the q_{2n} axis current controller.

$$V_{q2n} = \delta_{q2n} + \omega_r L_{ls} i_{d2n} \tag{6.165}$$

The *'q_{3n}'* and *'d_{3n}'* axis also have the same controller as *'q_{2n}' and 'd_{2n}'* therefore, they are not repeated here. To apply the generated voltages to the machine, they should be transformed to the natural variables using equation (6.166). It should be netted that according to section 4.5, for the machine equations to be diagonalizable, they need to have distinct eigen values. Therefore, the zero sequences are removed from the machine model to let the inductance matrix be diagonalizable.

$$\begin{bmatrix} V_{a1} \\ V_{b1} \\ V_{c1} \\ V_{a2} \\ V_{b2} \\ V_{c2} \\ V_{a3} \\ V_{b3} \\ V_{c3} \end{bmatrix} = T'^{-1}_{n}(\theta_r) \begin{bmatrix} V_{d1n} \\ V_{q1n} \\ V_{d2n} \\ V_{q2n} \\ V_{d3n} \\ V_{q3n} \end{bmatrix} \tag{6.166}$$

Where:

$$T'^{-1}{}_n(\theta_r) =$$

$$\begin{bmatrix} -S(\theta_r+\beta) & -C(\theta_r+\beta) & -C(\theta_r+\beta) & -S(\theta_r+\beta) & C(\theta_r+\beta) & S(\theta_r+\beta) \\ -S(\theta_r+\beta-\gamma) & -C(\theta_r+\beta-\gamma) & -C(\theta_r+\beta-\gamma) & -S(\theta_r+\beta-\gamma) & C(\theta_r+\beta-\gamma) & S(\theta_r+\beta-\gamma) \\ -S(\theta_r+\beta+\gamma) & -C(\theta_r+\beta+\gamma) & -C(\theta_r+\beta+\gamma) & -S(\theta_r+\beta+\gamma) & C(\theta_r+\beta+\gamma) & S(\theta_r+\beta+\gamma) \\ -S(\theta_r) & -C(\theta_r) & 0 & 0 & -2C(\theta_r) & -2S(\theta_r) \\ -S(\theta_r-\gamma) & -C(\theta_r-\gamma) & 0 & 0 & -2C(\theta_r-\gamma) & -2S(\theta_r-\gamma) \\ -S(\theta_r+\gamma) & -C(\theta_r+\gamma) & 0 & 0 & -2C(\theta_r+\gamma) & -2S(\theta_r+\gamma) \\ -S(\theta_r-\beta) & -C(\theta_r-\beta) & -C(\theta_r-\beta) & -S(\theta_r-\beta) & C(\theta_r-\beta) & S(\theta_r-\beta) \\ -S(\theta_r-\beta-\gamma) & -C(\theta_r-\beta-\gamma) & -C(\theta_r-\beta-\gamma) & -S(\theta_r-\beta-\gamma) & C(\theta_r-\beta-\gamma) & S(\theta_r-\beta-\gamma) \\ -S(\theta_r-\beta+\gamma) & -C(\theta_r-\beta+\gamma) & -C(\theta_r-\beta+\gamma) & -S(\theta_r-\beta+\gamma) & C(\theta_r-\beta+\gamma) & S(\theta_r-\beta+\gamma) \end{bmatrix} \quad (6.167)$$

$$\beta = \frac{2\pi}{9}\ ,\ \gamma = \frac{2\pi}{3}\ ,\ S = \sin,\ C = \cos$$

And the feedback currents can be generated using the transformation matrix as:

$$i_{qdn} = T'_n(\theta_r) i_s = T'_n(\theta_r) \times \begin{bmatrix} i_{a1} \\ i_{b1} \\ i_{c1} \\ i_{a2} \\ i_{b2} \\ i_{c2} \\ i_{a3} \\ i_{b3} \\ i_{c3} \end{bmatrix} \quad (6.168)$$

Where:

$$T'_n(\theta_r) =$$

$$\frac{2}{3}\begin{pmatrix}
\frac{C(\theta_r+\beta)}{6} & \frac{C(\theta_r+\beta-\gamma)}{6} & \frac{C(\theta_r+\beta+\gamma)}{6} & \frac{-C(\theta_r)}{3} & \frac{-C(\theta_r-\gamma)}{3} & \frac{-C(\theta_r+\gamma)}{3} & \frac{C(\theta_r-\beta)}{6} & \frac{C(\theta_r-\beta-\gamma)}{6} & \frac{C(\theta_r-\beta+\gamma)}{6} \\
\frac{C(\theta_r+\beta)}{3} & \frac{C(\theta_r+\beta-\gamma)}{3} & \frac{C(\theta_r+\beta+\gamma)}{3} & \frac{C(\theta_r)}{3} & \frac{C(\theta_r-\gamma)}{3} & \frac{C(\theta_r+\gamma)}{3} & \frac{C(\theta_r-\beta)}{3} & \frac{C(\theta_r-\beta-\gamma)}{3} & \frac{C(\theta_r-\beta+\gamma)}{3} \\
\frac{-C(\theta_r+\beta)}{2} & \frac{-C(\theta_r+\beta-\gamma)}{2} & \frac{-C(\theta_r+\beta+\gamma)}{2} & 0 & 0 & 0 & \frac{C(\theta_r-\beta)}{2} & \frac{C(\theta_r-\beta-\gamma)}{2} & \frac{C(\theta_r-\beta+\gamma)}{2} \\
\frac{-S(\theta_r+\beta)}{2} & \frac{-S(\theta_r+\beta-\gamma)}{2} & \frac{-S(\theta_r+\beta+\gamma)}{2} & 0 & 0 & 0 & \frac{S(\theta_r-\beta)}{2} & \frac{S(\theta_r-\beta-\gamma)}{2} & \frac{S(\theta_r-\beta+\gamma)}{2} \\
\frac{S(\theta_r+\beta)}{3} & \frac{S(\theta_r+\beta-\gamma)}{3} & \frac{S(\theta_r+\beta+\gamma)}{3} & \frac{S(\theta_r)}{3} & \frac{S(\theta_r-\gamma)}{3} & \frac{S(\theta_r+\gamma)}{3} & \frac{S(\theta_r-\beta)}{3} & \frac{S(\theta_r-\beta-\gamma)}{3} & \frac{S(\theta_r-\beta+\gamma)}{3} \\
\frac{S(\theta_r+\beta)}{6} & \frac{S(\theta_r+\beta-\gamma)}{6} & \frac{S(\theta_r+\beta+\gamma)}{6} & \frac{-S(\theta_r)}{3} & \frac{-S(\theta_r-\gamma)}{3} & \frac{-S(\theta_r+\gamma)}{3} & \frac{S(\theta_r-\beta)}{6} & \frac{S(\theta_r-\beta-\gamma)}{6} & \frac{S(\theta_r-\beta+\gamma)}{6}
\end{pmatrix} \tag{6.169}$$

$$\beta = \frac{2\pi}{9}\ ,\ \gamma = \frac{2\pi}{3}, S = \sin,\ C = \cos$$

6.4 The Position Estimation of the Triple-Star IPM

To obtain a precise control on the machine, the position of the rotor flux linkage is needed. Like the nine phase case, the rotor position can be estimated using a high frequency injection and a signal processing procedure. In the nine-phase machine the high frequency voltages were injected into the third sequence of the stationary reference frame reference frame. According to the equation (3.47), the higher order sequences (3^{th}, 5^{th} and 7^{th}) do not exist in the triple star machine model. Therefore, to be able to perform the high frequency voltage injection, the machine can be modelled by two separate models. The first model is the full order coupled model of the triple star machine (presented in 3.3) for low frequency analysis such as torque producing voltages, and the second one is the nine-phase coupled model (presented in 3.2) for high frequency analysis. First it will be shown that, the triple star machine has the same response as the single-star nine-phase one, with the high frequency voltage injection. From the nine phase results the currents due to the high frequency injection have the following forms in stationary reference frame:

$$i_{qd3} = \frac{18Ae^{j(\omega_s t - 6\theta_r - \frac{\pi}{2})}}{(\omega_i)a_2 N_3^{\,2}} + \frac{18Ae^{j(\omega_s t + 6\theta_r - \frac{\pi}{2})}}{(\omega_i)a_2 N_3^{\,2}} \Rightarrow$$

$$i_{q3} = \frac{18A}{(\omega_i)a_2 N_3^{\,2}} Cos\left(\omega_s t - 6\theta_r - \frac{\pi}{2}\right) + \frac{18A}{(\omega_i)a_2 N_3^{\,2}} Cos\left(\omega_s t + 6\theta_r - \frac{\pi}{2}\right) \tag{6.170}$$

$$i_{d3} = \frac{18A}{(\omega_i)a_2 N_3^{\,2}} Sin\left(\omega_s t - 6\theta_r - \frac{\pi}{2}\right) + \frac{18A}{(\omega_i)a_2 N_3^{\,2}} Sin\left(\omega_s t + 6\theta_r - \frac{\pi}{2}\right)$$

By transforming them to the natural variables using the transformation matrix of equation (3.13), the nine phase currents are:

$$\begin{bmatrix} i_a \\ i_b \\ i_c \\ i_d \\ i_e \\ i_f \\ i_g \\ i_h \\ i_m \end{bmatrix} = \frac{18A}{(\omega_i)a_2 N_3^{\,2}} \begin{bmatrix} \cos(\omega_s t - 6\theta_r - \frac{\pi}{2}) + \cos(\omega_s t + 6\theta_r - \frac{\pi}{2}) \\ \cos(-3\alpha + \omega_s t - 6\theta_r - \frac{\pi}{2}) + \cos(-3\alpha + \omega_s t + 6\theta_r - \frac{\pi}{2}) \\ \cos(-6\alpha + \omega_s t - 6\theta_r - \frac{\pi}{2}) + \cos(-6\alpha + \omega_s t + 6\theta_r - \frac{\pi}{2}) \\ \cos(-9\alpha + \omega_s t - 6\theta_r - \frac{\pi}{2}) + \cos(-9\alpha + \omega_s t + 6\theta_r - \frac{\pi}{2}) \\ \cos(-12\alpha + \omega_s t - 6\theta_r - \frac{\pi}{2}) + \cos(-12\alpha + \omega_s t + 6\theta_r - \frac{\pi}{2}) \\ \cos(-15\alpha + \omega_s t - 6\theta_r - \frac{\pi}{2}) + \cos(-15\alpha + \omega_s t + 6\theta_r - \frac{\pi}{2}) \\ \cos(-18\alpha + \omega_s t - 6\theta_r - \frac{\pi}{2}) + \cos(-18\alpha + \omega_s t + 6\theta_r - \frac{\pi}{2}) \\ \cos(-21\alpha + \omega_s t - 6\theta_r - \frac{\pi}{2}) + \cos(-21\alpha + \omega_s t + 6\theta_r - \frac{\pi}{2}) \\ \cos(-24\alpha + \omega_s t - 6\theta_r - \frac{\pi}{2}) + \cos(-24\alpha + \omega_s t + 6\theta_r - \frac{\pi}{2}) \end{bmatrix}, \alpha = \frac{2\pi}{9} \tag{6.171}$$

By substituting the α in equation 6.171 the currents of triple star machine can be represented as:

$$\begin{bmatrix} i_a \\ i_b \\ i_c \\ i_d \\ i_e \\ i_f \\ i_g \\ i_h \\ i_m \end{bmatrix} = \frac{18A}{(\omega_i)a_2 N_3^{\,2}} \begin{bmatrix} \cos(\omega_s t - 6\theta_r - \frac{\pi}{2}) + \cos(\omega_s t + 6\theta_r - \frac{\pi}{2}) \\ \cos(-2\frac{\pi}{3} + \omega_s t - 6\theta_r - \frac{\pi}{2}) + \cos(-2\frac{\pi}{3} + \omega_s t + 6\theta_r - \frac{\pi}{2}) \\ \cos(-4\frac{\pi}{3} + \omega_s t - 6\theta_r - \frac{\pi}{2}) + \cos(-4\frac{\pi}{3} + \omega_s t + 6\theta_r - \frac{\pi}{2}) \\ \cos(\omega_s t - 6\theta_r - \frac{\pi}{2}) + \cos(\omega_s t + 6\theta_r - \frac{\pi}{2}) \\ \cos(-2\frac{\pi}{3} + \omega_s t - 6\theta_r - \frac{\pi}{2}) + \cos(-2\frac{\pi}{3} + \omega_s t + 6\theta_r - \frac{\pi}{2}) \\ \cos(-4\frac{\pi}{3} + \omega_s t - 6\theta_r - \frac{\pi}{2}) + \cos(-4\frac{\pi}{3} + \omega_s t + 6\theta_r - \frac{\pi}{2}) \\ \cos(\omega_s t - 6\theta_r - \frac{\pi}{2}) + \cos(\omega_s t + 6\theta_r - \frac{\pi}{2}) \\ \cos(-2\frac{\pi}{3} + \omega_s t - 6\theta_r - \frac{\pi}{2}) + \cos(-2\frac{\pi}{3} + \omega_s t + 6\theta_r - \frac{\pi}{2}) \\ \cos(-4\frac{\pi}{3} + \omega_s t - 6\theta_r - \frac{\pi}{2}) + \cos(-4\frac{\pi}{3} + \omega_s t + 6\theta_r - \frac{\pi}{2}) \end{bmatrix} = \begin{bmatrix} i_{a1} \\ i_{a2} \\ i_{a3} \\ i_{b1} \\ i_{b2} \\ i_{b3} \\ i_{c1} \\ i_{c2} \\ i_{c3} \end{bmatrix} \tag{6.172}$$

Simplifying equation (6.172), the following relations hold for the high frequency currents in each machine sets:

$$
\begin{aligned}
&i_{a1} = i_{b1} = i_{c1} \Rightarrow i_{a1} + i_{b1} + i_{c1} \neq 0 \\
&i_{a2} = i_{b2} = i_{c2} \Rightarrow i_{a2} + i_{b2} + i_{c2} \neq 0 \\
&i_{a3} = i_{b3} = i_{c3} \Rightarrow i_{a3} + i_{b3} + i_{c3} \neq 0
\end{aligned}
\tag{6.173}
$$

The equations (6.173) indicates that the high frequency currents have the same magnitude and same phase angle, therefore, they cannot form a three phase balanced system. They cannot pass through the stator windings of the machines; therefore, the currents remain zero. The next sequence which can be used for the high frequency injection is the fifth sequence circuit. To obtain the currents due to the high frequency injection in to this circuit, the inductances of the fifth sequence circuit in the stationary reference frame are derived. The general form of the inductances is repeated in the equation (6.174).

$$
\begin{aligned}
L_{jk} = 2\mu_o rl[&a_o(N_1{}^2\cos(k-j)\alpha + \frac{N_7{}^2}{49}\cos 7(k-j)\alpha + \frac{N_5{}^2}{25}\cos 5(k-j)\alpha \\
&+ \frac{N_3{}^2}{9}\cos 3(k-j)\alpha) + \frac{1}{2}(a_1 N_1{}^2)\cos(-2(k-j)\alpha + 2\theta_r) \\
&+ \frac{1}{2}(\frac{a_2 N_3{}^2}{9})\cos(-6k(k-j)\alpha + 6\theta_r) + \frac{1}{2}(\frac{a_3 N_5{}^2}{25})\cos(-10k(k-j)\alpha \\
&+ 10\theta_r) + (\frac{a_4 N_7{}^2}{98})\cos(-14k(k-j)\alpha + 14\theta_r)], \qquad \alpha = \frac{2\pi}{9}
\end{aligned}
\tag{6.174}
$$

Where ‘k’ and ‘j’ represent the machine phase number according to Table 6.2. In equation (6.174), ‘ a_i ’ are the coefficients of the Fourier series of the air gap function, ‘ N_i ’ represents the coefficients of the Fourier series of the winding functions.

The inductances can be arranged in the following matrix.

$$L_{ss}=\begin{bmatrix} L_{ls}+L_{aa} & L_{ab} & L_{ac} & L_{ad} & L_{ae} & L_{af} & L_{ag} & L_{ah} & L_{ai} \\ L_{ba} & L_{ls}+L_{bb} & L_{bc} & L_{bd} & L_{be} & L_{bf} & L_{bg} & L_{bh} & L_{bi} \\ L_{ca} & L_{cb} & L_{ls}+L_{cc} & L_{cd} & L_{ce} & L_{cf} & L_{cg} & L_{ch} & L_{ci} \\ L_{da} & L_{db} & L_{dc} & L_{ls}+L_{dd} & L_{de} & L_{df} & L_{dg} & L_{dh} & L_{di} \\ L_{ea} & L_{eb} & L_{ec} & L_{ed} & L_{ls}+L_{ee} & L_{ef} & L_{eg} & L_{eh} & L_{ei} \\ L_{fa} & L_{fb} & L_{fc} & L_{fd} & L_{fe} & L_{ls}+L_{ff} & L_{fg} & L_{fh} & L_{fi} \\ L_{ga} & L_{gb} & L_{gc} & L_{gd} & L_{ge} & L_{gf} & L_{ls}+L_{gg} & L_{gh} & L_{gi} \\ L_{ha} & L_{hb} & L_{hc} & L_{hd} & L_{he} & L_{hf} & L_{hg} & L_{ls}+L_{hh} & L_{hi} \\ L_{ia} & L_{ib} & L_{ic} & L_{id} & L_{ie} & L_{if} & L_{ig} & L_{ih} & L_{ls}+L_{ii} \end{bmatrix} \quad (6.175)$$

Then using the transformation matrix of the equation (6.176) the various components of the inductances can be obtained using the equation (6.177).

$T(0)=$

$$\frac{2}{9}\begin{bmatrix} c(\theta) & c(\theta-\alpha) & c(\theta-2\alpha) & c(\theta-3\alpha) & c(\theta-4\alpha) & c(\theta-5\alpha) & c(\theta-6\alpha) & c(\theta-7\alpha) & c(\theta-8\alpha) \\ s(\theta) & s(\theta-\alpha) & s(\theta-2\alpha) & s(\theta-3\alpha) & s(\theta-4\alpha) & s(\theta-5\alpha) & s(\theta-6\alpha) & s(\theta-7\alpha) & s(\theta-8\alpha) \\ c(3\theta) & c3(\theta-\alpha) & c3(\theta-2\alpha) & c3(\theta-3\alpha) & c3(\theta-4\alpha) & c3(\theta-5\alpha) & c3(\theta-6\alpha) & c3(\theta-7\alpha) & c3(\theta-8\alpha) \\ s(3\theta) & s3(\theta-\alpha) & s3(\theta-2\alpha) & s3(\theta-3\alpha) & s3(\theta-4\alpha) & s3(\theta-5\alpha) & s3(\theta-6\alpha) & s3(\theta-7\alpha) & s3(\theta-8\alpha) \\ c(5\theta) & c5(\theta-\alpha) & c5(\theta-2\alpha) & c5(\theta-3\alpha) & c5(\theta-4\alpha) & c5(\theta-5\alpha) & c5(\theta-6\alpha) & c5(\theta-7\alpha) & c5(\theta-8\alpha) \\ s(5\theta) & s5(\theta-\alpha) & s5(\theta-2\alpha) & s5(\theta-3\alpha) & s5(\theta-4\alpha) & s5(\theta-5\alpha) & s5(\theta-6\alpha) & s5(\theta-7\alpha) & s5(\theta-8\alpha) \\ c(7\theta) & c7(\theta-\alpha) & c7(\theta-2\alpha) & c7(\theta-3\alpha) & c7(\theta-4\alpha) & c7(\theta-5\alpha) & c7(\theta-6\alpha) & c7(\theta-7\alpha) & c7(\theta-8\alpha) \\ s(7\theta) & s7(\theta-\alpha) & s7(\theta-2\alpha) & s7(\theta-3\alpha) & s7(\theta-4\alpha) & s7(\theta-5\alpha) & s7(\theta-6\alpha) & s7(\theta-7\alpha) & s7(\theta-8\alpha) \\ 1/2 & 1/2 & 1/2 & 1/2 & 1/2 & 1/2 & 1/2 & 1/2 & 1/2 \end{bmatrix} \quad (6.176)$$

$\alpha=\frac{2\pi}{9}, \quad \theta=0$

$$L_{qdo}=T(0)L_{ss}T^{-1}(0) \quad (6.177)$$

The qdo inductances of the machine are obtained by transforming the natural variable equations to the stationary reference frame. The fifth qd sequence equivalent circuit to be used for the rotor angle estimation has the q and d inductances expressed in equations (6.178) and (6.179),

which are clearly shown to be dependent to the rotor angle. Hence, the fifth sequence equivalent circuit, which is non-torque producing, will be used to modulate the high frequency voltage to estimate the position of the rotor.

$$L_{q5} = \frac{a_3}{2}\left(\frac{N_5^{\,2}}{25}\right)Cos(10\theta_r) \tag{6.178}$$

$$L_{d5} = \frac{a_3}{2}\left(\frac{N_5^{\,2}}{25}\right)Cos(10\theta_r + \frac{\pi}{2}) \tag{6.179}$$

A high frequency voltage set according the equation (6.180) is injected into the fifth sequence of the nine-phase IPM in the stationary reference frame to generate the rotor angle dependent component in the stator .

$$\begin{bmatrix} V_{q5} \\ V_{d5} \end{bmatrix} = A\begin{bmatrix} Cos(\omega_s t) \\ Cos(\omega_s t + \frac{\pi}{2}) \end{bmatrix} \tag{6.180}$$

The voltages of the equation (6.180) can be transformed back to natural reference frame and result in:

$$\begin{bmatrix} V_a \\ V_b \\ V_c \\ V_d \\ V_e \\ V_f \\ V_g \\ V_h \\ V_m \end{bmatrix} = V\begin{bmatrix} \cos(\omega_s t) \\ \cos(-3\alpha + \omega_s t) \\ \cos(-6\alpha + \omega_s t) \\ \cos(-9\alpha + \omega_s t) \\ \cos(-12\alpha + \omega_s t) \\ \cos(-15\alpha + \omega_s t) \\ \cos(-18\alpha + \omega_s t) \\ \cos(-21\alpha + \omega_s t) \\ \cos(-24\alpha + \omega_s t) \end{bmatrix} \quad , \alpha = \frac{2\pi}{9} \tag{6.181}$$

Table 6.2 K and j corresponding to the machine phases.

Name of The Phase	K	j
A	0	0
B	1	1
C	2	2
D	3	3
E	4	4
F	5	5
G	6	6
H	7	7
I	8	8

Using the qd inductances in equations (6.178) and (6.179), the voltage equation for fifth sequence of the machine in stationary reference frame can be expressed as:

$$\begin{bmatrix} V_{q5} \\ V_{d5} \end{bmatrix} = A \begin{bmatrix} Cos(\omega_s t) \\ Cos(\omega_s t - \frac{\pi}{2}) \end{bmatrix} = r_s \begin{bmatrix} i_{q5} \\ i_{d5} \end{bmatrix} + p \begin{bmatrix} \lambda_{q5} \\ \lambda_{d5} \end{bmatrix} \tag{6.182}$$

The $q_5 d_5$ flux linkage equations are:

$$\begin{bmatrix} \lambda_{q5} \\ \lambda_{d5} \end{bmatrix} = \begin{bmatrix} L_{q5} & 0 \\ 0 & L_{d5} \end{bmatrix} \begin{bmatrix} i_{q5} \\ i_{d5} \end{bmatrix} \tag{6.183}$$

From the equations (6.182) and (6.183), the equation (6.184) can be derived.

$$A \begin{bmatrix} Cos(\omega_s t) \\ Cos(\omega_s t - \frac{\pi}{2}) \end{bmatrix} = r_s \begin{bmatrix} i_{q5} \\ i_{d5} \end{bmatrix} + p \begin{bmatrix} \frac{a_3}{2}\left(\frac{N_5^{\,2}}{25}\right) Cos(10\theta_r) & 0 \\ 0 & \frac{a_3}{2}\left(\frac{N_5^{\,2}}{25}\right) Sin(10\theta_r) \end{bmatrix} \begin{bmatrix} i_{q5} \\ i_{d5} \end{bmatrix} \tag{6.184}$$

After simplifying:

$$A\cos(\omega_s t) = r_s i_{q5} - \frac{10\omega_r a_3 N_9^{\,2}}{50} \sin(10\theta_r) i_{q3} + \frac{a_3}{2}\left(\frac{N_5^{\,2}}{25}\right) Cos(10\theta_r)\, p i_{q5} \tag{6.185}$$

$$A\sin(\omega_s t) = r_s i_{d5} + \frac{10\omega_r a_5 N_5^{\,2}}{50}\cos(10\theta_r) i_{d5} + \frac{a_3}{2}\left(\frac{N_5^{\,2}}{25}\right) Sin(10\theta_r)\, p i_{d5} \tag{6.186}$$

The general form of high frequency current (i_{qd5}) can be considered as:

$$i_{qd5} = Ie^{j(\theta_i)} \tag{6.187}$$

Substituting the current of the equation (6.187) into the voltage equation results in:

$$Ae^{j(\omega_s t)} = r_s Ie^{j(\theta_i)} + pL_{qd5} Ie^{j(\theta_i)} \tag{6.188}$$

Separating the real and the imaginary parts of the equation (6.188) results in:

$$A\sin(\omega_s t) = r_s i_{q5} - \frac{10\omega_r a_3 N_9^{\,2}}{50}\sin(10\theta_r) I\sin(\theta_i) + \frac{a_3}{2}\left(\frac{N_5^{\,2}}{25}\right) Cos(10\theta_r)\, pI\cos(\theta_i) \tag{6.189}$$

$$A\cos(\omega_s t) = r_s i_{d5} + \frac{10\omega_r a_5 N_5^{\,2}}{50}\cos(10\theta_r) I\cos(\theta_i) + \frac{a_3}{2}\left(\frac{N_5^{\,2}}{25}\right) Sin(10\theta_r)\, pI\sin(\theta_i) \tag{6.190}$$

The equations (6.189) and (6.190) can be expanded to:

$$A\cos(\omega_s t) = r_s i_{q5} - \frac{5\omega_r a_3 N_5^{\,2} I}{50}\left[\sin(10\theta_r + \theta_i) + \sin(10\theta_r - \theta_i)\right] - \frac{\omega_i a_3 N_5^{\,2} I}{100}\left[\sin(10\theta_r + \theta_i) + \sin(\theta_i - 10\theta_r)\right] \tag{6.191}$$

$$A\sin(\omega_s t) = r_s i_{d5} + \frac{5\omega_r a_3 N_5^{\,2} I}{50}\left[\sin(10\theta_r + \theta_i) + \sin(\theta_i - 10\theta_r)\right] + \frac{\omega_i a_3 N_5^{\,2} I}{100}\left[\cos(10\theta_r + \theta_i) + \cos(10\theta_r - \theta_i)\right] \tag{6.192}$$

Where: $\omega_i = \frac{d\theta_i}{dt}$, $\omega_r = \frac{d\theta_r}{dt}$. Since $\omega_i >> \omega_r$ (ω_i is the frequency of the high signal and ω_r is the rotor frequency) the first and the second terms of the equations (6.191) and (6.192) are negligible compared to the third term. By neglecting the first and the second terms, these equations can be expressed as:

$$A[\cos(\omega_s t) + j\sin(\omega_s t)] =$$

$$\frac{\omega_i a_3 N_5{}^2 I}{100}[-\sin(10\theta_r + \theta_i) - \sin(\theta_i - 10\theta_r) + j\cos(10\theta_r + \theta_i) + j\cos(10\theta_r - \theta_i)] \quad (6.193)$$

$$Ae^{j(\omega_s t)} = 0.01\omega_i a_3 N_5{}^2 I\left[e^{j(10\theta_r + \theta_i + \frac{\pi}{2})} + e^{-j(10\theta_r - \theta_i - \frac{\pi}{2})}\right] \quad (6.194)$$

The two sides of the equation (6.194) should be equal. Therefore, the harmonic balance technique results in [167]:

$$\begin{aligned}(10\theta_r + \theta_i + \frac{\pi}{2}) = \omega_s t \rightarrow \theta_i = \omega_s t - 10\theta_r - \frac{\pi}{2} \\ -(10\theta_r - \theta_i - \frac{\pi}{2}) = \omega_s t \rightarrow \theta_i = \omega_s t + 10\theta_r - \frac{\pi}{2}\end{aligned} \quad (6.195)$$

By substituting the 'θ_i' into the (6.194), the $q_5 d_5$ currents due to the high frequency voltage set can be expressed in complex variable form as:

$$I = I_1 e^{j(\omega_s t - 10\theta_r - \frac{\pi}{2})} + I_2 e^{j(\omega_s t + 10\theta_r - \frac{\pi}{2})},\ \theta_r = \omega_r t \quad (6.196)$$

Where:

$$I_1 = I_2 = \frac{100A}{\omega_i a_3 N_5{}^2} \quad (6.197)$$

Separating the q and d axis currents of the above currents can result in:

$$i_{qd5} = I_1 e^{j(-10\theta_r + \omega_s t - \frac{\pi}{2})} + I_2 e^{j(10\theta_r + \omega_s t - \frac{\pi}{2})} \Rightarrow$$

$$i_{q5} = I_1 Cos\left(-10\theta_r + \omega_s t - \frac{\pi}{2}\right) + I_2 Cos\left(10\theta_r + \omega_s t - \frac{\pi}{2}\right) \tag{6.198}$$

$$i_{d5} = I_1 Sin\left(-10\theta_r + \omega_s t - \frac{\pi}{2}\right) + I_2 Sin\left(10\theta_r + \omega_s t - \frac{\pi}{2}\right)$$

Transforming the resulting currents to the natural variables using the transformation matrix of equation (3.13), the currents of equation (6.199) are obtained.

$$\begin{bmatrix} i_a \\ i_b \\ i_c \\ i_d \\ i_e \\ i_f \\ i_g \\ i_h \\ i_m \end{bmatrix} = T_r^{-1}(0) \begin{bmatrix} 0 \\ 0 \\ 0 \\ 0 \\ i_{q5} \\ i_{d5} \\ 0 \\ 0 \\ 0 \end{bmatrix} = \begin{bmatrix} i_{a1} \\ i_{a2} \\ i_{a3} \\ i_{b1} \\ i_{b2} \\ i_{b3} \\ i_{c1} \\ i_{c2} \\ i_{c3} \end{bmatrix} = \frac{100A}{\omega_i a_3 N_5^{\,2}} \begin{bmatrix} \cos(-10\theta_r + \omega_s t - \frac{\pi}{2}) + \cos(+10\theta_r + \omega_s t - \frac{\pi}{2}) \\ \cos(-10\frac{\pi}{9} - 10\theta_r + \omega_s t - \frac{\pi}{2}) + \cos(-10\frac{\pi}{9} + 10\theta_r + \omega_s t - \frac{\pi}{2}) \\ \cos(-2\frac{\pi}{9} - 10\theta_r + \omega_s t - \frac{\pi}{2}) + \cos(-2\frac{\pi}{9} + 10\theta_r + \omega_s t - \frac{\pi}{2}) \\ \cos(-12\frac{\pi}{9} - 10\theta_r + \omega_s t - \frac{\pi}{2}) + \cos(-12\frac{\pi}{9} + 10\theta_r + \omega_s t - \frac{\pi}{2}) \\ \cos(-4\frac{\pi}{9} - 10\theta_r + \omega_s t - \frac{\pi}{2}) + \cos(-4\frac{\pi}{9} + 10\theta_r + \omega_s t - \frac{\pi}{2}) \\ \cos(-14\frac{\pi}{9} - 10\theta_r + \omega_s t - \frac{\pi}{2}) + \cos(-14\frac{\pi}{9} + 10\theta_r + \omega_s t - \frac{\pi}{2}) \\ \cos(-6\frac{\pi}{9} - 10\theta_r + \omega_s t - \frac{\pi}{2}) + \cos(-6\frac{\pi}{9} + 10\theta_r + \omega_s t - \frac{\pi}{2}) \\ \cos(-16\frac{\pi}{9} - 10\theta_r + \omega_s t - \frac{\pi}{2}) + \cos(-16\frac{\pi}{9} + 10\theta_r + \omega_s t - \frac{\pi}{2}) \\ \cos(-8\frac{\pi}{9} - 10\theta_r + \omega_s t - \frac{\pi}{2}) + \cos(-8\frac{\pi}{9} + 10\theta_r + \omega_s t - \frac{\pi}{2}) \end{bmatrix} \tag{6.199}$$

Therefore, the currents of equation (6.200) are 3 phase balanced currents and their sum for each machine is be zero:

$$i_{a1} + i_{b1} + i_{c1} = i_{a2} + i_{b2} + i_{c2} = i_{a3} + i_{b3} + i_{c3} = 0 \tag{6.200}$$

Since the sum of the currents in each machine phases is zero, from the fifth sequence view point, the triple star machine can be considered as a balance nine-phase single-star machine. The currents have two components, one component is related to the frequency of the injected high frequency voltage and the Second component related to the rotor angle. To extract the rotor position information, the signal of equation (6.196), can be first multiplied by $e^{-j(\omega_s t)}$ which results in:

$$i_{qd5} = \frac{100Ae^{j(10\theta_r - \frac{\pi}{2})}}{(\omega_i)a_3 {N_5}^2} + \frac{100Ae^{j(-10\theta_r - \frac{\pi}{2})}}{(\omega_i)a_5 {N_5}^2} \tag{6.201}$$

Low pass filter can extract the low frequency terms of the equation (6.201) from the remaining of the high frequency components after heterodyning. The outputs of the filters have variable magnitudes which vary with the rotor speed. Using equation (6.202), the signals can be normalized to have fixed magnitudes equal to unity.

$$i_{nq5} = \frac{i_{q5}}{\sqrt{{i_{q5}}^2 + {i_{d5}}^2}}, i_{nd5} = \frac{i_{d5}}{\sqrt{{i_{q5}}^2 + {i_{d5}}^2}} \tag{6.202}$$

After normalizing the signals change to equation (6.203) which can be used for heterodyning and feeding the observer.

$$i_{nqd5} = e^{j(10\theta_r - \frac{\pi}{2})} \tag{6.203}$$

The signals of the equation (6.203) can be used as the input signals of the Luenberger observer designed in the chapter 5. It should be noted that the heterodyning part of the observer presented in the chapter 5 needs to be modified to be compatible with the new input signals. By separating the real and imaginary parts of the signal in equation (6.203) they can be represented as:

$$i_{nq5} = Sin\ (10\theta_r) \tag{6.204}$$

$$i_{nd5} = Cos(10\theta_r) \tag{6.205}$$

To extract the position from the above signals, a function is needed to extract the 'θ_r' and subtract the estimated output value ($\hat{\theta}_r$) from it and obtain the error. The first solution for this case is proposed according to the equation (6.206).

$$\varepsilon = i_{nq5} Cos\left(10\hat{\theta}_r\right) - i_{nd5} Sin\left(10\hat{\theta}_r\right) \tag{6.206}$$

Substituting the currents from equations (6.204) and (6.205) in to the (6.206) results in:

$$\varepsilon = Sin(10\theta_r) Cos\left(10\hat{\theta}_r\right) - Cos(10\theta_r) Sin\left(10\hat{\theta}_r\right) = Sin\left(10\theta_r - 10\hat{\theta}_r\right) \tag{6.207}$$

When the observer is tracking the real position equation (6.208) can be approximated as:

$$\varepsilon = Sin\left(10\theta_r - 10\hat{\theta}_r\right) \cong \left(10\theta_r - 10\hat{\theta}_r\right) \tag{6.208}$$

Using equation (6.208), the observer of the Figure 5.9 can be modified as Figure 6.18. Using the designed controller and the estimator, the controller for the machine can be generated as Figure 6.19. This controller has 6 loops for controlling the currents of the different axis of the decoupled model. The rotor speed and the position are estimated using the observer that operates on the fifth sequence of the machine currents in the stationary reference frame. According to this Figure, the high frequency signals are injected in the fifth channel of the stationary reference frame in controller. After the signals are added, the voltages are transformed to natural variables and the resulted nine-phase voltages are applied to the machine phases.

Equation (6.209) can be rewritten in standard form as equation (6.210).

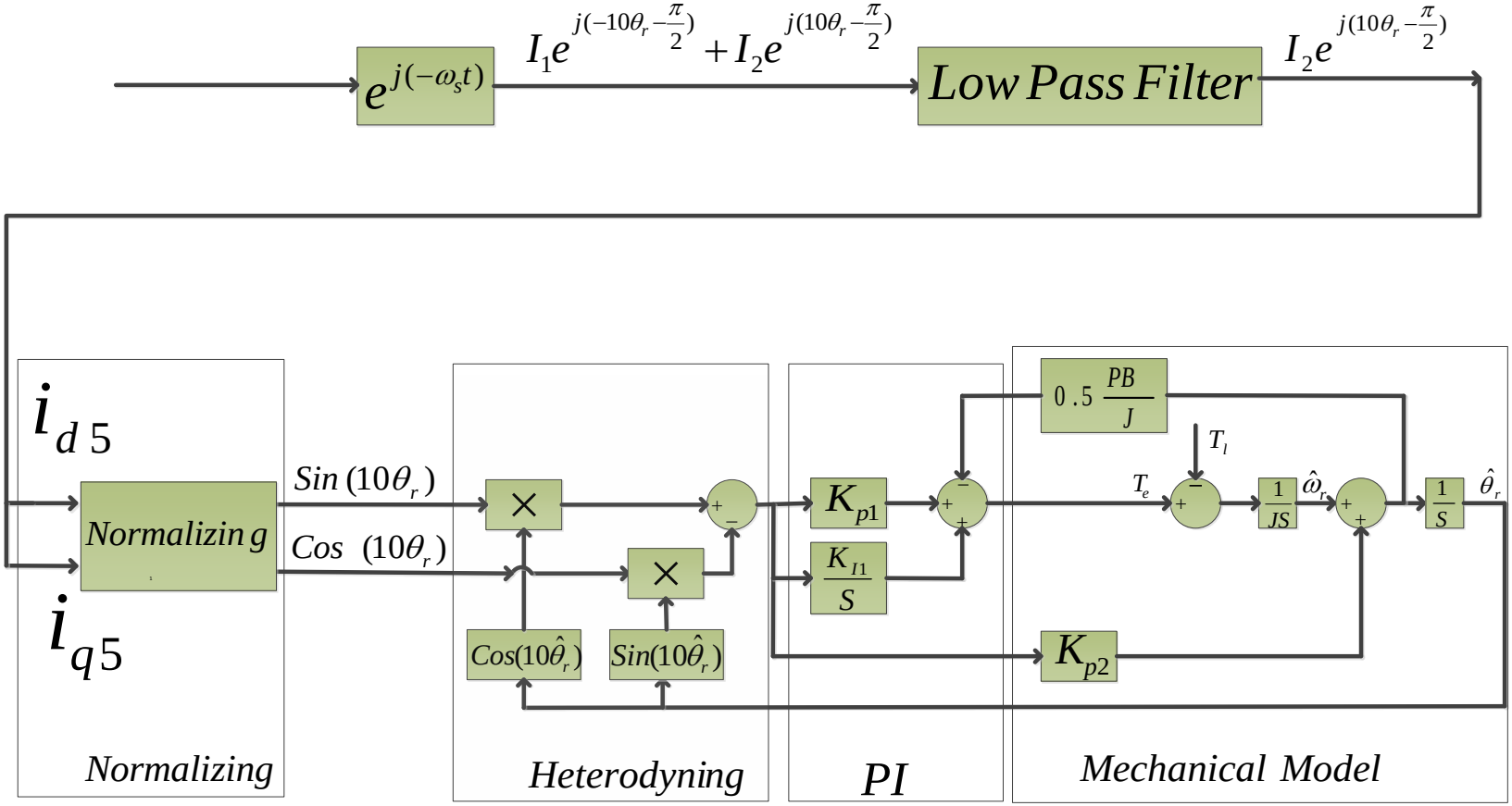

Figure 6.18: The position observer.

$$pX = AX + Bu$$
$$Y = CX + Du \tag{6.210}$$

After generating the voltages of the decoupled axis they are transformed to the natural variables (using the transformation matrix of equation (6.169)) to obtain the three sets of the three phase voltages. From there the voltages are transformed to the stationary reference frame using transformation matrix of equation (3.10). Now the high frequency voltages can be added to the fifth sequence voltage. After adding the high frequency voltages, they are transformed back to the natural variables to obtain the nine-phase voltages to be applied to the machine. The stator currents are also measured using a nine-phase current sensor. The currents can be transformed to the stationary reference frame to extract the fifth sequence current for the position estimator. Also they are transformed to the decoupled reference frame to get the feedback currents for the drive.

6.4.1 Robustness of the Observer

Similar to the single-star case the stability of the observer that is designed in this section can be evaluated by changing of the fifth sequence inductances of the machine due to the saturation caused by the stator currents. In this section the poles of the fifth sequence circuit are plotted for different stator current levels. The dynamic equation for the fifth sequence circuit is presented in the equation (6.182). To investigate the stability of this circuit, the fifth sequence inductances are needed for the all ranges of the stator current. The equation (6.182) can be expanded as equation (6.209).

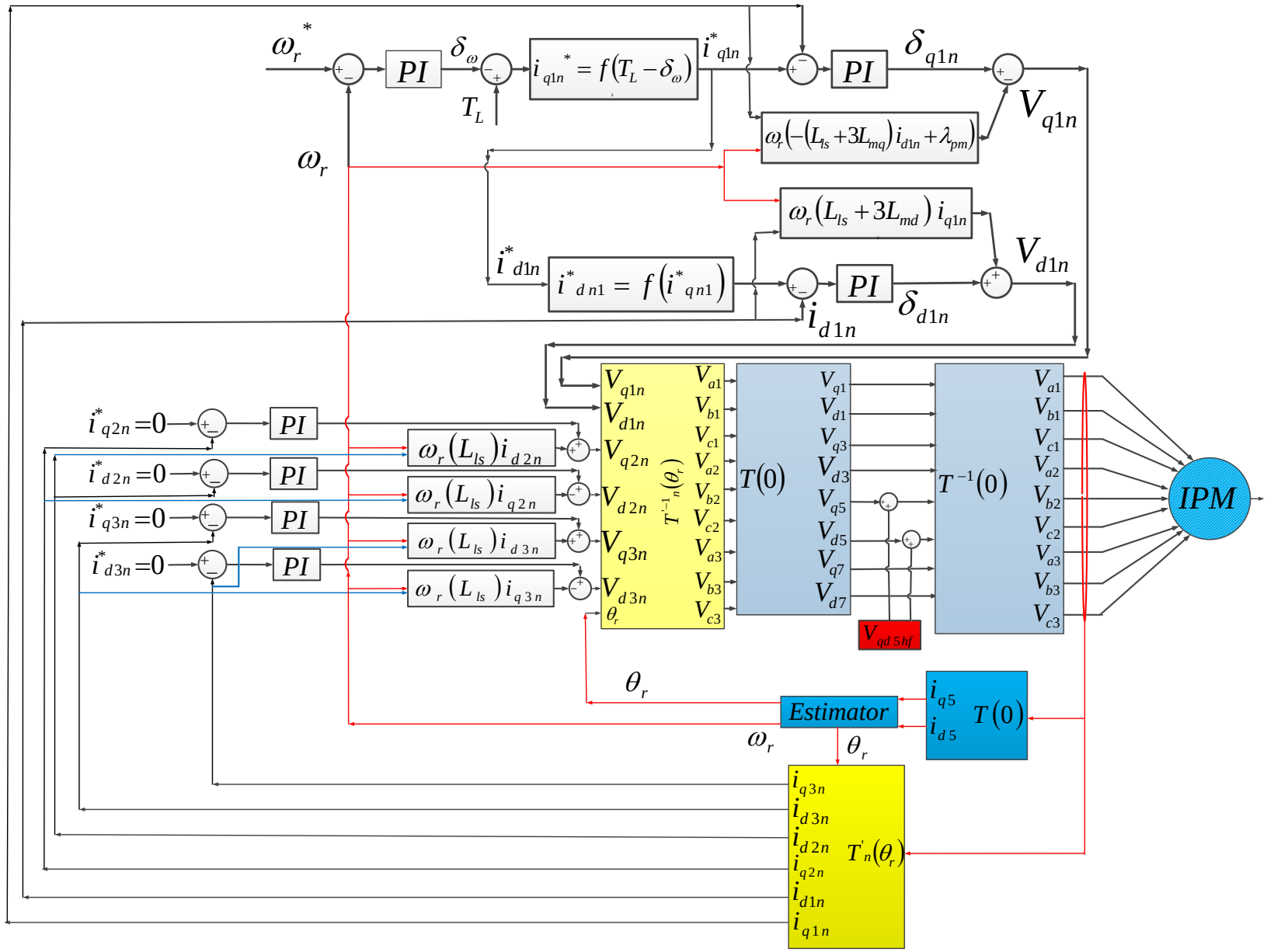

Figure 6.19: The controller of the symmetrical machine.

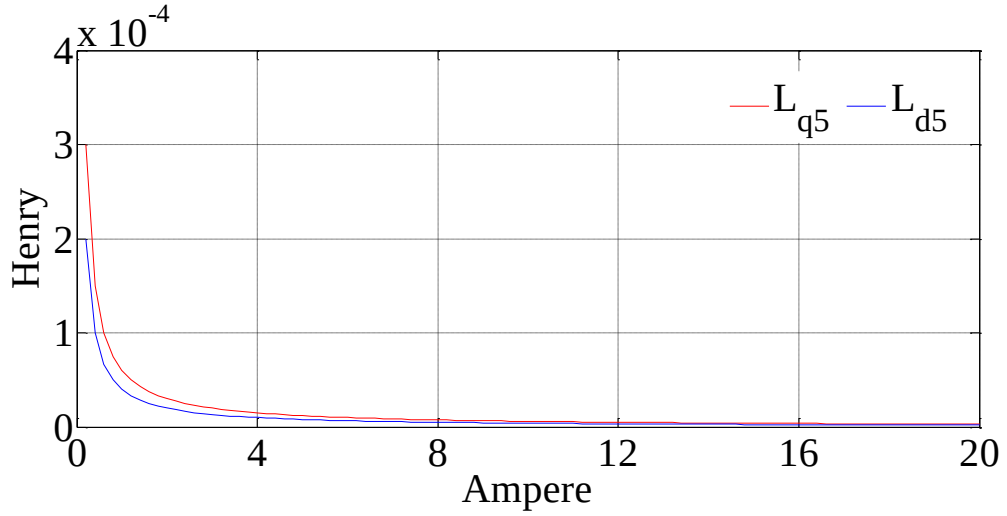

Figure 6.20: The magnitude of fifth sequence inductance of the stationary reference frame versus stator current.

$$\begin{bmatrix} V_{q5} \\ V_{d5} \end{bmatrix} = r_s \begin{bmatrix} i_{q5} \\ i_{d5} \end{bmatrix} + \begin{bmatrix} -10\omega_r L_{q5} \sin(10\theta_r) & 0 \\ 0 & 10\omega_r L_{d5} \cos(10\theta_r) \end{bmatrix} \begin{bmatrix} i_{q5} \\ i_{d5} \end{bmatrix} + \begin{bmatrix} L_{q5} \cos(10\theta_r) & 0 \\ 0 & L_{d5} \sin(10\theta_r) \end{bmatrix} p \begin{bmatrix} i_{q5} \\ i_{d5} \end{bmatrix} \tag{6.209}$$

$$p \begin{bmatrix} i_{q5} \\ i_{d5} \end{bmatrix} = -\begin{bmatrix} \dfrac{L_{d5} \sin(10\theta_r)\left(10\omega_r L_{q5} \sin(10\theta_r) - r_s\right)}{0.5 L_{q5} L_{d5} \sin(5\theta_r)} & 0 \\ 0 & \dfrac{L_{q5} \cos(10\theta_r)\left(10\omega_r L_{d5} \cos(10\theta_r) - r_s\right)}{0.5 L_{q5} L_{d5} \sin(5\theta_r)} \end{bmatrix} \begin{bmatrix} i_{q5} \\ i_{d5} \end{bmatrix} - \frac{1}{0.5 L_{q5} L_{d5} \sin(5\theta_r)} \begin{bmatrix} L_{d5} \sin(10\theta_r) & 0 \\ 0 & L_{q5} \cos(10\theta_r) \end{bmatrix} \begin{bmatrix} V_{q5} \\ V_{d5} \end{bmatrix} \tag{6.211}$$

$$Y = \begin{bmatrix} 1 & 0 \\ 0 & 1 \end{bmatrix} \begin{bmatrix} i_{q5} \\ i_{d5} \end{bmatrix} \tag{6.212}$$

For $\theta_r = K\frac{\pi}{5}, K = 1,2,3,...$ the 'A' matrix is not defied. Therefore, the stability of such points need to be checked separately. For $\theta_r = K\frac{\pi}{5}, K = 1,2,3,...$ the fifth sequence circuit model can be presented as equation (6.213).

$$\begin{bmatrix} V_{q5} \\ V_{d5} \end{bmatrix} = r_s \begin{bmatrix} i_{q5} \\ i_{d5} \end{bmatrix} + \begin{bmatrix} 0 & 0 \\ 0 & 10\omega_r L_{d5} \end{bmatrix} \begin{bmatrix} i_{q5} \\ i_{d5} \end{bmatrix} + \begin{bmatrix} L_{q5} & 0 \\ 0 & 0 \end{bmatrix} p \begin{bmatrix} i_{q5} \\ i_{d5} \end{bmatrix} \tag{6.213}$$

First and second rows of the equation (6.213) can be separated as shown in equations (6.214) and (6.215).

$$V_{q5} = r_s i_{q5} + pL_{q5} i_{q5} \tag{6.214}$$

$$V_{d5} = r_s i_{d5} + 10\omega_r L_{d5} i_{d5} \tag{6.215}$$

The equation (6.214) has a pole in ($S = -r_s / L_{q5}$) therefore, it is stable. The equation (6.215) is algebraic and it is stable. For the rest of the points the characteristic equation of the system is needed. The characteristic equation of the matrix 'A' can be presented as equation (6.216).

$$\begin{aligned} &|SI - A| = \\ &\left(S + \frac{L_{d5}\sin(10\theta_r)\left(10\omega_r L_{q5}\sin(10\theta_r) - r_s\right)}{0.5L_{q5}L_{d5}\sin(5\theta_r)} \right)\left(S + \frac{L_{q5}\cos(10\theta_r)\left(10\omega_r L_{d5}\cos(10\theta_r) - r_s\right)}{0.5L_{q5}L_{d5}\sin(5\theta_r)} \right) = \\ &S^2 + S\left(\frac{L_{d5}\sin(10\theta_r)\left(10\omega_r L_{q5}\sin(10\theta_r) - r_s\right) + L_{q5}\cos(10\theta_r)\left(10\omega_r L_{d5}\cos(10\theta_r) - r_s\right)}{0.5L_{q5}L_{d5}\sin(5\theta_r)} \right) + \\ &\frac{\left(L_{d5}\sin(10\theta_r)\left(10\omega_r L_{q5}\sin(10\theta_r) - r_s\right)\right)\left(L_{q5}\cos(10\theta_r)\left(10\omega_r L_{d5}\cos(10\theta_r) - r_s\right)\right)}{\left(0.5L_{q5}L_{d5}\sin(10\theta_r)\right)^2} \end{aligned} \tag{6.216}$$

Using FEMM, the magnitude of q and d inductances of the fifth sequence versus the RMS value of the stator current are generated as Figure 6.20. Using the inductances of the Figure 6.19 the poles of the equation (6.211) can be plotted as Figure 6.21. It can be seen that for all the ranges of the stator current the poles are stable.

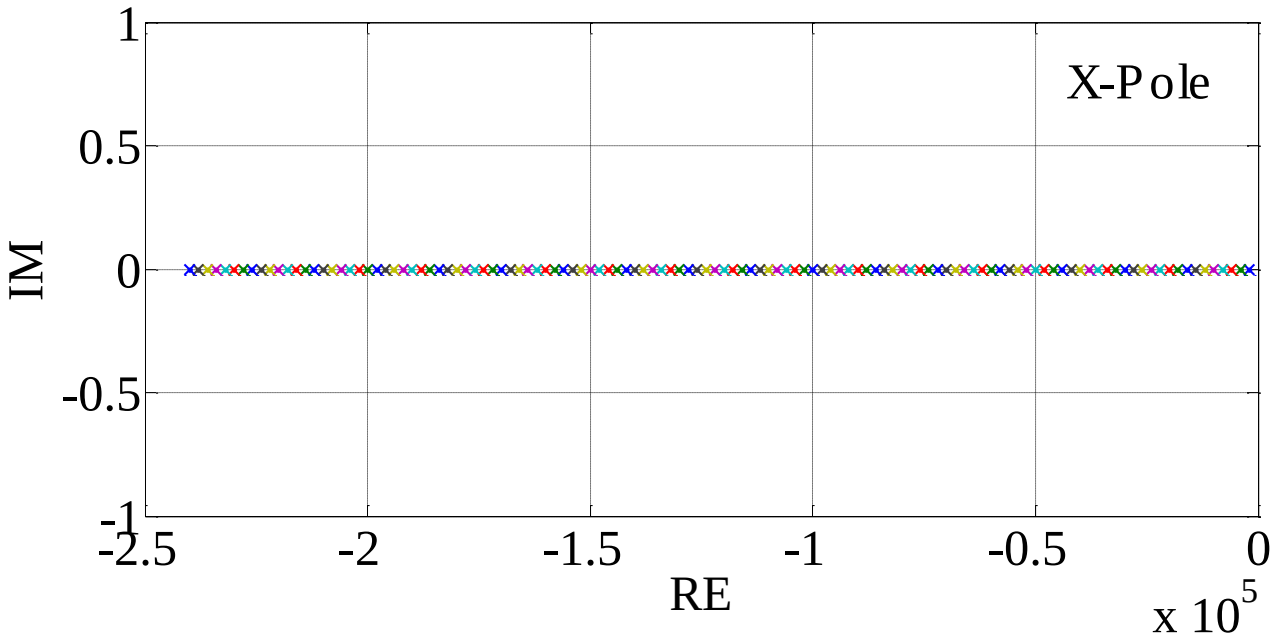

Figure 6.21: The poles of the fifth sequence circuit in different stator current levels.

6.5 Implementation of the Sensorless Controller of the Symmetrical Triple-Star IPM

6.5.1 Discretizing the Controller

In this section the controller that is designed in the previous sections of this chapter is discretized to be implemented in the DSP using C++ language. The controller equations are

represented here to be converted to the 'Z' domain. The dynamic equation for the speed loop in 'S' domain, is presented in the equation (6.217).

$$\sigma_{\omega r} = \left(K_{P\omega} + \frac{K_{I\omega}}{S} \right) \left(\omega_r^* - \omega_r \right) \tag{6.217}$$

Using Tustin's approximation which is one of the simplest 'Z' domain approximations and therefore, it is easy to implement in DSP [159], the term 'S' can be replaced by:

$$S = \frac{2}{T} \frac{1 - z^{-1}}{1 + z^{-1}} \tag{6.218}$$

Where, T is the sampling period. Substituting the 'S' from equation (6.218) into the equation (6.217) results in:

$$2\sigma_{\omega r} \left(1 - z^{-1}\right) = \left(2K_{P\omega} \left(1 - z^{-1}\right) + T\left(1 + z^{-1}\right) K_{I\omega}\right) \left(\omega_r^* - \omega_r\right) \tag{6.219}$$

The equation (6.219) can be rewritten as:

$$2\sigma_{\omega r} - 2\sigma_{\omega r} z^{-1} = 2K_{P\omega} e_{\omega r} - 2K_{P\omega} z^{-1} e_{\omega r} + TK_{I\omega} e_{\omega r} + TK_{I\omega} z^{-1} e_{\omega r} \tag{6.220}$$

Where:

$$e_{\omega r} = \omega_r^* - \omega_r \tag{6.221}$$

In equation (6.220) the term 'z^{-1}' simply represents a step of delay. Therefore, the equation 6.220 can be represented as:

$$\sigma_{\omega r}(K) = K_{P\omega} e_{\omega r}(K) - K_{P\omega} e_{\omega r}(K-1) + \frac{T}{2} K_{I\omega} e_{\omega r}(K) + \frac{T}{2} K_{I\omega} e_{\omega r}(K-1) + \sigma_{\omega r}(K-1) \tag{6.222}$$

Where: 'K' is the sample number. The output of the equation (6.222) is $\sigma_{\omega r}(K)$ which can be replaced in the equation (6.223) to generate the reference of the q_{1n} axis current. The equation (6.223) is the discretized version of equation (6.133).

$$i^{4}{}_{q1n}{}^{*}(K)+\frac{4\lambda_{pm}i_{q1n}{}^{*}(K)\left(\delta_{\omega_r}(K)-T_L(K)\right)}{27P\left(L_{md}-L_{mq}\right)^2}-\left(\frac{4\left(\delta_{\omega_r}(K)-T_L(K)\right)}{27P\left(L_{md}-L_{mq}\right)^2}\right)^2=0 \tag{6.223}$$

Using the q_{1n} axis reference, the reference of the d_{1n} axis current can be generated from the equation (6.224).

$$i_{d1n}{}^{*}(K)=-\frac{\lambda_{pm}}{6\left(L_{md}-L_{mq}\right)}+\sqrt{\left(\frac{\lambda_{pm}}{6\left(L_{md}-L_{mq}\right)}\right)^2+i^{2}{}_{q1n}{}^{*}(K)} \tag{6.224}$$

The q_{1n} and d_{1n} axis current references can be used in the current regulators. The dynamic equation of the current regulator of the q_{1n} axis is repeated in equation (6.225).

$$\delta_{q1n}=\left(K_{Pq1}+\frac{K_{Iq1}}{S}\right)\left(i_{q1n}{}^{*}-i_{q1n}\right) \tag{6.225}$$

Substituting the 'S' from the equation (6.218) results in:

$$\delta_{q1n}(K)=K_{Pq1}e_{i_{q1n}}(K)-K_{Pq1}e_{i_{q1n}}(K-1)+\frac{T}{2}K_{Iq1}e_{i_{q1n}}(K)+\frac{T}{2}K_{Iq1}e_{i_{q1n}}(K-1)+\delta_{q1n}(K-1) \tag{6.226}$$

Where:

$$e_{i_{q1n}}(K)=\left(i_{q1n}{}^{*}(K)-i_{q1n}(K)\right) \tag{6.227}$$

The dynamic equation of the d_{1n} axis current also can be represented as:

$$\delta_{d1n} = \left(K_{Pd1} + \frac{K_{Id1}}{S} \right) \left(i_{d1n}^{*} - i_{d1n} \right) \tag{6.228}$$

Substituting the 'S' from the equation (6.218) results in:

$$\delta_{d1n}(K) = K_{Pd1} e_{i_{d1n}}(K) - K_{Pd1} e_{i_{d1n}}(K-1) + \frac{T}{2} K_{Id1} e_{i_{d1n}}(K) + \frac{T}{2} K_{Id1} e_{i_{d1n}}(K-1) + \delta_{d1n}(K-1) \tag{6.229}$$

Where:

$$e_{i_{d1n}}(K) = \left(i_{d1n}^{*}(K) - i_{d1n}(K) \right) \tag{6.230}$$

Now the output of the current regulators can be used in to the equations (6.135) and (6.143) to generate the q_{1n} and d_{1n} axis voltages. Equations (6.231) and (6.232) show the final voltage equations in the 'Z' domain.

$$V_{q1n}(K) = \delta_{q1n}(K) - \omega_r(K) \left(-\left(L_{ls} + 3L_{mq} \right) i_{d1n}(K) + \lambda_{pm} \right) \tag{6.231}$$

$$V_{d1n}(K) = \delta_{d1n}(K) + \omega_r(K) \left(L_{ls} + 3L_{md} \right) i_{q1n}(K) \tag{6.232}$$

Using the discretized equations, the controller flow chart can be drawn as Figure 6.22. The controllers for the q_{2n} and d_{2n} can also be discretized to be implemented in the DSP. The dynamic equations for the qd_{2n} controllers are repeated here.

$$\delta_{d2n} = \left(K_{Pd2} + \frac{K_{Id2}}{S} \right) \left(i_{d2n}^{*} - i_{d2n} \right) \tag{6.233}$$

$$\delta_{q2n} = \left(K_{Pq2} + \frac{K_{Iq2}}{S} \right) \left(i_{q2n}^{*} - i_{q2n} \right) \tag{6.234}$$

By substituting the 'S' from the equation (6.218) in to the above equations, they can be discretized as:

$$\delta_{d2n}\left(1-z^{-1}\right)=\left(K_{Pd2}\left(1-z^{-1}\right)+\frac{TK_{Id2}\left(1+z^{-1}\right)}{2}\right)\left(i_{d2n}{}^{*}-i_{d2n}\right) \tag{6.235}$$

$$\delta_{q2n}\left(1-z^{-1}\right)=\left(K_{Pq2}\left(1-z^{-1}\right)+\frac{TK_{Iq2}\left(1+z^{-1}\right)}{2}\right)\left(i_{q2n}{}^{*}-i_{q2n}\right) \tag{6.236}$$

The term ‘ Z^{-1} ’ is one single delay in the sampling procedure. The final discrete controller can be expressed as equation (6.237).

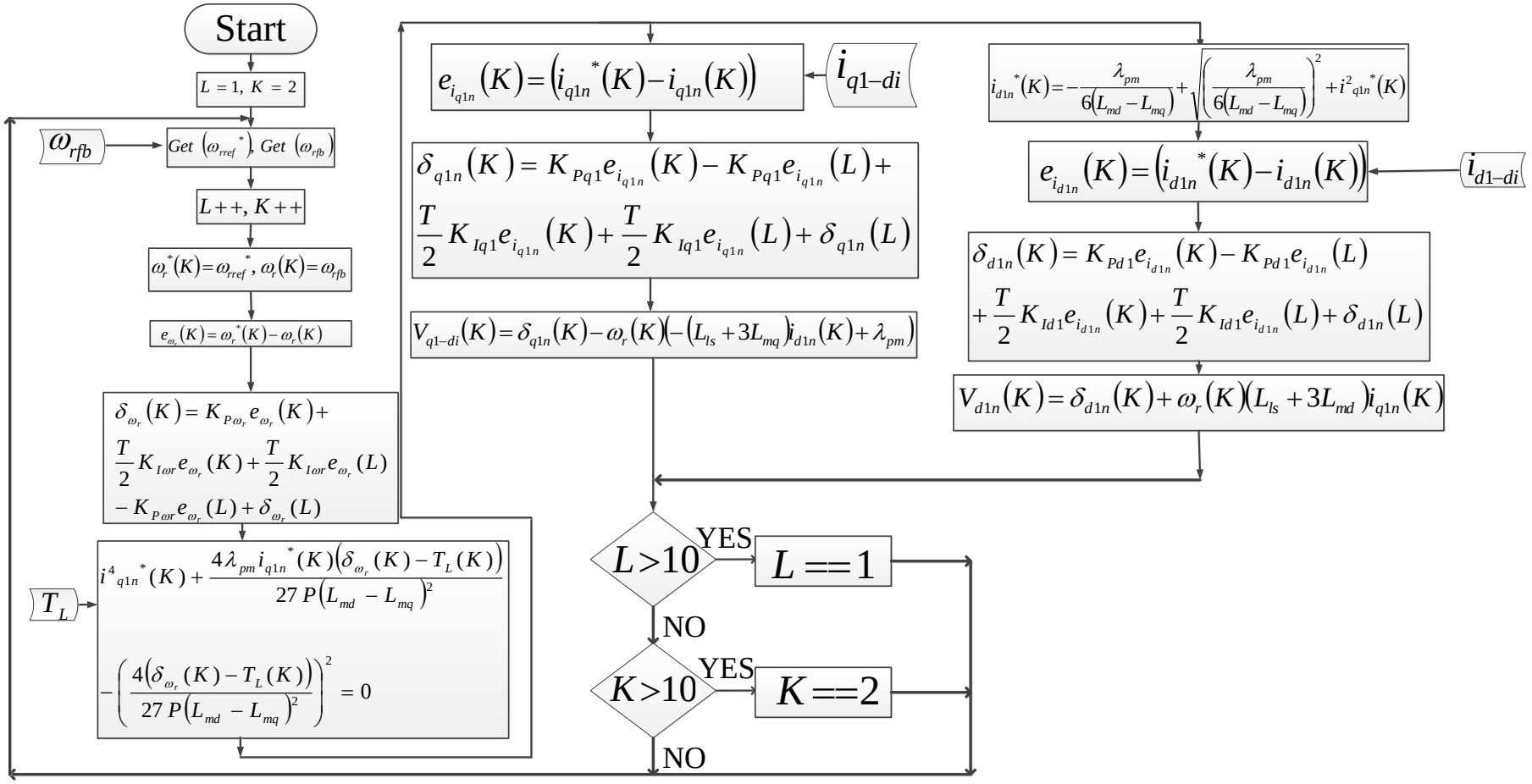

Figure 6.22: The controller flow chart for q_{1n} and d_{1n} axis.

$$\delta_{d2n}(K) = K_{Pd2}e_{d2n}(K) - K_{Pd2}e_{d2n}(K-1) + \frac{T}{2}K_{Id2}e_{d2n}(K) + \frac{T}{2}K_{Id2}e_{d2n}(K-1) + \delta_{d2n}(K-1) \quad (6.237)$$

Where:

$$e_{d2n}(K) = \left(i_{d2n}{}^{*}(K) - i_{d2n}(K)\right) \quad (6.238)$$

$$\delta_{q2n}(K) = K_{Pq2}e_{q2n}(K) - K_{Pq2}e_{q2n}(K-1) + \frac{T}{2}K_{Iq2}e_{q2n}(K) + \frac{T}{2}K_{Iq2}e_{q2n}(K-1) + \delta_{q2n}(K-1) \quad (6.239)$$

Where:

$$e_{q2n}(K) = \left(i_{q2n}{}^{*}(K) - i_{q2n}(K)\right) \quad (6.240)$$

The output of the above loops can be fed to the dynamic voltage equations of the controller to generate the q_{2n} and d_{2n} voltages. Equations (6.241) and (6.242) show the discretized equations for the voltages.

$$V_{d2n}(K) = \delta_{d2n}(K) - \omega_r(K)L_{ls}i_{q2n}(K) \quad (6.241)$$

$$V_{q2n}(K) = \delta_{q2n}(K) + \omega_r(K)L_{ls}i_{d2n}(K) \quad (6.242)$$

Figure 6.23 shows the flow chart of the current controllers of the q_{2n} and d_{2n}. Because of the symmetry, the controller for q_{3n} and d_{3n} axis can also be discretized according to the same procedure as q_{2n} and d_{2n} axis.

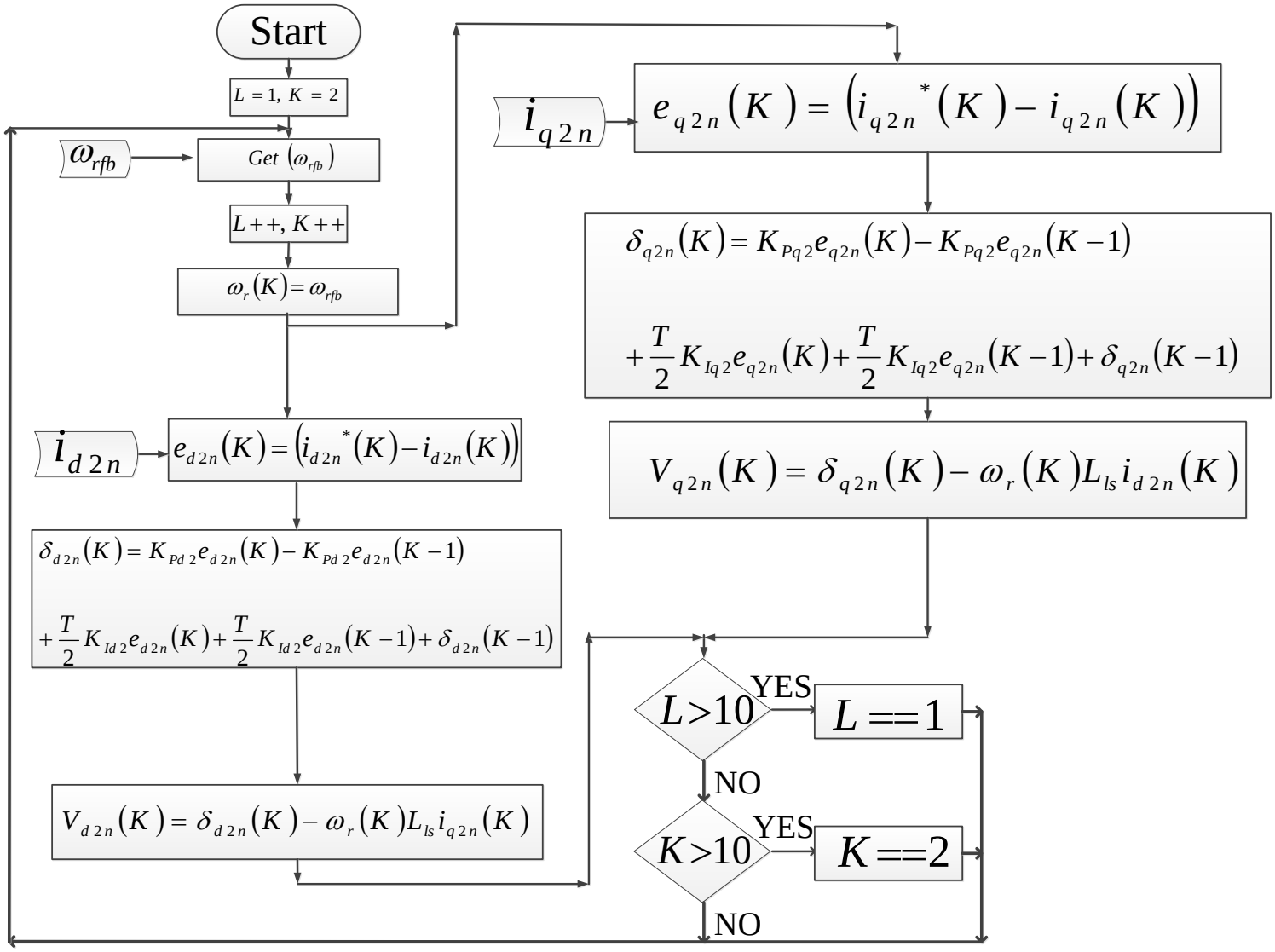

Figure 6.23: The controller flow chart for q_{2n} and d_{2n} axis.

6.5.2 Discretizing the Position Estimator

The position observer (designed in section 4.3) is composed of low pass filter, heterodyning block and Luenberger observer. All the components should be discretized to be implemented in the DSP. The first step is to discretize the filter. The filters transfer function is shown in equation (6.243).

$$f = \frac{10^6}{S^2 + 1414S + 10^6} \tag{6.243}$$

Now to get the discretized function the term S can be substituted with the equation (6.218):

$$f = \frac{i_o}{i_{in}} = \frac{10^6}{\left(\frac{2}{T}\frac{1-z^{-1}}{1+z^{-1}}\right)^2 + 1414\left(\frac{2}{T}\frac{1-z^{-1}}{1+z^{-1}}\right) + 10^6} \tag{6.244}$$

Then finally to implement the equation in the DSP it need to be rewritten in the below form.

$$f = \frac{i_o}{i_{in}} = \frac{\left(T\left(1+z^{-1}\right)\right)^2 10^6}{4\left(1-z^{-1}\right)^2 + 2828\left(T\left(1+z^{-1}\right)\right)\left(1-z^{-1}\right) + 10^6\left(T\left(1+z^{-1}\right)\right)^2} \tag{6.245}$$

$$i_o(K) = \frac{\left(\begin{array}{l}\left(10^6 T\, i_{in}(K) + 2\times 10^6 T\, i_{in}(K-1) + 10^6 T\, i_{in}(K-2)\right)\\ -\left(997172T + 4\right)i_o(K-2) - \left(2\times 10^6 - 8\right)i_o(K-1)\end{array}\right)}{\left(1002828\, T + 4\right)} \tag{6.246}$$

Now the filter can be shown in the flow chart of Figure 6.24. For the observer itself (with B=0) transfer functions can be generated.

$$\frac{\hat{\omega}_r}{\varepsilon} = \frac{\frac{K_{I1}}{S} + K_{p1}}{JS} + K_{p2} \tag{6.247}$$

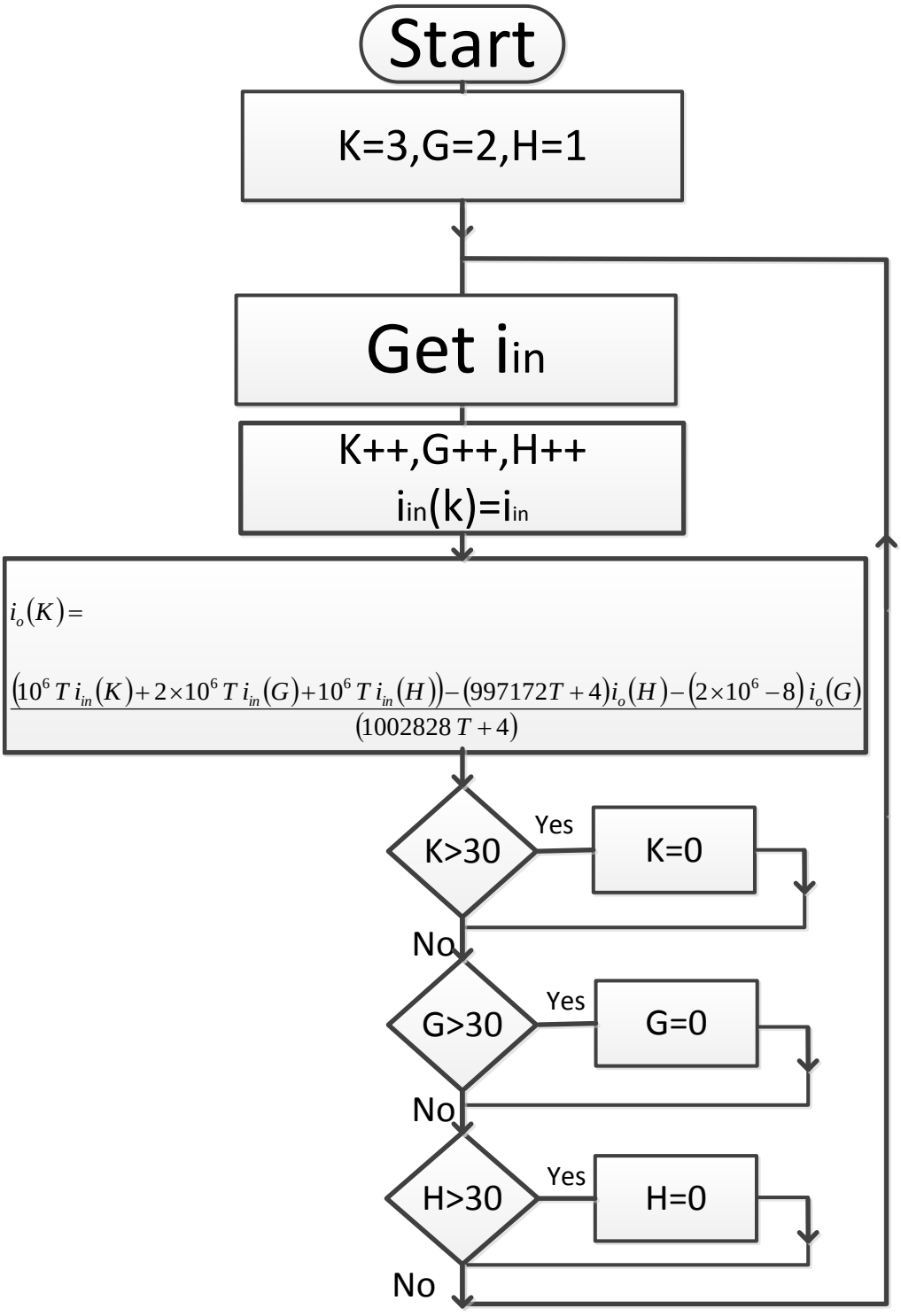

Figure 6.24: The flow chart for the filter.

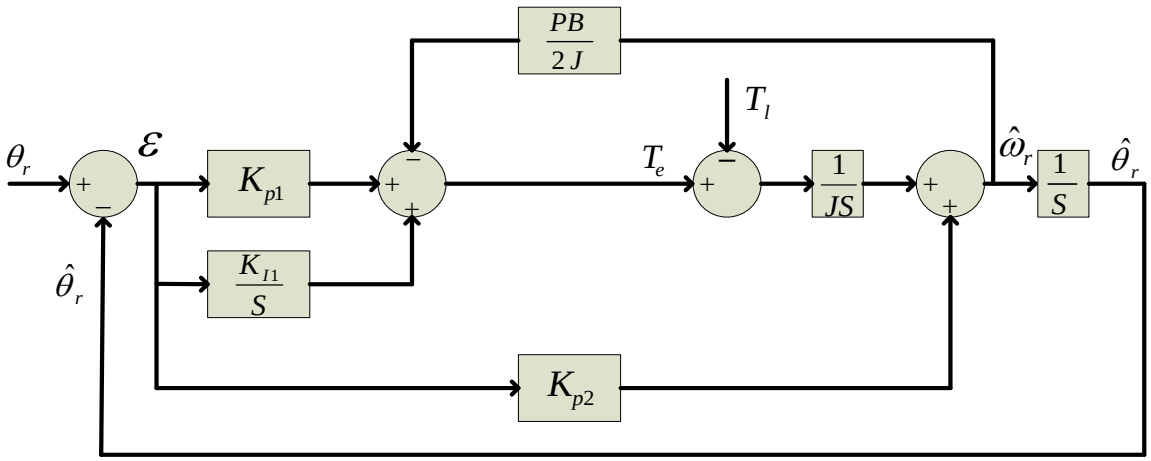

Figure 6.25: The position observer.

$$\hat{\theta}_r = \frac{\hat{\omega}_r}{S} \tag{6.248}$$

By combining the equations (6.247) and (6.248) the transfer function between the input error and the output can be generated as:

$$\frac{\hat{\theta}_r}{\varepsilon} = \frac{K_{I1} + SK_{p1} + JK_{p2}S^2}{JS^3} \tag{6.249}$$

Finally, after transforming the equation (6.249) to the 'Z' domain the observer transformation matrix can be represented as:

$$\frac{\hat{\theta}_r}{\varepsilon} = \frac{K_{I1}\left(T\left(1+z^{-1}\right)\right)^3 + 2K_{p1}\left(1-z^{-1}\right)\left(T\left(1+z^{-1}\right)\right)^2 + JK_{p2}\left(2\left(1-z^{-1}\right)\right)^2\left(T\left(1+z^{-1}\right)\right)}{2J\left(1-z^{-1}\right)^3} \tag{6.250}$$

And from there

$$2J\hat{\theta}_r = -2J\hat{\theta}_r\left(-3z^{-1}+3z^{-2}-z^{-3}\right) + K_{I1}T^3\left(1+3z^{-1}+3z^{-2}+z^{-3}\right) \tag{6.251}$$

$$+ 2K_{p1}T^2\left(1+z^{-1}-z^{-2}-z^{-3}\right) + 4TJK_{p2}\left(1-z^{-1}-z^{-2}+z^{-3}\right)$$

$$2J\hat{\theta}_r(K)=6J\hat{\theta}_r(K-1)-6J\hat{\theta}_r(K-2)+2J\hat{\theta}_r(K-3)+K_{I1}T^3\varepsilon(K)$$

$$+3K_{I1}T^3\varepsilon(K-1)+3K_{I1}T^3\varepsilon(K-2)+K_{I1}T^3\varepsilon(K-3)+2K_{p1}T^2\varepsilon(K)$$

$$+2K_{p1}T^2\varepsilon(K-1)-2K_{p1}T^2\varepsilon(K-2)-2K_{p1}T^2\varepsilon(K-3)+4TJK_{p2}\varepsilon(K) \quad (6.252)$$

$$-4TJK_{p2}\varepsilon(K-1)-4TJK_{p2}\varepsilon(K-2)+4TJK_{p2}\varepsilon(K-3)$$

Where:

$$\varepsilon(K)=\theta_r(K)-\hat{\theta}_r(K) \quad (6.253)$$

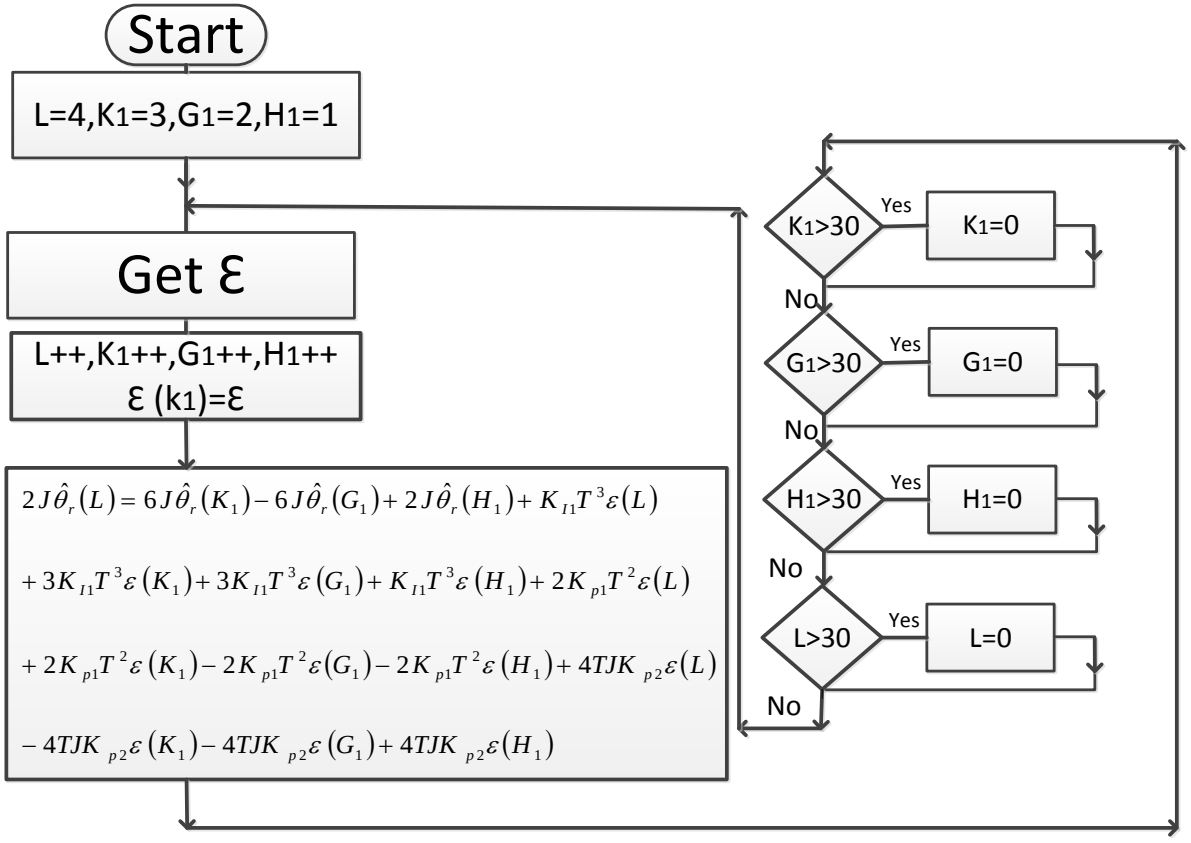

Figure 6.26: The flow chart for the observer.

6.6 Simulation and Experimental Results of the Sensorless Control of Symmetrical Triple-Star IPM

The sensorless controller that was designed in this chapter was simulated with the full order coupled model of the machine presented in the chapter 3. The simulation is done using MATLAB/ Simulink. In this simulation the controller and the position estimator are connected to the machine and the estimator provides the essential rotor angle for the converter. The designed controller is also implemented using a DSP-FPGA controller and simulation results are verified with experimental results. In this section the simulation and experimental results of three different speed profiles are presented.

6.6.1 Trapezoidal Speed Reference

In this test the motor controller receives a trapezoidal speed reference as the input command. The speed reference starts from the zero and goes to the positive rated speed from the positive rated speed it goes to the negative rated speed and returns to zero. The load torque is a damping load which is proportional to the rotor speed ($T_L = 0.013\omega_r$). Figures 6.27 and 6.28 show the reference speed, rotor speed and the speed error for simulation and experimental results respectively. It can be seen that; in all operating regions the rotor speed can accurately follow the reference speed. The Figure 6.29 (a) shows the electromagnetic torque generated by each machine and the total electromagnetic torque. The spectrum of the torque is shown in Figure 6.29 (b) and (c). Figure 6.30 (a) also shows the electromagnetic torque of the machine for experimental results and the spectrum of that is shown in Figures 6.30 (b) and (c). From these figures, it can be seen that at the frequency of 920 (Hz) where the high frequency signals are injected the machine does not produce any torque.

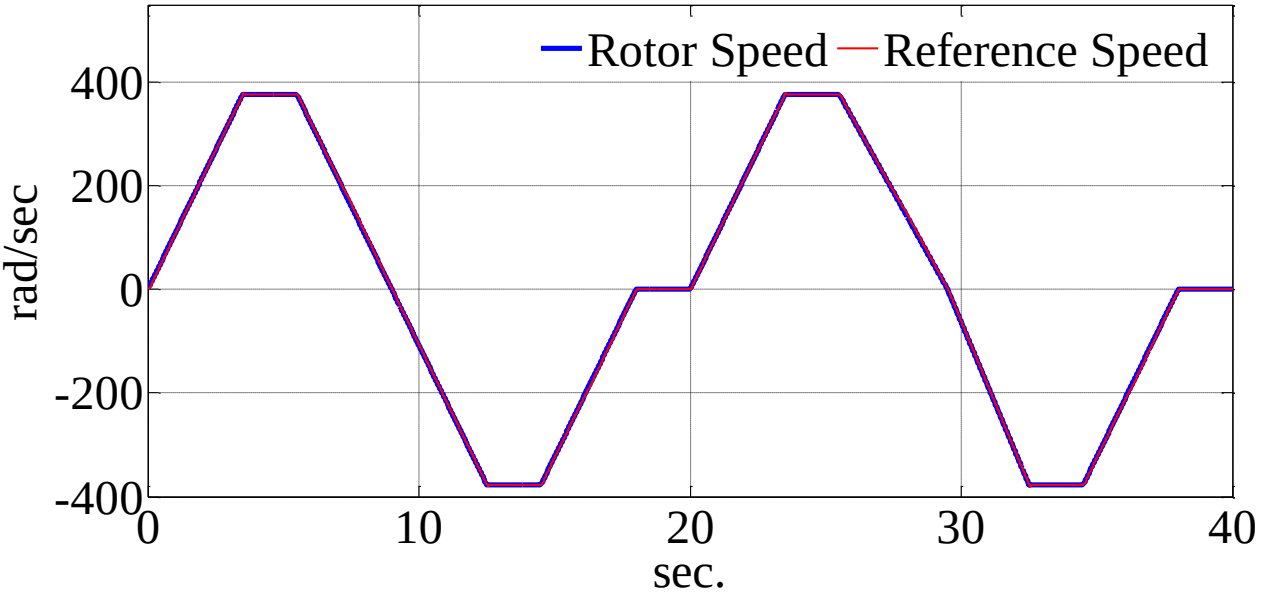

(a)

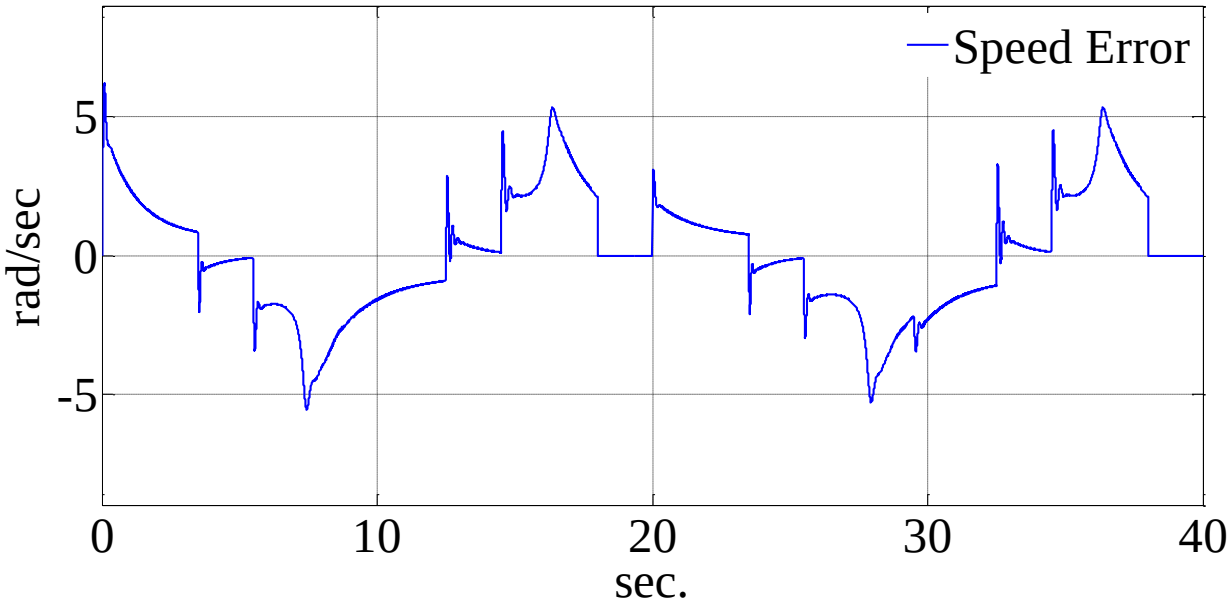

(b)

Figure 6.27: (a) The reference and rotor speed (simulation results), (b) The speed error (simulation results).

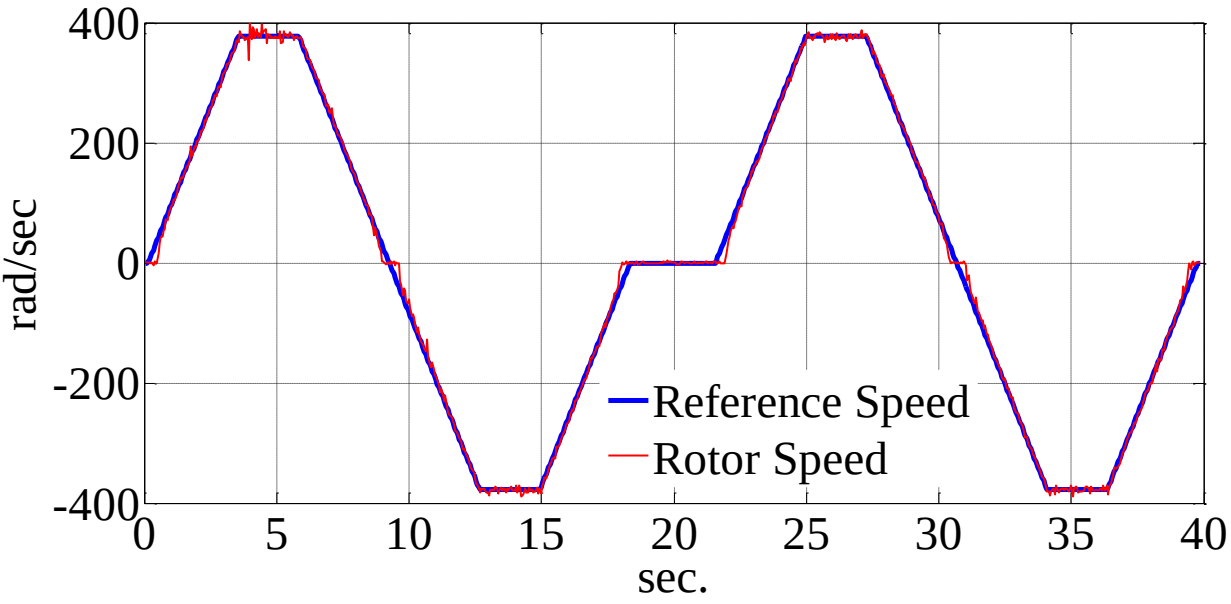

(a)

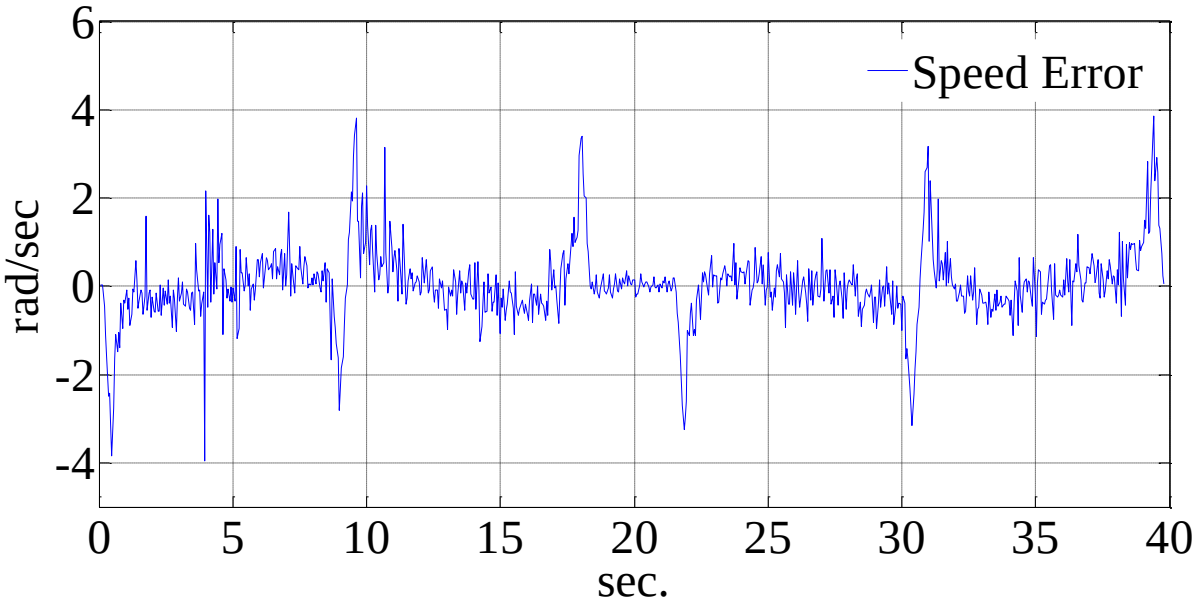

(b)

Figure 6.28: (a) The reference and rotor speed (experimental results), (b) The speed error (experimental results).

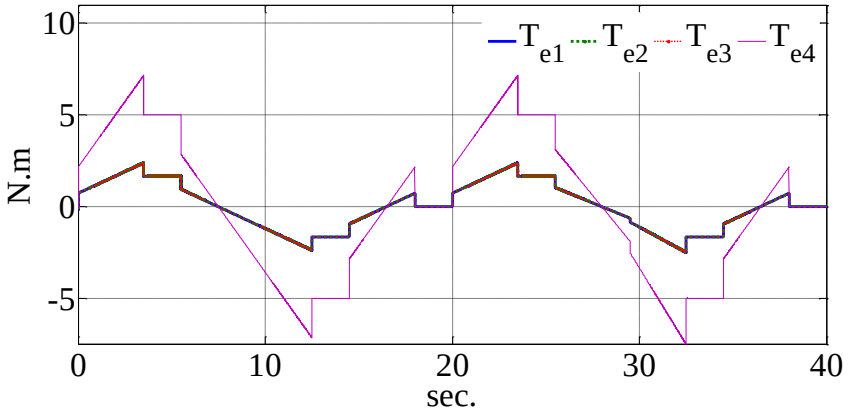

(a)

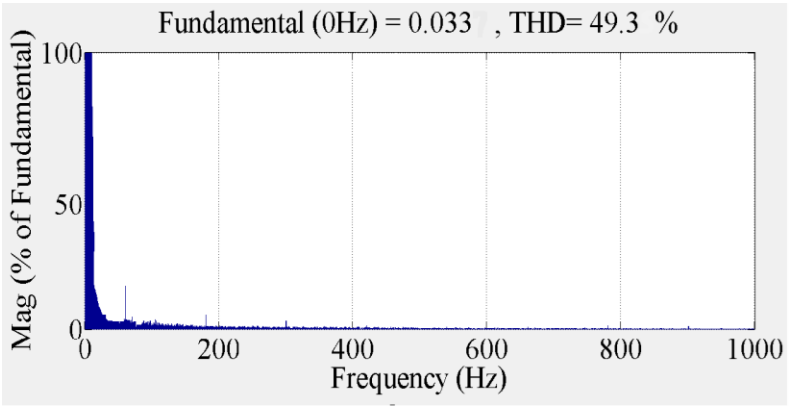

(b)

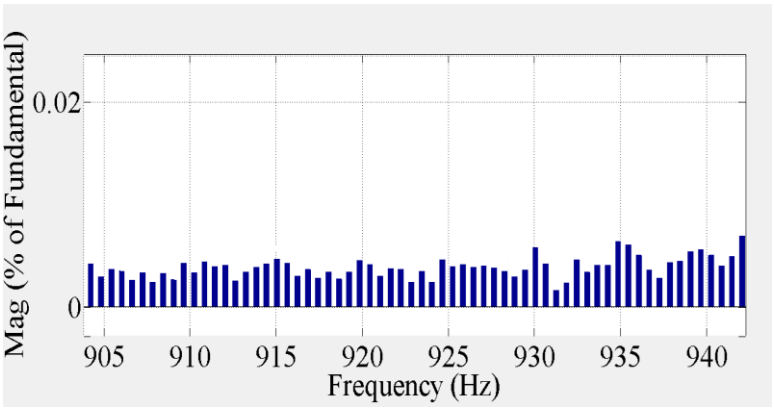

(c)

Figure 6.29: (a) The electromagnetic torque of each machine and the total, (b) The spectrum of the total electromagnetic torque, (c) The zoomed view of the spectrum of the electromagnetic torque around the frequency of 920 (Hz) (simulation results).

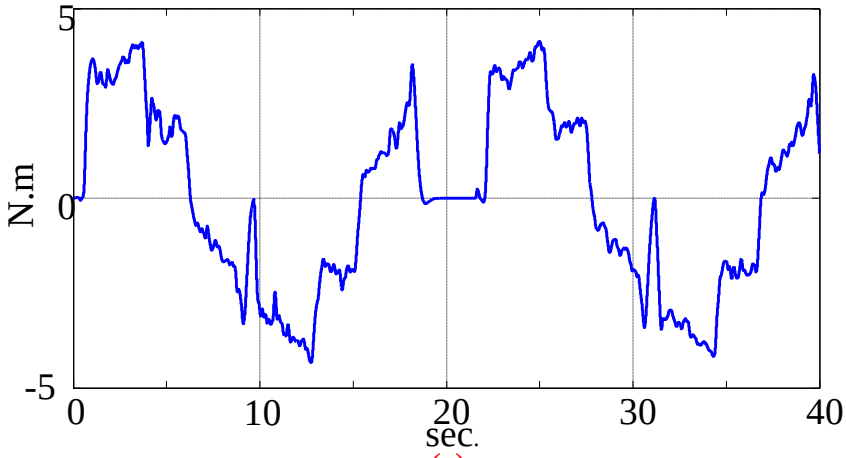

(a)

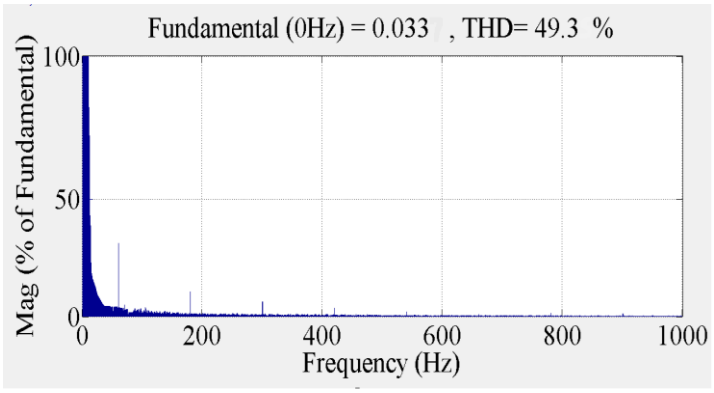

(b)

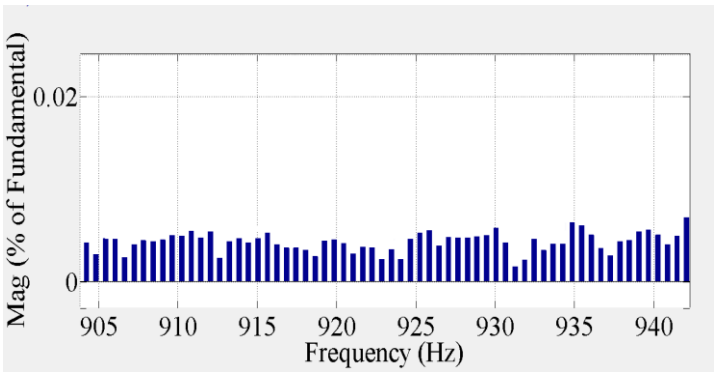

(c)

Figure 6.30: (a) The electromagnetic torque of each machine and the total, (b) The spectrum of the total electromagnetic torque, (c) The zoomed view of the spectrum of the electromagnetic torque around the frequency of 920 (Hz) (experimental results).

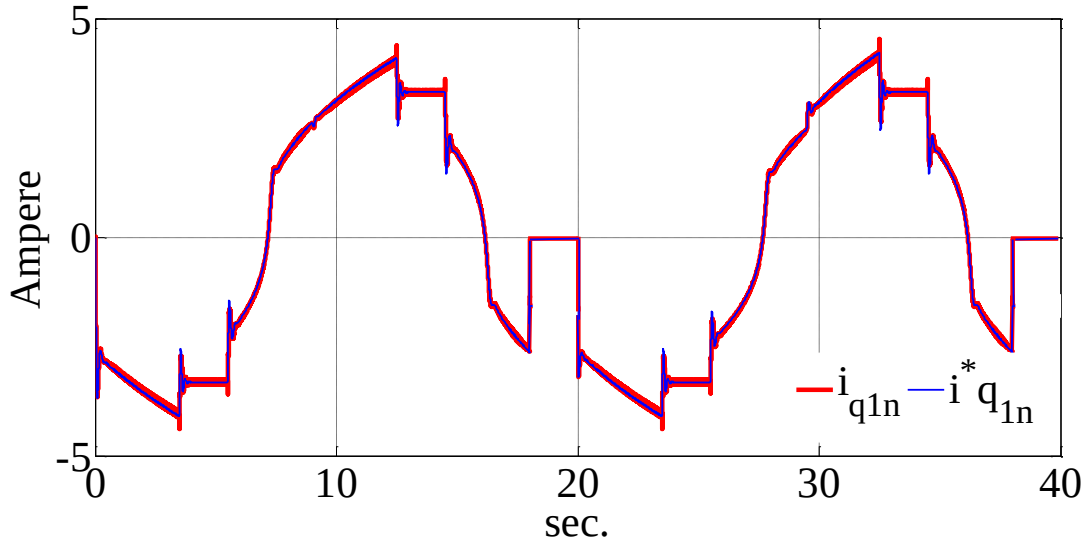

(a)

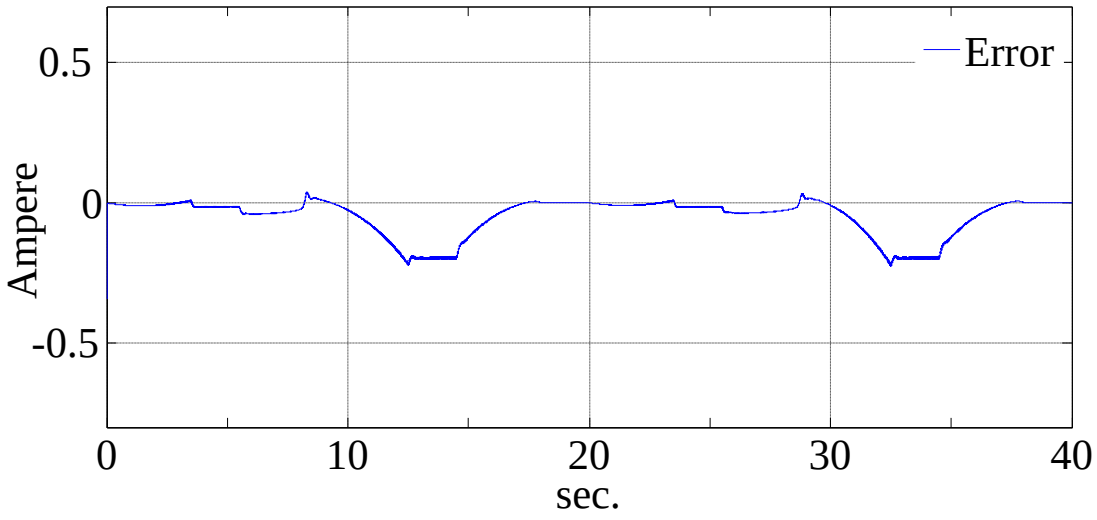

(b)

Figure 6.31: (a) The q_{1n} reference and feedback currents, (b) The current regulator error (simulation results).

From the speed error and the torque equation, the reference value of the q_{1n} axis current is generated and the reference current is given to current regulator of the q_{1n} axis. Figures 6.31 and 6.32 show the reference and feedback currents of the q_{1n} axis along with the regulator error for simulation and experimental results respectively.

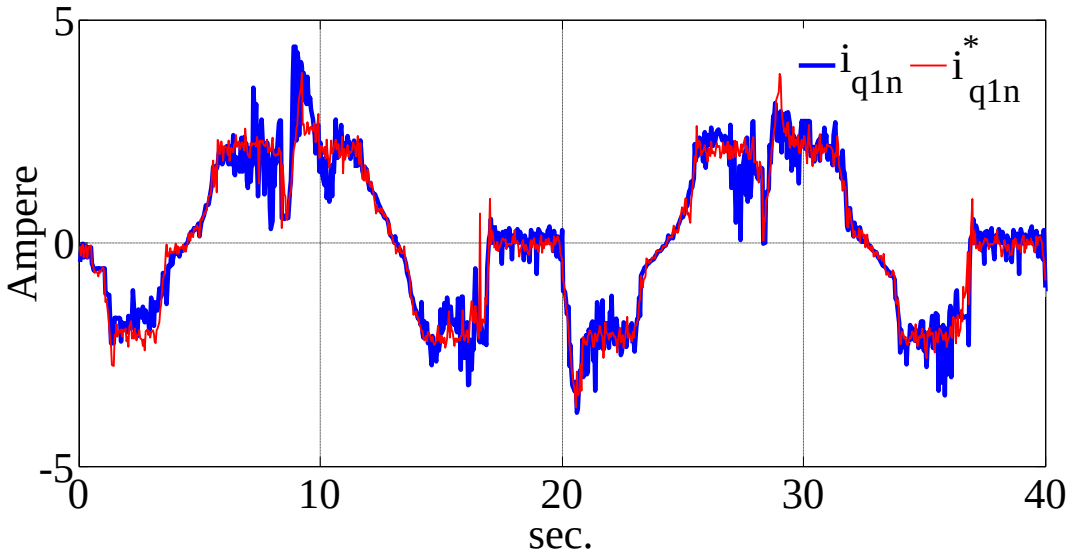

(a)

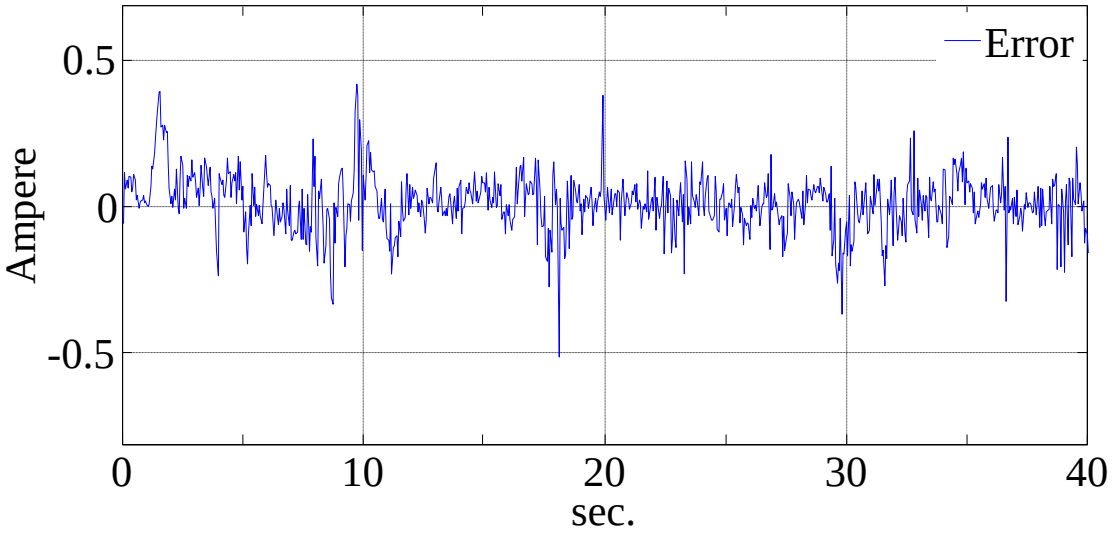

(b)

Figure 6.32: (a) The reference and actual q_{1n} axis current, (b) The current regulator error (experimental results).

From the q_{1n} reference current, the reference current of the d_{1n} axis current can be generated according to the equation (6.126). The generated reference current is used by the current regulator loop as reference. Figures 6.33 and 6.34 show the reference and the feedback currents for this axis along with the regulator error for simulation and experimental results respectively.

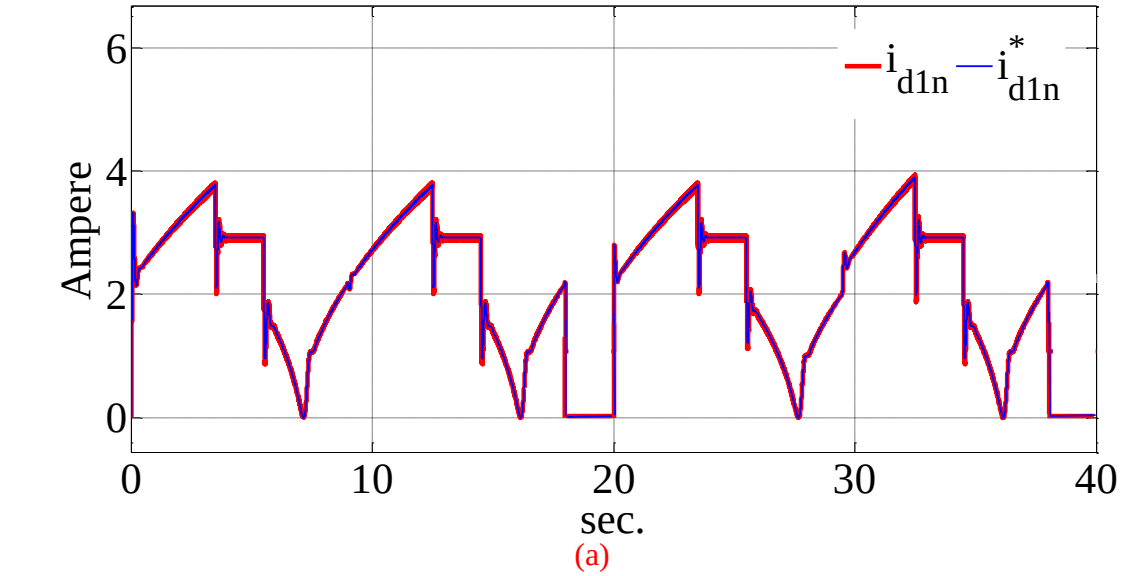

(a)

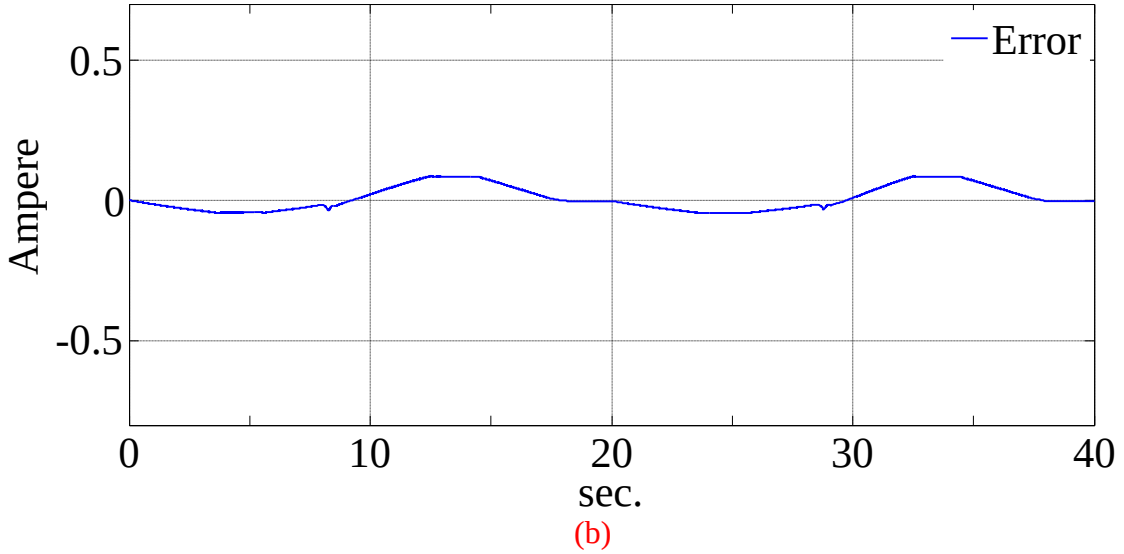

(b)

Figure 6.33: (a) The d_{1n} reference and feedback currents, (b) The current regulator error (simulation results).

The rest of the axis in the decoupled reference frame have zero as their reference currents. The Figures 6.35 to 6.38 show the non-torque producing axis currents generated by the current regulators for ' $d_{2,3n}$ ' and ' $q_{2,3n}$ ' for simulation and experimental results respectively.

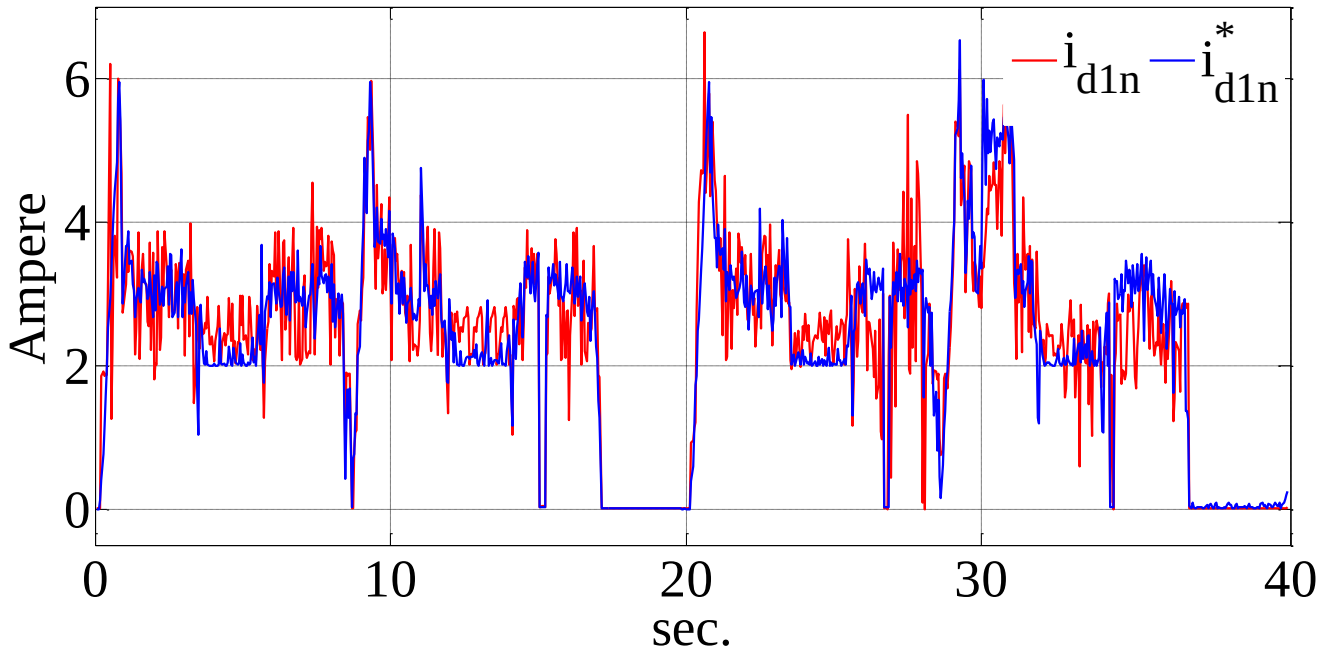

(a)

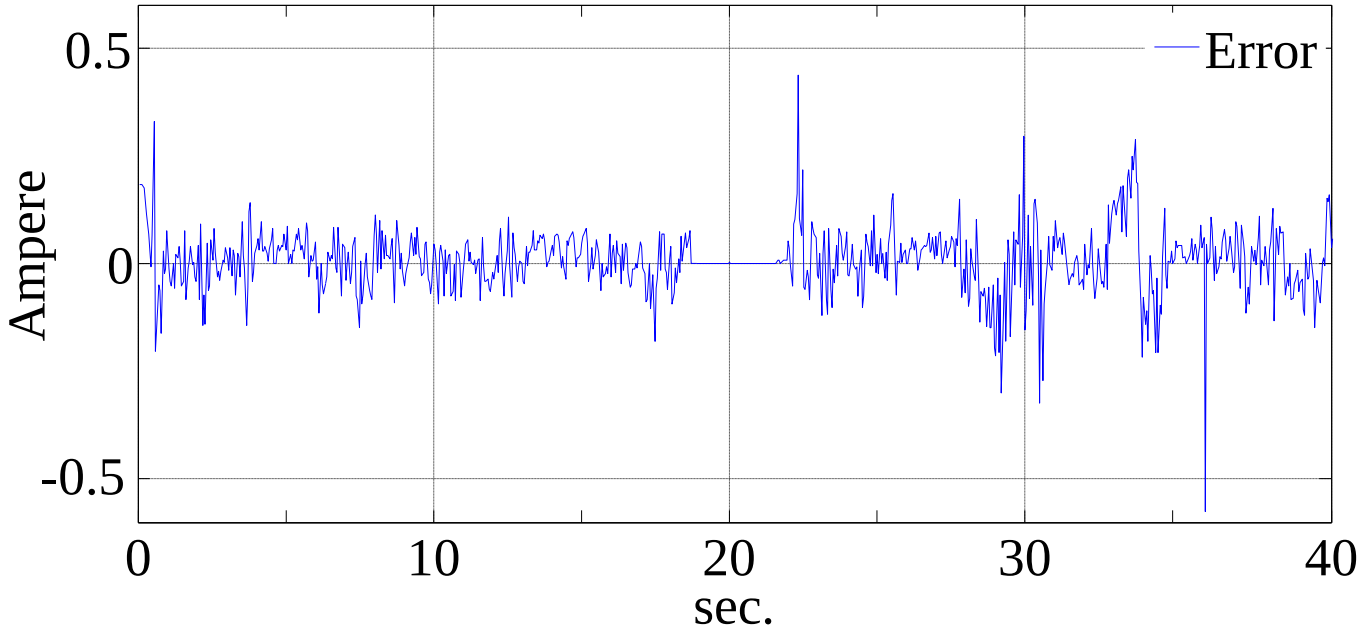

(b)

Figure 6.34: The reference and actual d_{1n} axis current, (b) The current regulator error (experimental results).

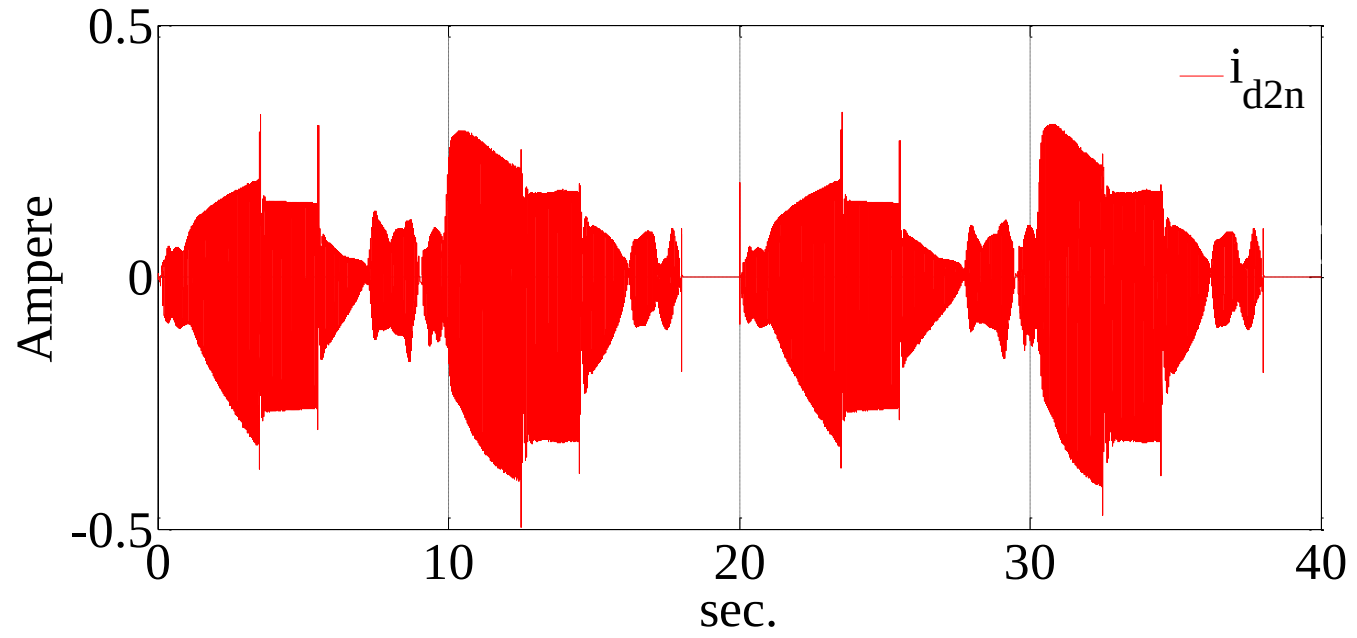

(a)

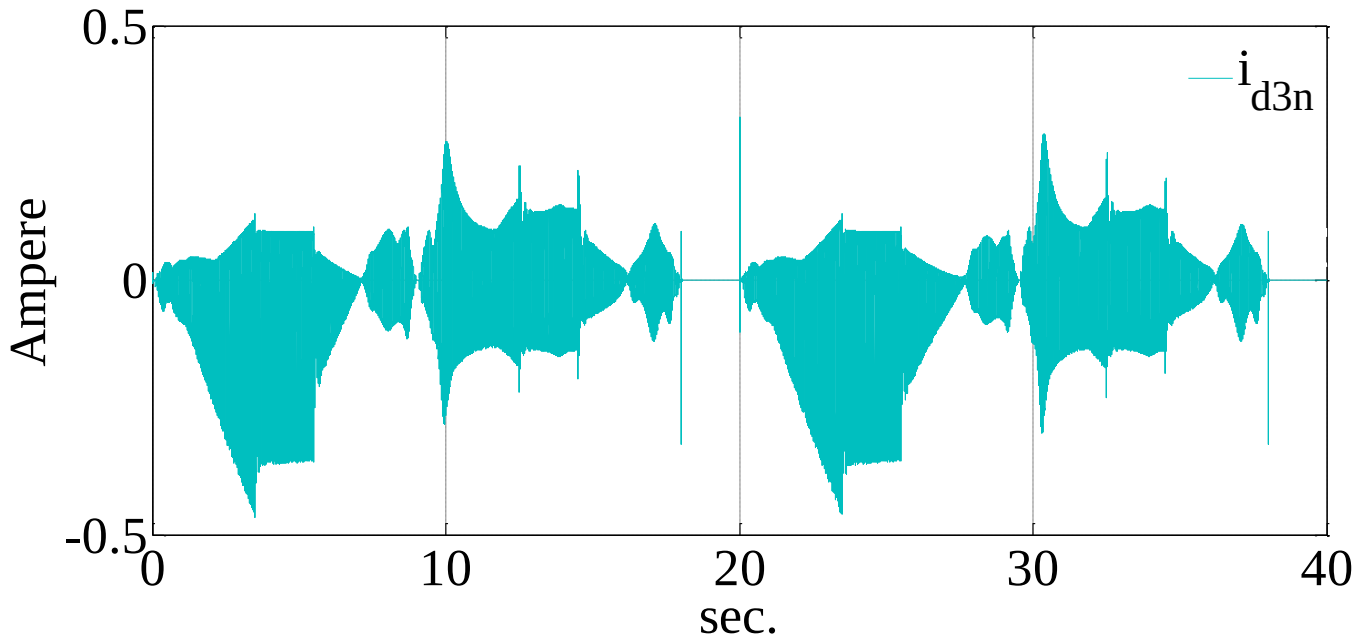

(b)

Figure 6.35: The currents of the non-torque producing axis for, (a) d_{2n}, (b) d_{3n} (simulation results).

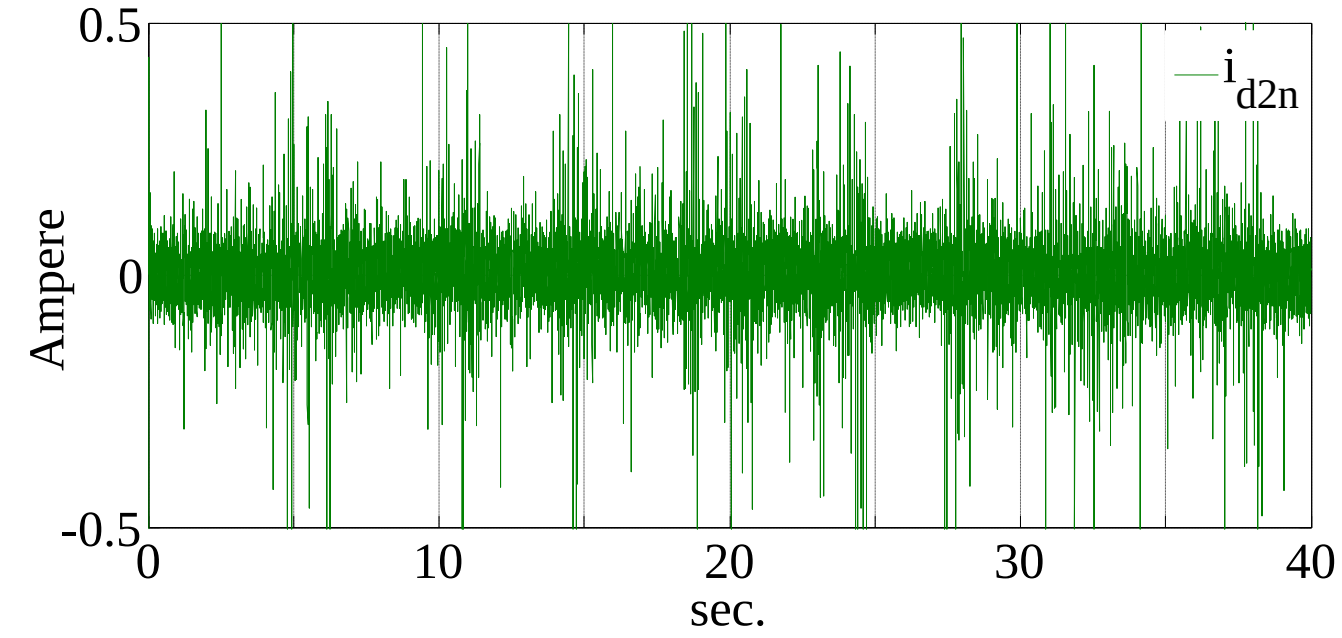

(a)

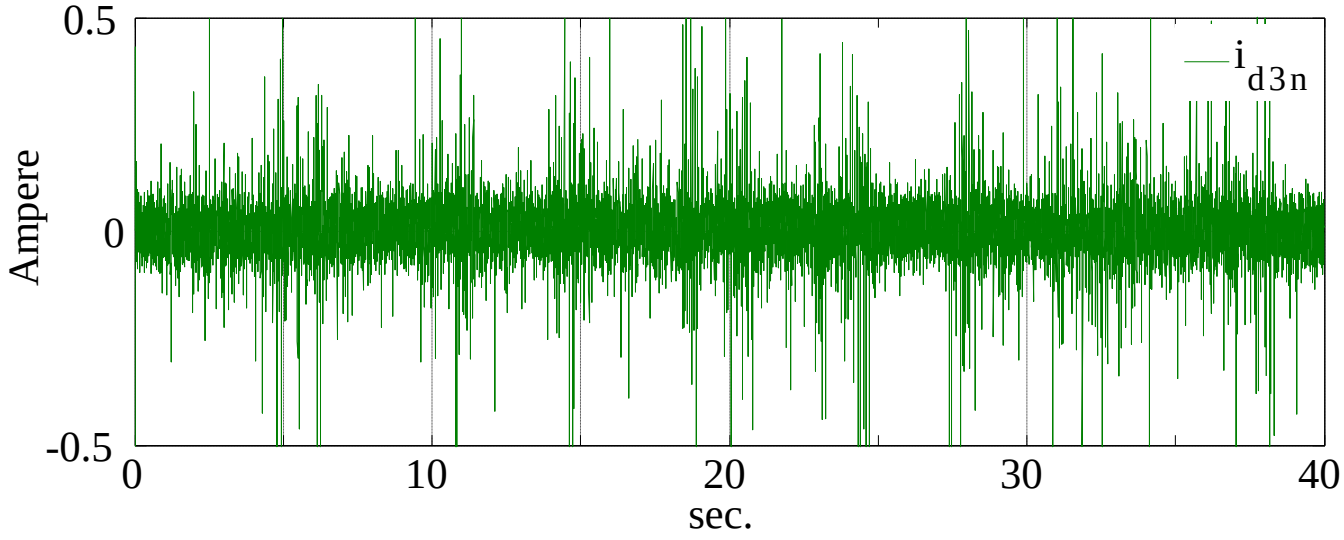

(b)

Figure 6.36: The currents of the non-torque producing axis for, (a) d_{2n}, (b) d_{3n} (experimental results).

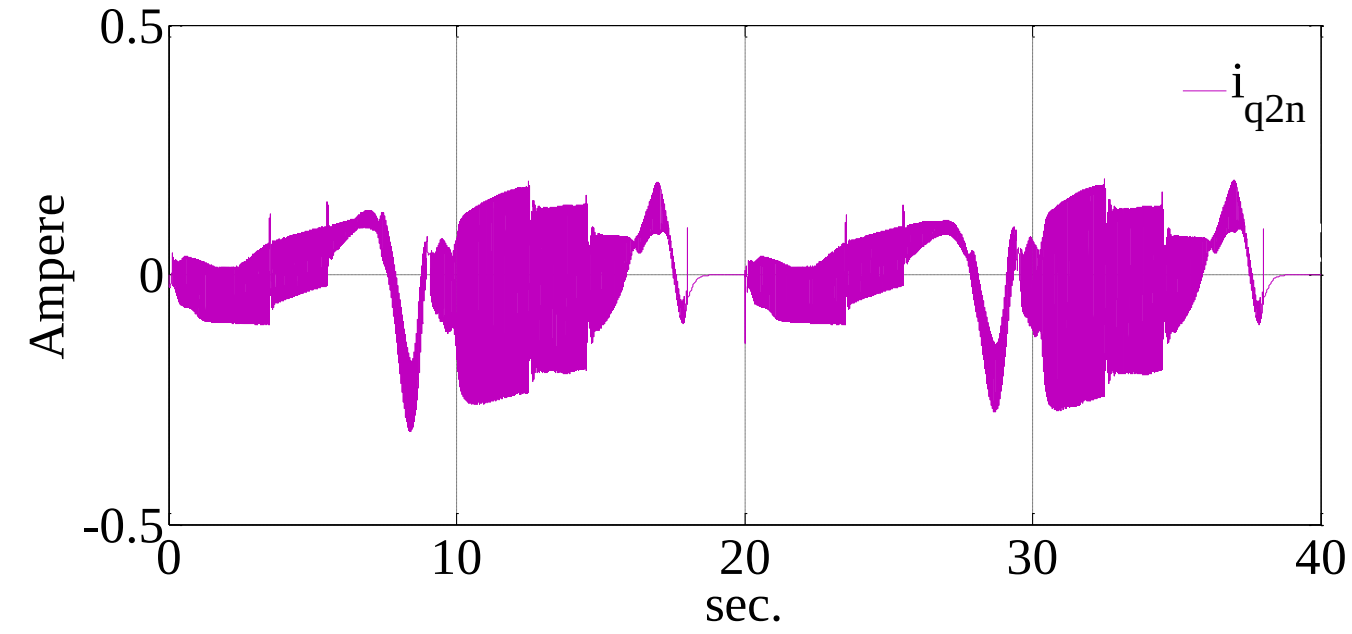

(a)

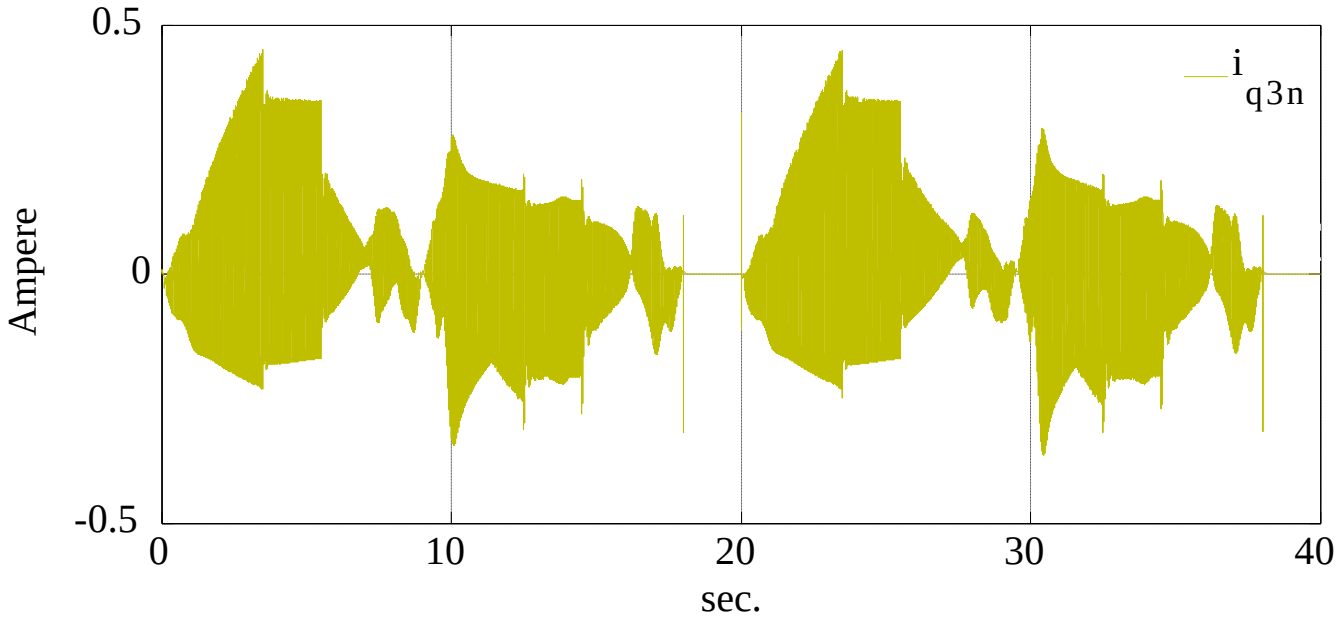

(b)

Figure 6.37: The currents of the non-torque producing axis for, (a) q_{2n}, (b) q_{3n} (simulation results).

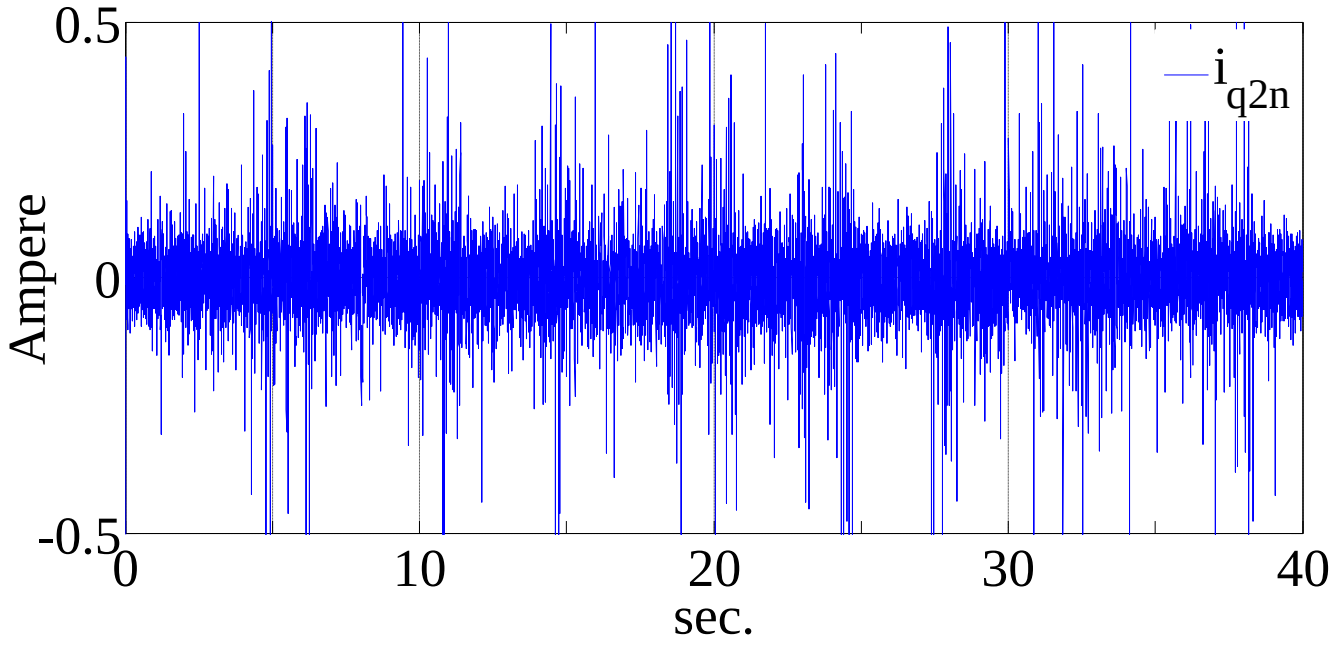

(a)

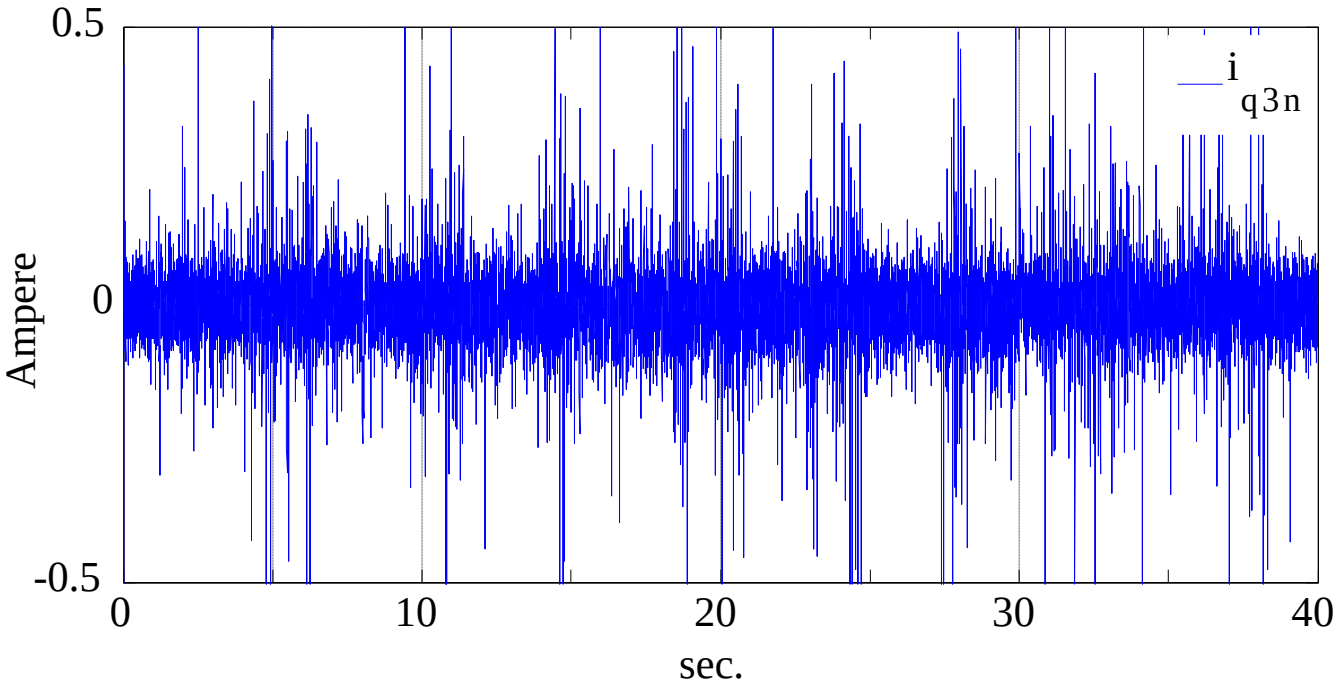

(b)

Figure 6.38: The currents of the non-torque producing axis for, (a) q_{2n}, (b) q_{3n} (experimental result).

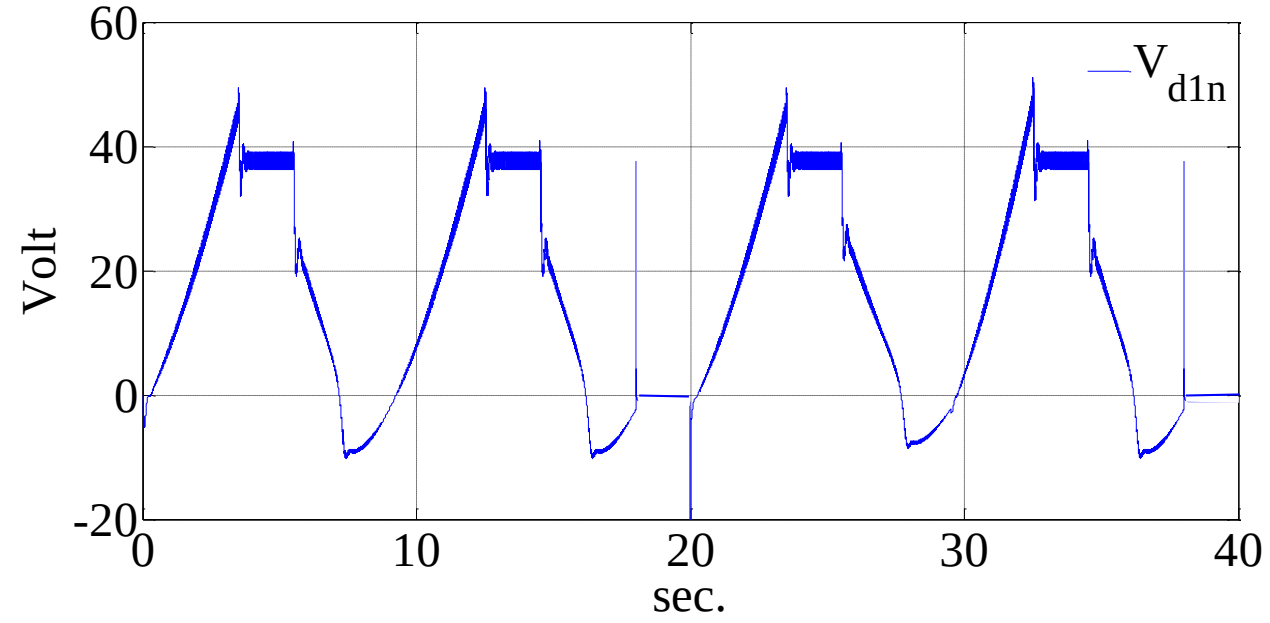

(a)

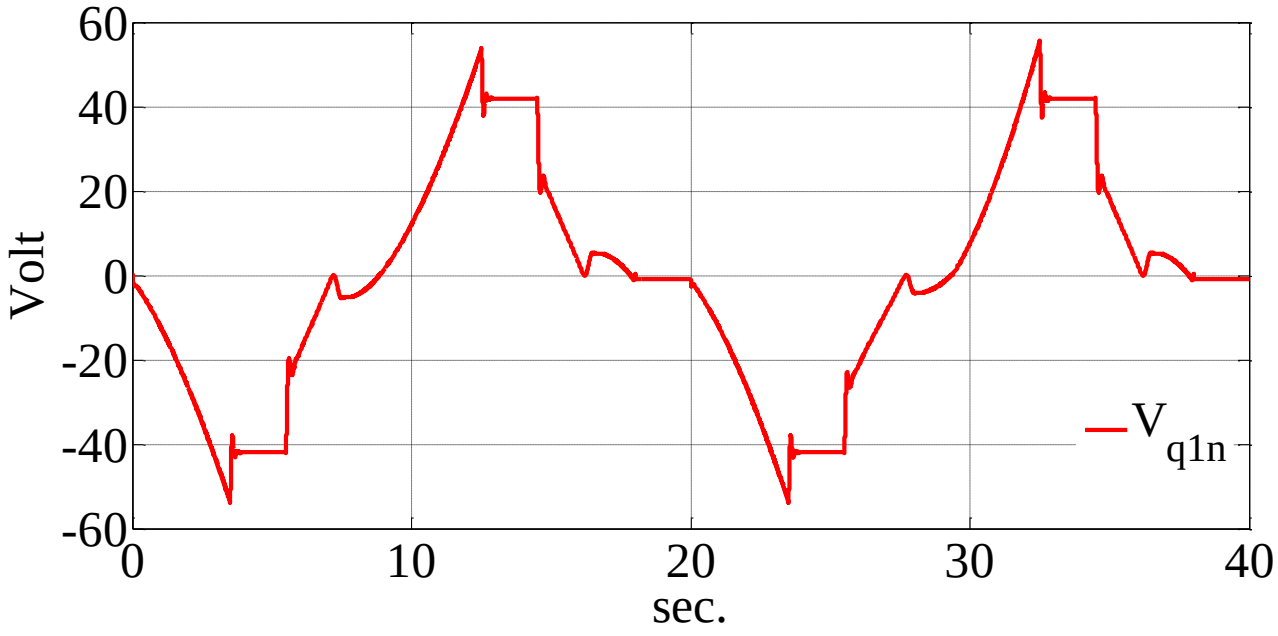

(b)

Figure 6.39: The voltages generated by the current regulators in the decoupled reference frame, (a) d_{1n} axis, (b) q_{1n} axis (simulation results)

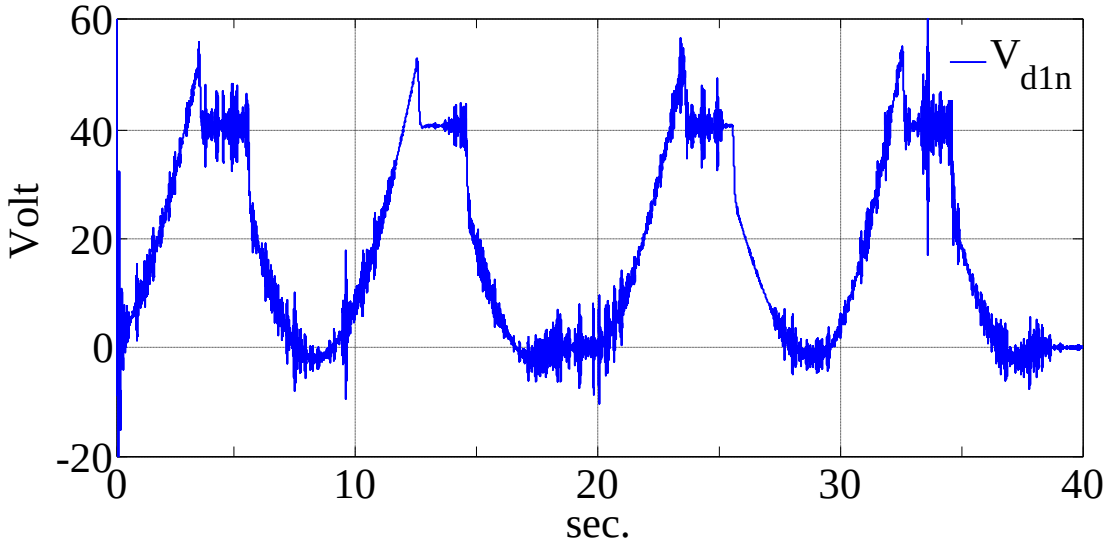

(a)

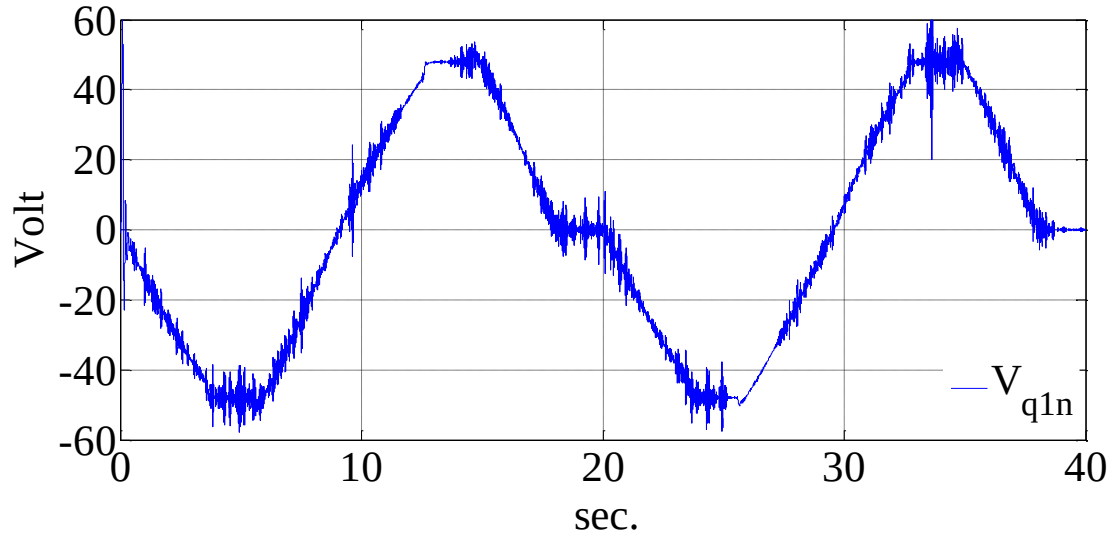

(b)

Figure 6.40: The voltages generated by the current regulators in the decoupled reference frame, (a) d_{1n} axis, (b) q_{1n} axis (experimental results).

The currents shown for the decoupled axis are generated by the output voltages of the current regulators. Figures 6.39 and 6.40 show the output voltages of the current regulators in the decoupled reference frame for simulation and experimental results respectively. It can be seen that, the voltages are regulating the stator currents and they are proportional to the stator currents. The

voltages of the qd_{2n} axis are presented in Figures 6.41 and 6.42 for simulation and experimental results respectively.

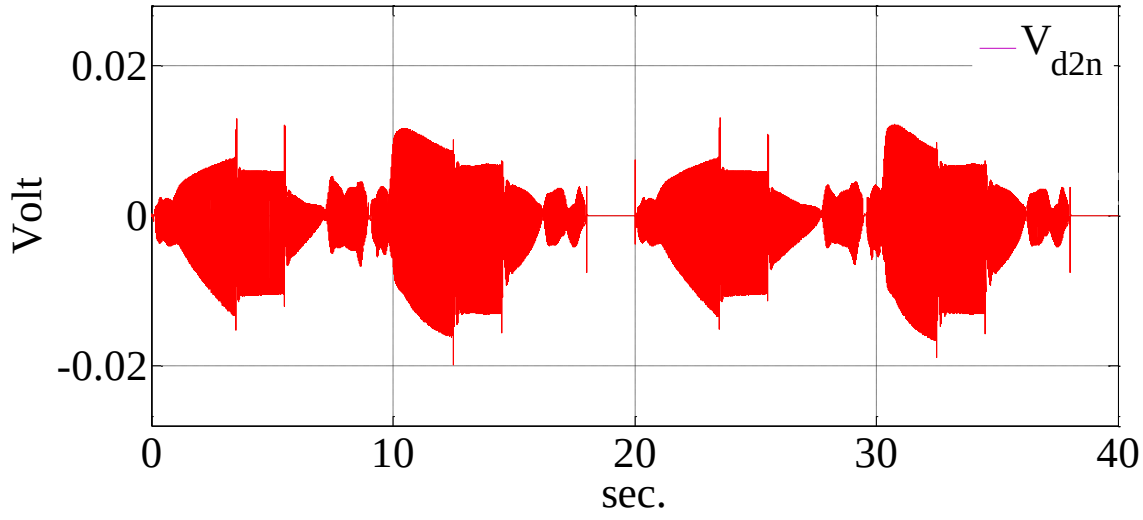

(a)

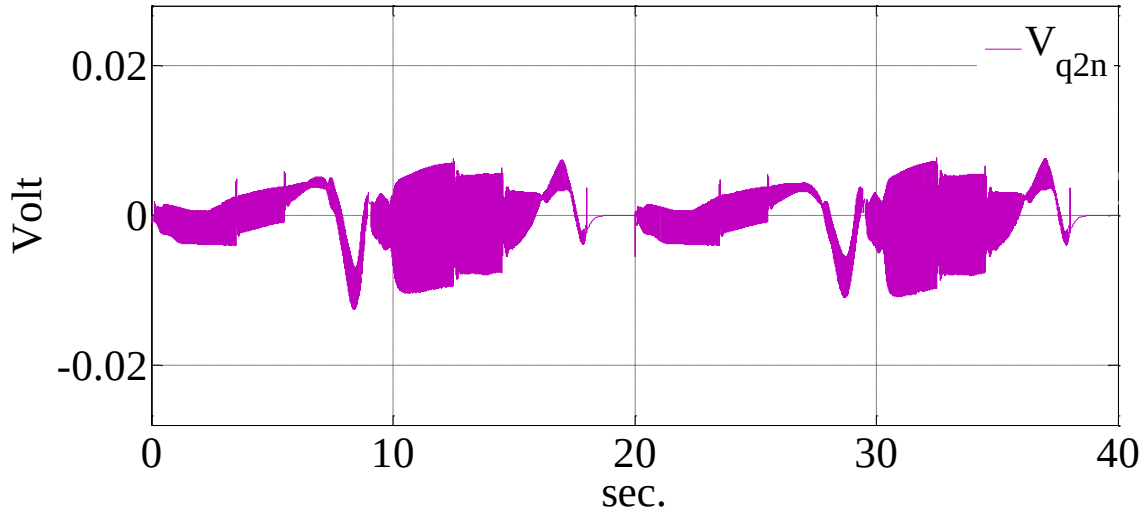

(b)

Figure 6.41: The voltages generated by the current regulators in the decoupled reference frame, (a) d_{2n} axis, (b) q_{2n} axis (simulation results).

Similarly, the voltages of qd_{3n} axis are shown in Figures 6.43 and 6.44 for simulation and experimental results respectively. These voltages are regulating currents of very small inductances of non-torque producing channels therefore, their magnitudes are relatively small.

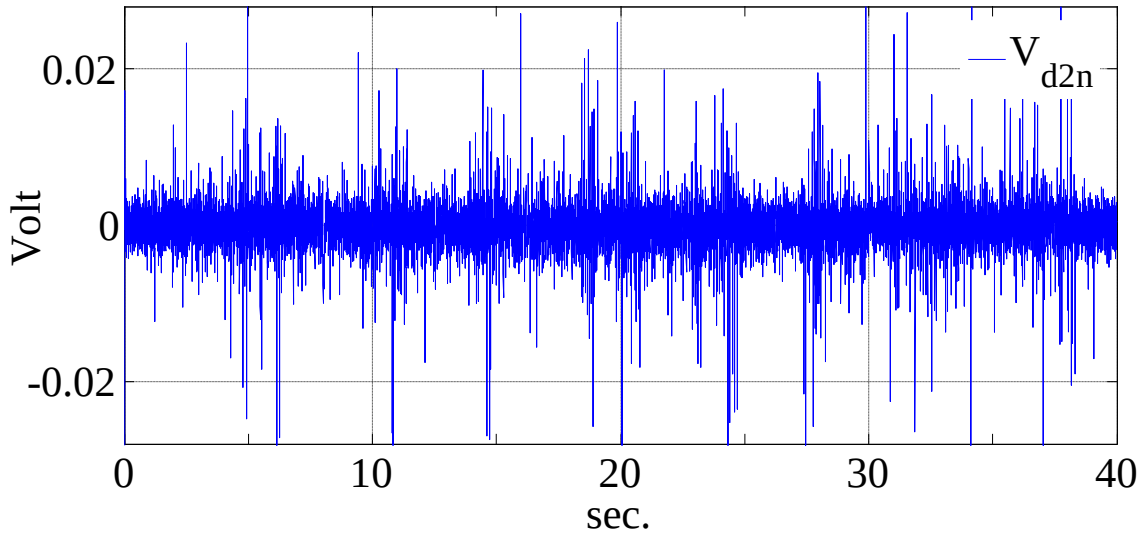

(a)

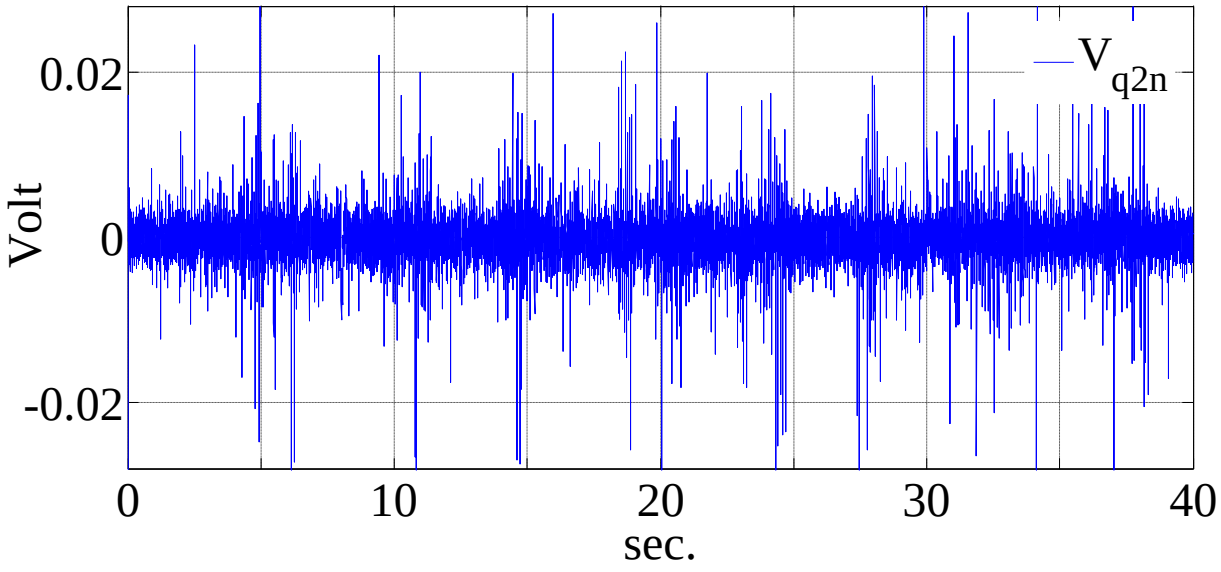

(b)

Figure 6.42: The voltages generated by the current regulators in the decoupled reference frame, (a) d_{2n} axis, (b) q_{2n} axis (experimental results).

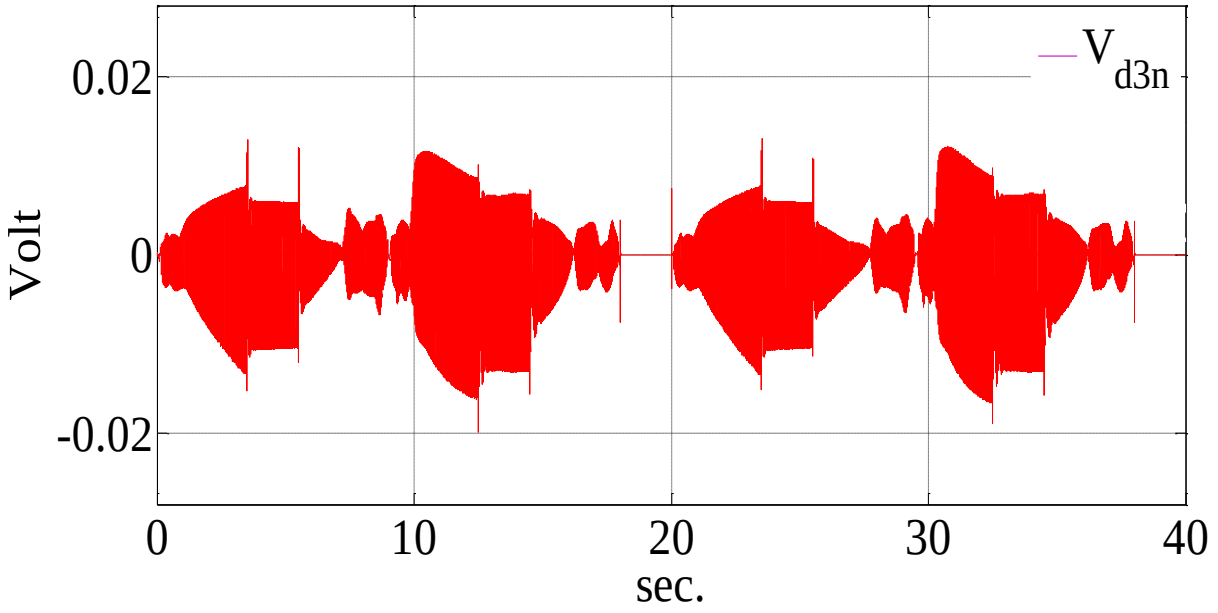

(a)

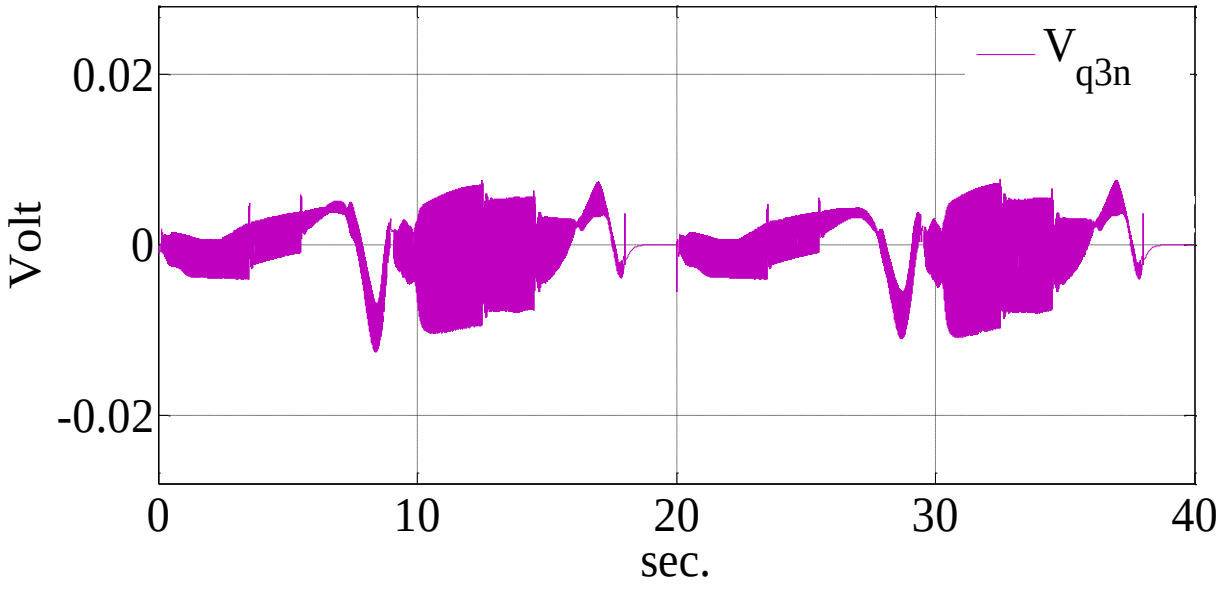

(b)

Figure 6.43: The voltages generated by the current regulators in the decoupled reference frame, (a) d_{3n} axis, (b) q_{3n} axis (simulation results).

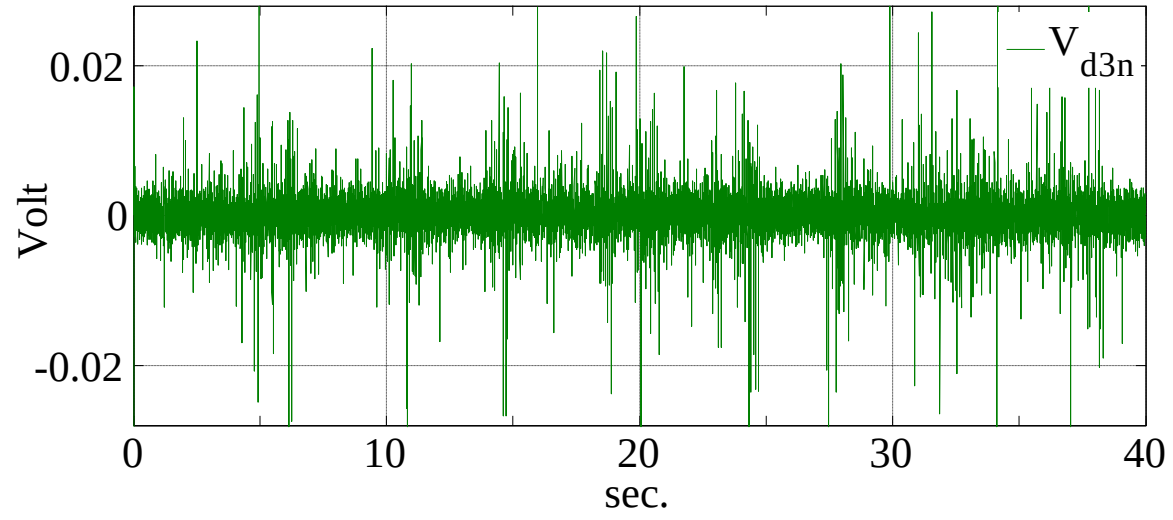

(a)

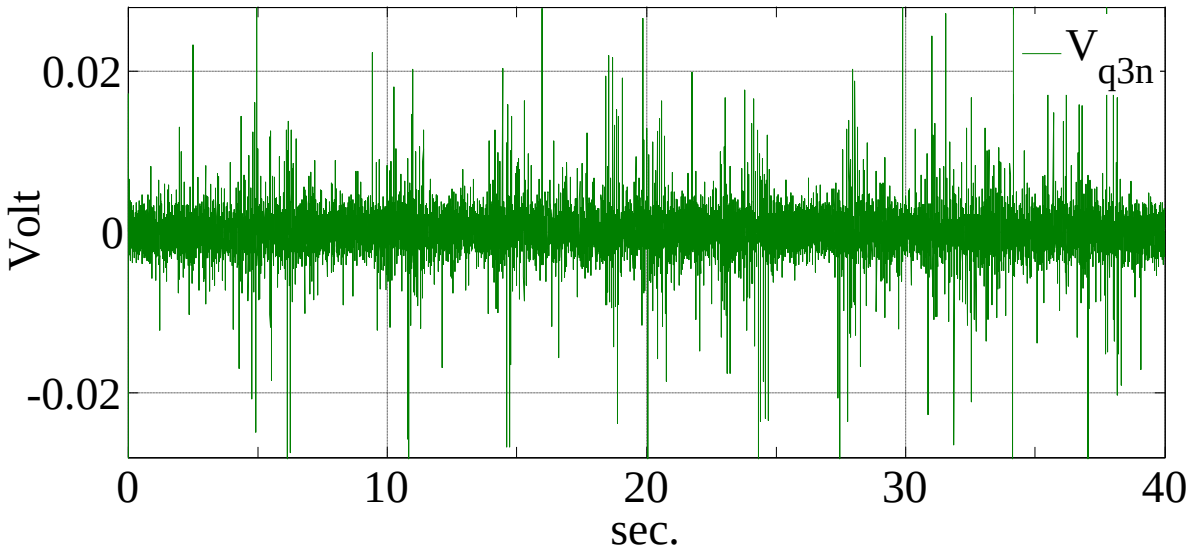

(b)

Figure 6.44: The voltages generated by the current regulators in the decoupled reference frame, (a) d_{3n} axis, (b) q_{3n} axis (experimental results).

The voltages that are generated by current regulators need to be transformed to natural variables to be applied to machine. Before they can be transformed to natural variables, they are

transformed to rotor reference frame. Figures 6.45 and 6.46 show the voltages of the machines in rotor reference frame for simulation and experimental results respectively.

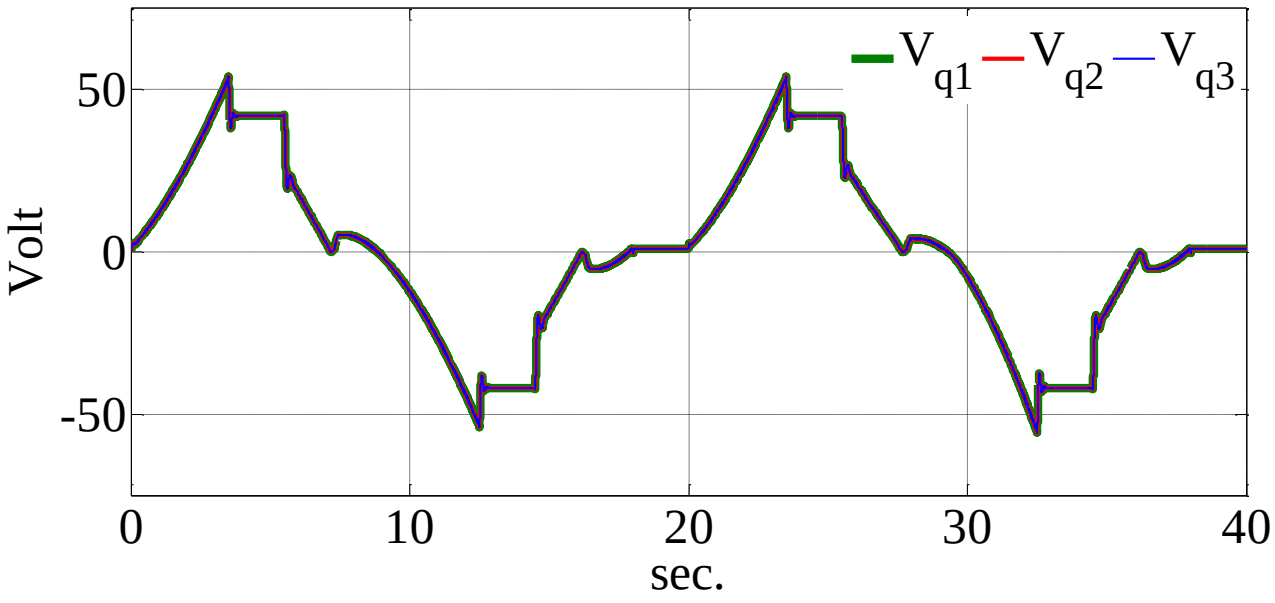

(a)

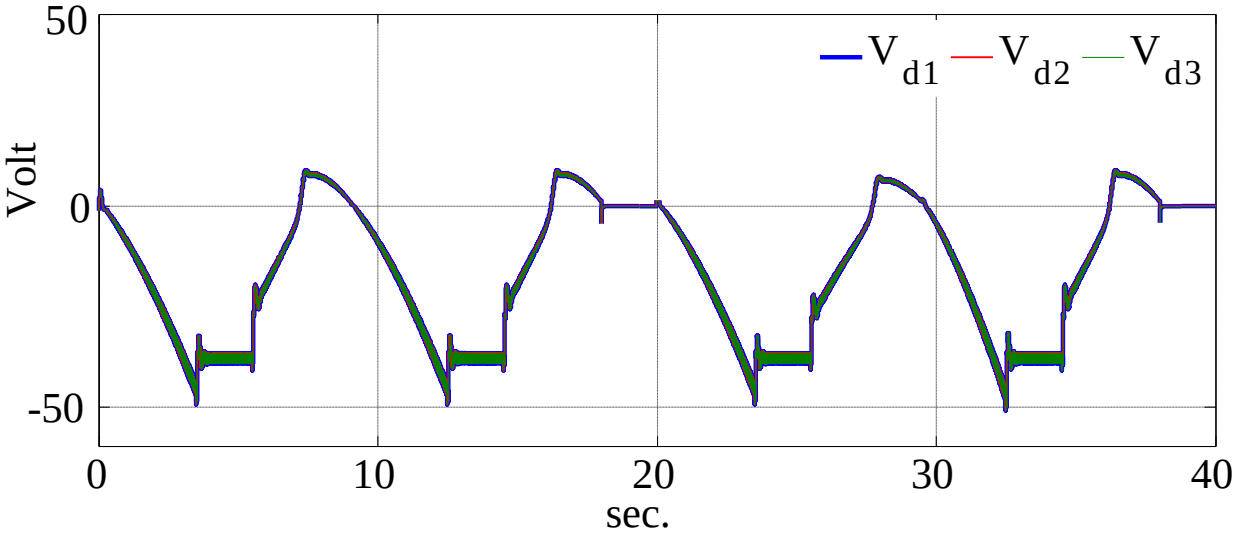

(b)

Figure 6.45: The voltages generated by the current regulators in the rotor reference frame (a) q axis, (b) d axis (simulation results).

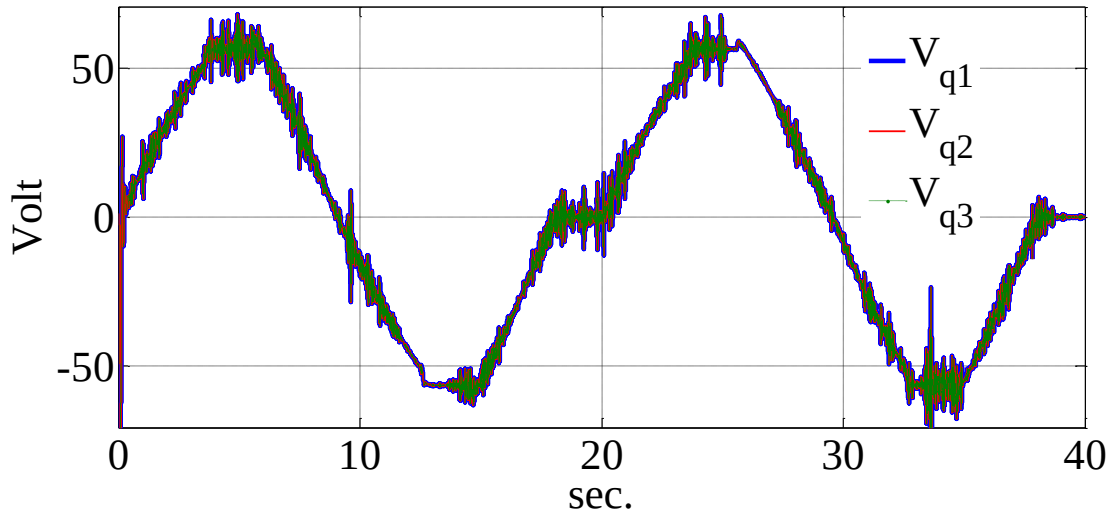

(a)

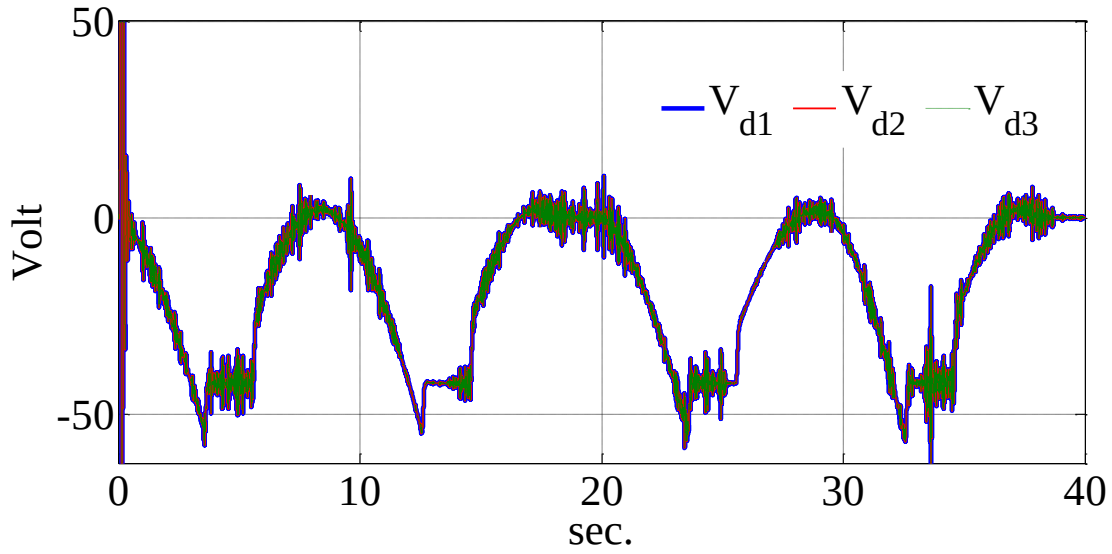

(b)

Figure 6.46: The voltages generated by the current regulators in the rotor reference frame, (a) q axis, (b) d axis (experimental results).

The currents and the machine stator in the rotor reference frame for simulation and experimental results are also shown in the Figure 6.47 and Figure 6.48 respectively.

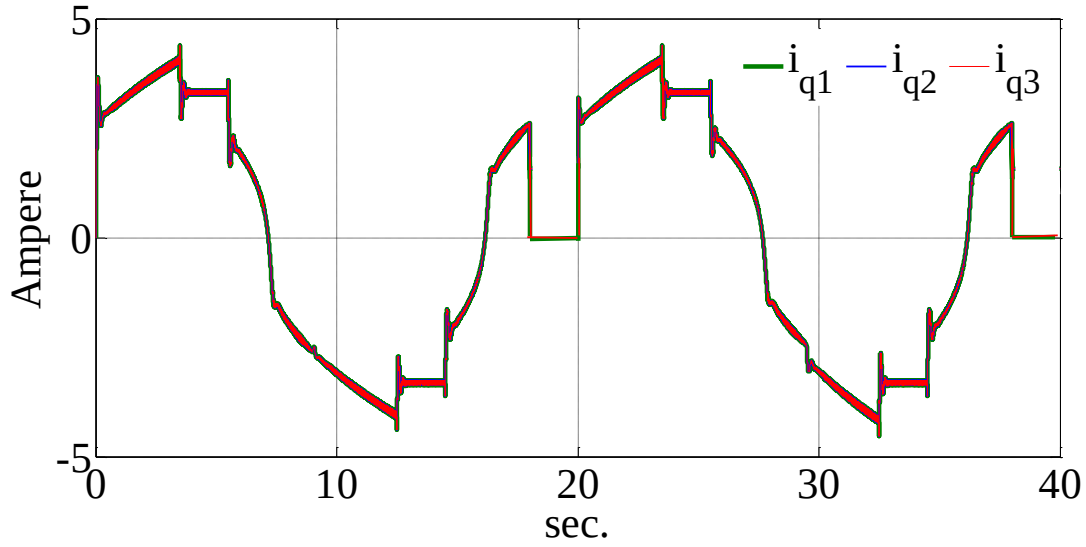

(a)

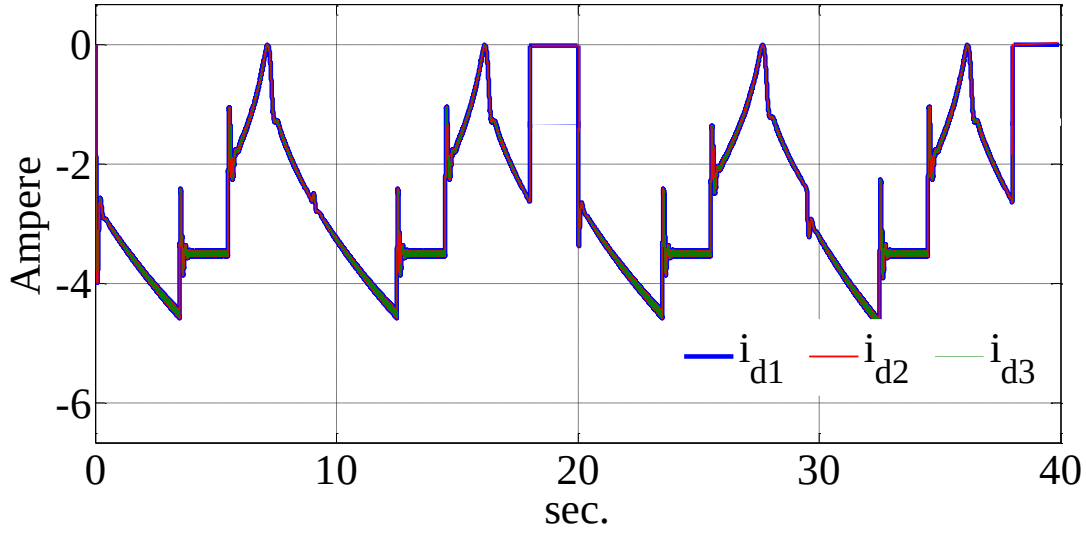

(b)

Figure 6.47: The stator current generated by the current regulators in the rotor reference frame, (a) q axis, (b) d axis (simulation results).

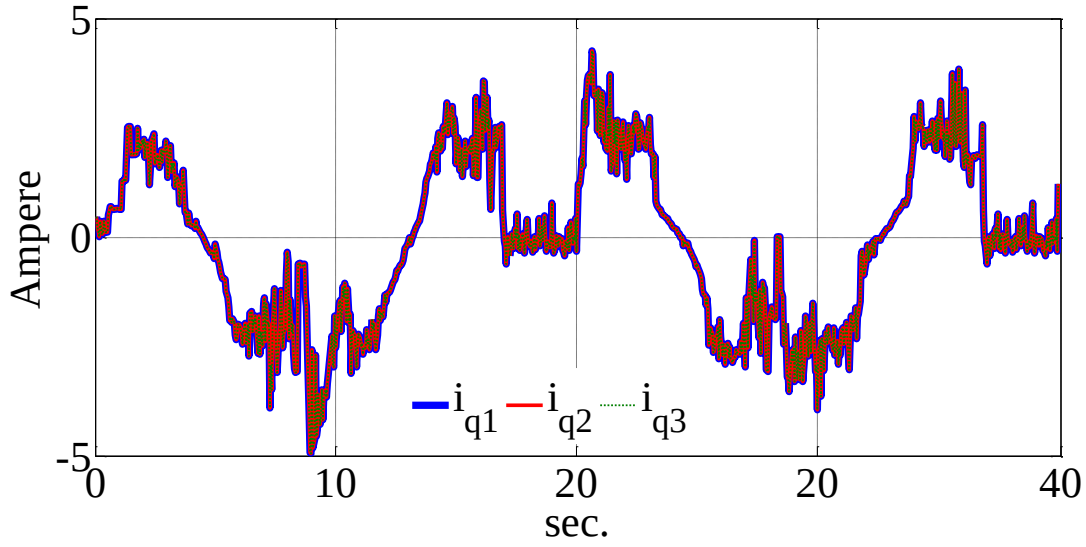

(a)

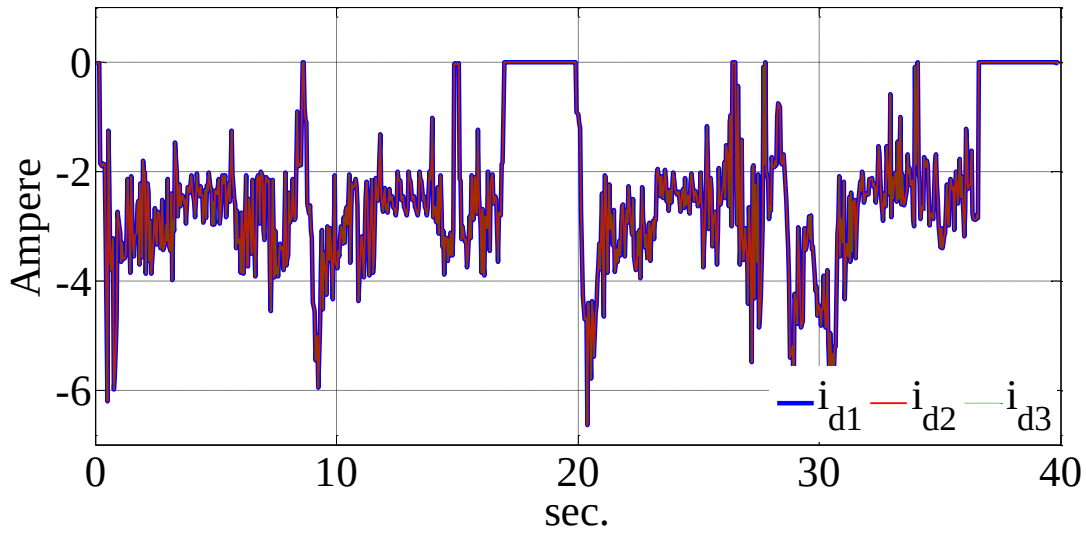

(b)

Figure 6.48: The stator current generated by the current regulators in the rotor reference frame, (a) q axis, (b) d axis (experimental results).

Figure 6.49 and 6.50 show the same voltages and currents in the natural variables respectively. Also the spectrum of the phase currents is shown in the Figure 6.51. The speed

dependent components can be seen around the main 920 (Hz). These components are used for position estimation.

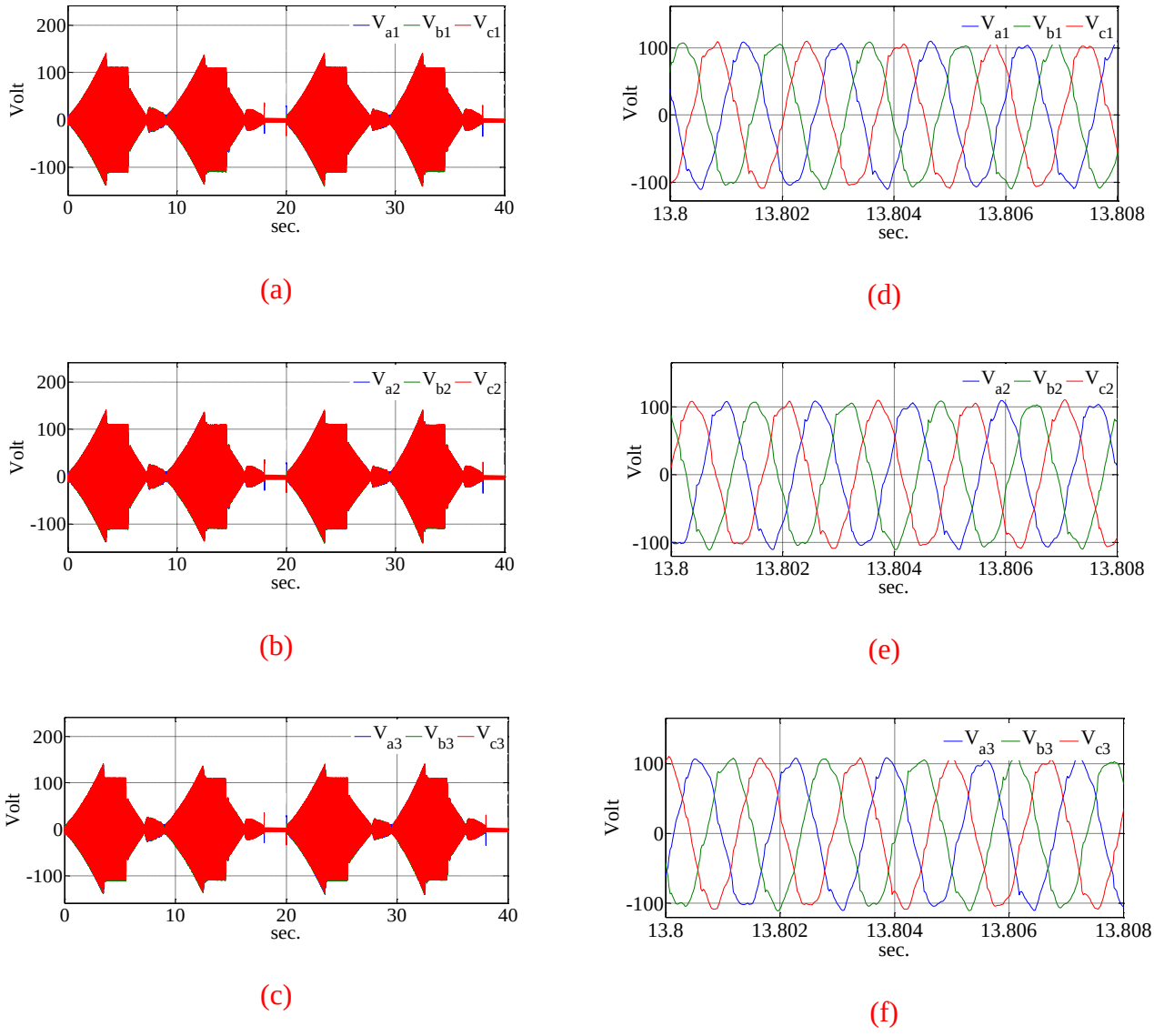

Figure 6.49: The voltages generated by the current regulators in natural variables for, (a) Machine 1, (b) Machine 2 ,(c) Machine 3 and the zoomed view of the voltages for, (d) Machine 1,(e) Machine 2 ,(f) Machine 3.

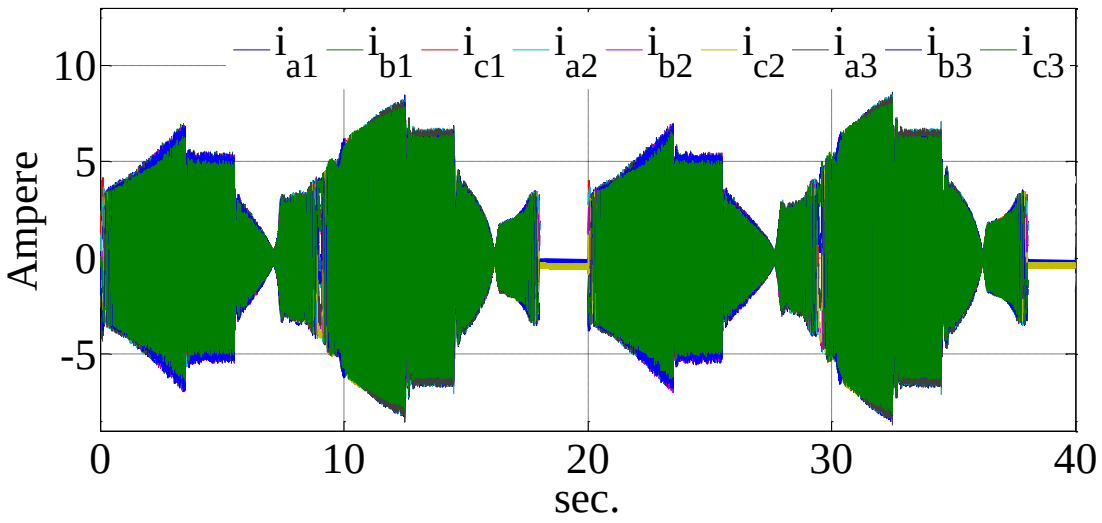

Figure 6.50: The stator current generated by the current regulators in the natural variables.

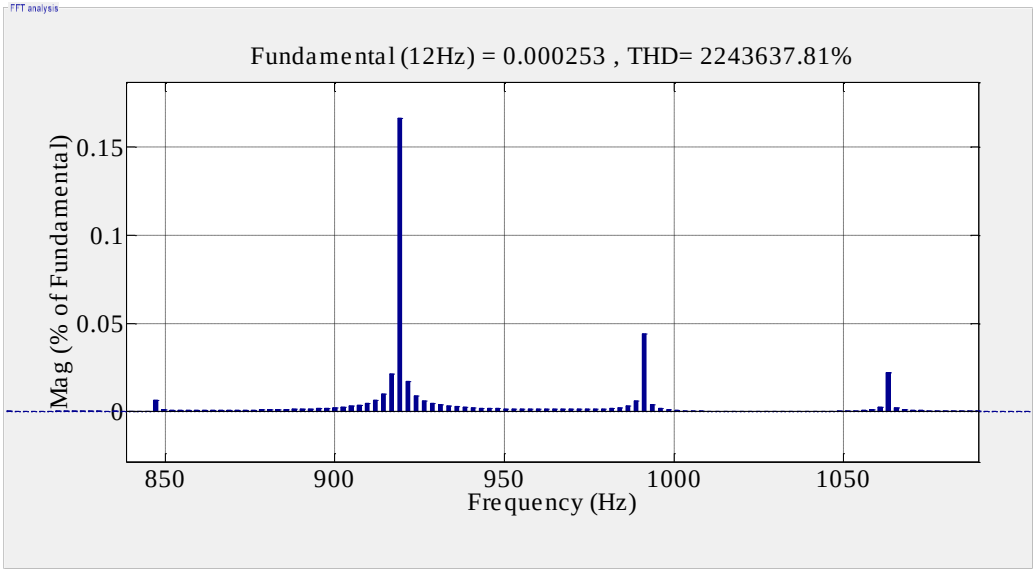

Figure 6.51: The spectrum of the phase ‘a’ current.

Figure 6.52 shows the current of each machine separately for a short time interval. For simulation results. The high frequency ripples can be seen on the phase currents.

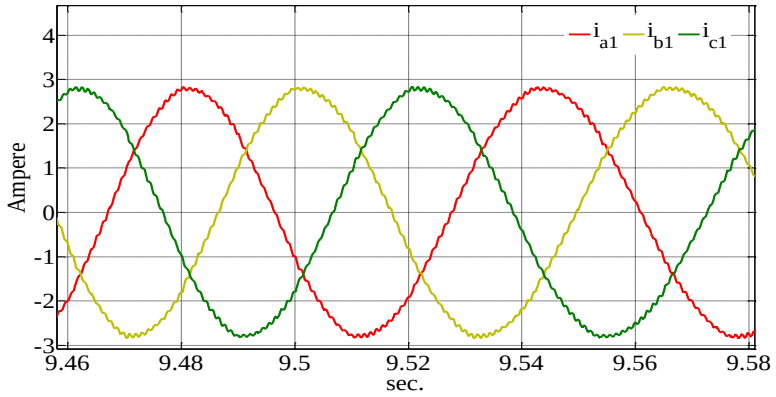

(a)

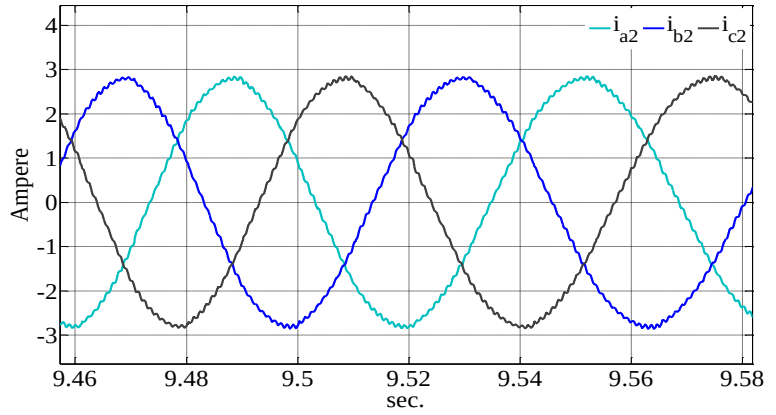

(b)

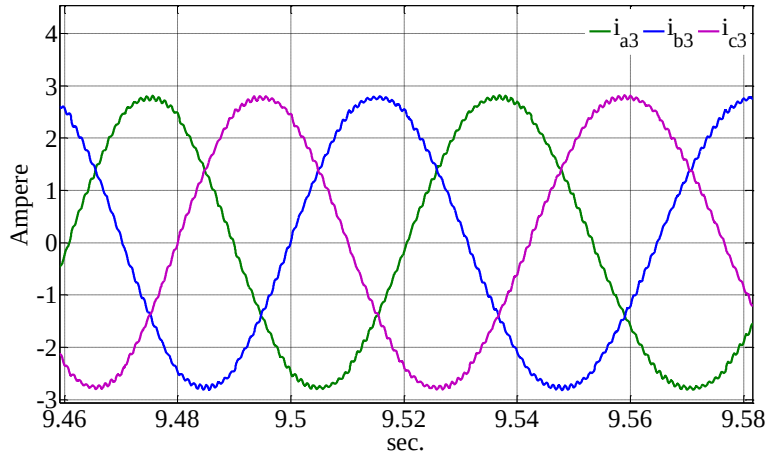

(c)

Figure 6.52: The current generated by the current regulators in natural variables, (a) Machine 1, (b) Machine 2, (c) Machine 3 (simulation results).

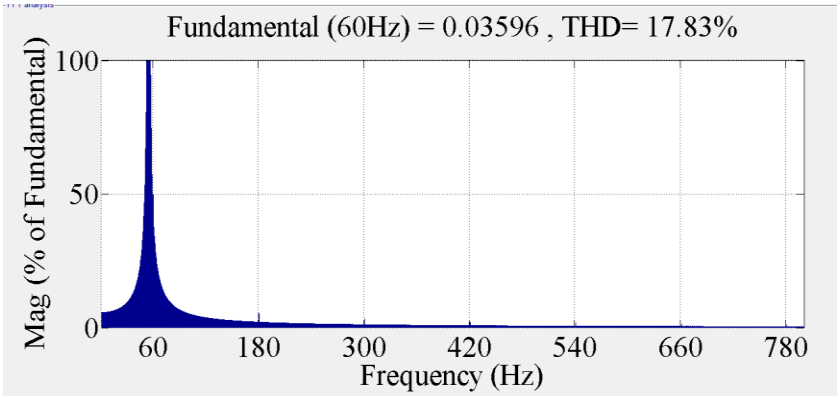

(a)

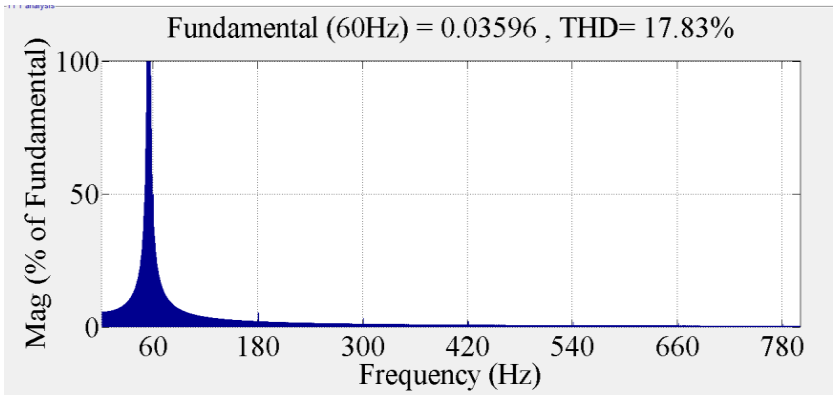

(b)

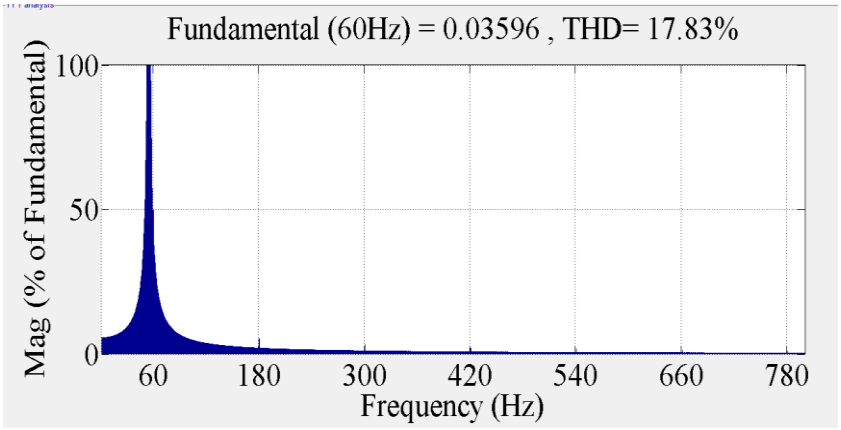

(c)

Figure 6.53: The spectrum of the phase ‘a’ current generated by the current regulators in natural variables, (a) Machine 1, (b) Machine 2, (c) Machine 3 (simulation results).

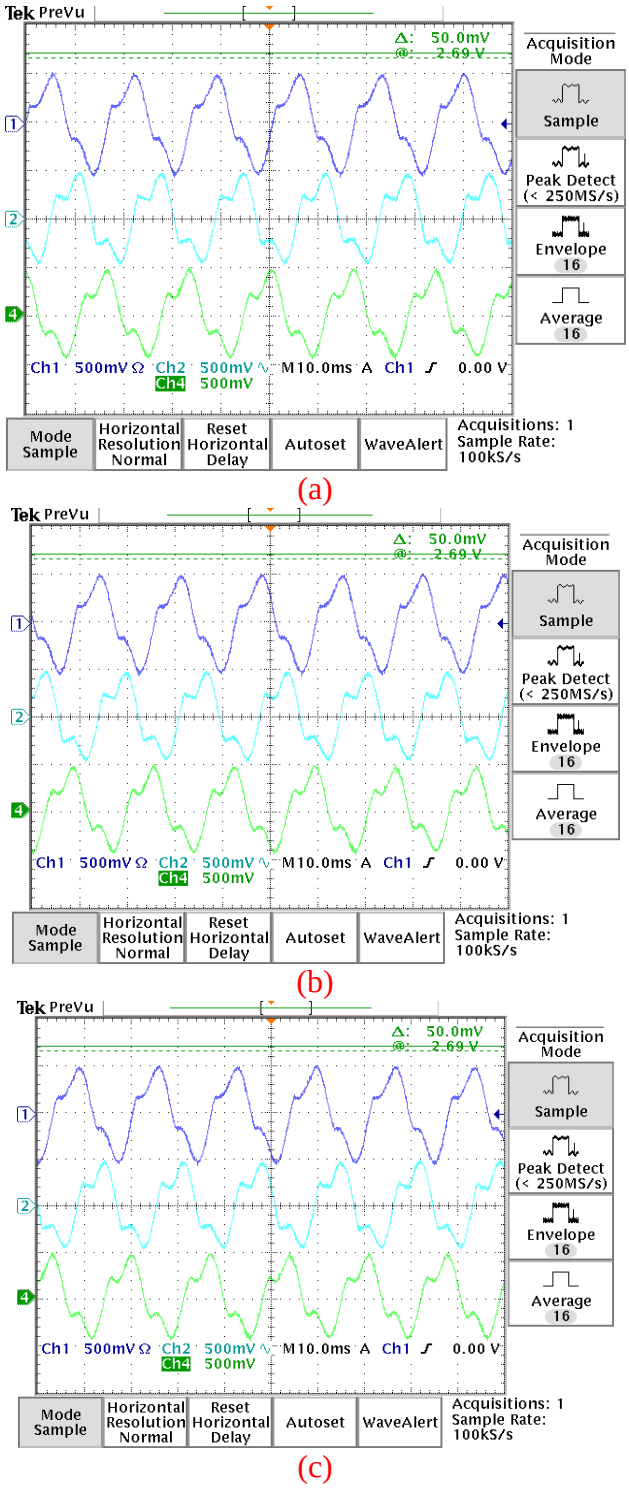

Figure 6.54: The nine-phase currents of the machine for phases, (a) 'a_1', 'b_1' and 'c_1', (b) 'a_2', 'b_2' and 'c_2' (c) 'a_2', 'b_2' and 'c_2' (experimental results) (5 A/ scale) (experimental results).

The spectrum of the phase ‘a’ currents of each machine are also shown in the Figure 6.53. From the spectrum it can be seen that the currents have less ripples than the currents of the open loop machine simulated in chapter 3. The lower ripples are due to the effect of the current regulators. The main component is used for the controller feedback and the high frequency component is used for the signal processing procedure and position estimation. The high frequency part is extracted using the transformation matrix in the equation (6.176), by considering the currents as a 9 phase set and extract the fifth sequence. Figure 6.54 shows the machines currents for experimental results. The effect of the nonlinear parameters of machine such as magnetic saturation which are neglected in simulation can cause some differences in the simulation and experimental results. The ripples on the experimental results are due to the un-modeled nonlinearities of the machine. The spectrums of the machine currents are also show in the Figure 6.55. The fifth sequence currents of the stator that are extracted using equation (6.167) are shown in Figures 6.56 and 6.57 for simulation and experimental results respectively. The fifth sequence currents can be used for position estimation. The currents in the Figure 6.56 and 6.57 pass through a heterodyning block then, they pass through a low pass filter to remove their redundant high frequency parts. Figures 6.58 and 6.59 show the resulting currents after filtering and heterodyning for simulator and experimental results respectively.

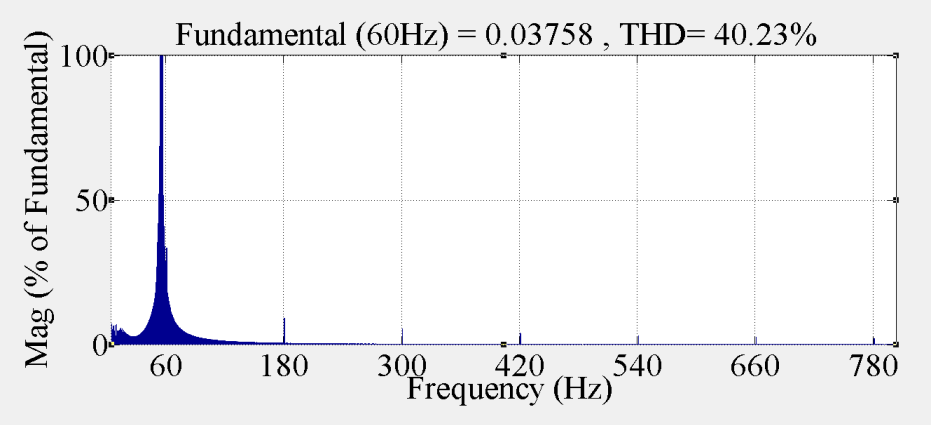

(a)

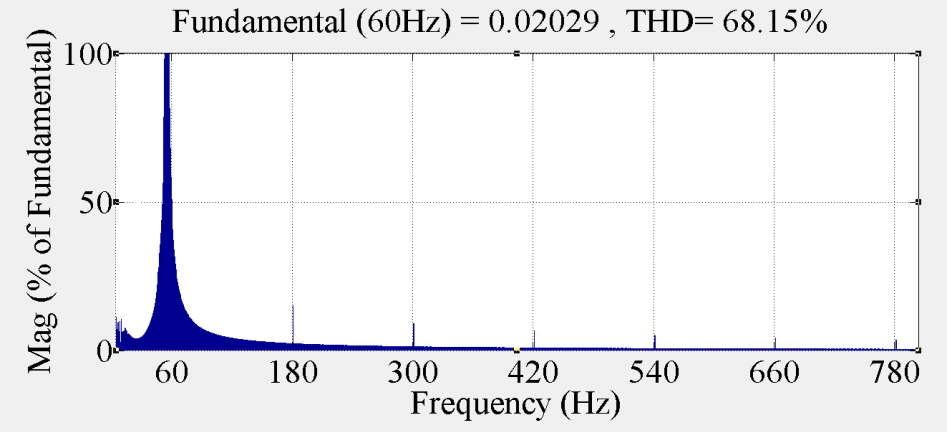

(b)

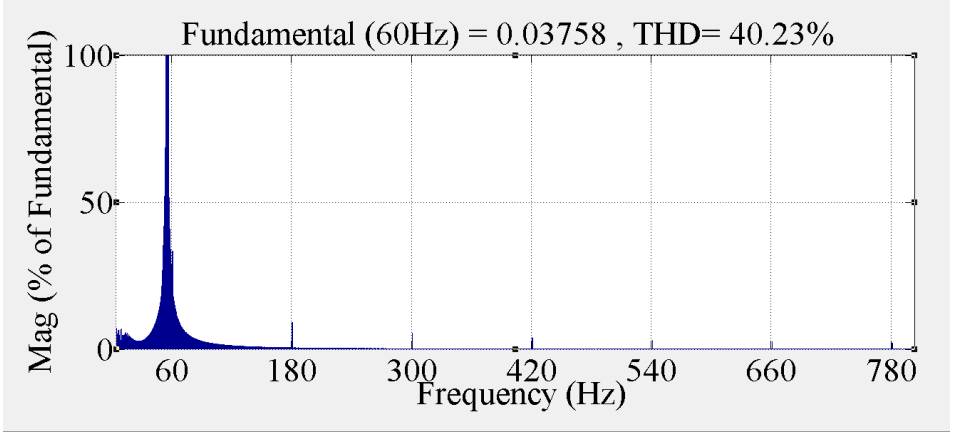

(c)

Figure 6.55: The spectrum of the phase ‘a’ current of the machines for, (a) Machine 1, (b) Machine 2, (c) Machine 3 (experimental results).

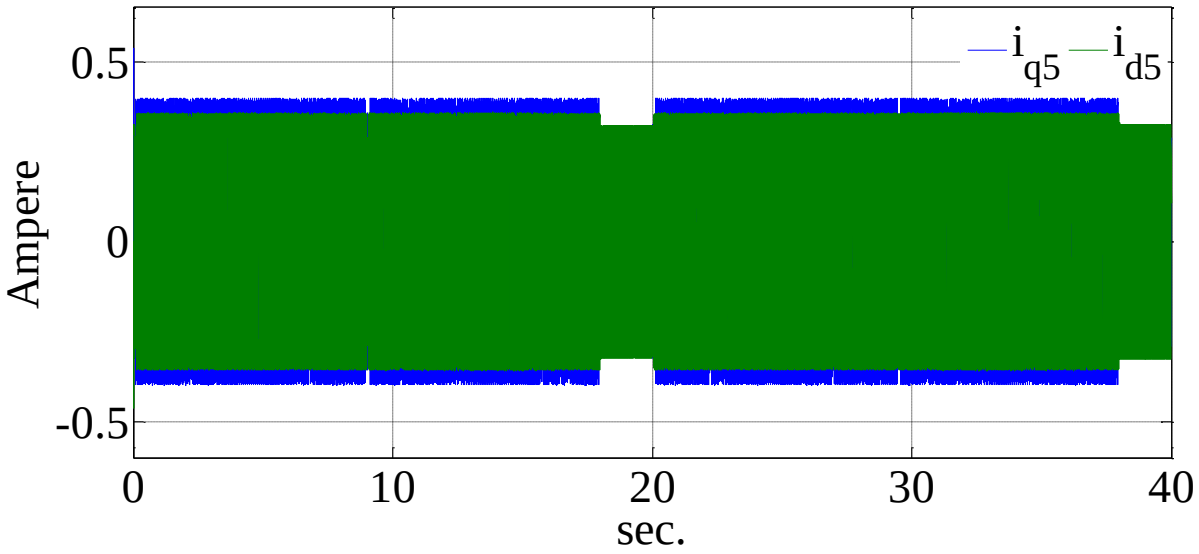

(a)

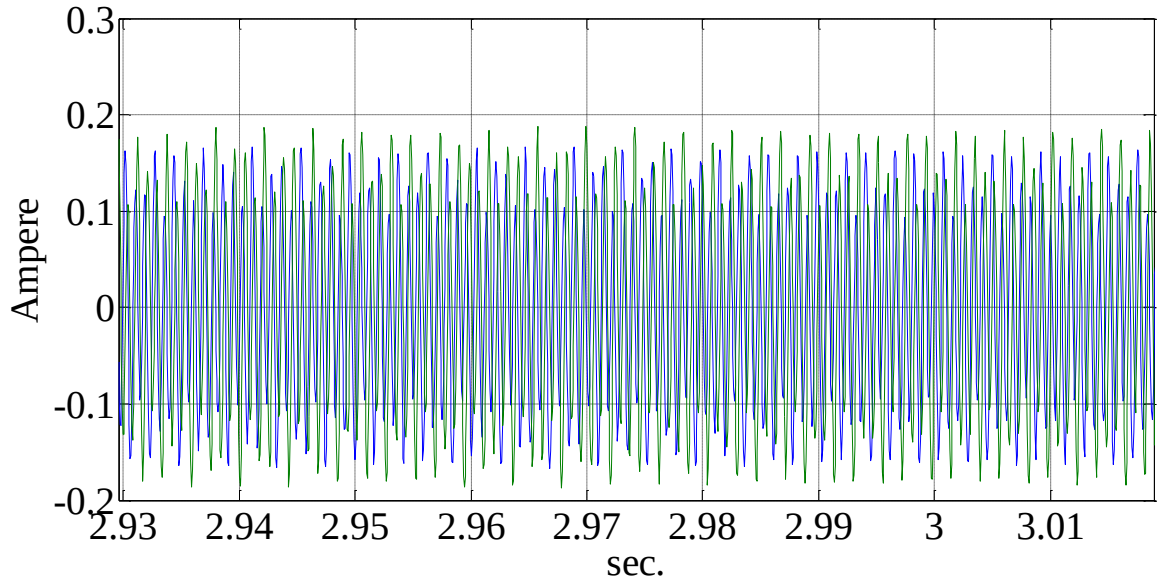

(b)

Figure 6.56: (a) The fifth sequence of the stator current in the stationary reference frame, (b) The zoomed view (simulation results).

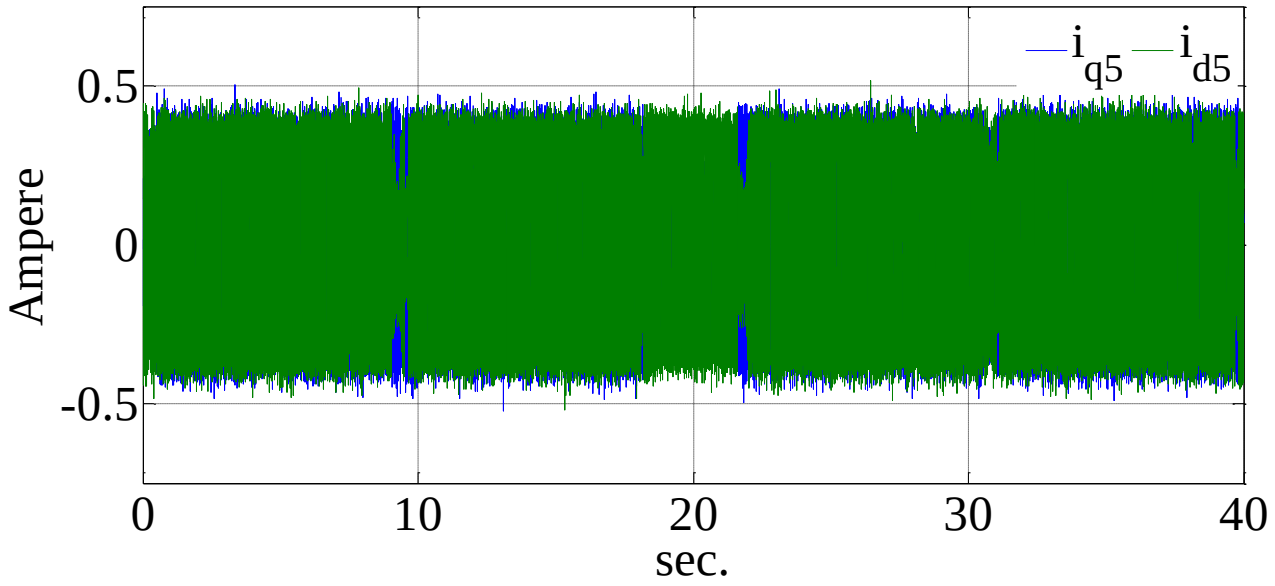

(a)

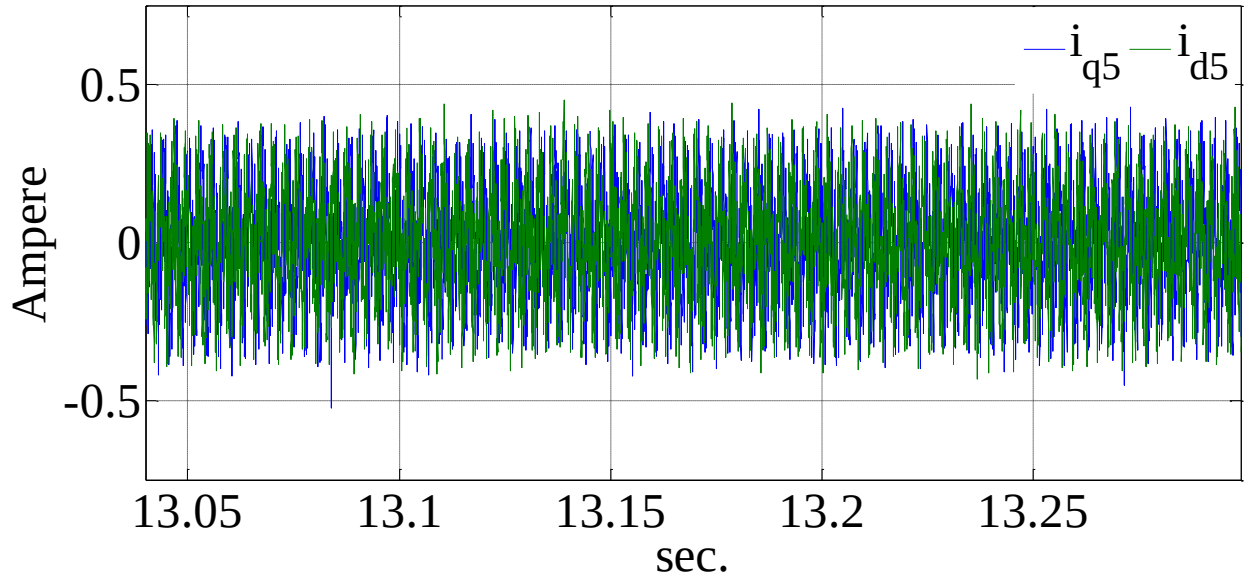

(b)

Figure 6.57: (a) The fifth sequence of the stator current in the stationary reference frame, (b) The zoomed view (experimental results).

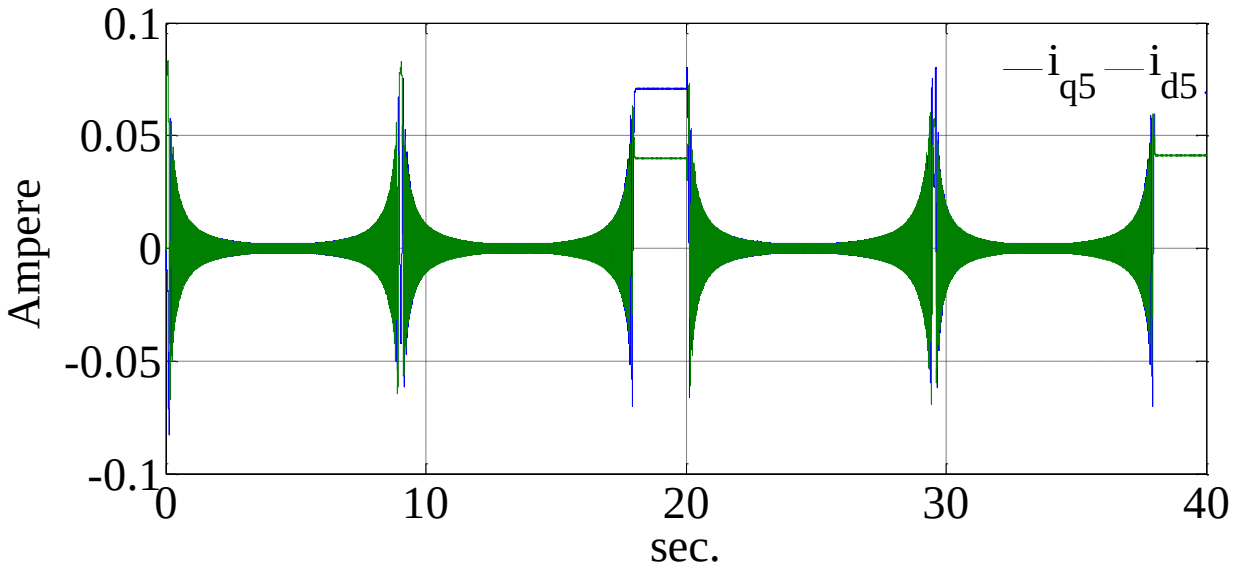

(a)

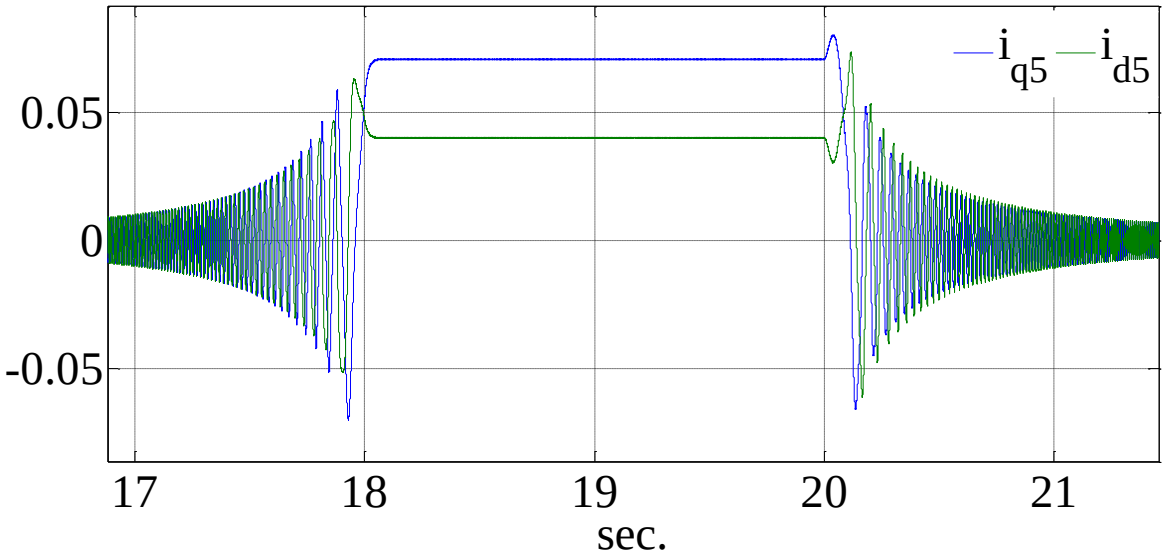

(b)

Figure 6.58: (a) The fifth sequence of the stator current in the stationary reference frame after heterodyning and filtering, (b) The zoomed view (simulation results).

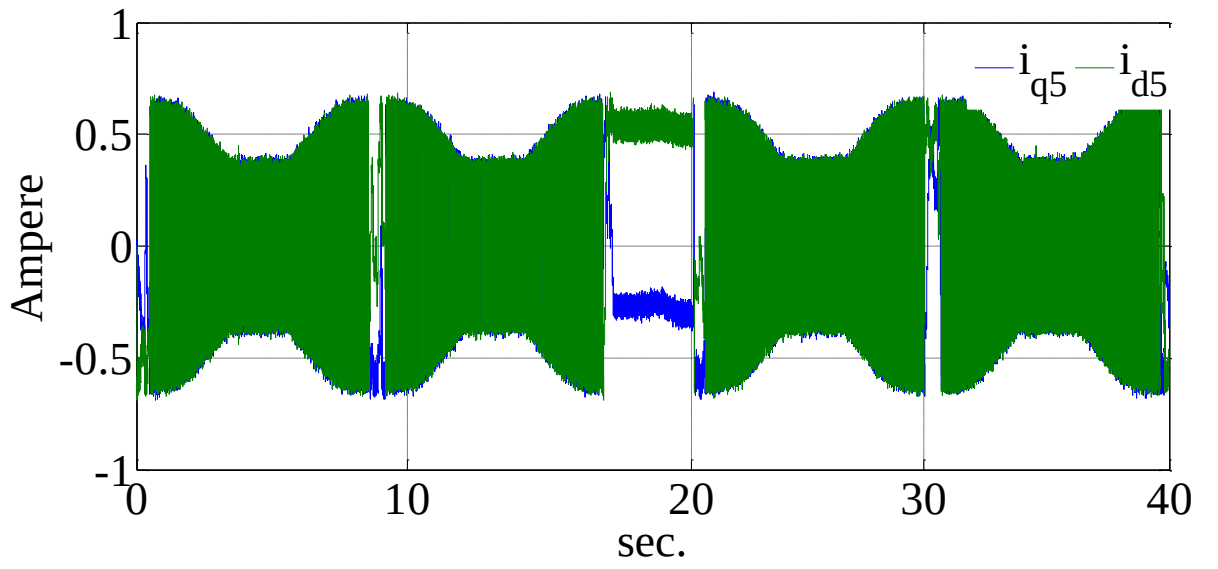

(a)

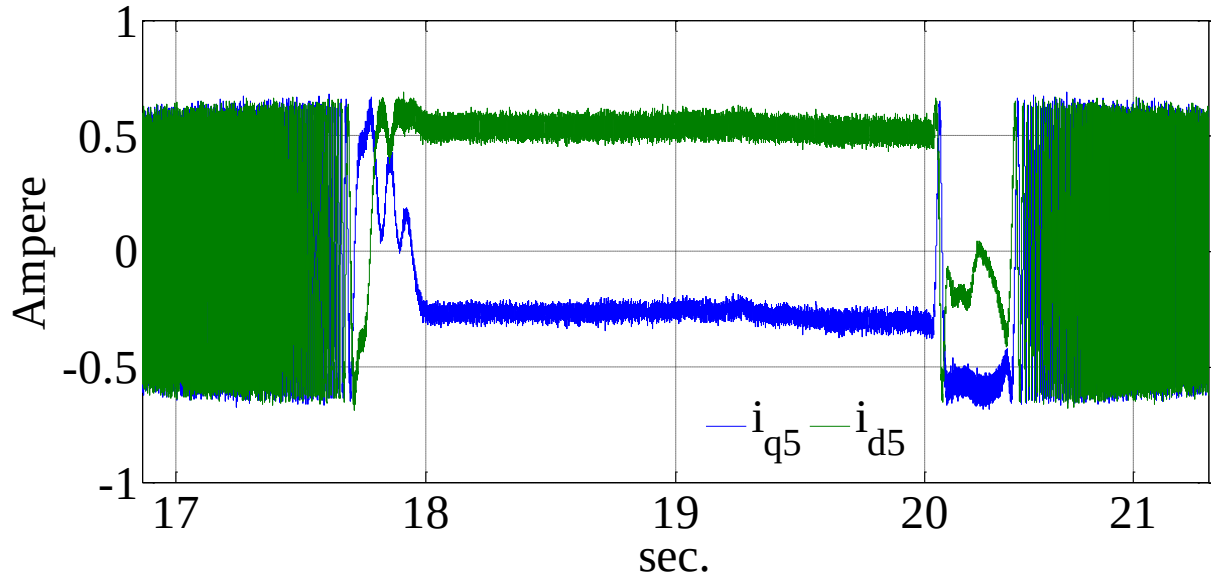

(b)

Figure 6.59: (a) The fifth sequence of the stator current in the stationary reference frame after heterodyning and filtering, (b) The zoomed view (experimental results).

Figures 6.58 and 6.59 show the resulting current after heterodyning and filtering for simulation and experimental results respectively. The currents of the Figures 6.58 and 6.59 need to be normalized to have unity magnitude. After normalizing they are used as the input signals of the observer.

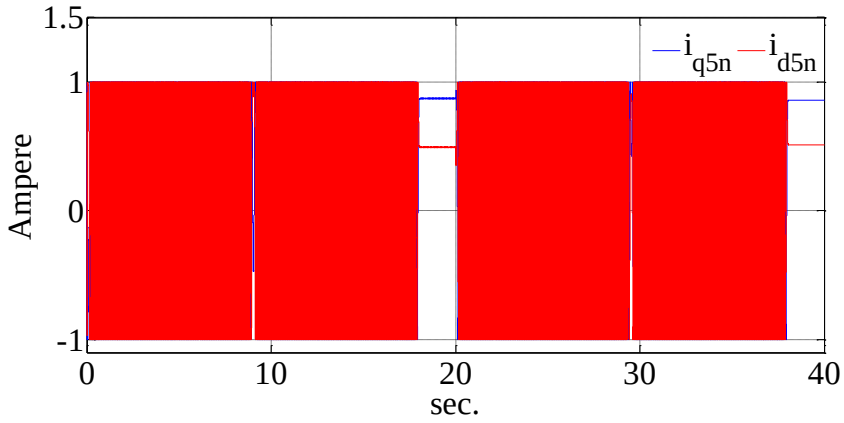

(a)

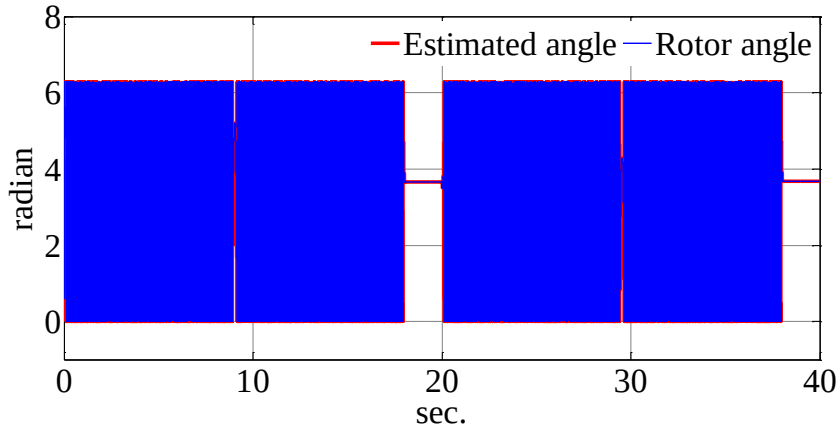

(b)

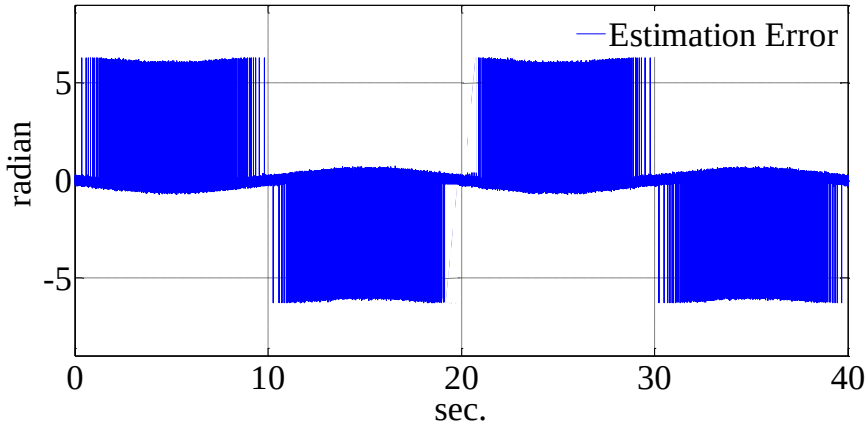

(c)

Figure 6.60: (a) The normalized currents of the fifth sequence (b) The simulated and estimated angle, (c) The estimation error (simulation results).

Figures 6.60 and 6.61 show the normalized currents with the estimated position angle along with estimation error for simulation and experimental results respectively.

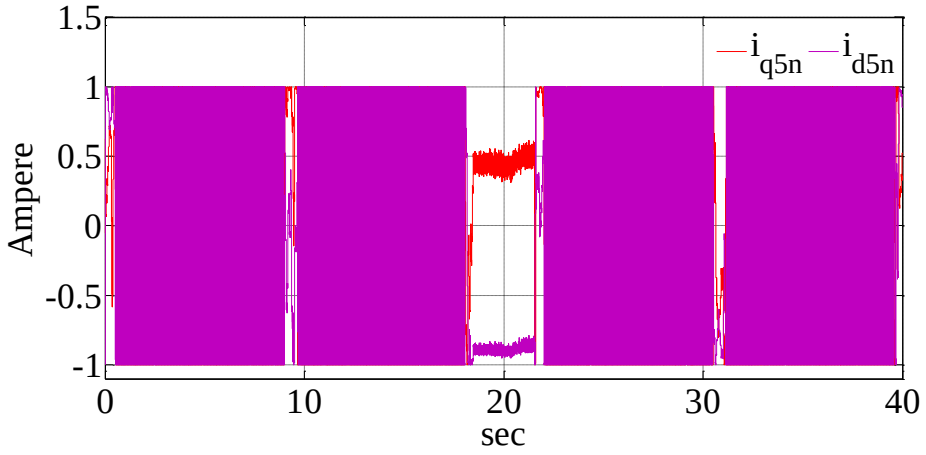

(a)

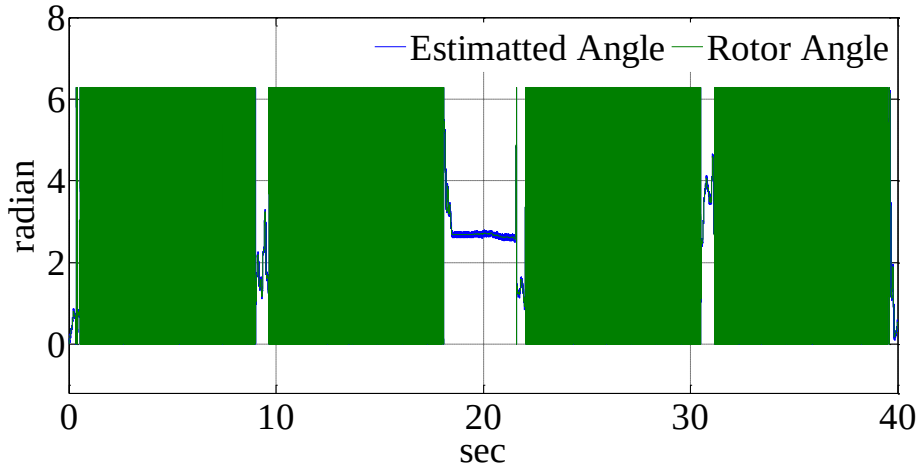

(b)

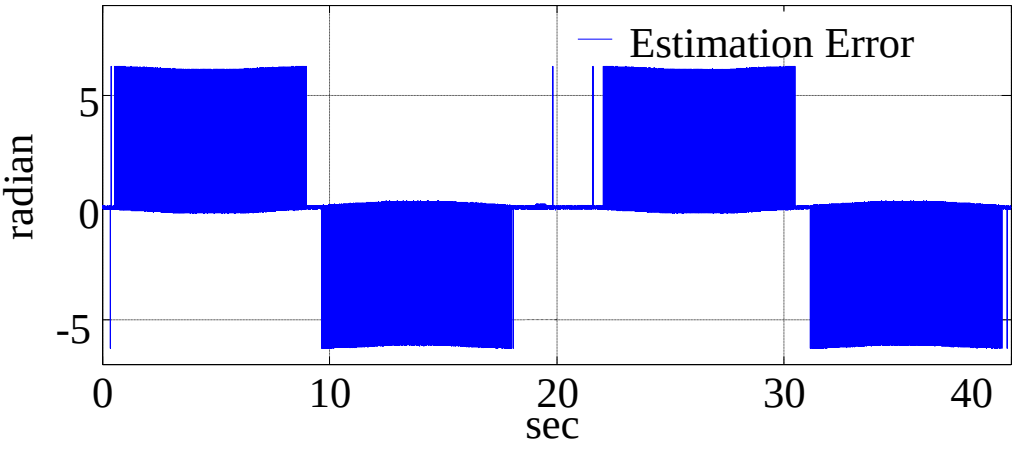

(c)

Figure 6.61: (a) The normalized currents of the fifth sequence, (b) Actual and estimated angle, (c) The estimation error (experimental results).

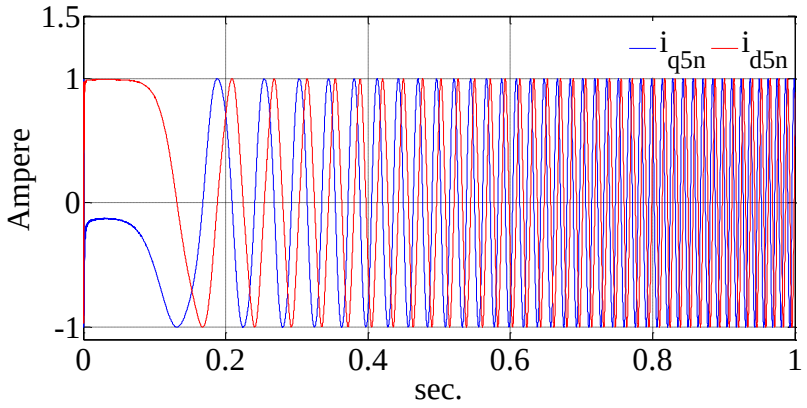

(a)

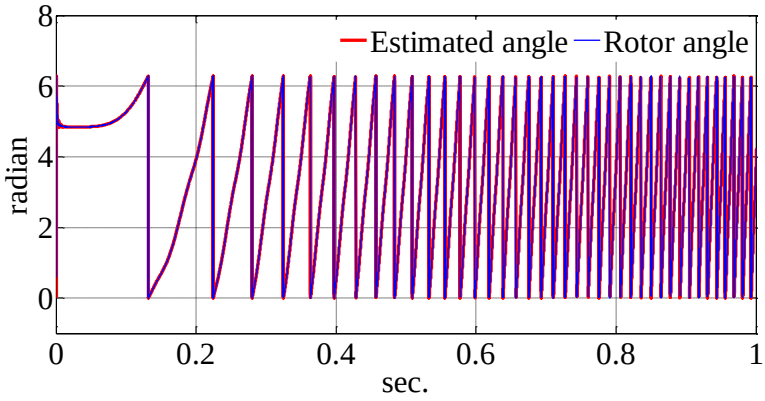

(b)

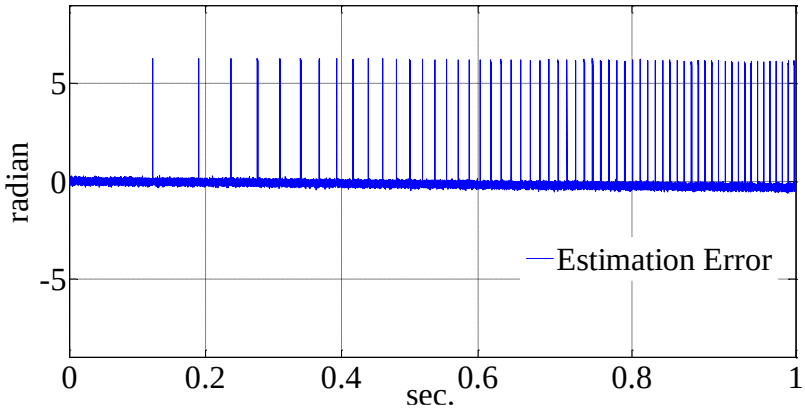

(c)

Figure 6.62: (a) The normalized currents of the fifth sequence, (b) The simulated and estimated angle at the starting interval, (c) Estimation error (simulation results).

The Figures 6.62 to 6.65 show the zoomed views of the same figure during different intervals. From these figures it can be seen that in each operating condition, the estimator tracts the rotor position precisely.

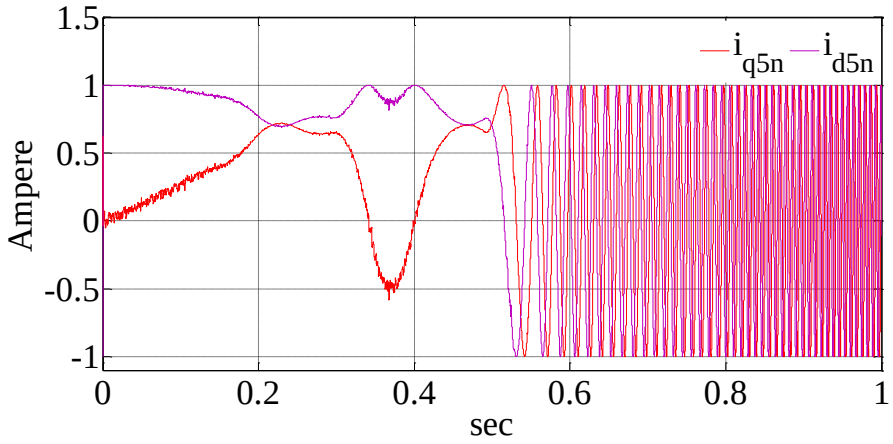

(a)

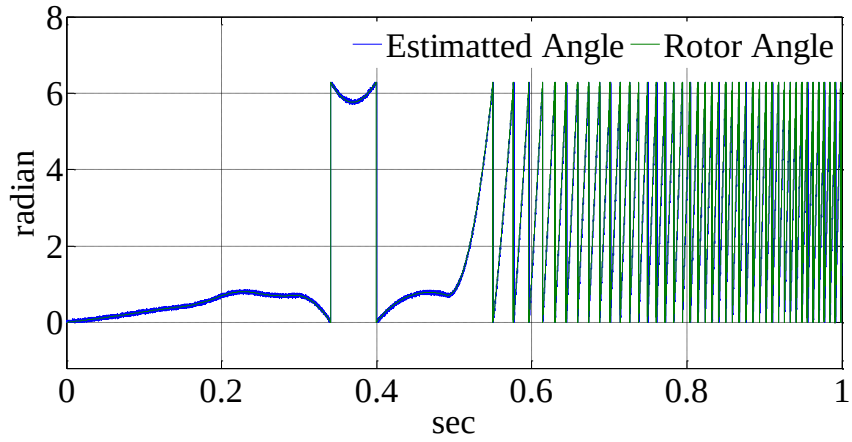

(b)

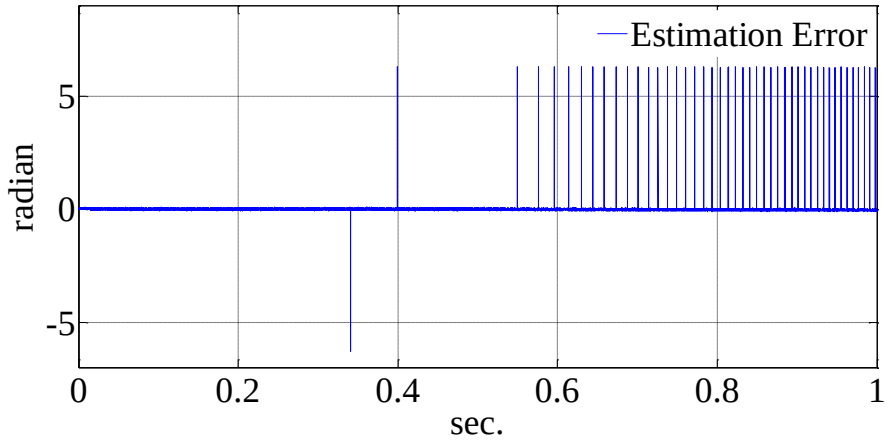

(c)

Figure 6.63: (a) The normalized currents of the fifth sequence, (b) Actual and estimated angle, (c) The estimation error (experimental results).

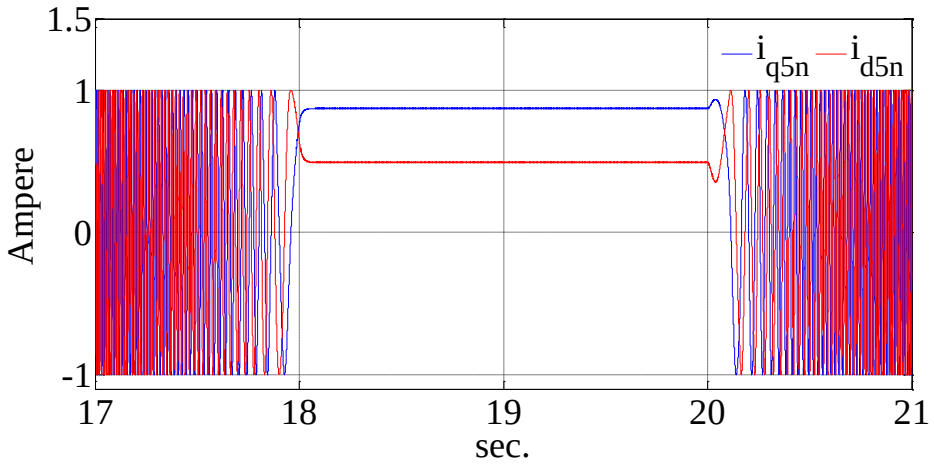

(a)

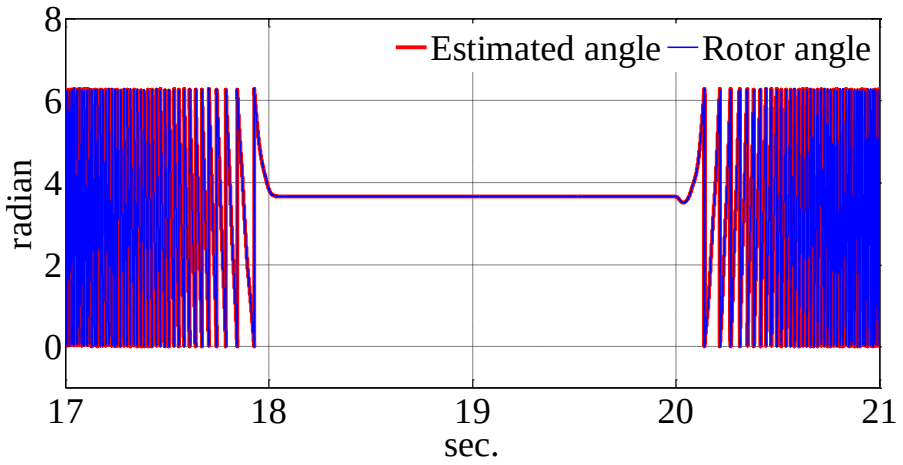

(b)

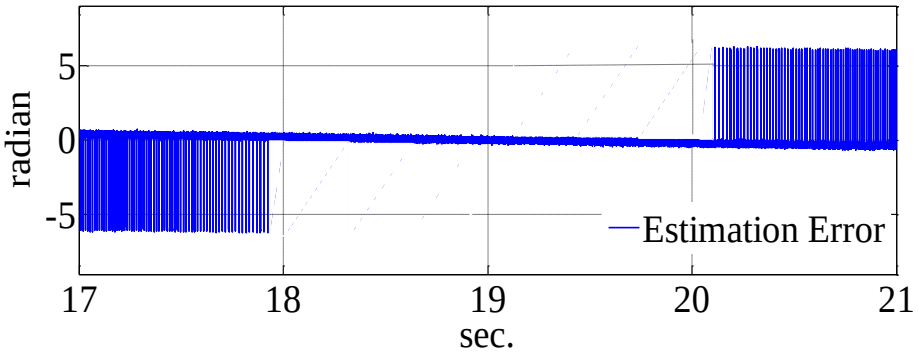

(c)

Figure 6.64: (a) The normalized currents of the fifth sequence, (b) The simulated and estimated angle, (c) Estimation error during the zero speed intervals (simulation results).

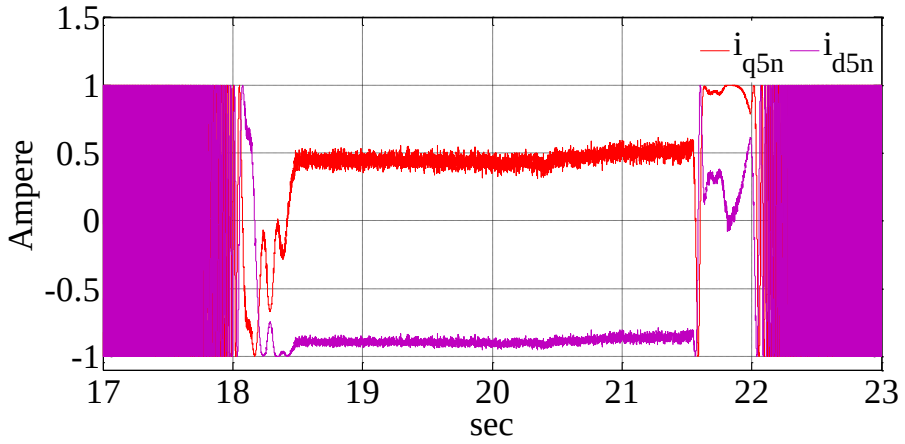

(a)

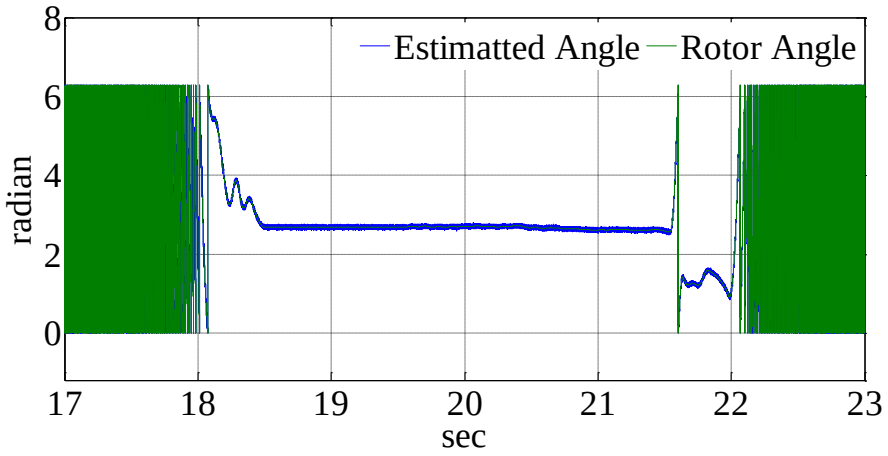

(b)

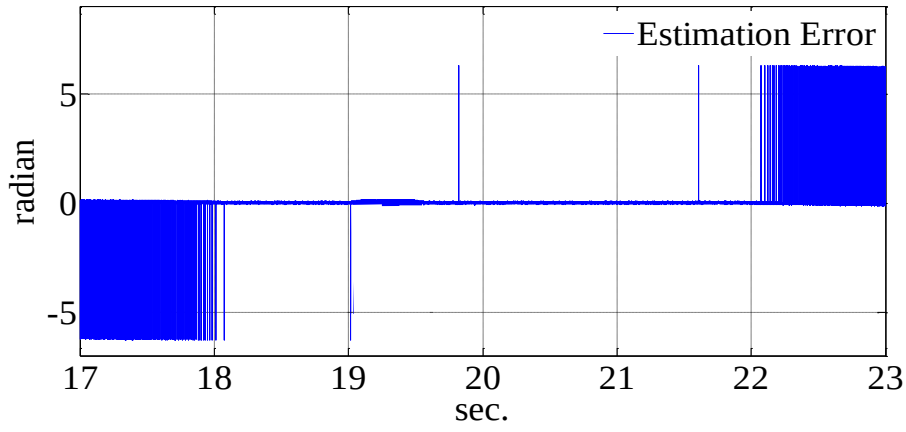

(c)

Figure 6.65: (a) The normalized currents of the fifth sequence, (b) The simulated and estimated angle, (c) Estimation error during the zero speed intervals (experimental results).

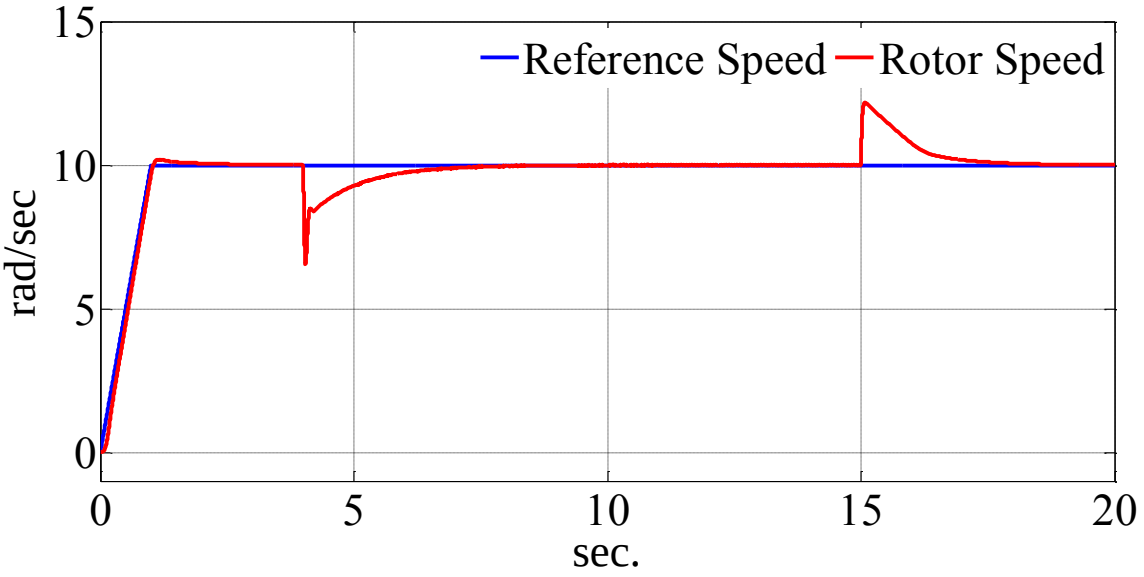

(a)

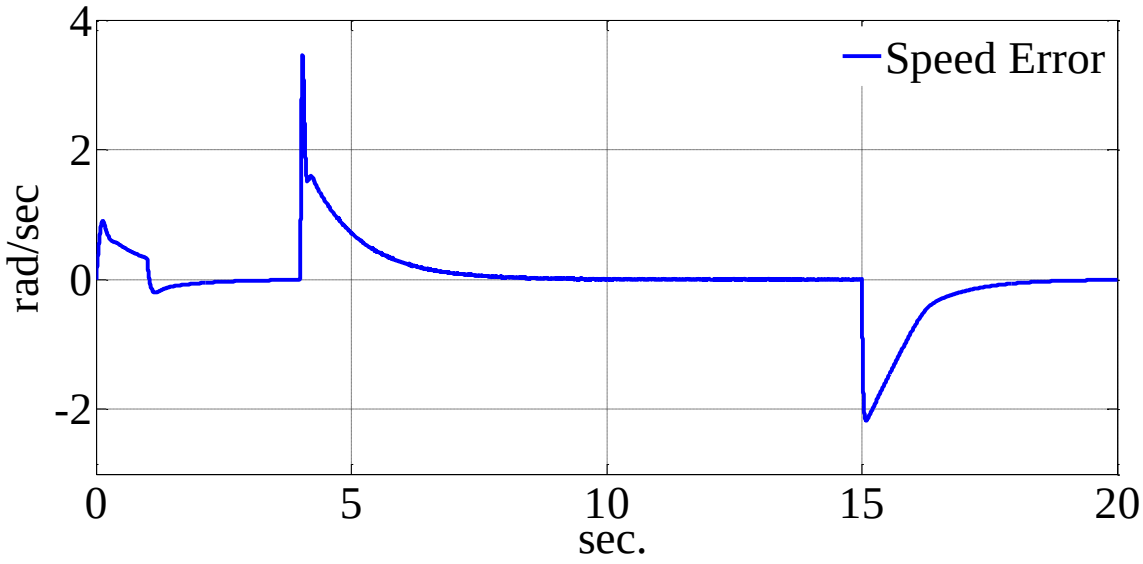

(b)

Figure 6.66: (a) The reference and rotor speed, (b) The speed error (simulation results).

6.6.2 Low Speed Test

In this test the motor controller receives a low speed reference as the input command. The speed reference starts from zero and goes to a fixed speed at 10 (rad/sec). After the machine settles down to the steady state condition a step load torque is applied to the rotor and finally, after transients, the load is removed.

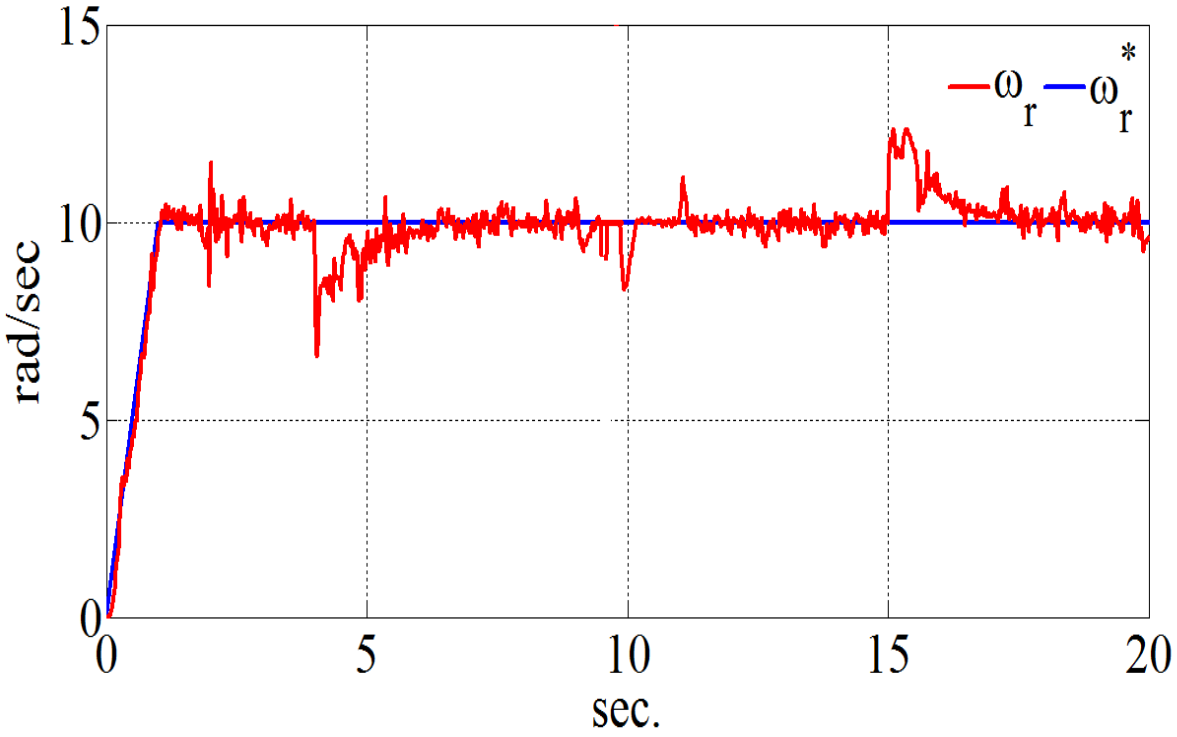

(a)

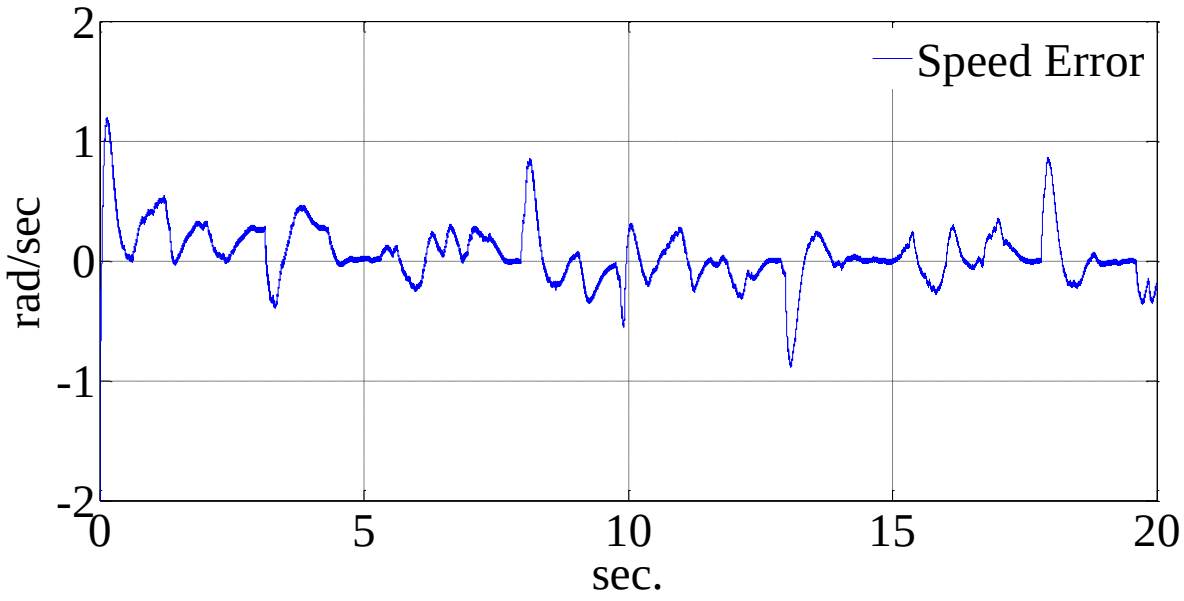

(b)

Figure 6.67: (a) The reference and rotor speed, (b) The speed error (experimental results).

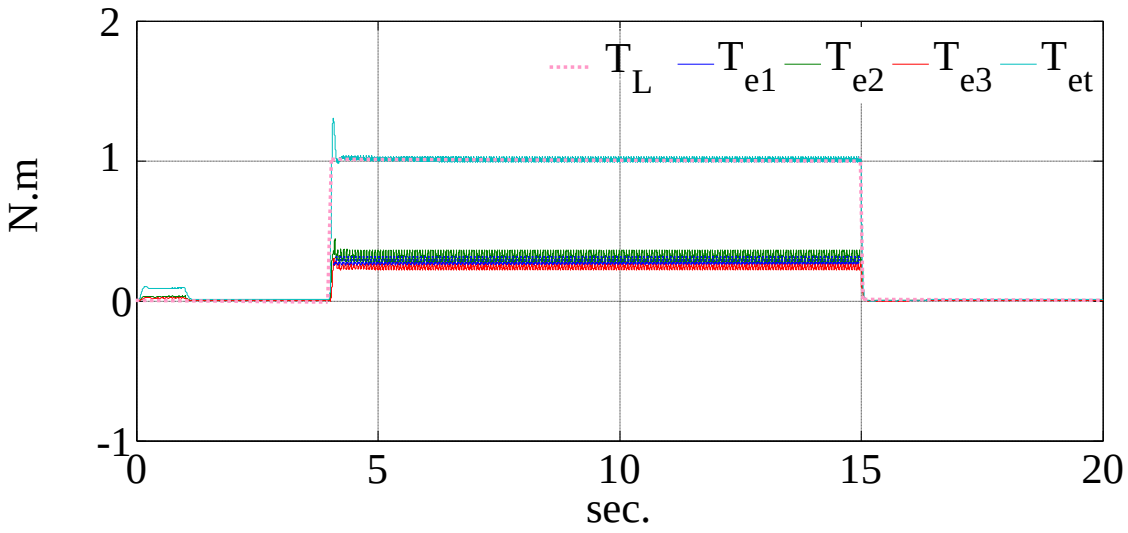

Figure 6.68: The electromagnetic torque of each machine and the total (simulation results).

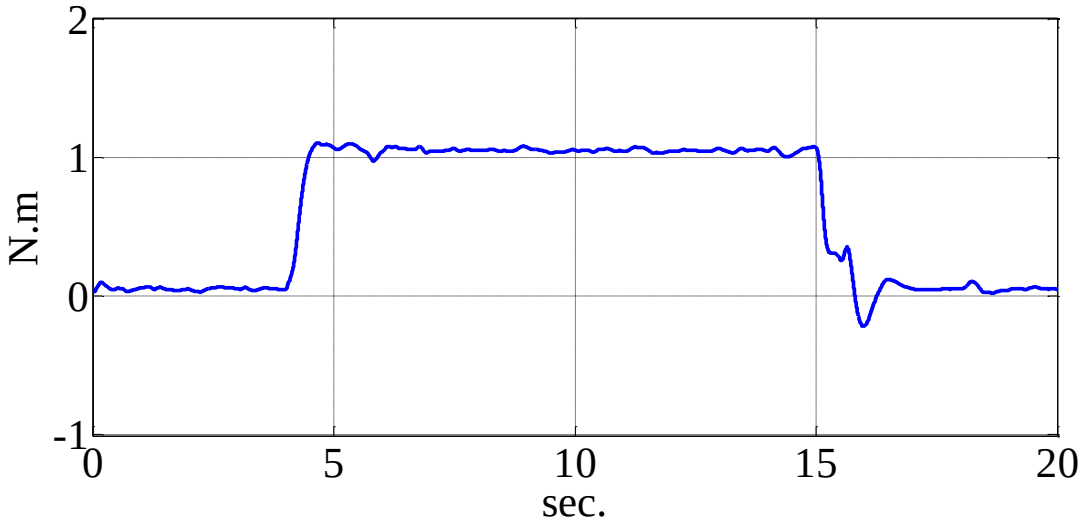

Figure 6.69: The electromagnetic torque of the machine (experimental results).

Figure 6.68 shows the electromagnetic torque of each machine and also the total electromagnetic torque together with the load torque for simulation results. The electromagnetic torque of the machine for experimental result is also shown in Figure 6.69. From these figures, it can be seen that, by applying the load torque, machine generates torque to keep the rotor speed constant. Figures 6.70 and 6.71 show the reference and the feedback of q_{1n} axis currents for

simulation and experiment respectively. From these figures, the reaction of the controller to the step load application can be seen.

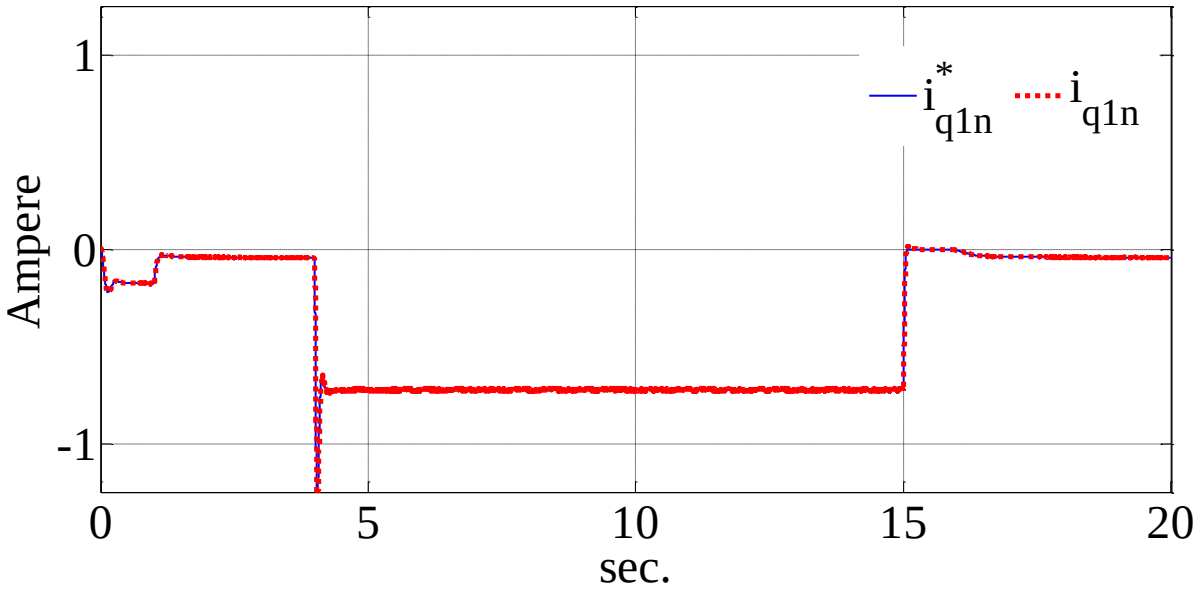

Figure 6.70: The q_{1n} reference and feedback currents (simulation results).

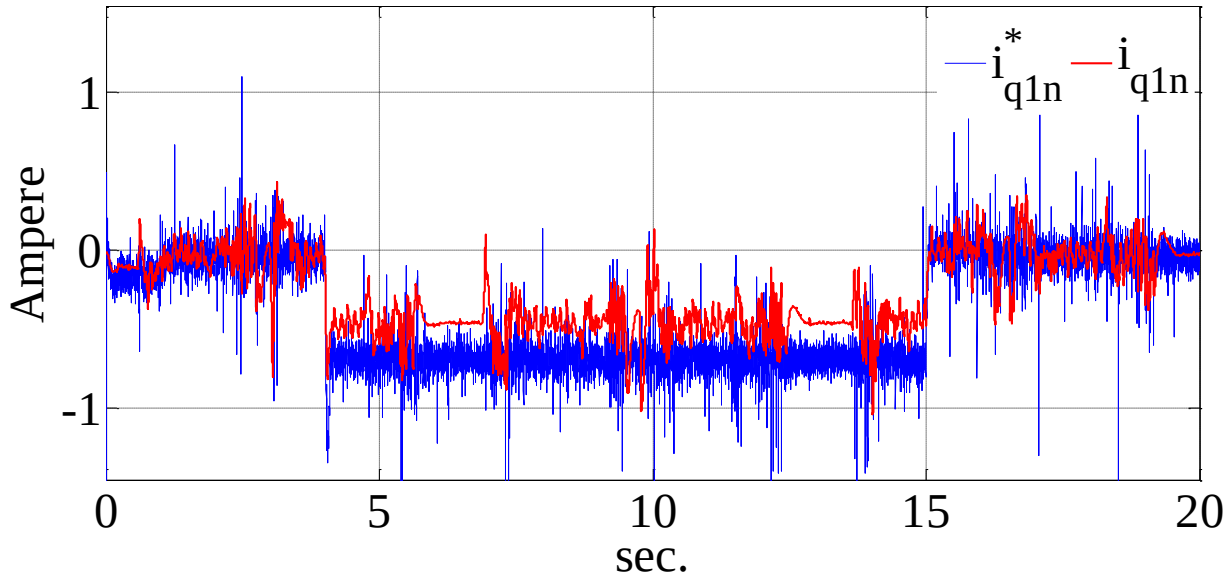

Figure 6.71: The q_{1n} reference and feedback currents (experimental results).

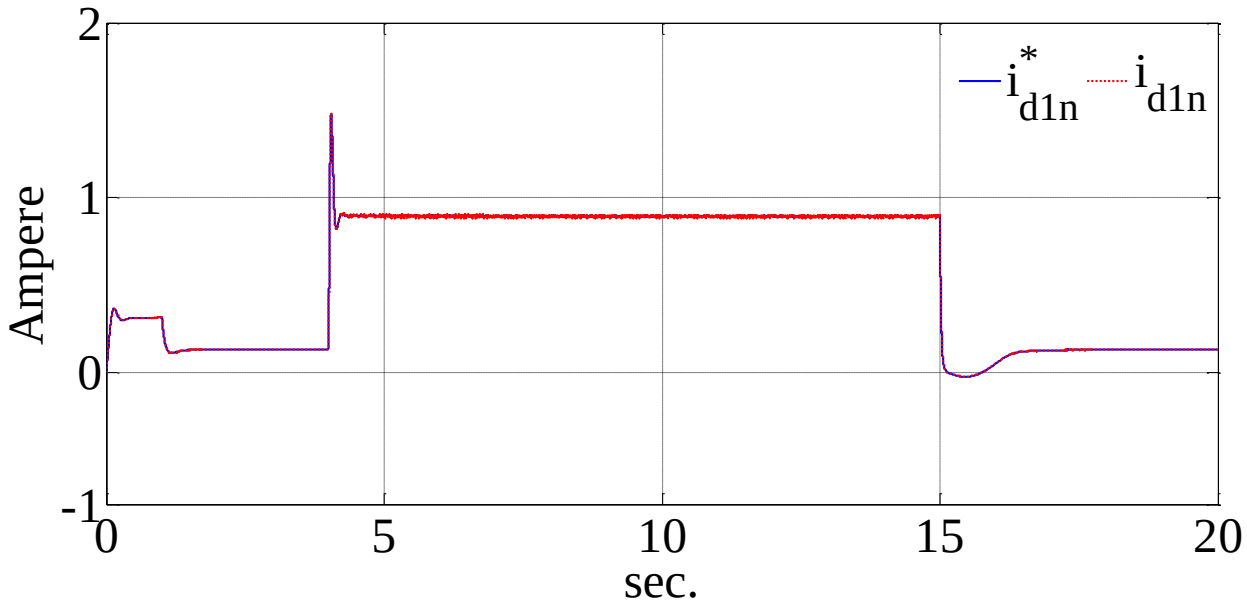

Figure 6.72: The d_{1n} reference and feedback currents (simulation results).

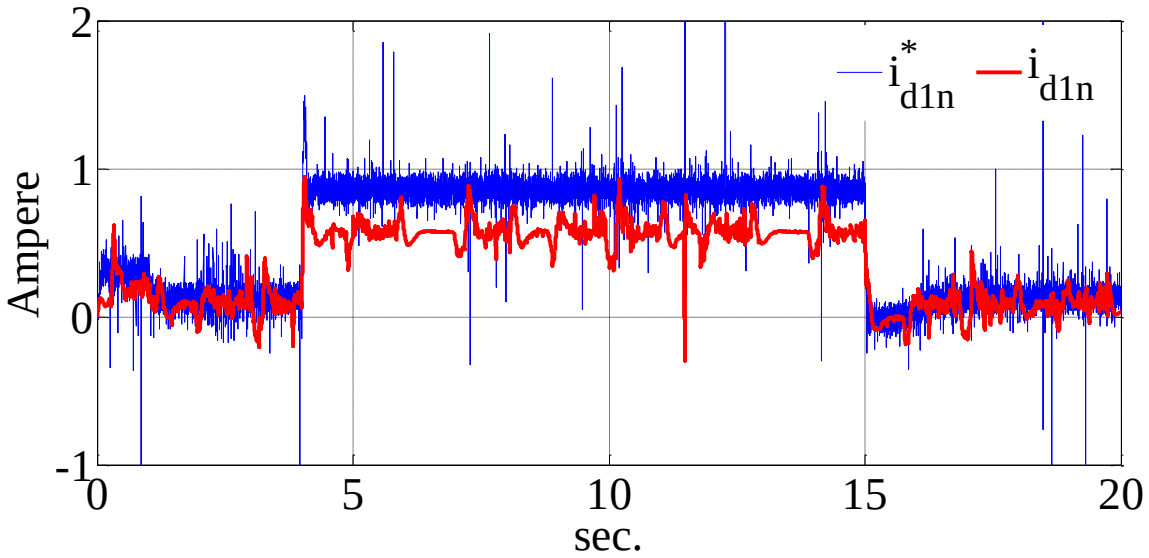

Figure 6.73: The reference and actual current of the d_{1n} axis of the decoupled reference frame (experimental results).

Figures 6.72 and 6.73 show the reference and the feedback currents for d_{1n} axis for simulation and experimental tests respectively. The reference current is generated using the q_{1n} axis current and the equation (6.127).

The rest of the axis in the decoupled reference frame have zero as their reference currents. The Figure 6.74 and 6.75 show the currents of qd_{2n} axis generated by the current regulators for simulation and experimental results respectively.

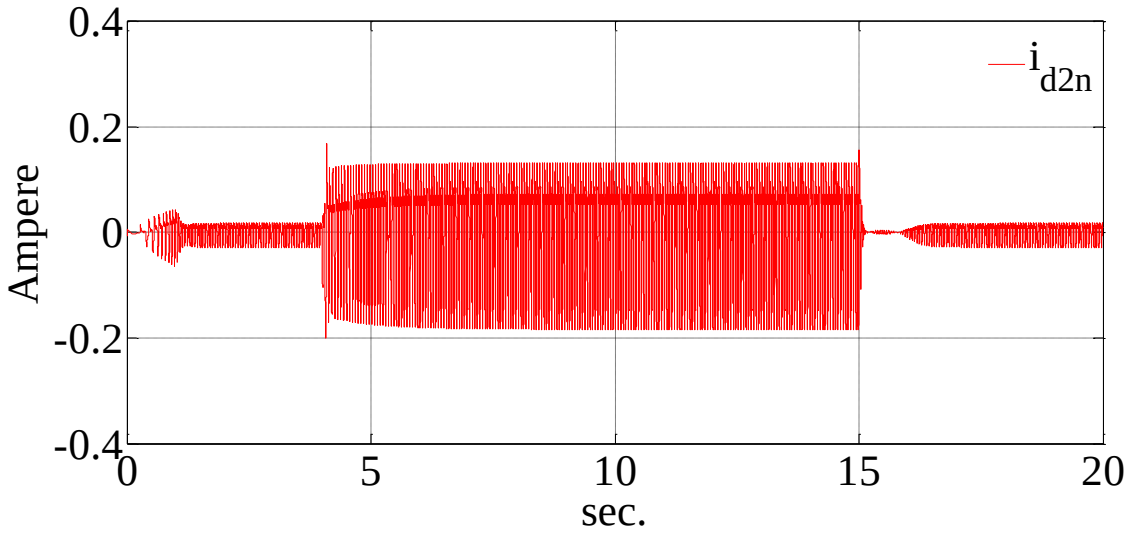

(a)

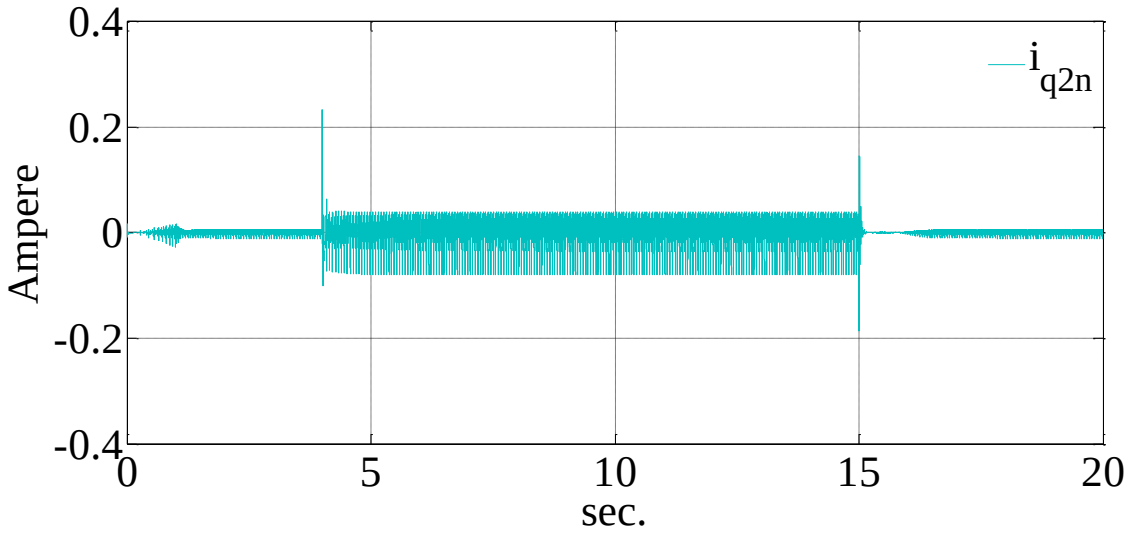

(b)

Figure 6.74: The simulated dq_{2n} axis current, (a) d_{2n}, (b) q_{2n} (simulation results).

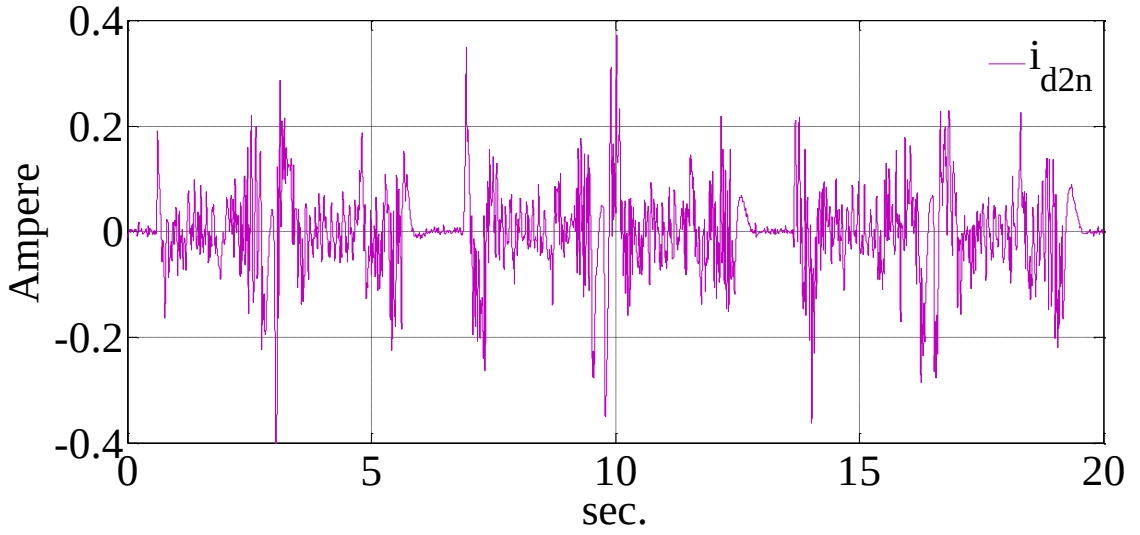

(a)

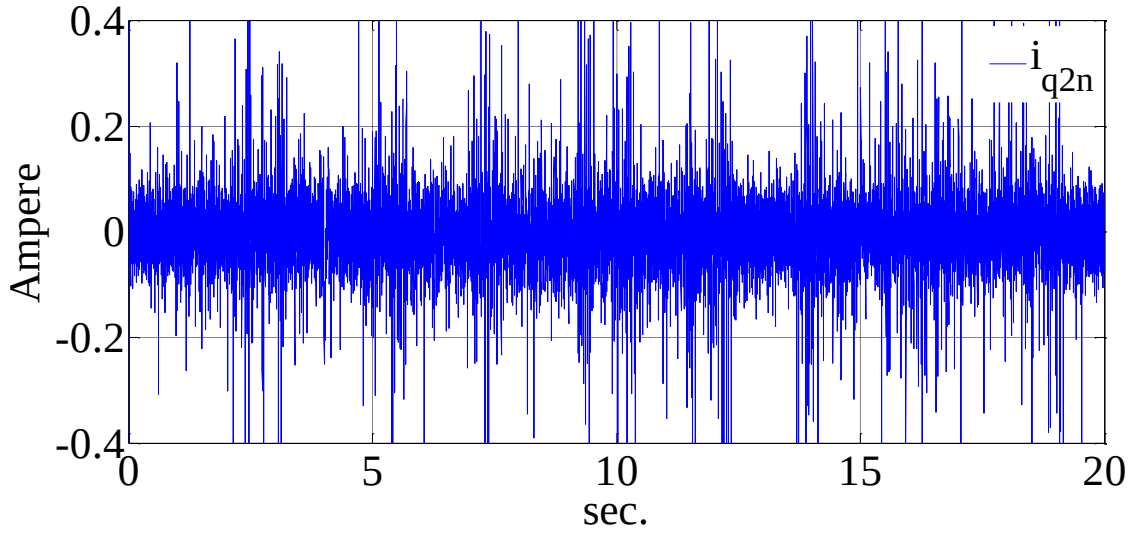

(b)

Figure 6.75: The measured dq_{2n} axis current, (a) d_{2n}, (b) q_{2n} (experimental results).

The Figure 6.76 and 6.77 also show the currents of qd_{3n} axis generated by the current regulators for simulation and experimental results respectively.

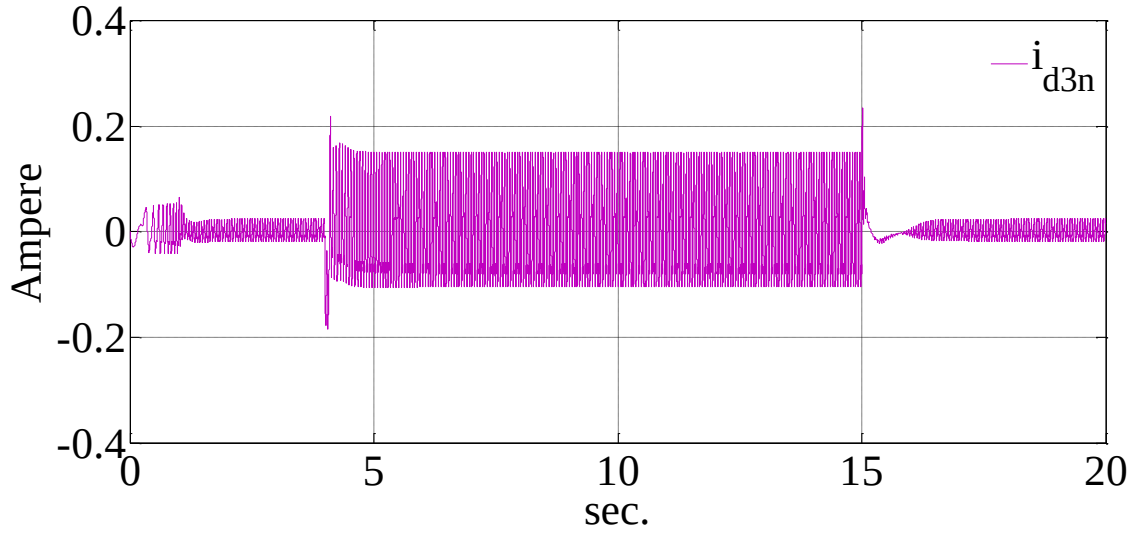

(a)

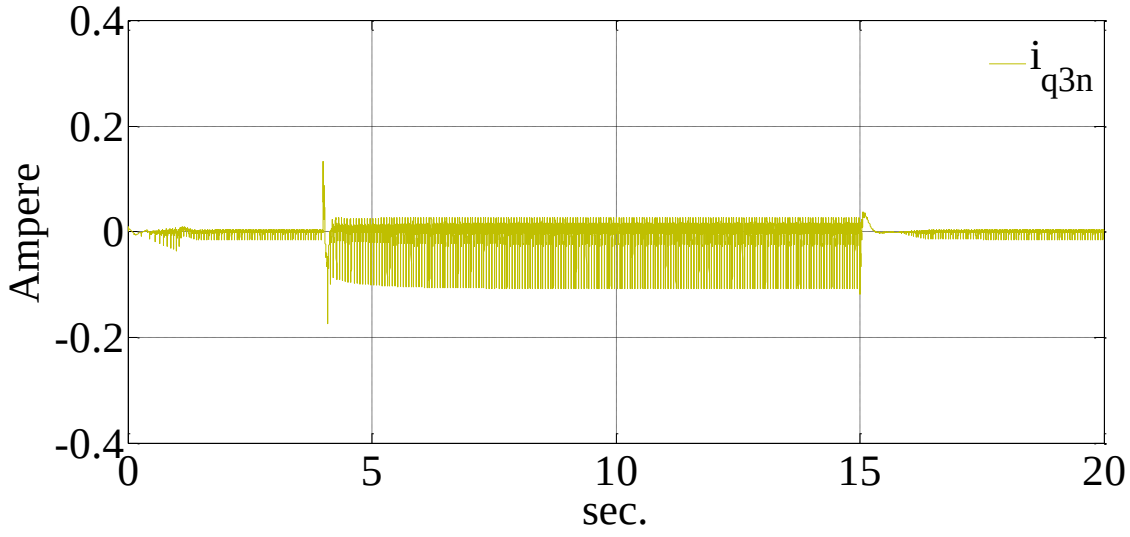

(b)

Figure 6.76: The simulated dq_{3n} axis current, (a) d_{3n}, (b) q_{3n} (simulation results).

Figures 6.78 and 6.79 show the generated voltages by current regulators in the decoupled reference frame for simulation and experimental results respectively. From Figures 6.78 (a) and 6.79 (a) it can be seen that, the voltages of axis qd_{1n} vary with the load torque to let stator current increase and supply the load.

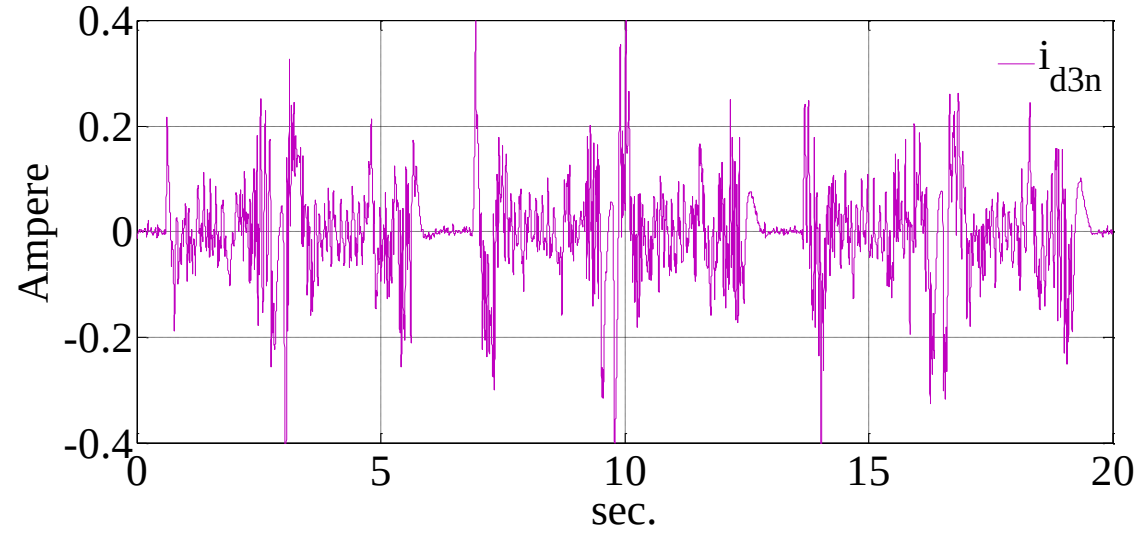

(a)

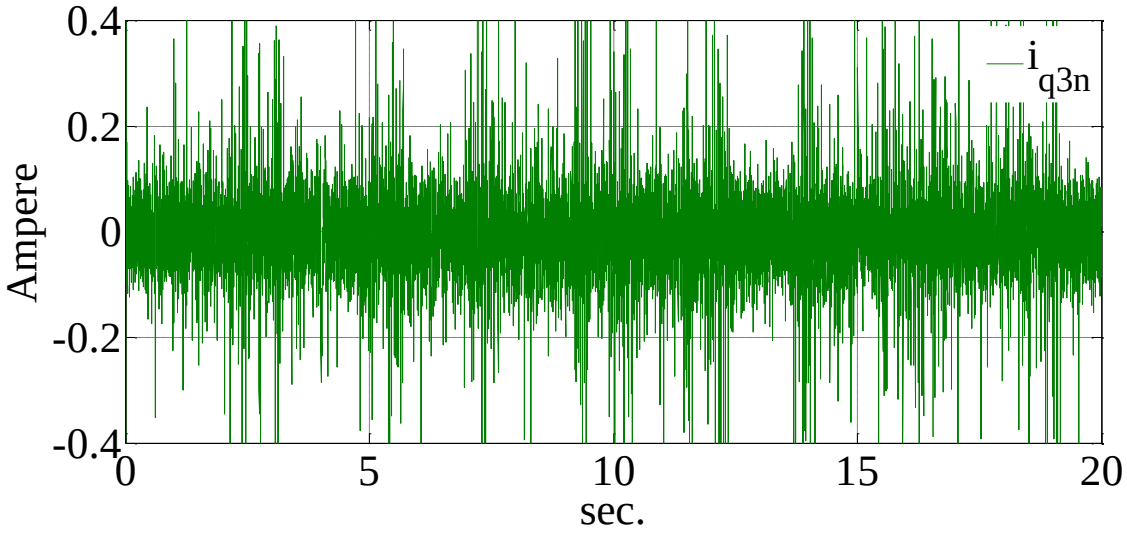

(b)

Figure 6.77: The measured dq_{3n} axis current, (a) d_{3n}, (b) q_{3n} (experimental results).

The voltages of the machine stator in the rotor reference frame are shown in the Figures 6.80 and 6.81 for simulation and experimental results respectively. Theas voltages are generated from the output voltages of current regulators and can be transformed to natural reference frame to be applied to stator. Again the effect of the applying load torque to the rotor of the machine can be seen from these voltages.

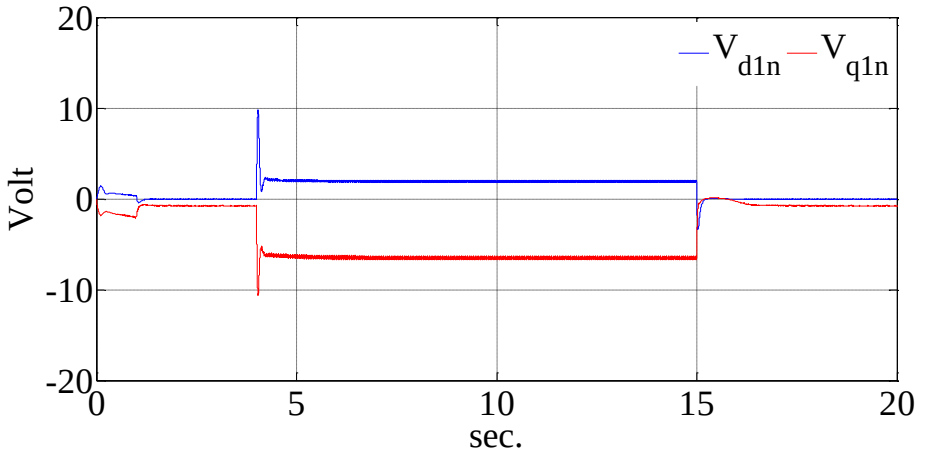

(a)

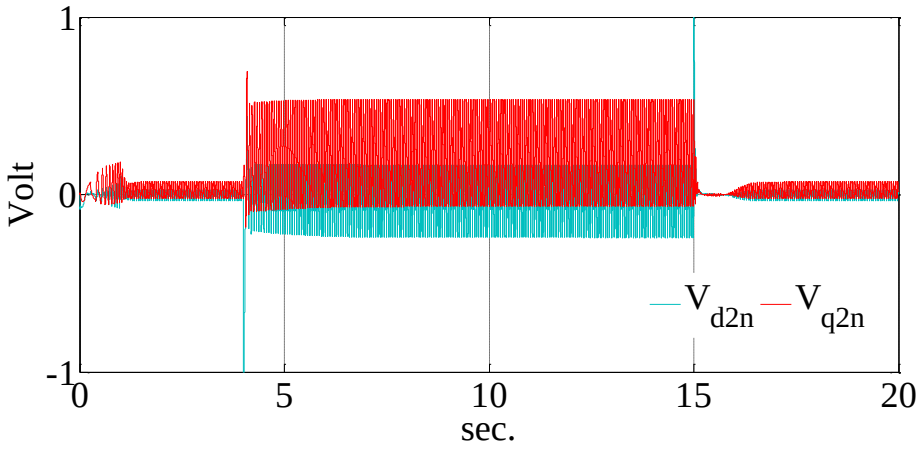

(b)

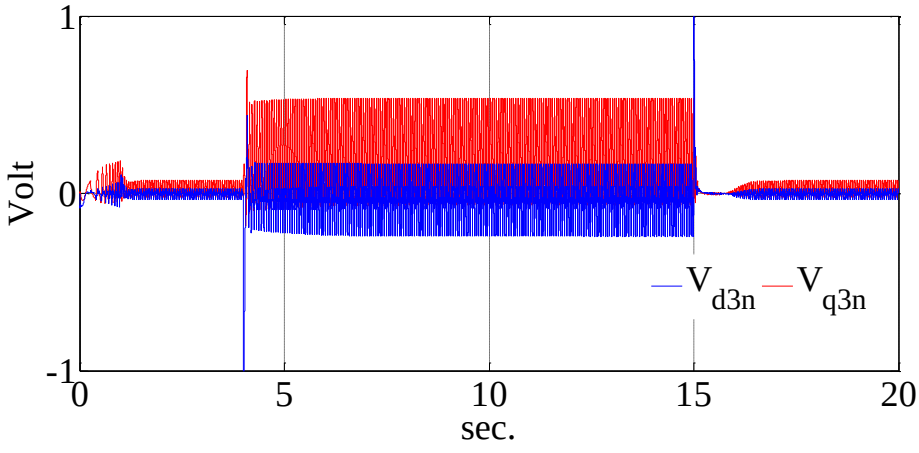

(c)

Figure 6.78: The voltage of the machines in the decoupled reference frame for axis, (a) qd_{1n}, (b) qd_{2n}, (c) qd_{3n} (simulation results).

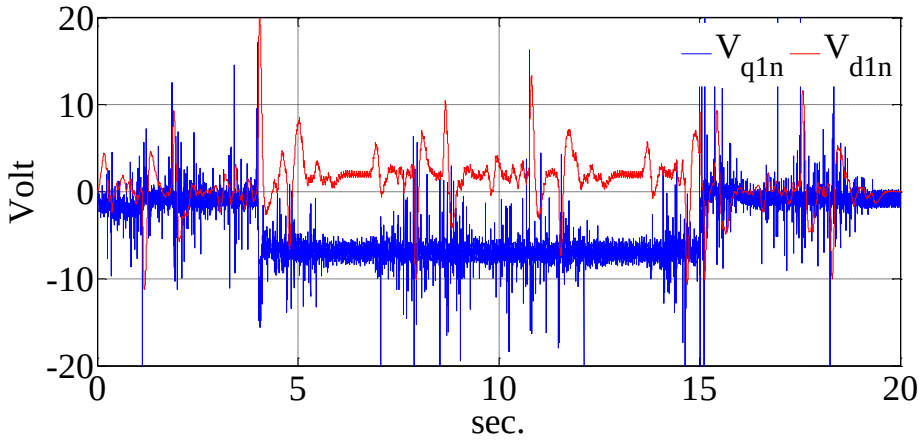

(a)

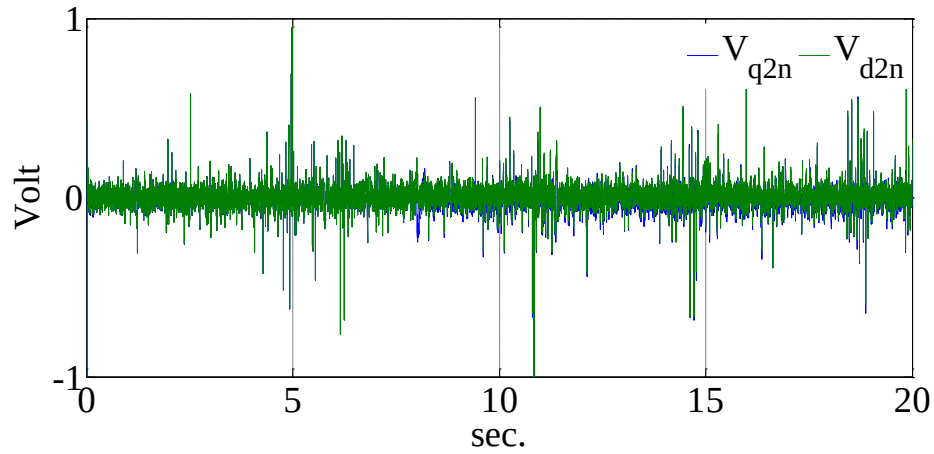

(b)

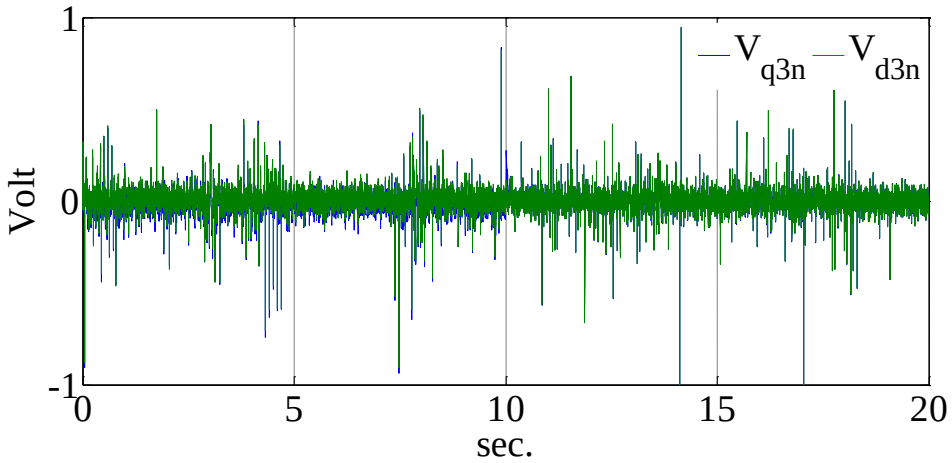

(c)

Figure 6.79: The voltage of the machines in the decoupled reference frame for axis, (a) qd_{1n}, (b) qd_{2n}, (c) qd_{3n} (experimental results).

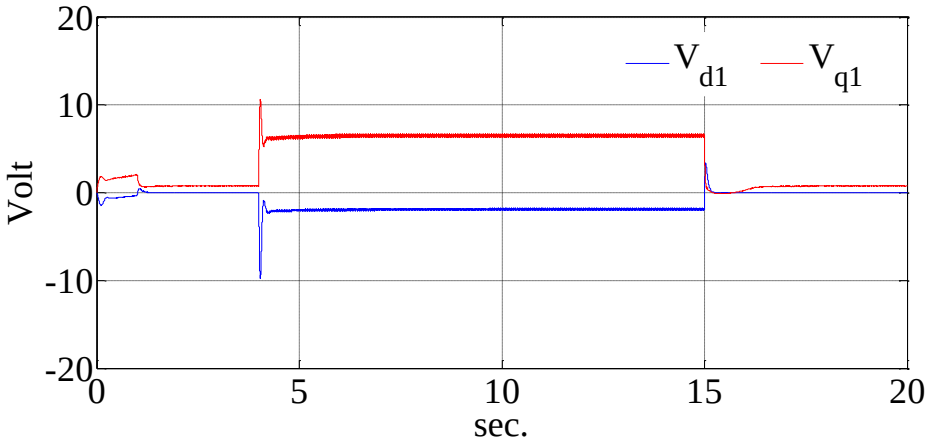

(a)

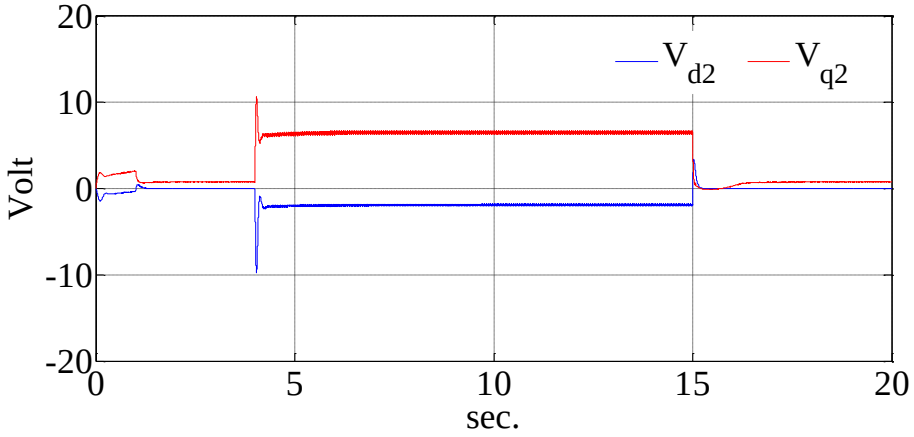

(b)

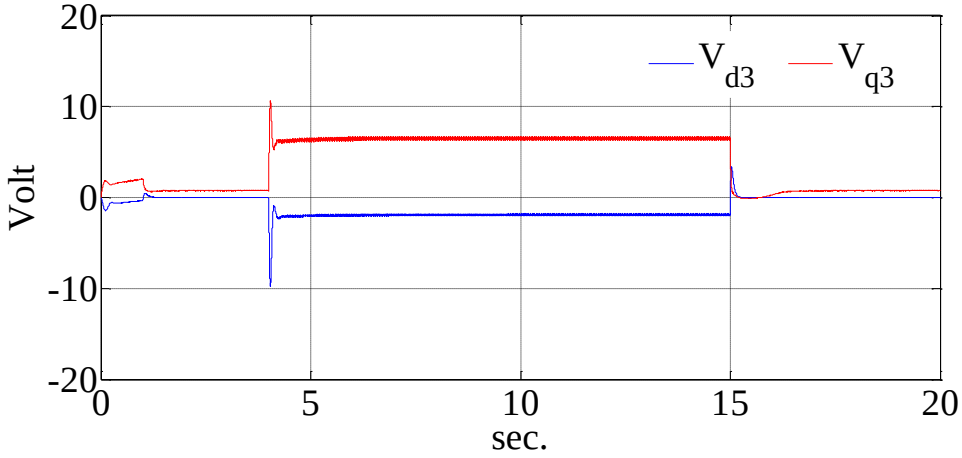

(c)

Figure 6.80: The q axis voltage of the machines in the rotor reference frame for, (a) Machine 1, (b) Machine 2, (c) Machine 3 (simulation results)

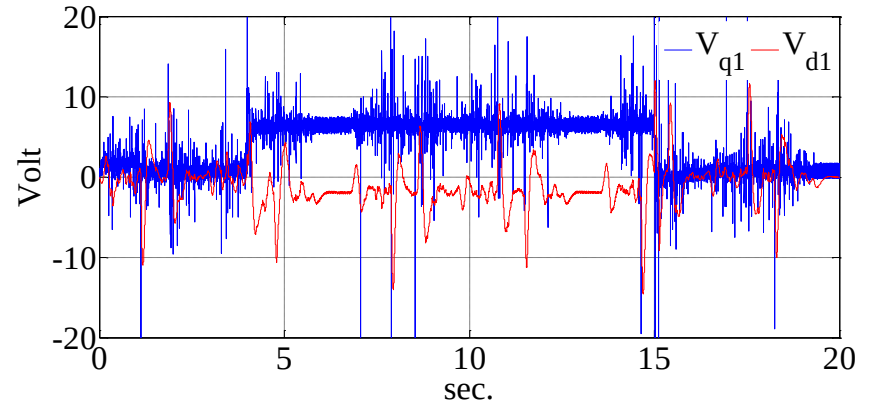

(a)

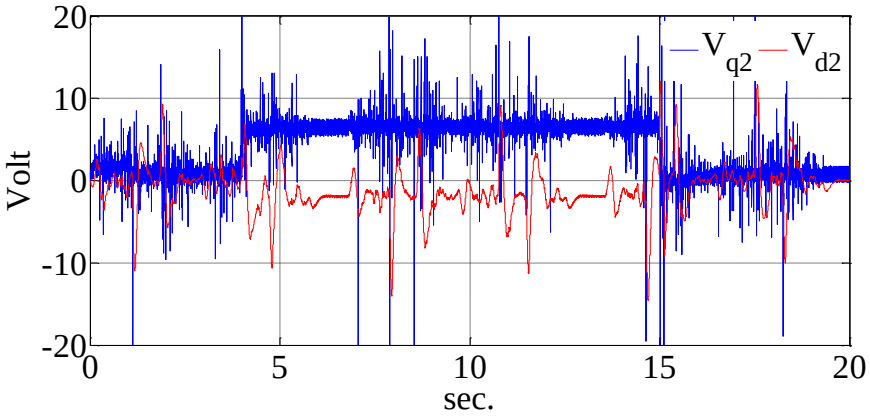

(b)

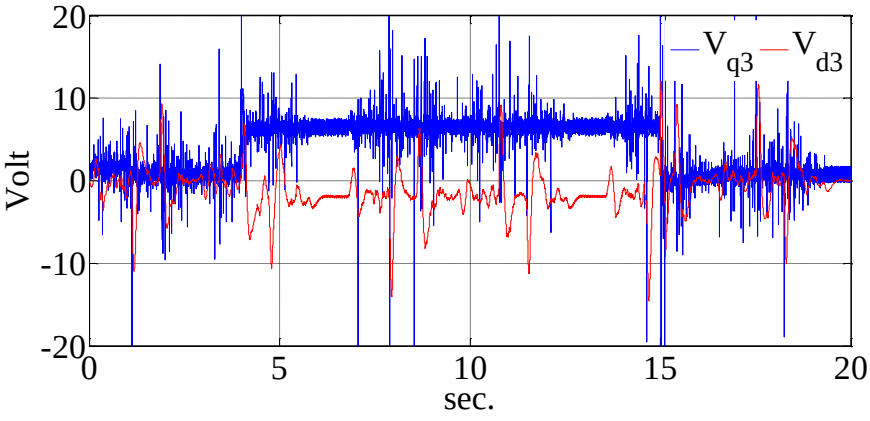

(c)

Figure 6.81: The q axis voltage of the machines in the rotor reference frame for, (a) Machine 1, (b) Machine 2, (c) Machine 3 (experimental results).

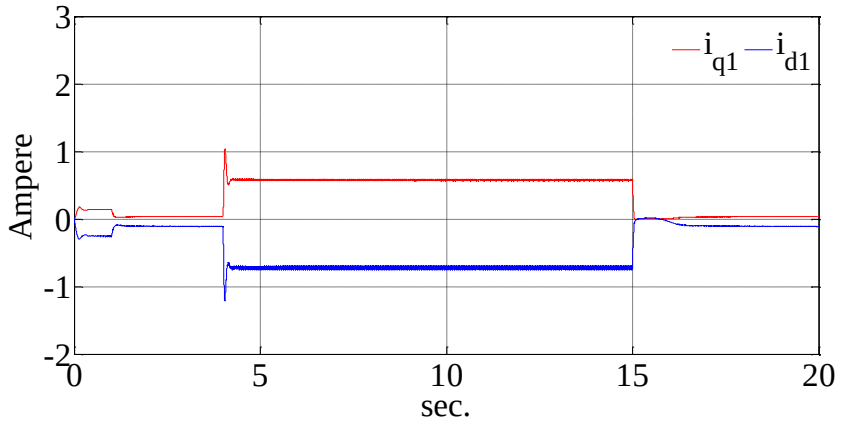

(a)

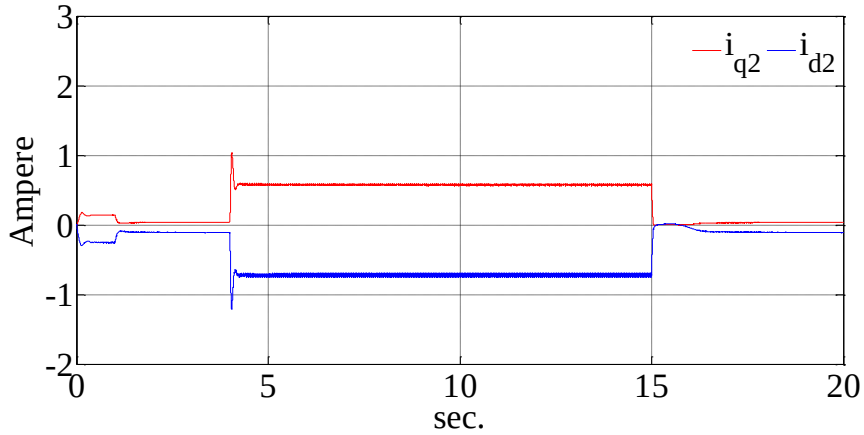

(b)

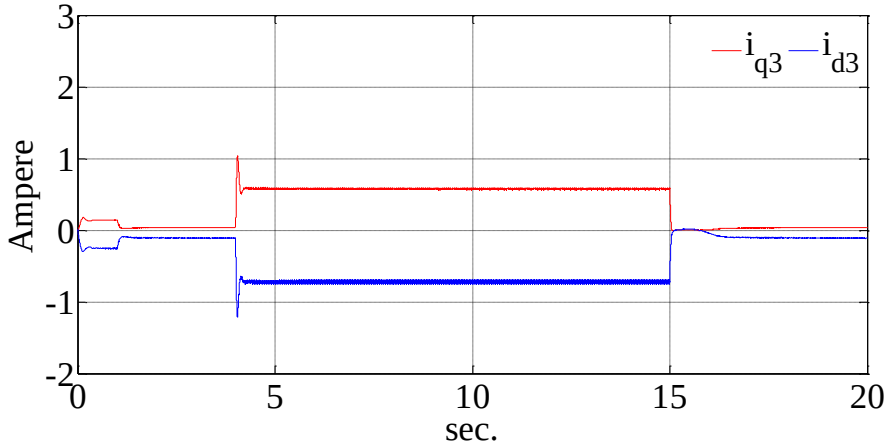

(c)

Figure 6.82: The q and d axis currents of the machines in the rotor reference frame for, (a) Machine 1, (b) Machine 2, (c) Machine 3 (simulation results).

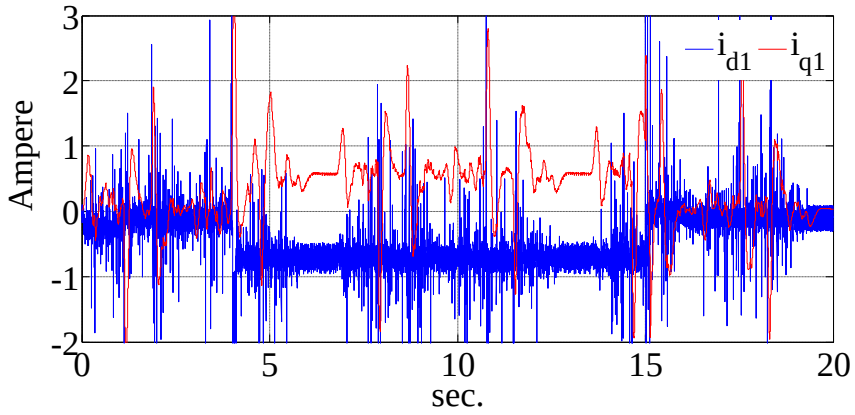

(a)

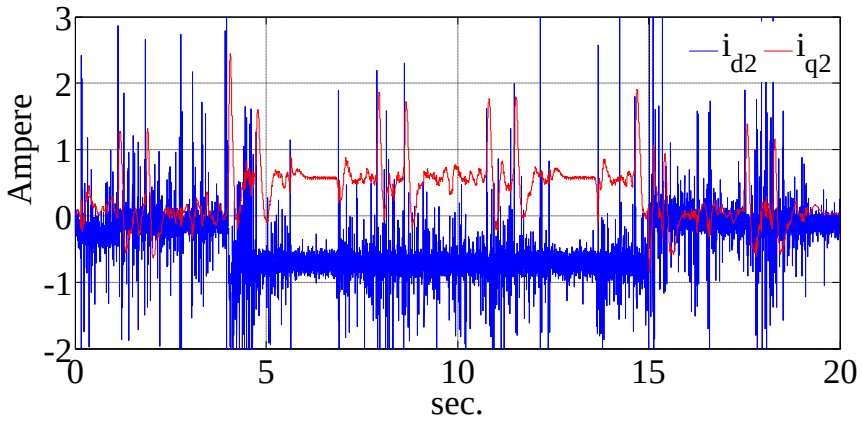

(b)

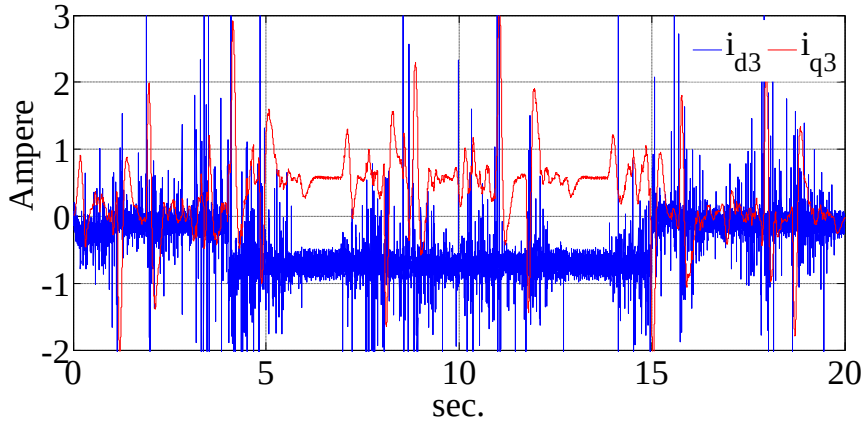

(c)

Figure 6.83: The q and d axis currents of the machines in the rotor reference frame for, (a) Machine 1, (b) Machine 2, (c) Machine 3 (experimental results).

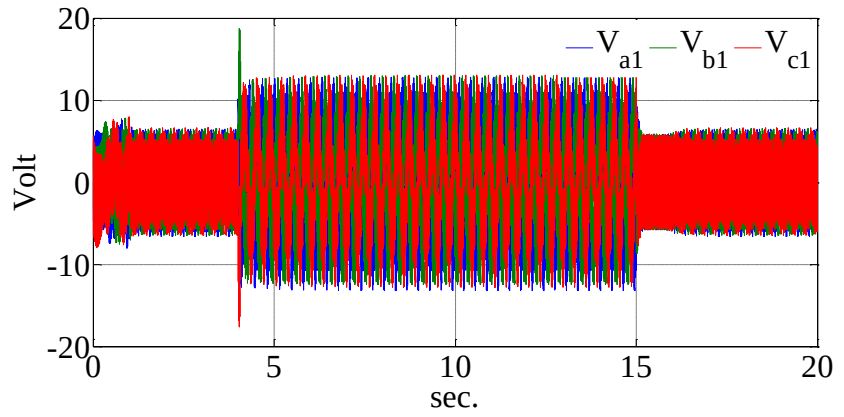

(a)

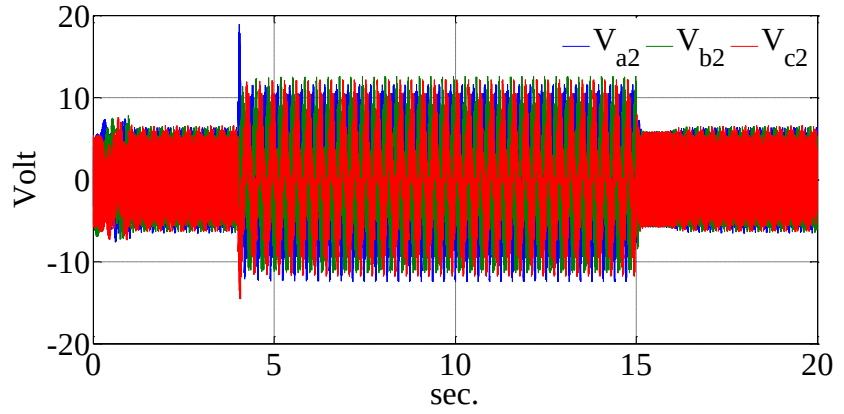

(b)

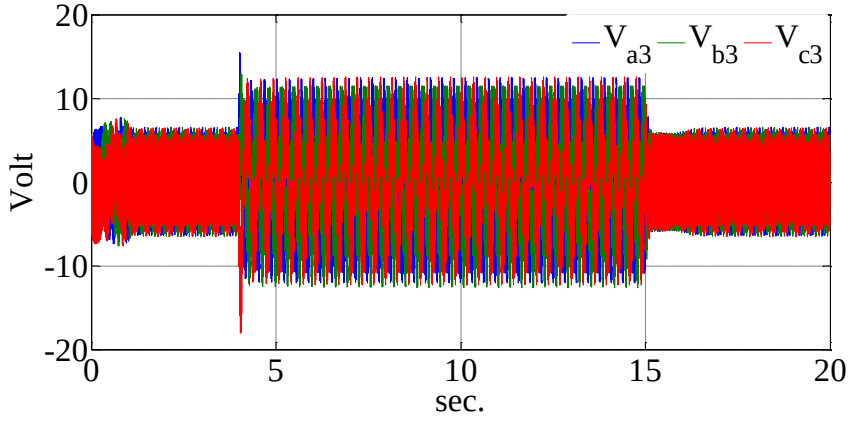

(c)

Figure 6.84: The voltages generated by the current regulators in natural variables, (a) Machine 1, (b) Machine 2, (c) Machine 3 (simulation results).

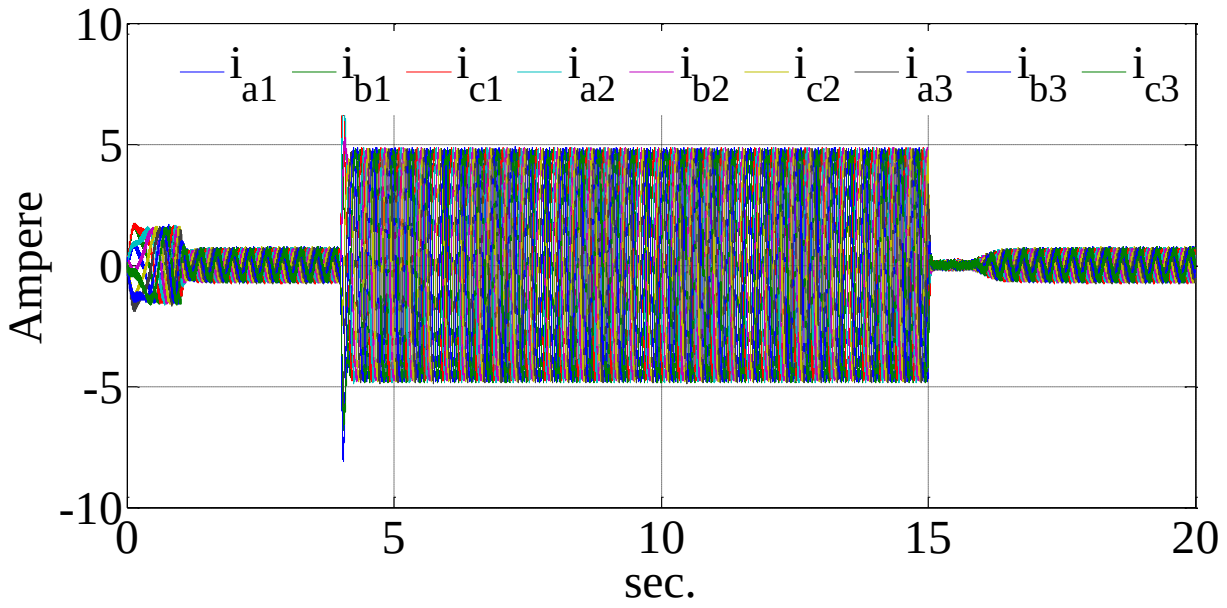

Figure 6.85: The stator current generated by the current regulators in the natural variables (simulation results)

The stator current in rotor reference frame for simulation and experimental are also shown in Figures 6.82 and 6.83 respectively. Form this figures, it can be seen that, by applying the load torque, q axis current increases and d axis current also reacts to the q axis current changes to keep the minimum loss copper conditions. The voltages of equation (6.132) are transformed to natural variables and they are applied to the machine phases. Figure 6.84 shows the machine voltages in natural variables for simulation results. Figure 6.85 shows the machine currents in natural variables. From this Figure, it can be seen that the magnitude of the currents varies with the load application. Figures 6.86 and 6.87 show the currents of each machine separately after load torque is applied for simulation and experimental results respectively. Figures 6.88 and 6.89 show the machine currents before applying load torque for simulation and experimental results respectively. Again there are some low frequency ripples on the experimental results which are due to the nonlinearities of the machine.

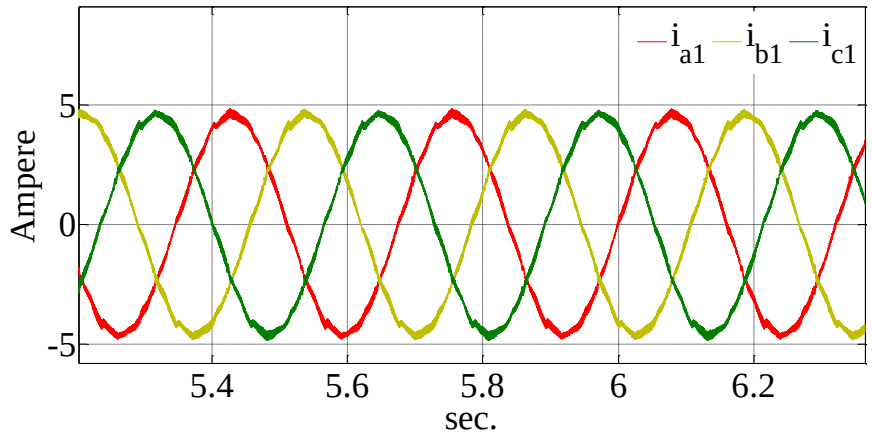

(a)

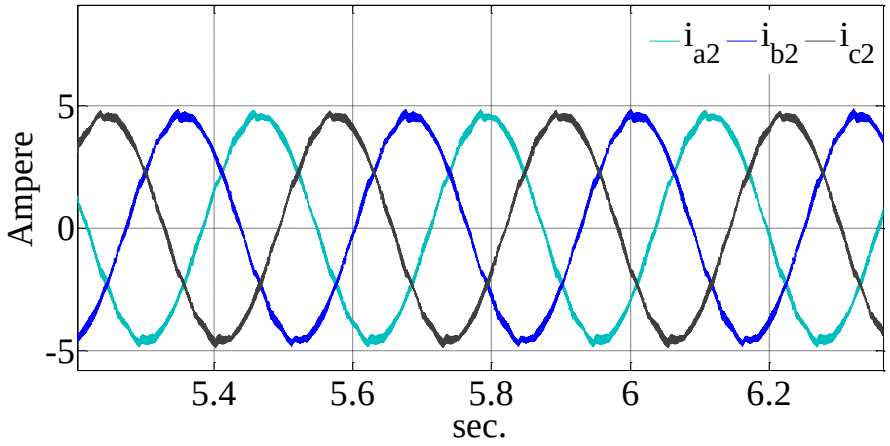

(b)

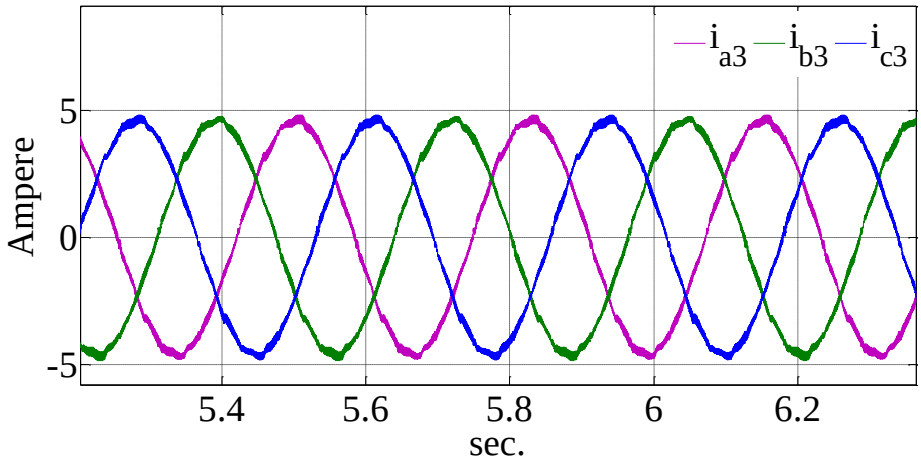

(c)

Figure 6.86: The currents generated by the current regulators in natural variables after applying load, (a) Machine 1, (b) Machine 2, (c) Machine 3 (simulation results).

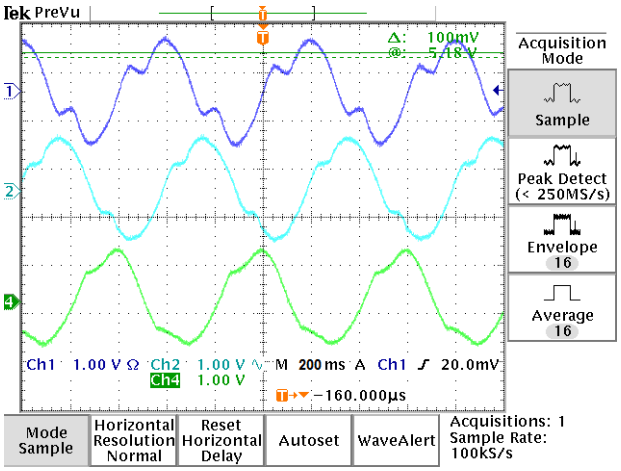

(a)

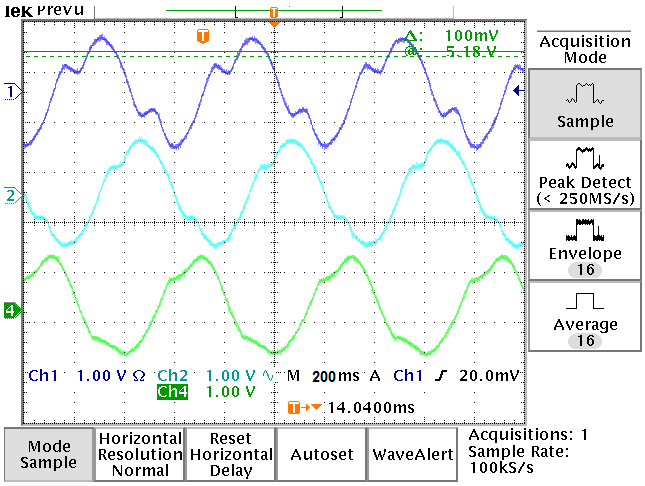

(b)

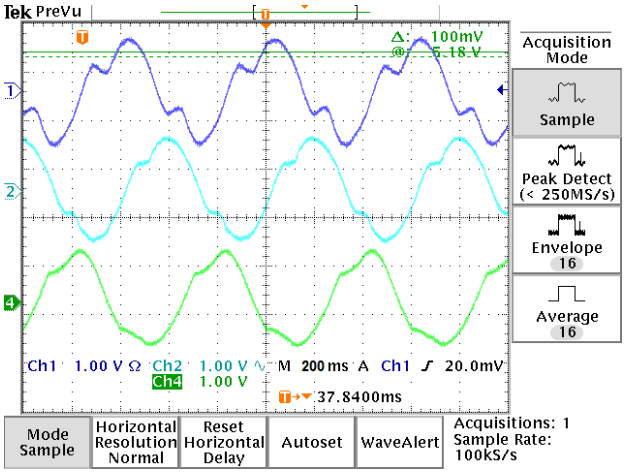

(c)

Figure 6.87: The currents generated by the current regulators in natural variables after applying load, (a) Machine 1, (b) Machine 2, (c) Machine 3 (5 A/ scale) (experimental results).

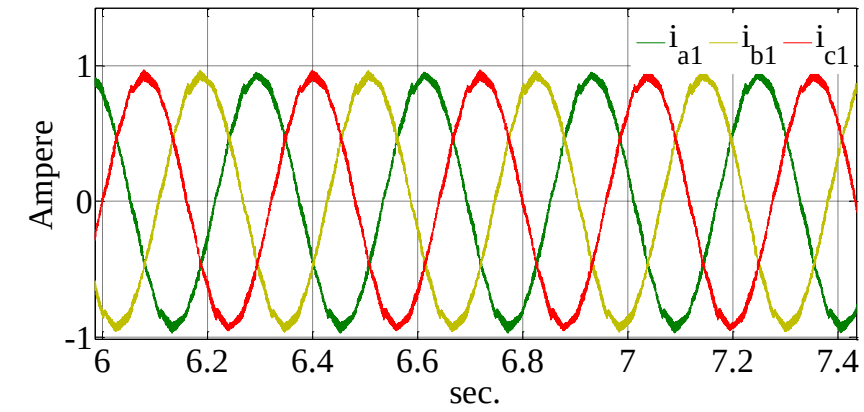

(a)

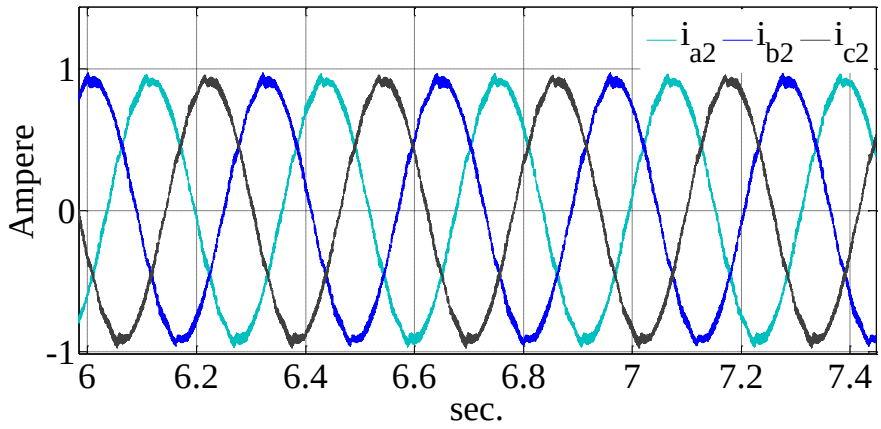

(b)

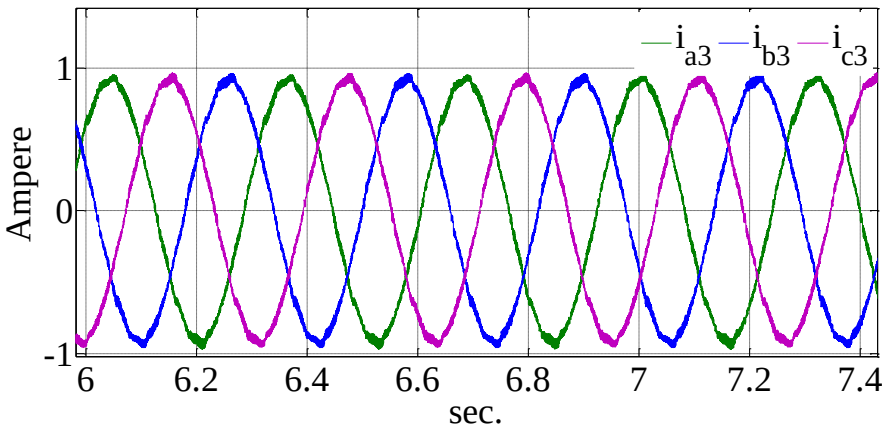

(c)

Figure 6.88: The currents generated by the current regulators in natural variables before applying load, (a) Machine 1, (b) Machine 2, (c) Machine 3 (simulation results).

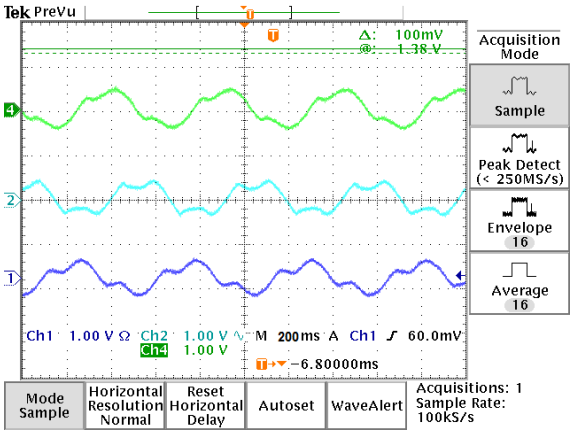

(a)

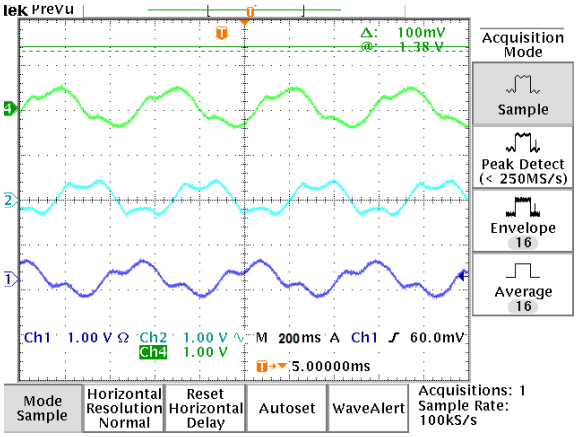

(b)

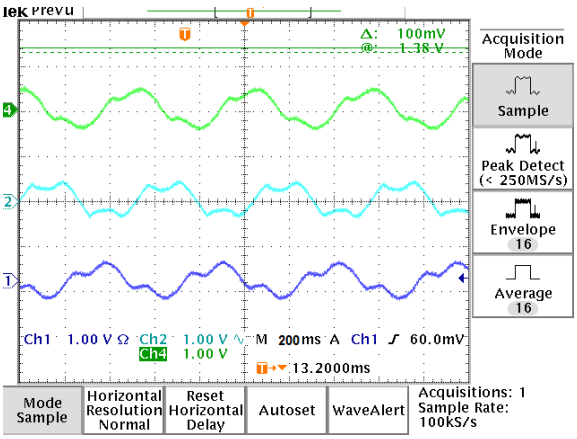

(c)

Figure 6.89: The currents generated by the current regulators in natural variables before applying load, (a) Machine 1, (b) Machine 2, (c) Machine 3 (5 A/ scale) (experimental results).

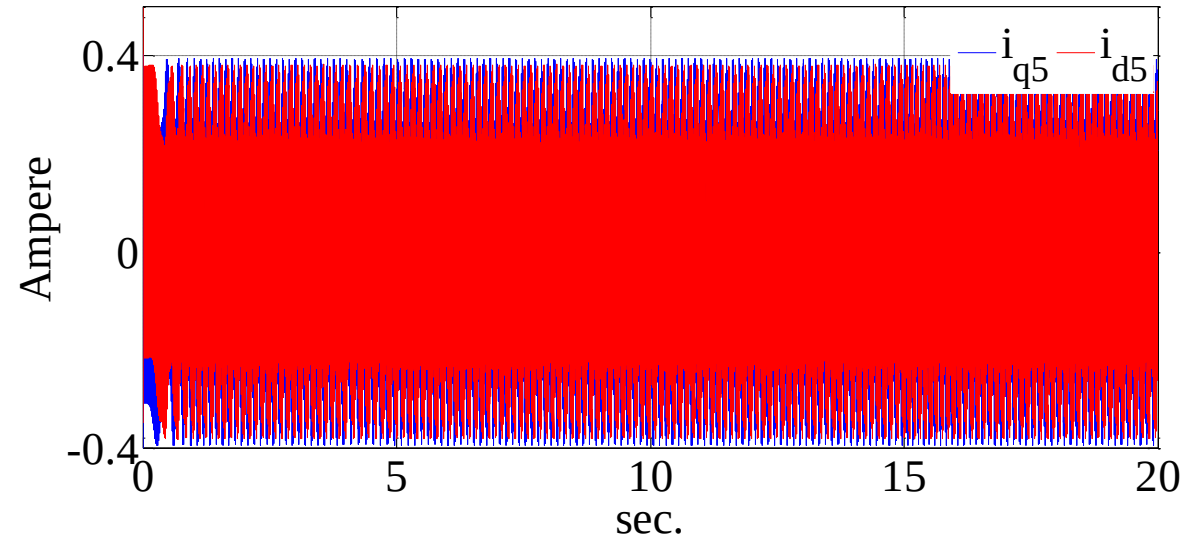

(a)

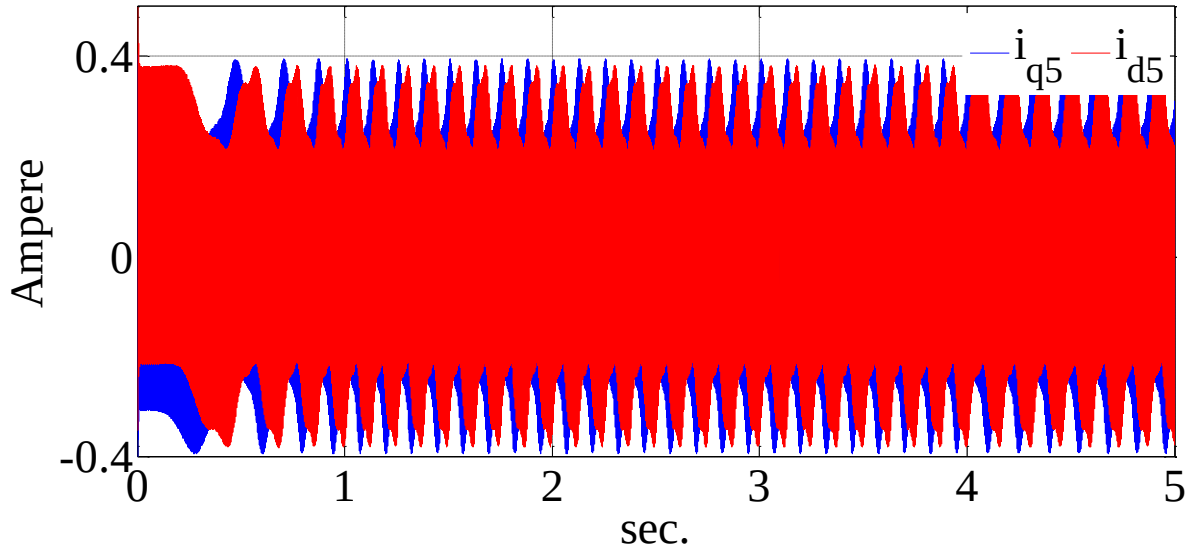

(b)

Figure 6.90: (a) The fifth sequence of the stator current in the stationary reference frame, (b) The zoomed view (simulation results).

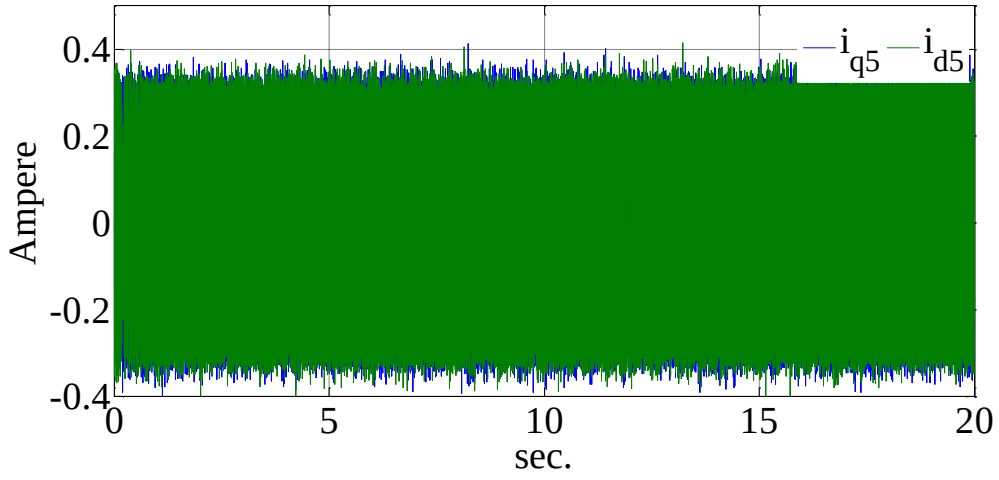

(a)

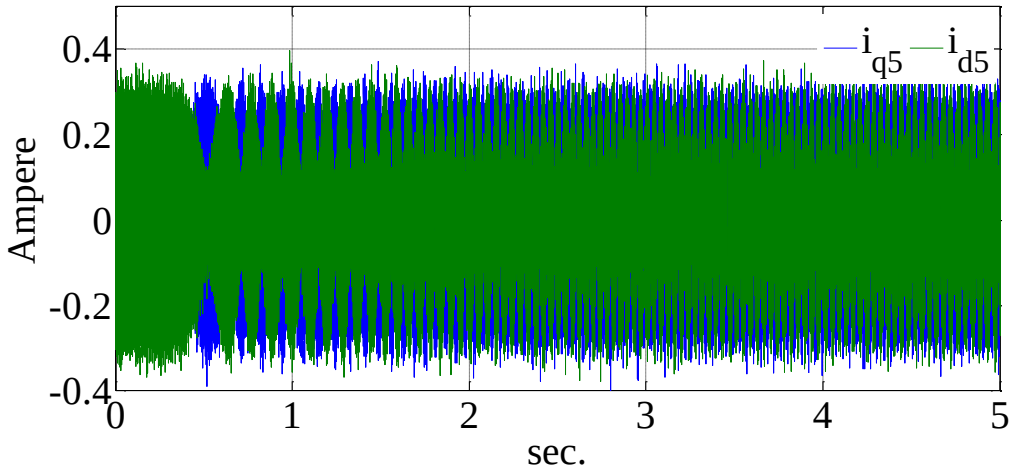

(b)

Figure 6.91: (a) The fifth sequence of the stator current in the stationary reference frame, (b) The zoomed view (experimental results).

The fifth sequence of the stator currents can be used for position estimation. The fifth sequence of the stator currents are extracted and shown in Figures 6.90 and 6.91 for simulation and experimental results respectively. The currents in these Figures pass through a heterodyning block then, they pass through a low pass filter to remove their redundant high frequency parts. Figures 6.92 and 6.93 show the resulting currents after heterodyning and filtering for simulation and experimental results respectively.

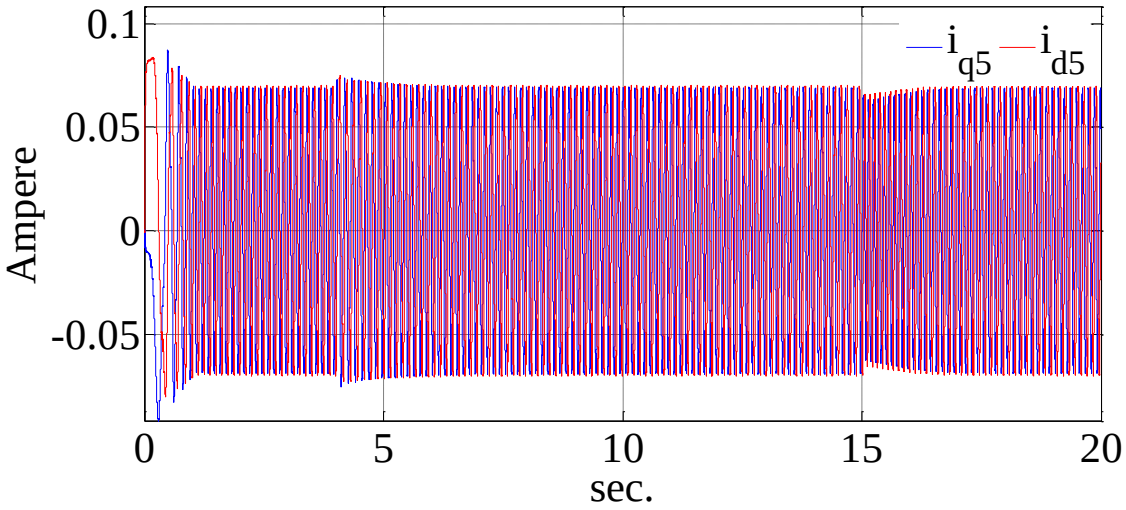

(a)

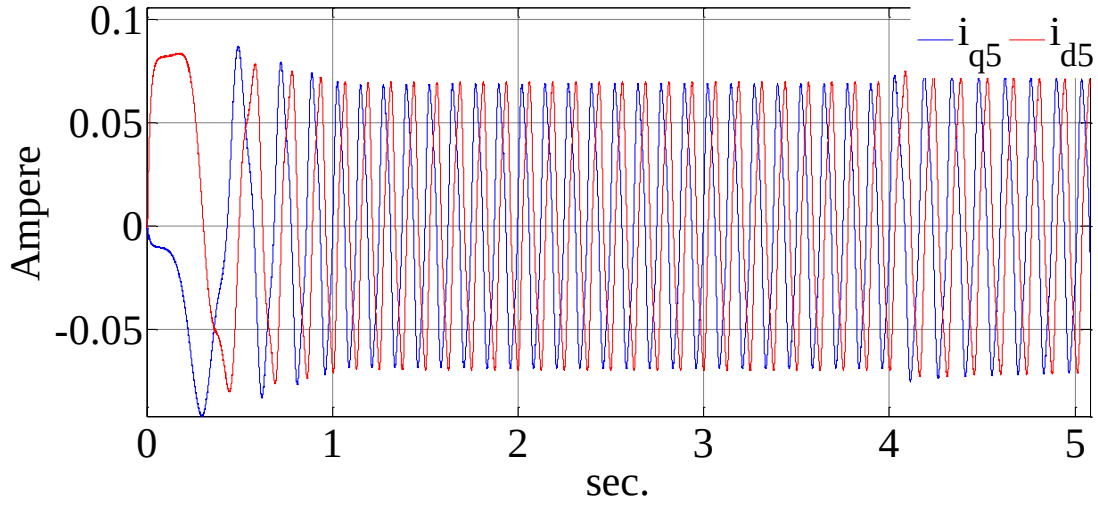

(b)

Figure 6.92: (a) The fifth sequence of the stator current in the stationary reference frame after heterodyning and filtering, (b) The zoomed view (simulation results).

The Currents of Figures 6.92 and 6.93 have variable magnitudes. To be able to use them as the input of the Luenberger observer their magnitudes need to be unity. The currents need to be normalized to fix their magnitudes to unity. After normalizing currents of the Figures 6.92 and 6.93, they can be used as the input signals of the observer. Figures 6.94 and 6.95 show the normalized currents with the estimated position angle along with estimation error for simulation and

experimental results respectively. Figures 6.96 and 6.97 show the zoomed view of the same figures during starting intervals. From this figures it can be seen that, the estimator can tract the rotor position precisely.

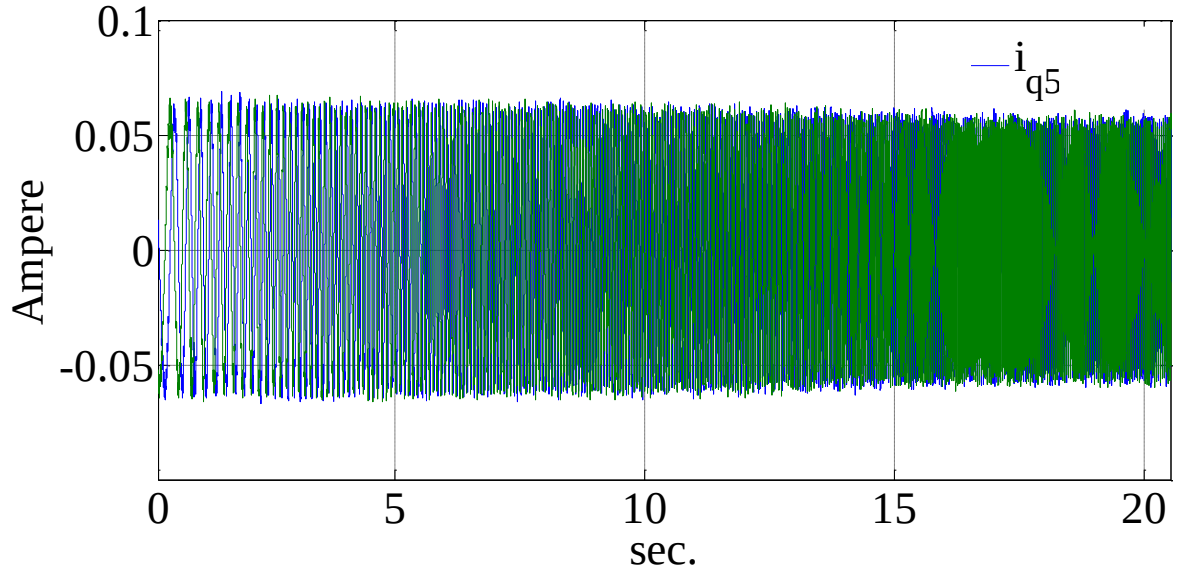

(a)

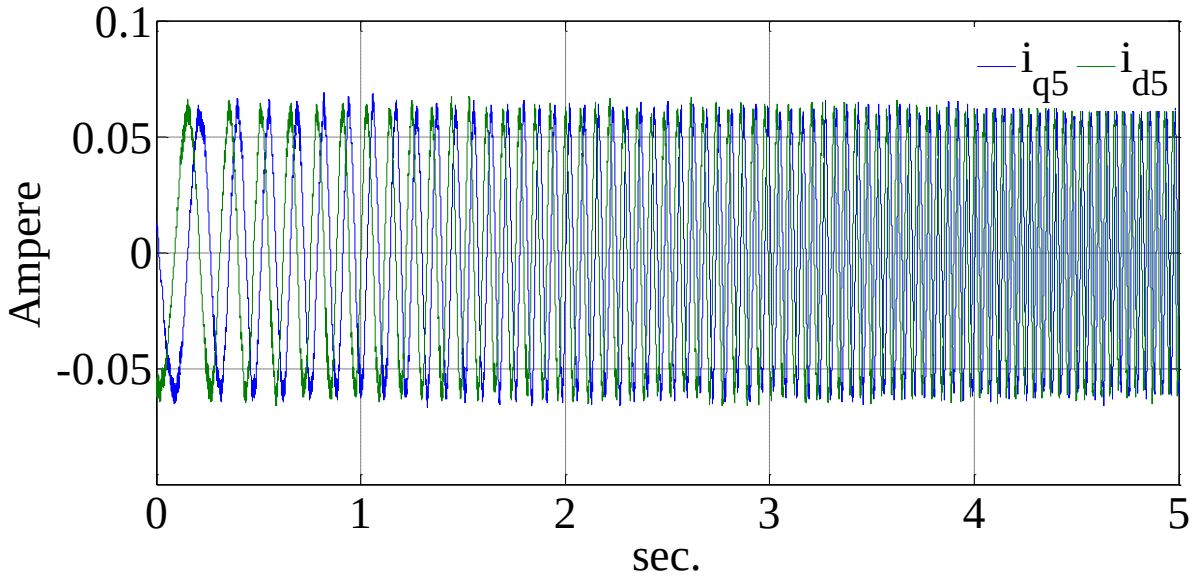

(b)

Figure 6.93: (a) The fifth sequence of the stator current in the stationary reference frame after heterodyning and filtering, (b) The zoomed view (experimental results).

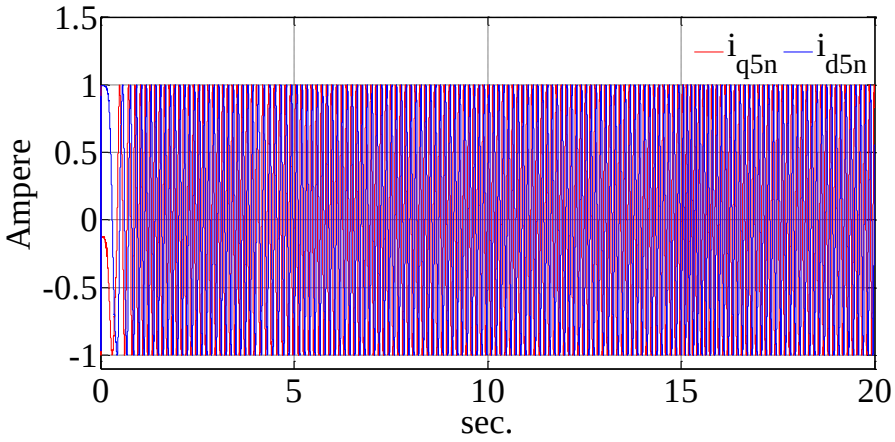

(a)

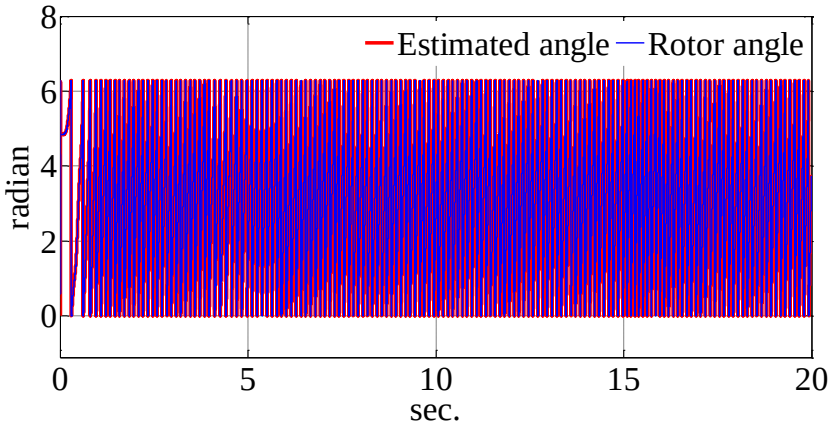

(a)

(b)

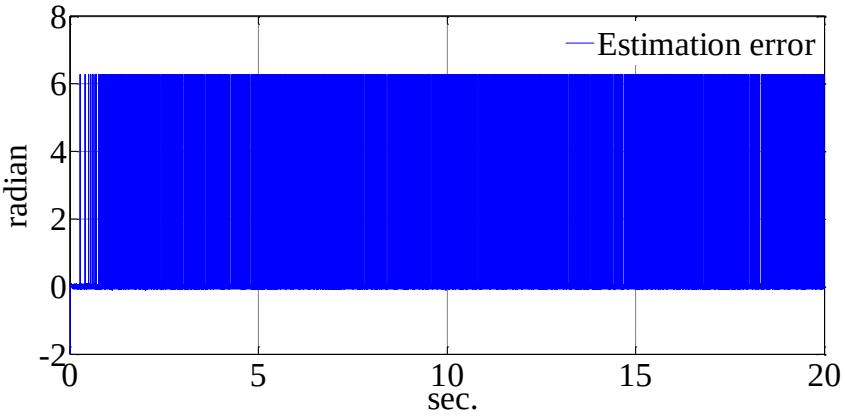

(c)

Figure 6.94: (a) The normalized currents of the fifth sequence, (b) Simulated and estimated angle, (c) The estimation error (simulation results).

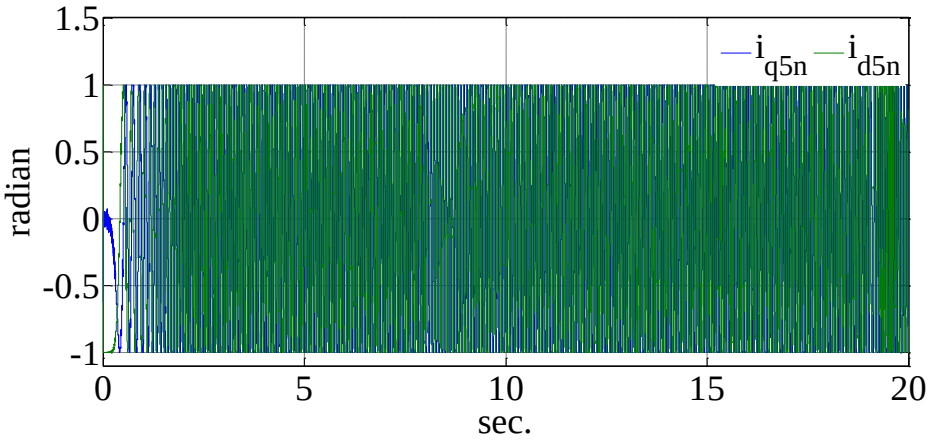

(a)

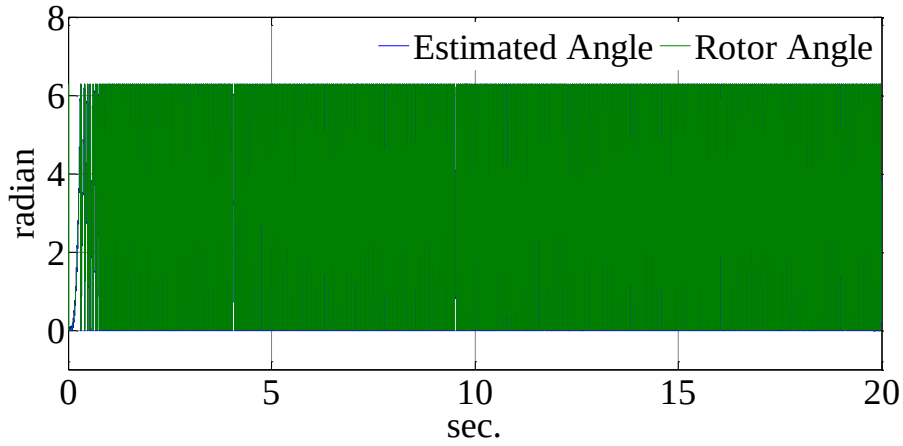

(b)

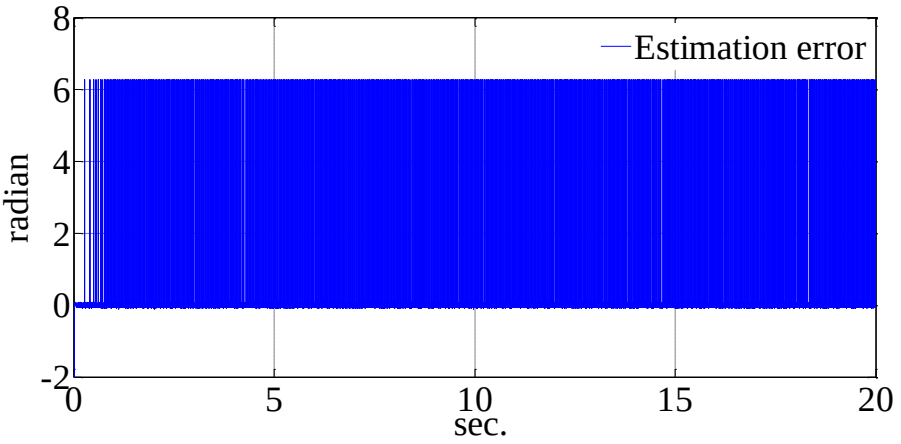

(c)

Figure 6.95: (a) The normalized currents of the fifth sequence, (b) Actual and estimated angle, (c) The estimation error (experimental results).

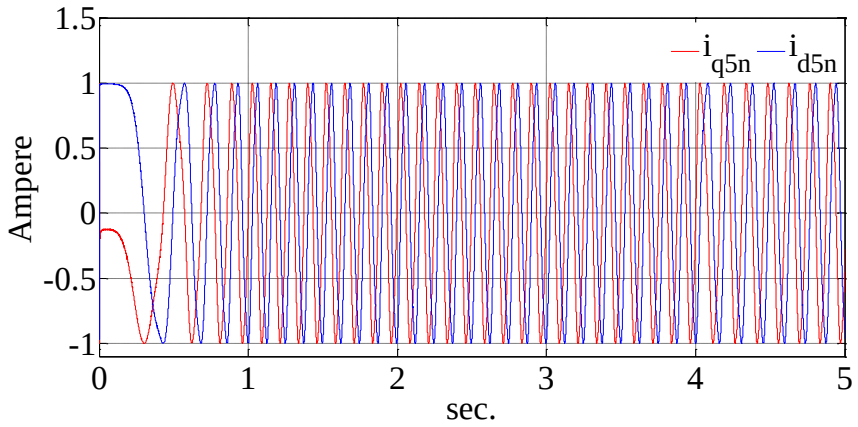

(a)

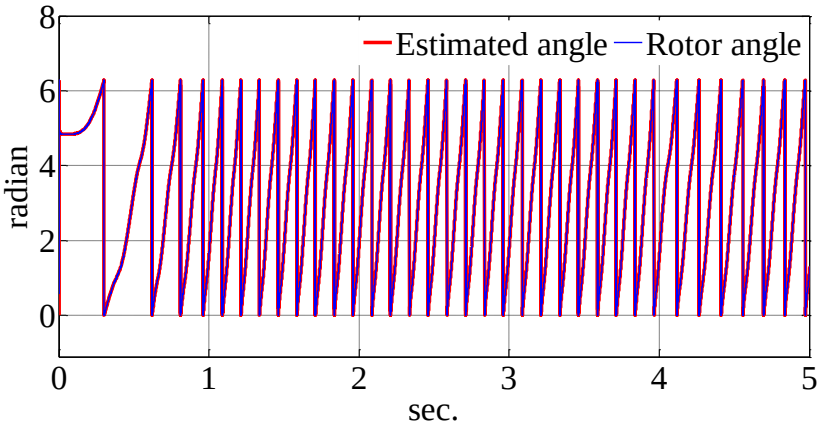

(b)

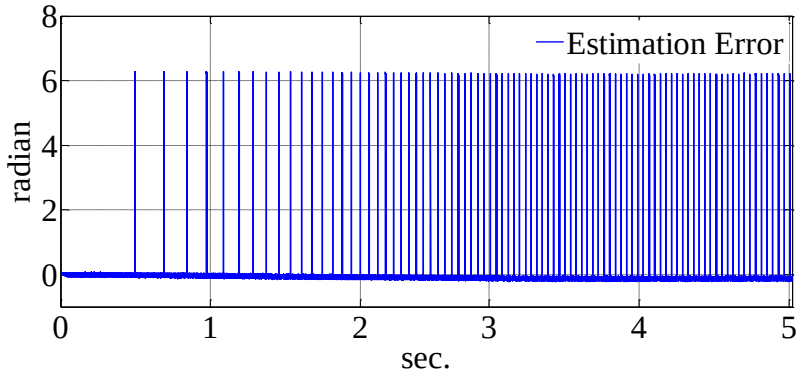

(c)

Figure 6.96: (a) The normalized currents of the fifth sequence, (b) Simulated and estimated angle, (c) The estimation error (simulation results).

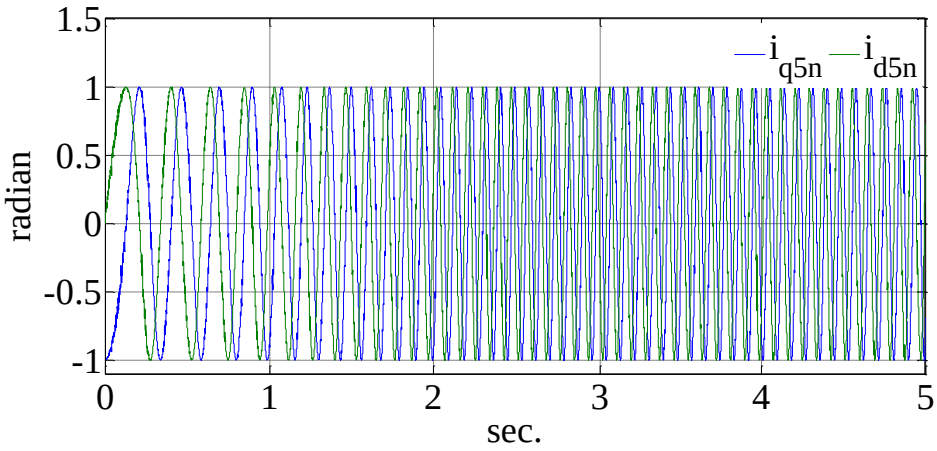

(a)

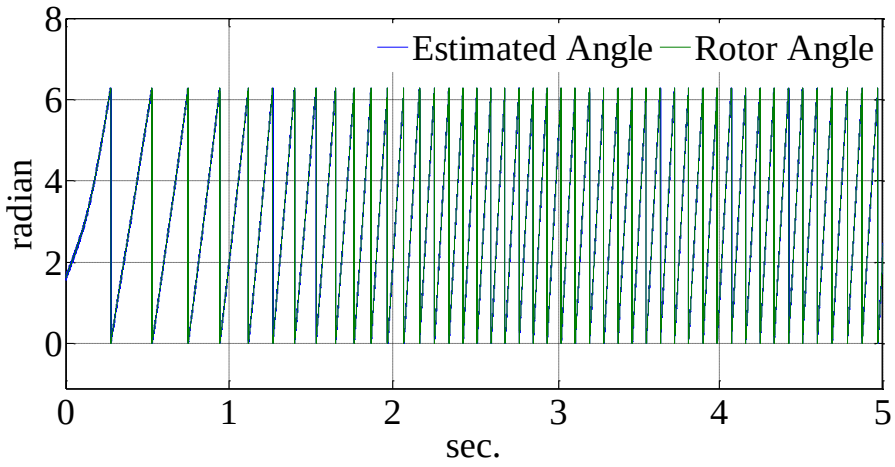

(b)

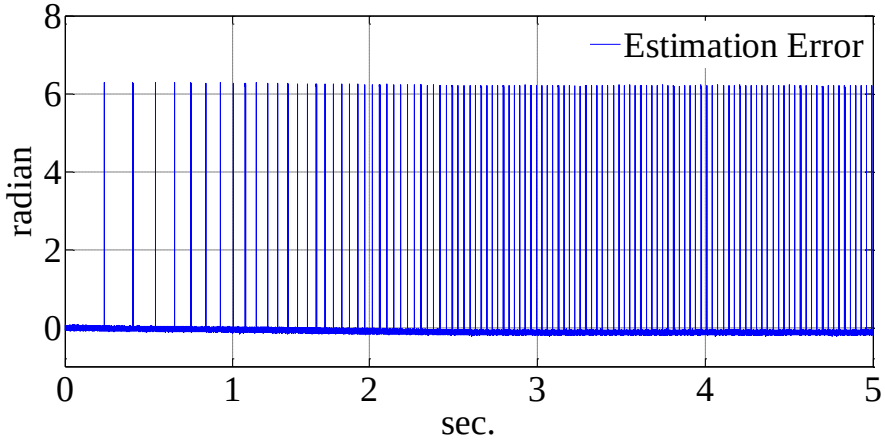

(c)

Figure 6.97: (a) The normalized currents of the fifth sequence, (b) Actual and estimated angle, (c) The estimation error (experimental results).

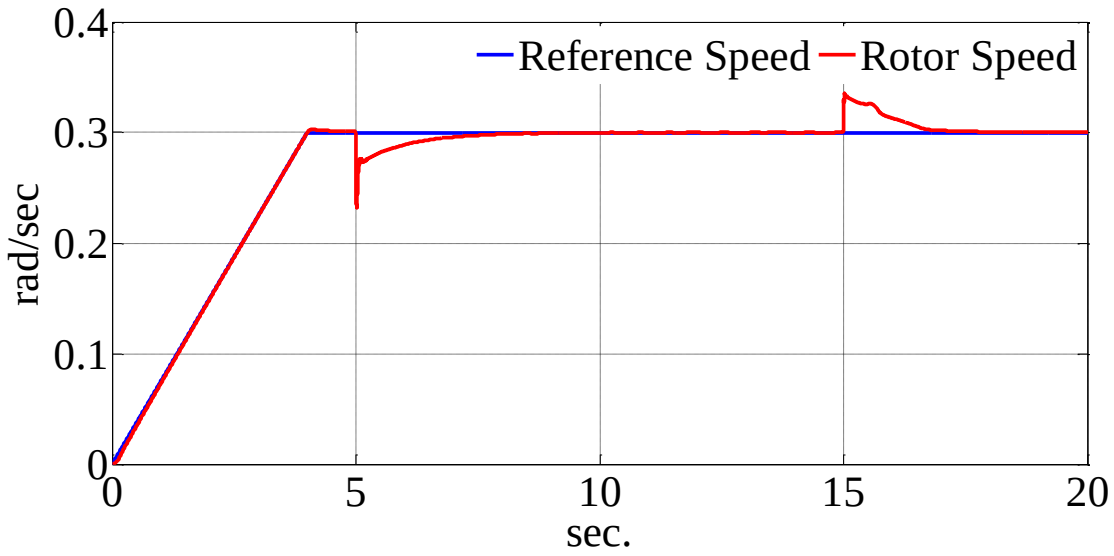

(a)

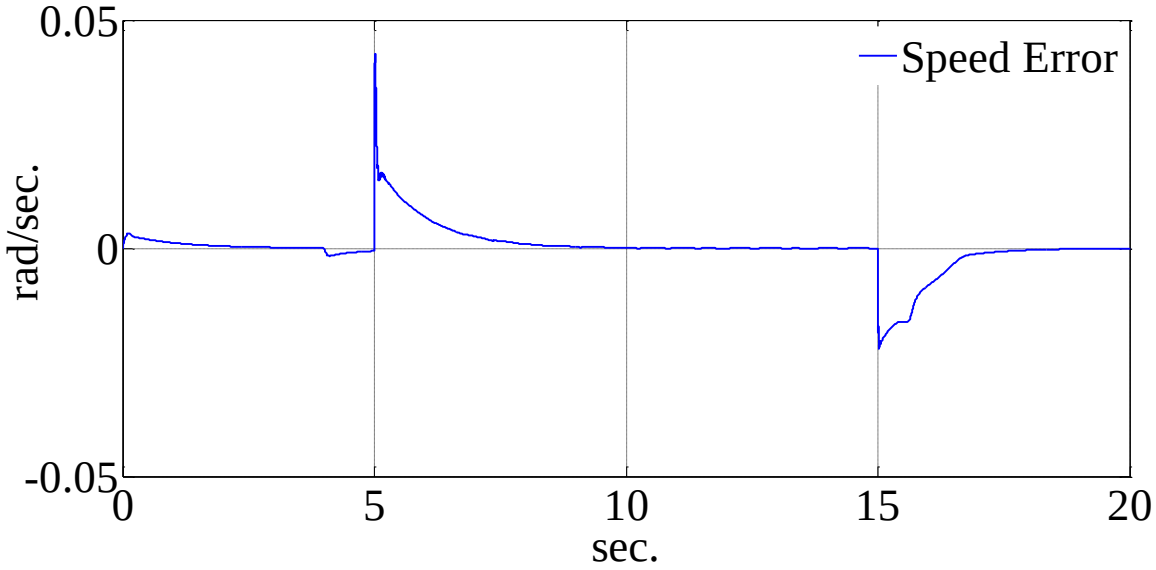

(b)

Figure 6.98: (a) The reference and rotor speed, (b) The speed error (simulation results).

6.6.3 Very Low Speed Test

In this section the drive receives a very low speed reference as the input command. The speed reference starts from the zero and goes to a fixed speed at 0.3 (rad/sec) after the rotor of the

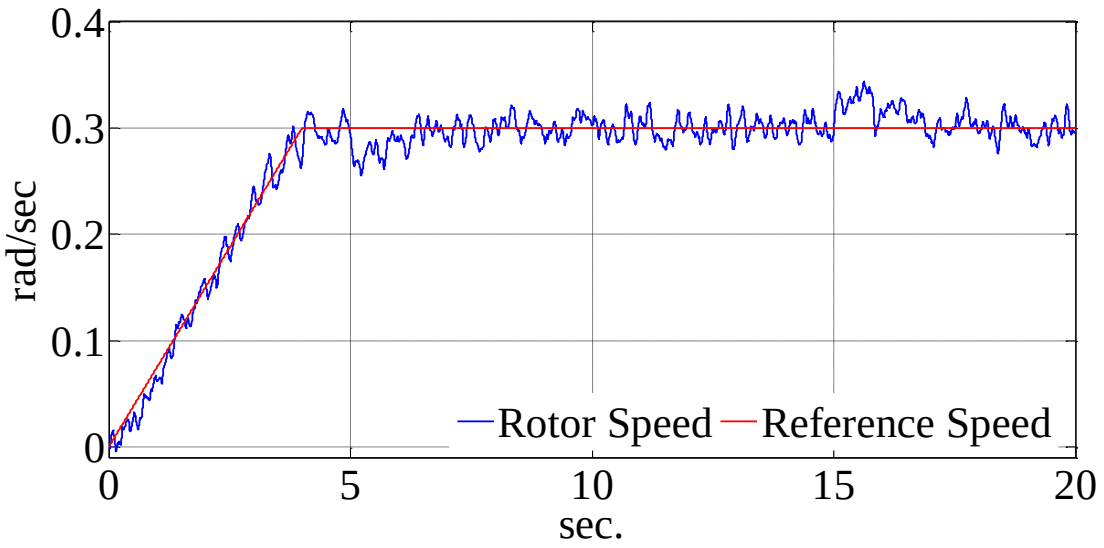

(a)

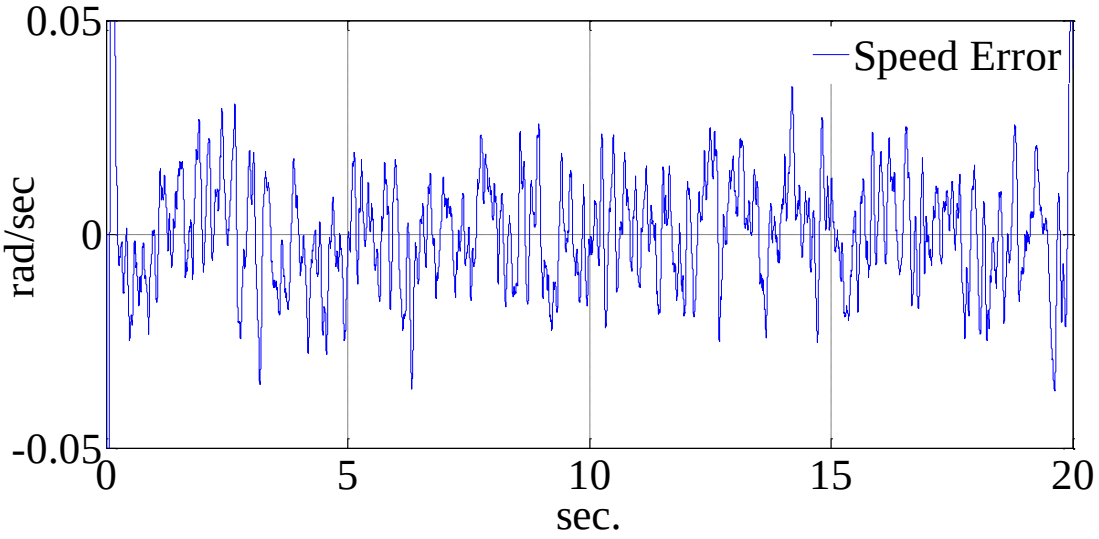

(b)

Figure 6.99: (a) The reference and rotor speed, (b) The speed error (experimental results).

Machine reaches the final speed, a step load torque of 1 N.m is applied to the rotor and later removed. Figures 6.98 and 6.99 show the reference speed and the rotor speed together along with the speed error for simulation and experimental results respectively. It can be seen that the drive can accurately follow the reference speed.

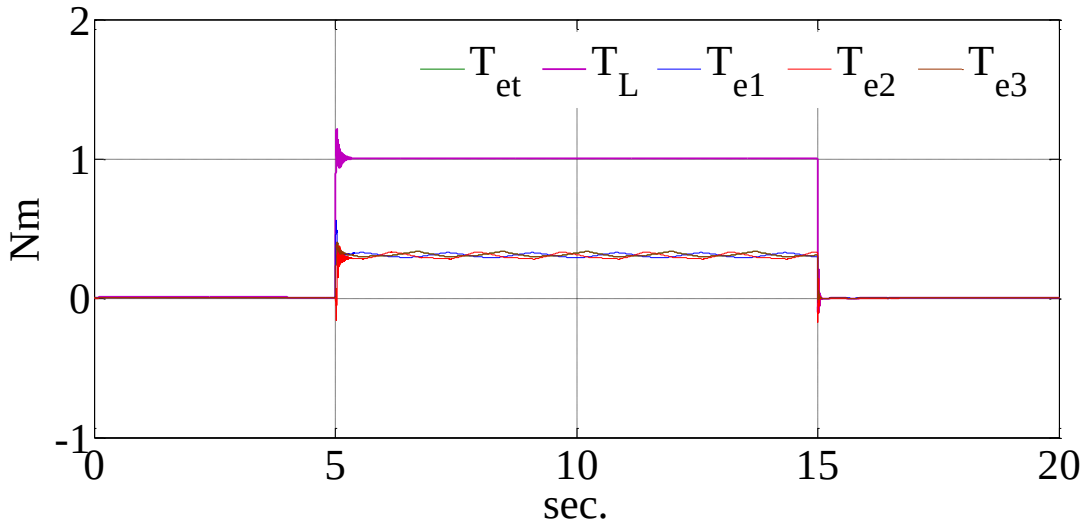

Figure 6.100: The electromagnetic torque of each machine and the total (simulation results).

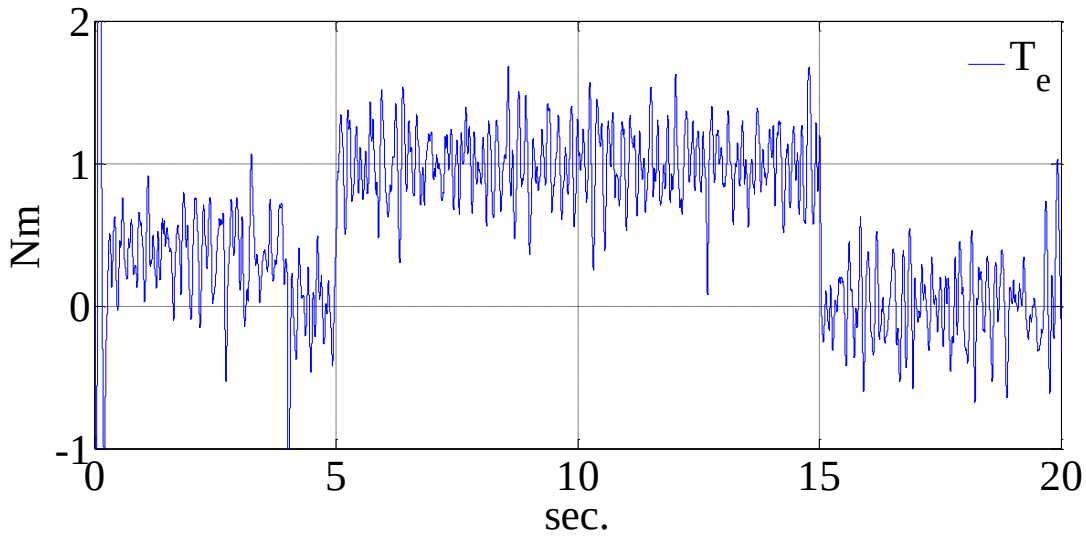

Figure 6.101: The electromagnetic torque of each machine and the total (experimental result).

Figure 6.100 shows the electromagnetic torque of each machine and the total torque for simulation results. It can be seen that by increasing the load torque, the machine generates electromagnetic torque to supply the load. The electromagnetic torque generated by machine in experiment is also shown in Figure 6.101.

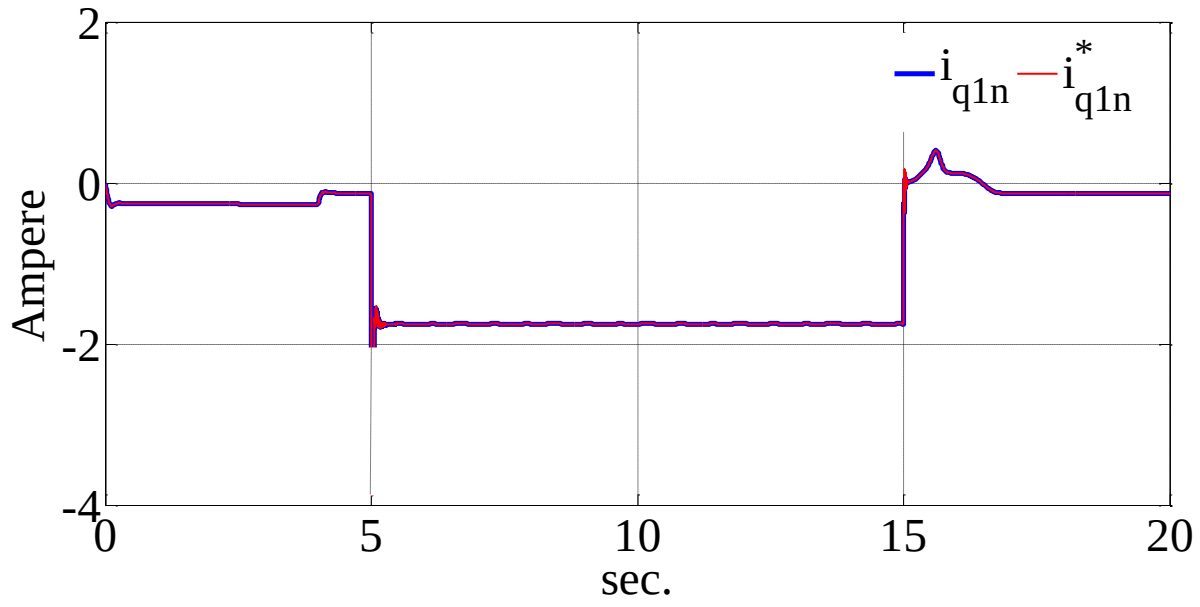

(a)

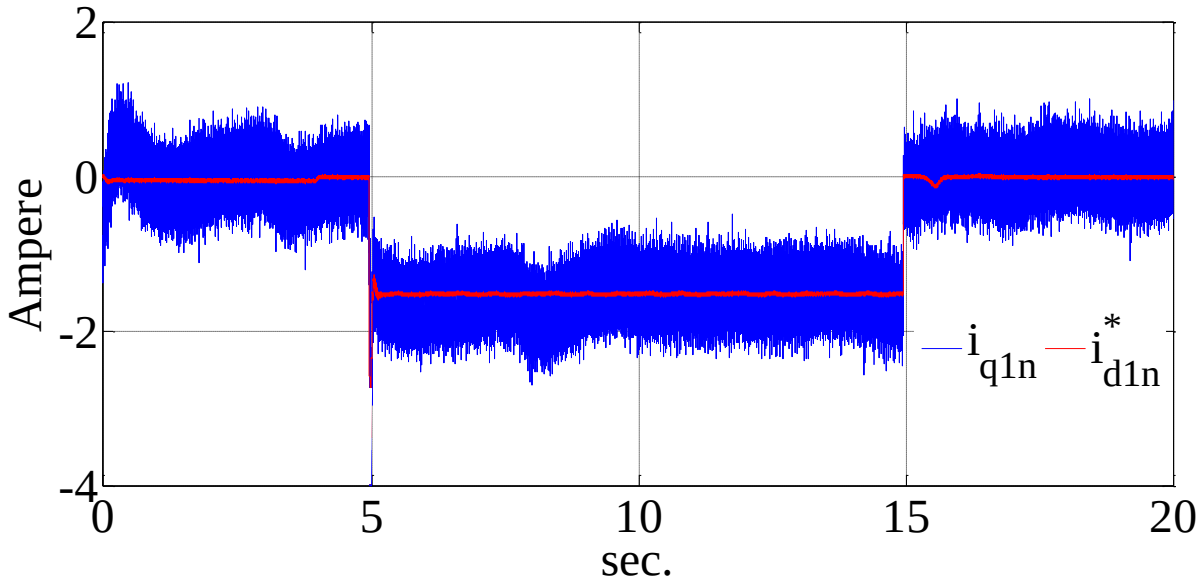

(b)

Figure 6.102: The q_{1n} reference and feedback currents for, (a) Simulation results, (b) Experimental results.

Figure 6.102 shows the reference and the feedback currents of q_{1n} - axis for simulation and experimental results. It can be seen that, by applying load torque the q axis current increases to let the machine generate torque and keep the speed constant. Similarly, Figure 6.103 shows the reference and feedback currents of d axis in decoupled reference frame. The d axis current reference

is generated from q axis current using minimum copper loss strategy. Therefore, the current of the d axis varies with the variations of the q axis current.

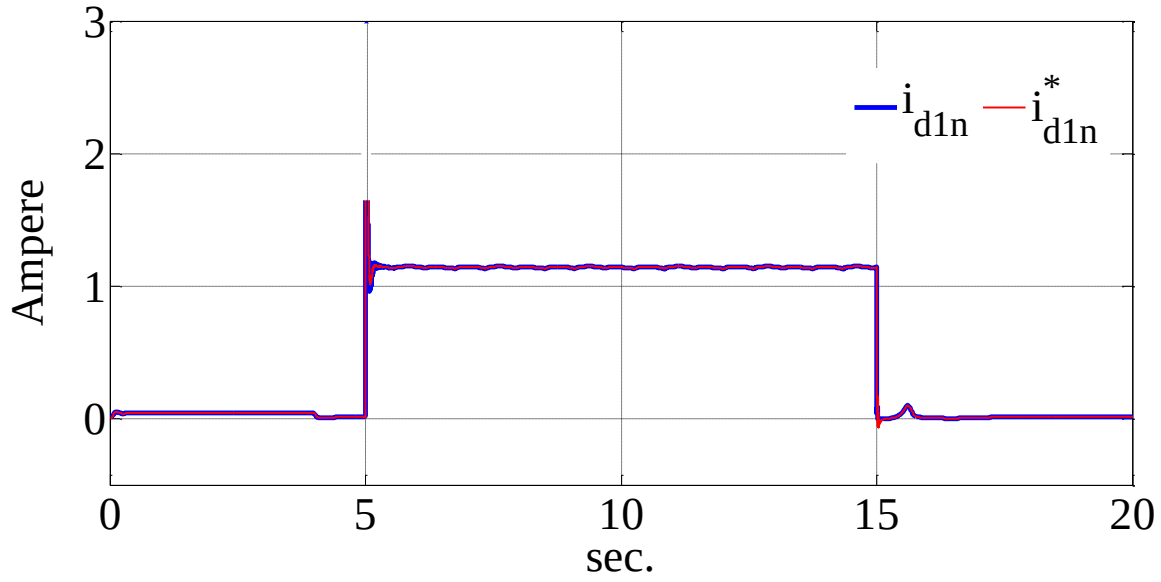

(a)

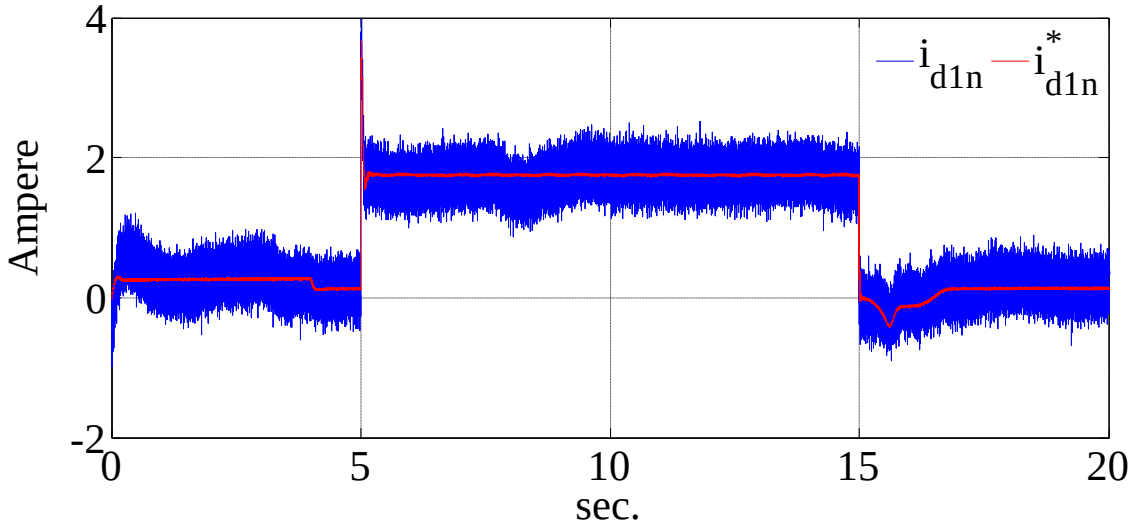

(b)

Figure 6.103: The d_{1n} reference and feedback currents for, (a) Simulation results, (b) Experimental results.

The rest of the axis of decoupled reference frame receive zero as their current reference. Their currents are shown in Figures 6.104 to 6.106 for simulation and experimental results. Figure 6.104 shows the currents of d_{2n} axis for simulation and experimental results.

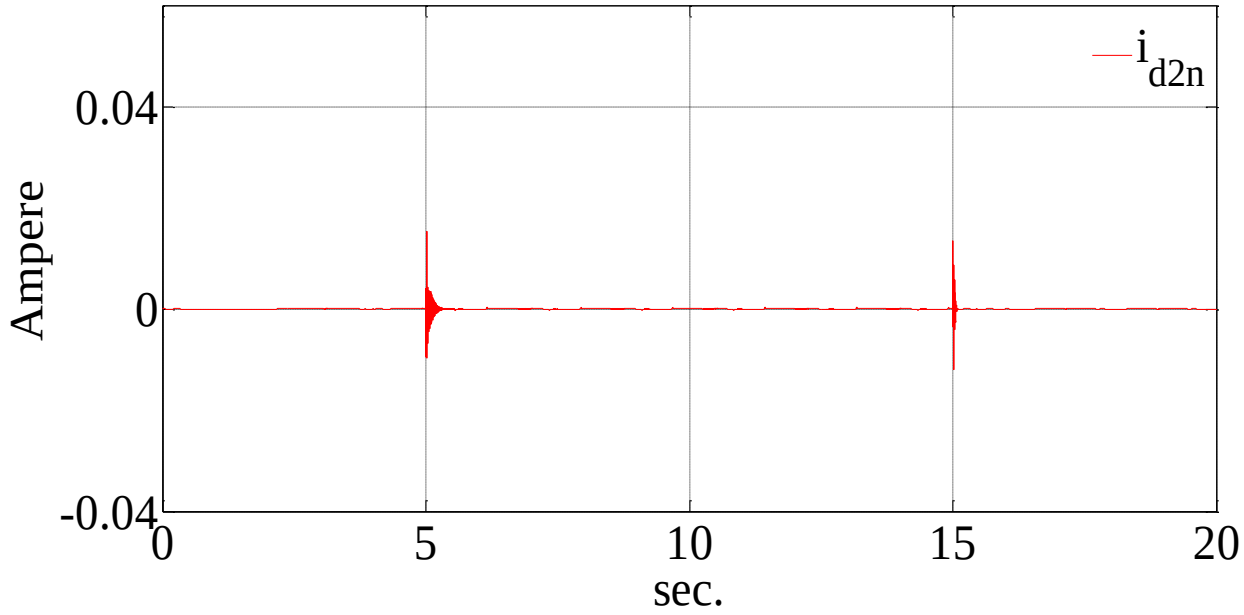

(a)

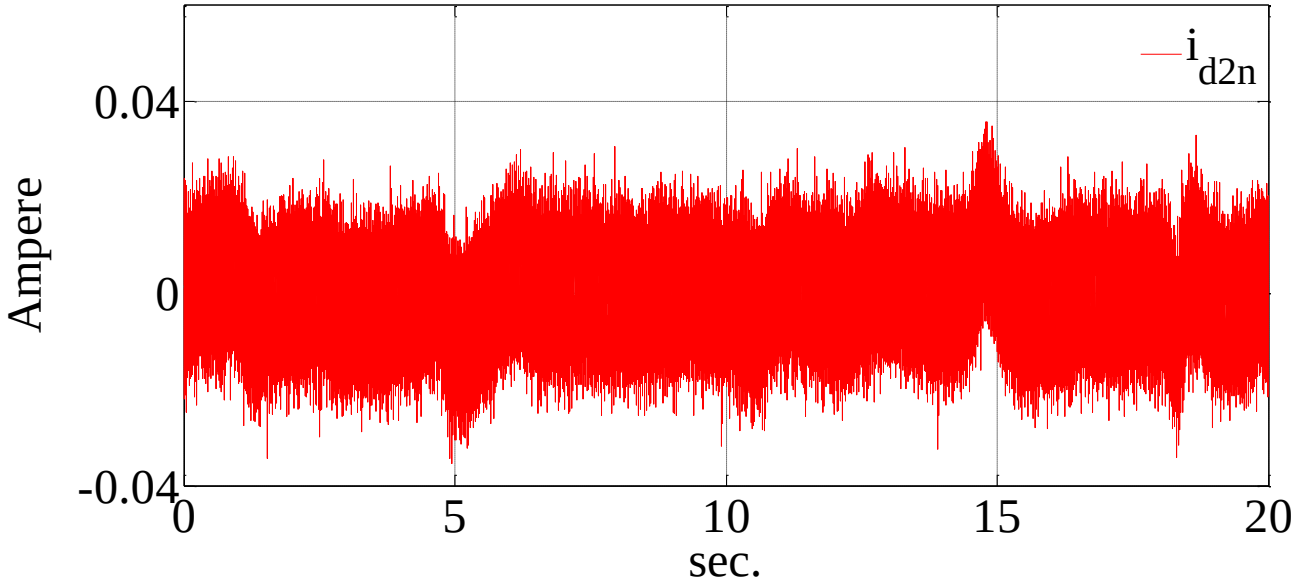

(b)

Figure 6.104: The d_{2n} reference and feedback currents for, (a) Simulation results, (b) Experimental results.

Currents of q_{2n} axis for simulation and experimental results are shown in Figure 6.105.

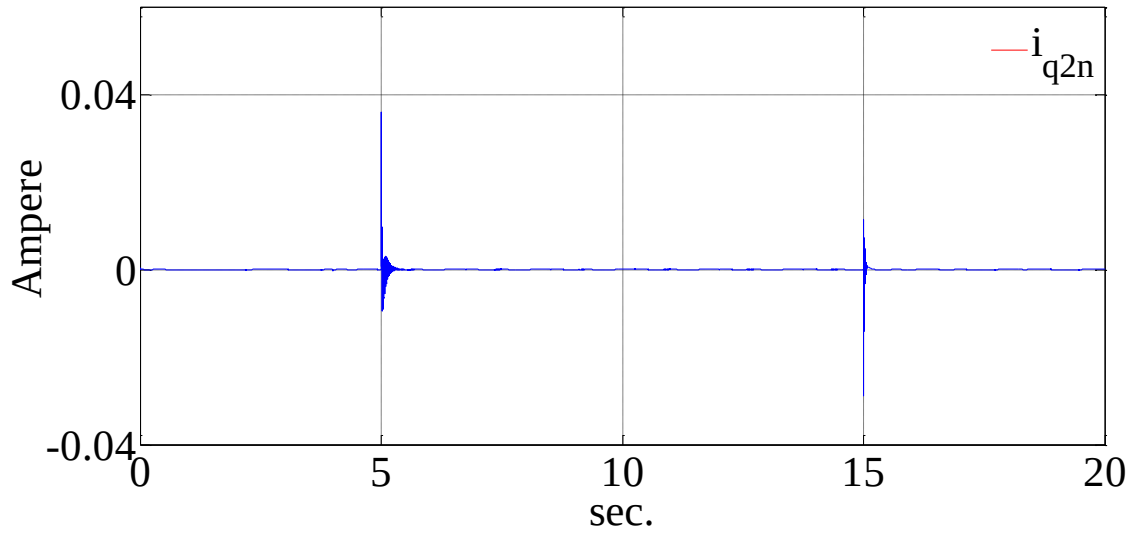

(a)

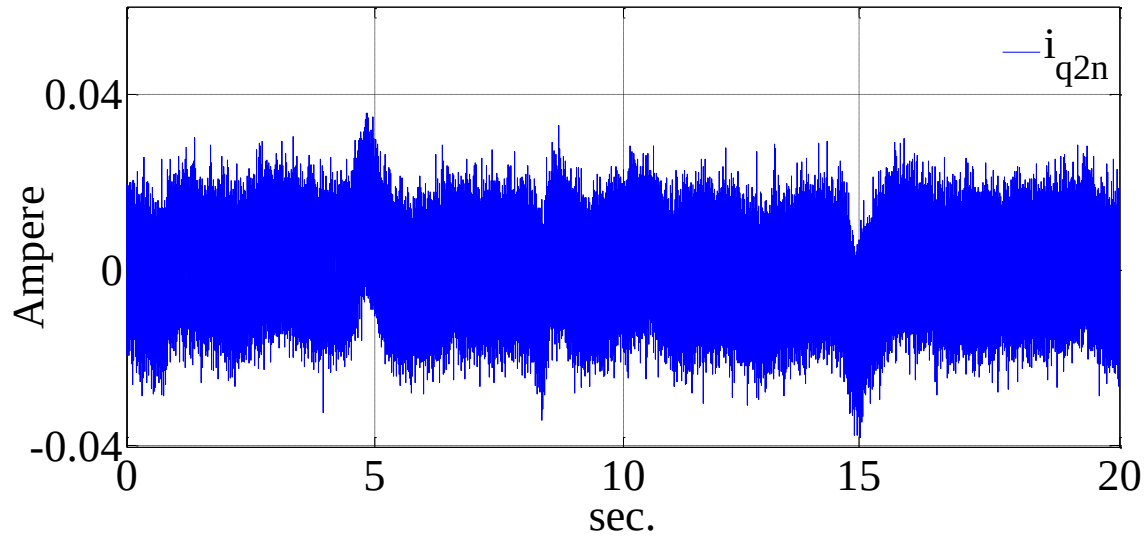

(b)

Figure 6.105: The q_{2n} reference and feedback currents for, (a) Simulation results, (b) Experimental results.

Currents of d_{3n} axis for simulation and experimental results are shown in Figure 6.106.

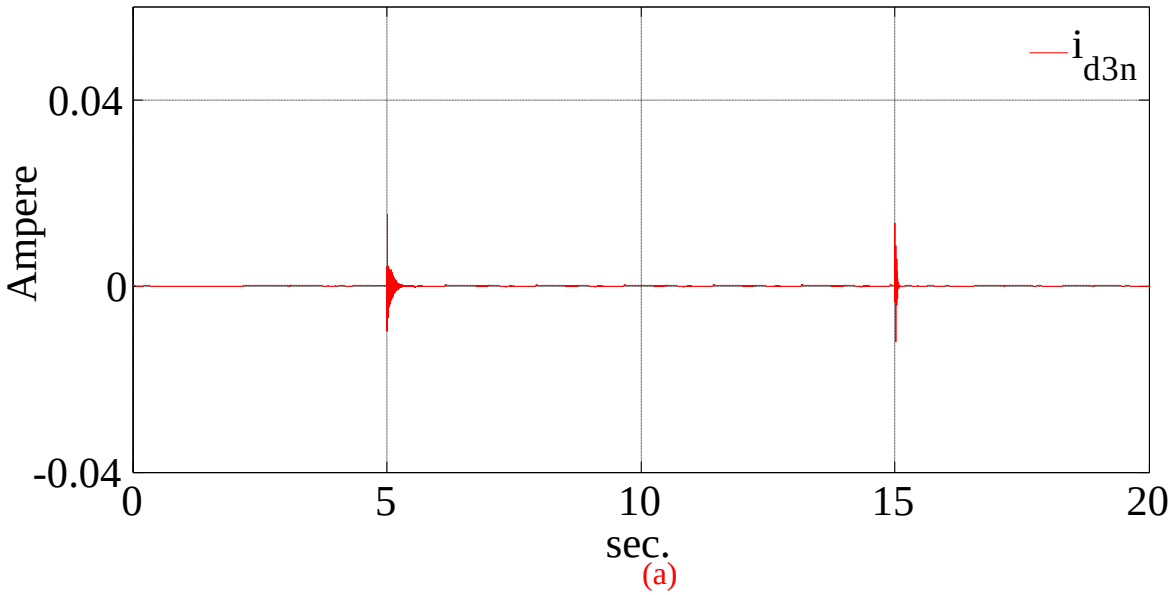

(a)

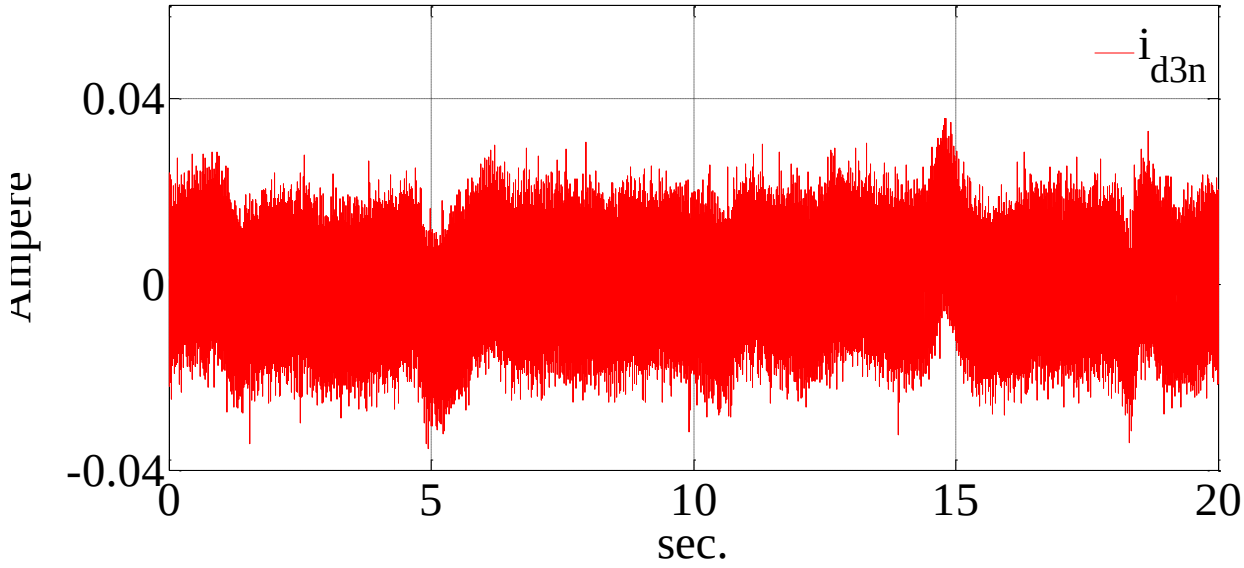

(b)

Figure 6.106: The d_{3n} reference and feedback currents for, (a) Simulation results, (b) Experimental results.

Currents of q_{3n} axis for simulation and experimental results are shown in Figure 6.107.

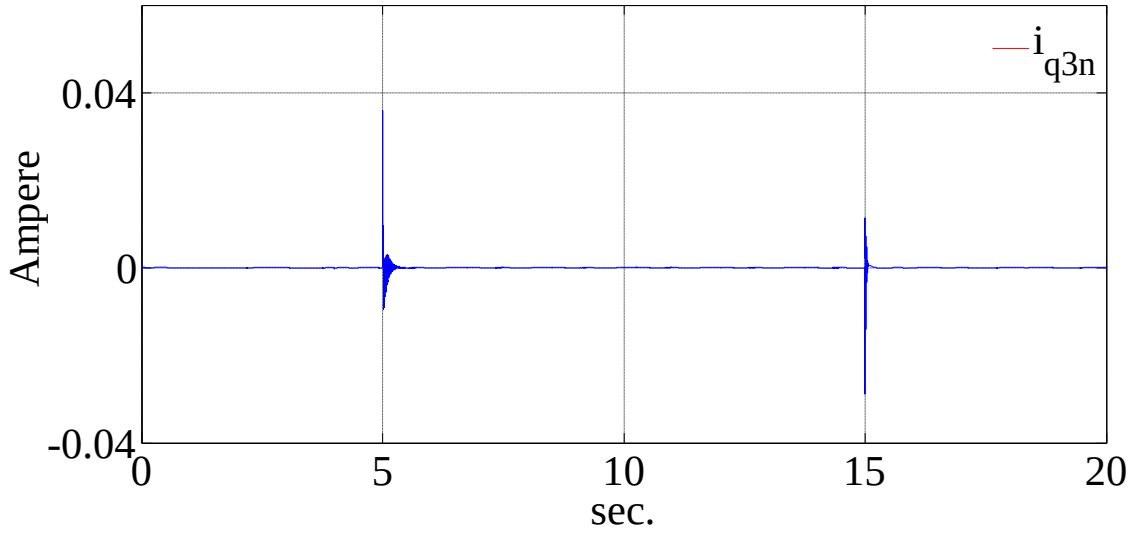

(a)

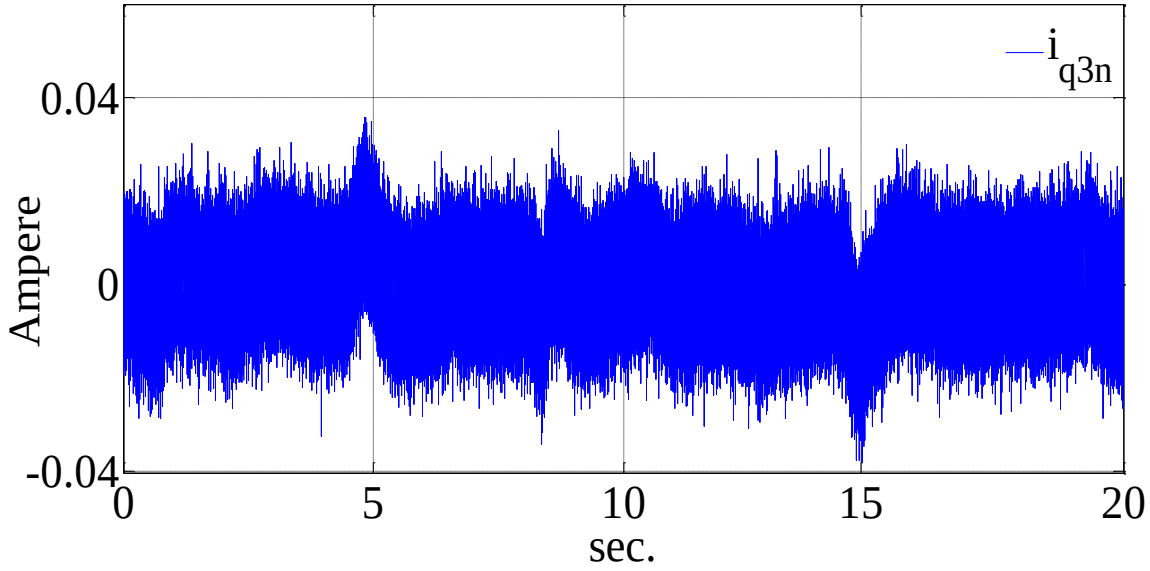

(b)

Figure 6.107: The q_{3n} reference and feedback currents for, (a) Simulation results, (b) Experimental results.

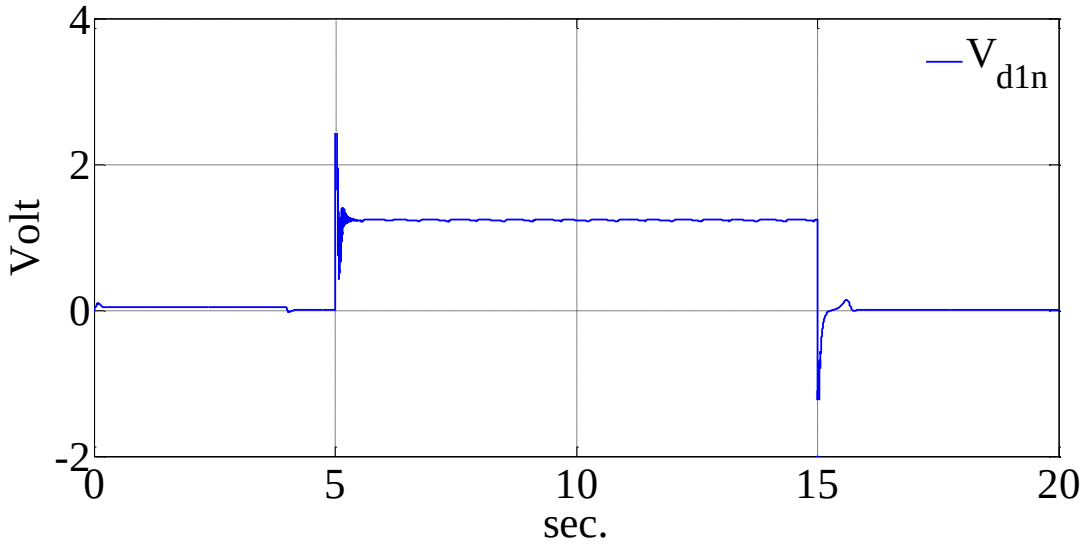

(a)

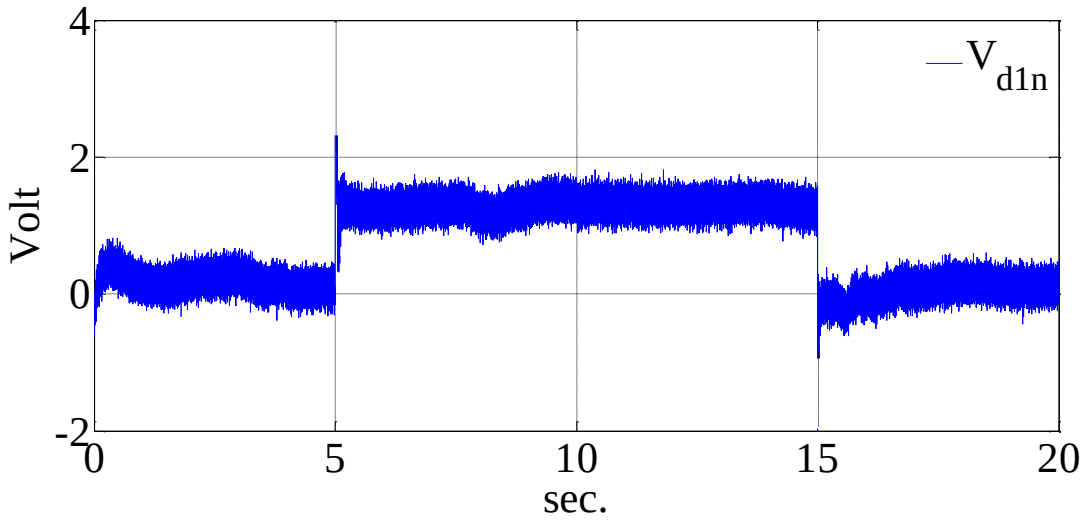

(b)

Figure 6.108: The voltages generated by the current regulators in d_{1n} axis for, (a) Simulation results, (b) Experimental results.

The output voltages of the current regulators are also shown in this section. Figure 6.108 shows the voltages of d axis of the decoupled reference frame for simulation and experimental results. Figure 6.109 shows the voltage of the q axis of the decoupled reference frame for simulation and experimental results. From these figures the variations of dq_{1n} axis voltages with the load torque can be seen.

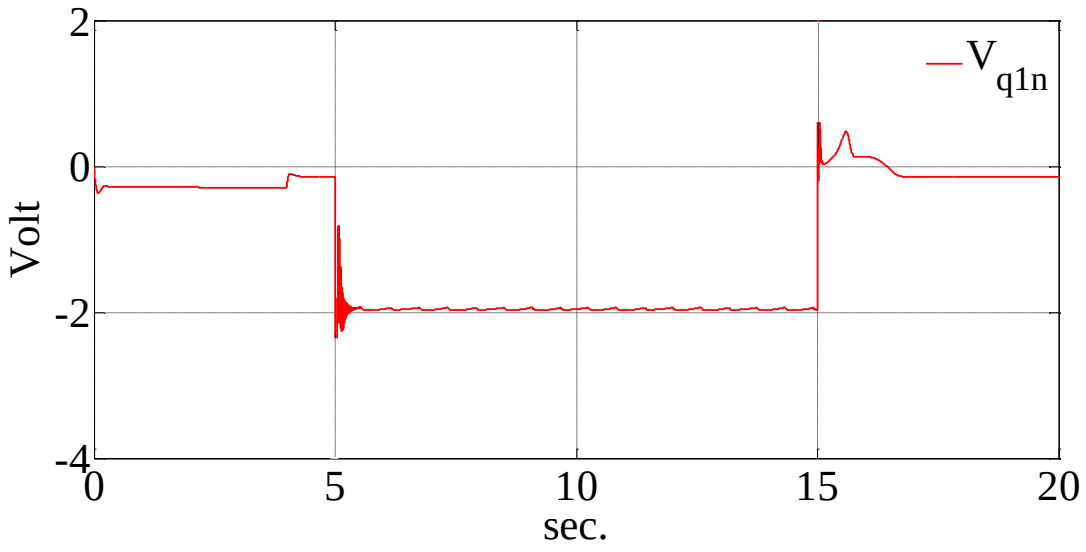

(a)

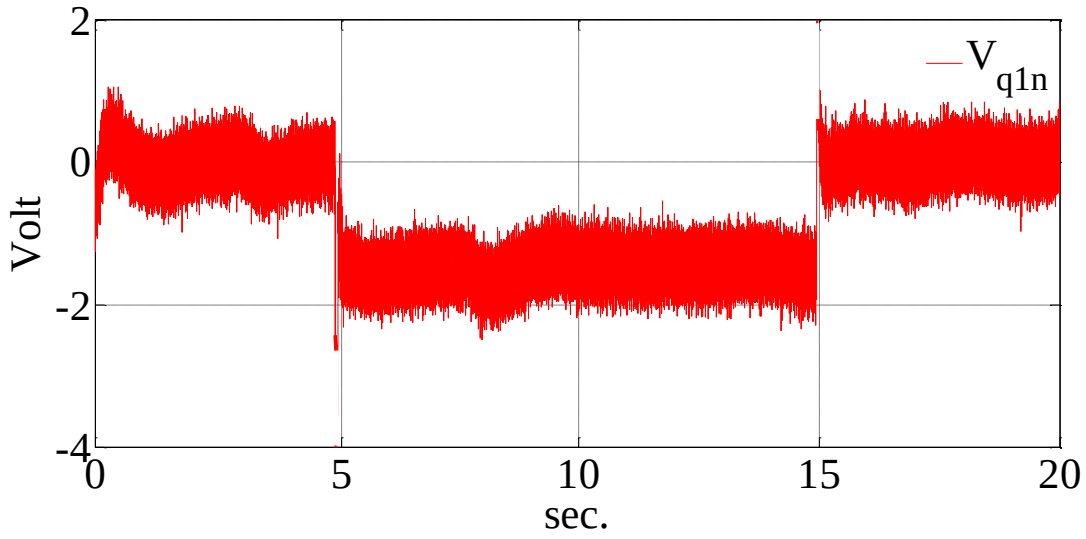

(b)

Figure 6.109: The voltages generated by the current regulators in q_{1n} axis for, (a) Simulation results, (b) Experimental results.

The voltages of the non-torque producing axis are also shown in Figures 6.110 to 6.113. Figure 6.110 shows the simulation and experimental results of q_{2n} axis for simulation and experimental results. Figure 6.111 also shows the simulation and experimental results of d_{2n} axis for simulation and experimental results.

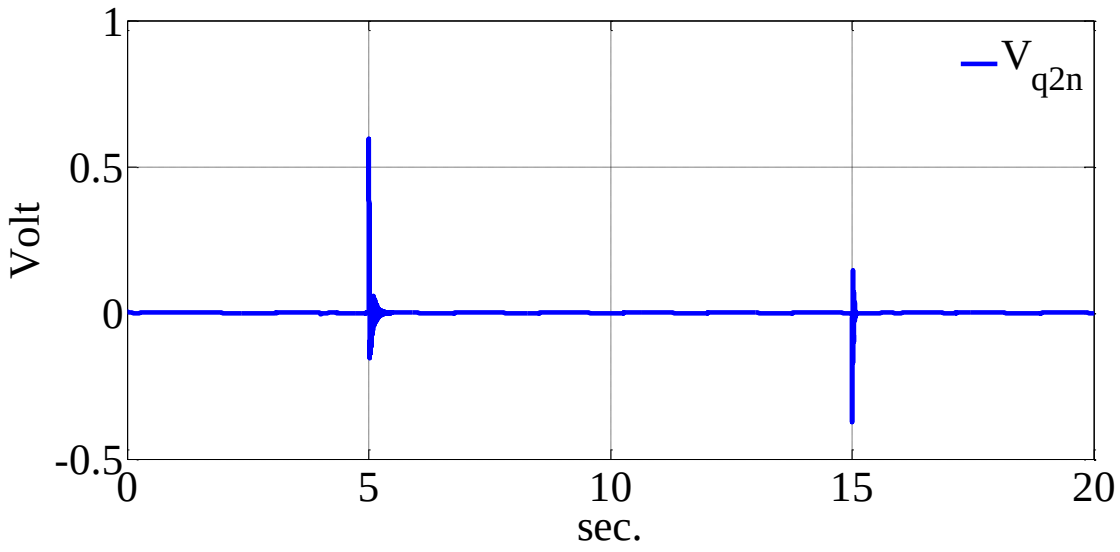

(a)

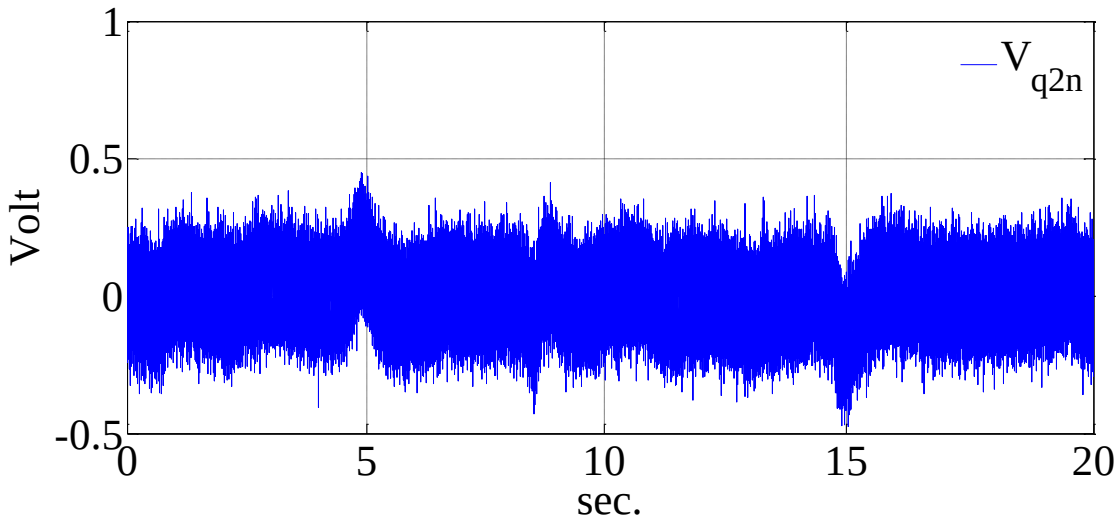

(b)

Figure 6.110: The voltages generated by the current regulators in q_{2n} axis for, (a) Simulation results, (b) Experimental results.

Figure 6.112 shows the simulation and experimental results of q_{3n} axis for simulation and experimental results.

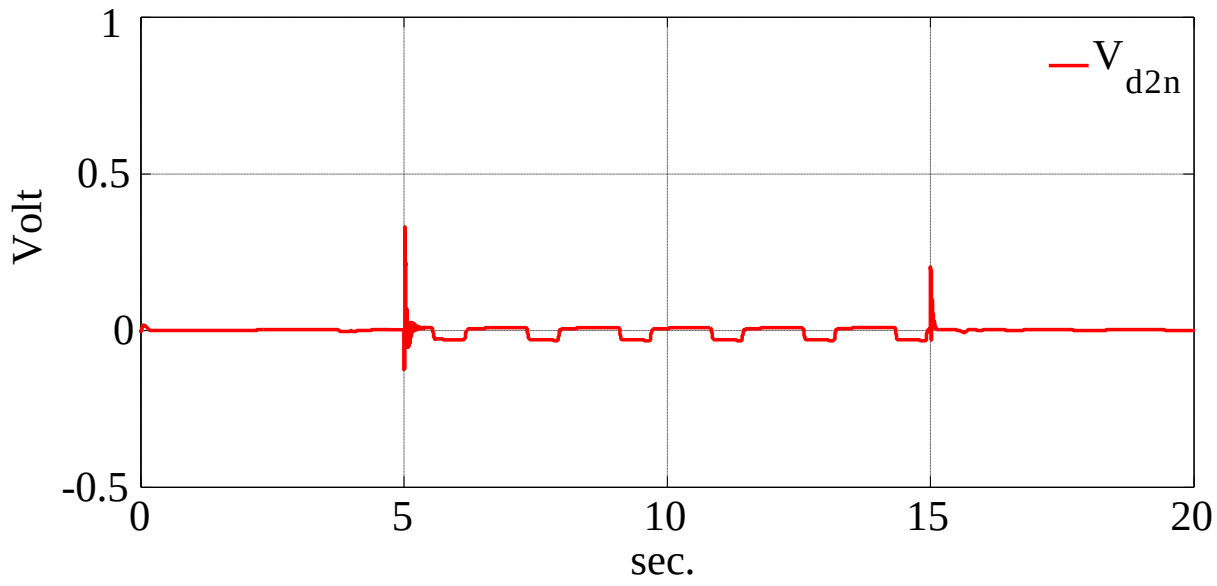

(a)

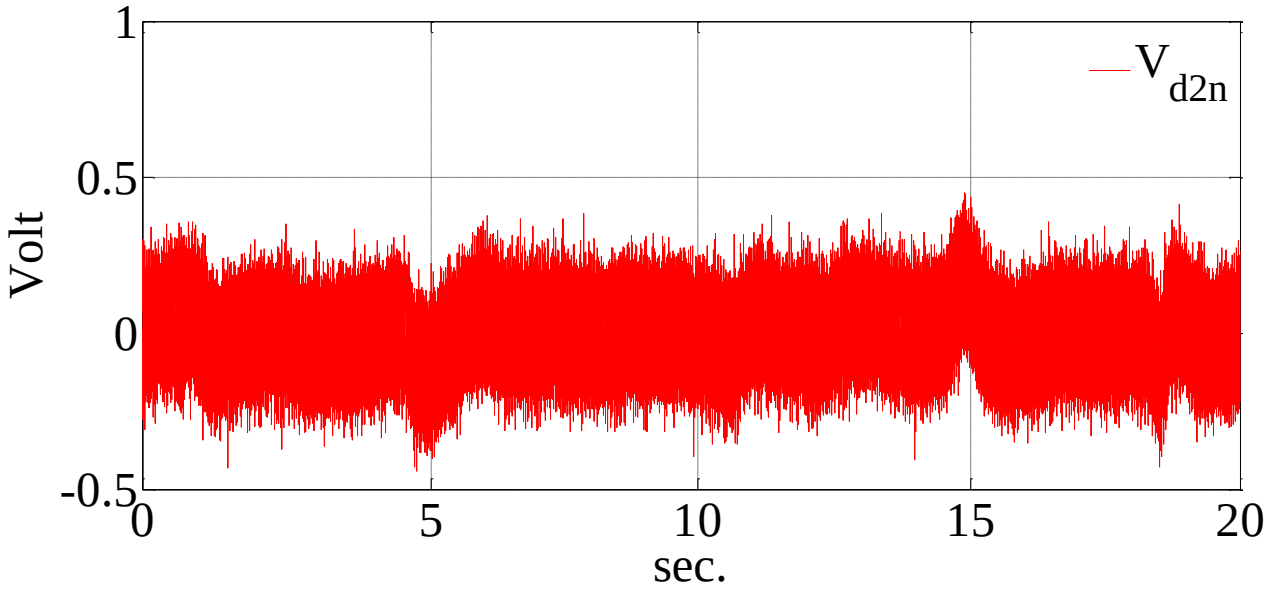

(b)

Figure 6.111: The voltages generated by the current regulators in d_{2n} axis for, (a) Simulation results, (b) Experimental results.

Figure 6.113 also shows the simulation and experimental results of d_{3n} axis for simulation and experimental results. From these figures it can be seen that the voltages have relatively low magnitudes because they are operating on small inductances.

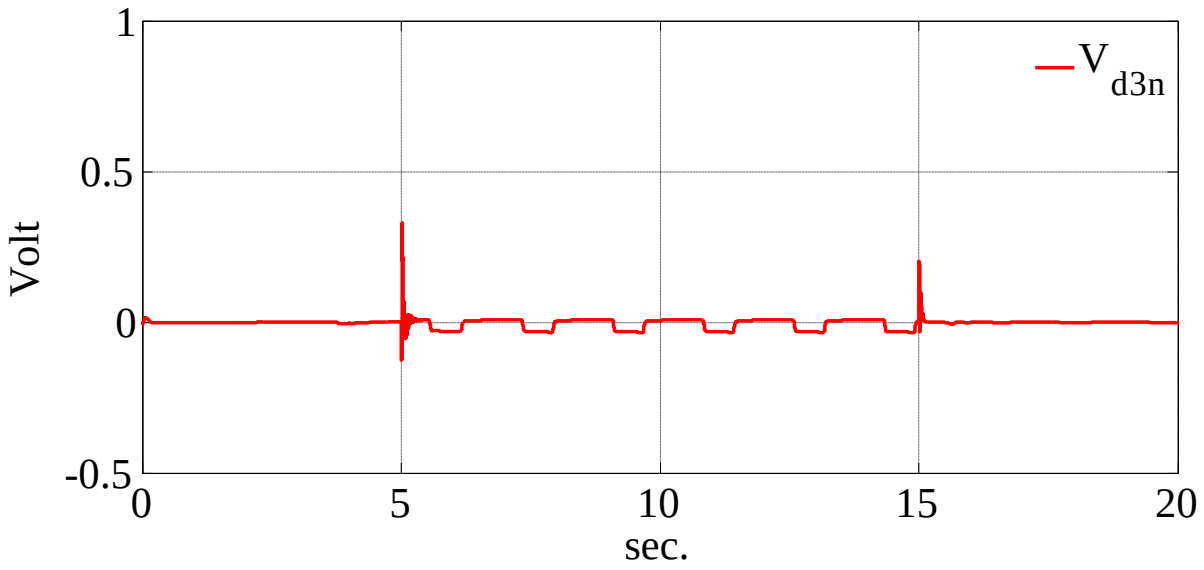

(a)

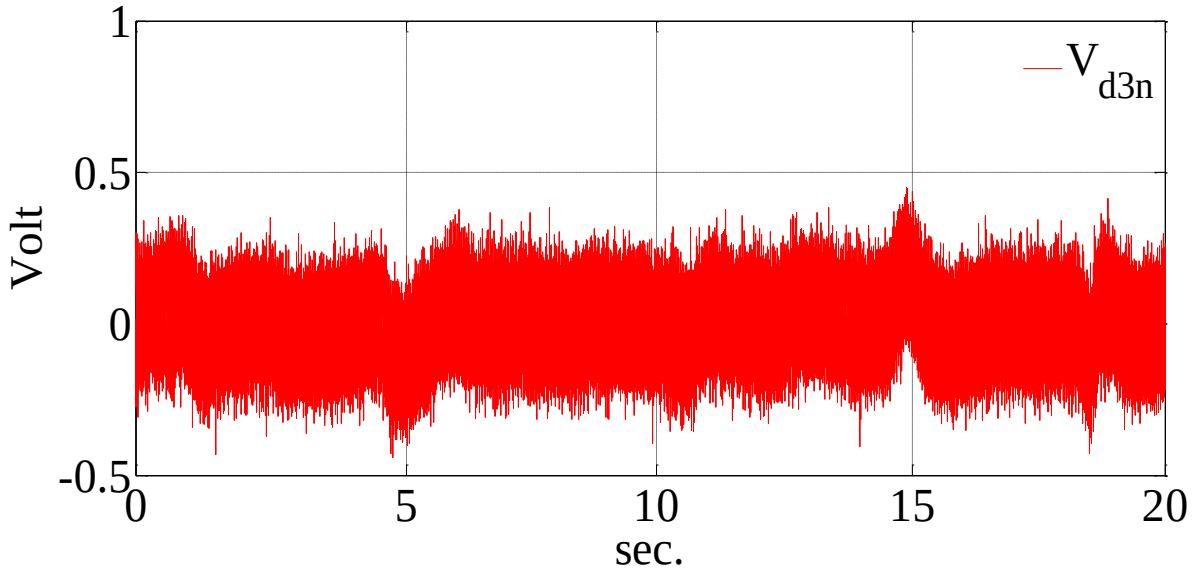

(b)

Figure 6.112: The voltages generated by the current regulators in d_{3n} axis for, (a) Simulation results, (b) Experimental results.

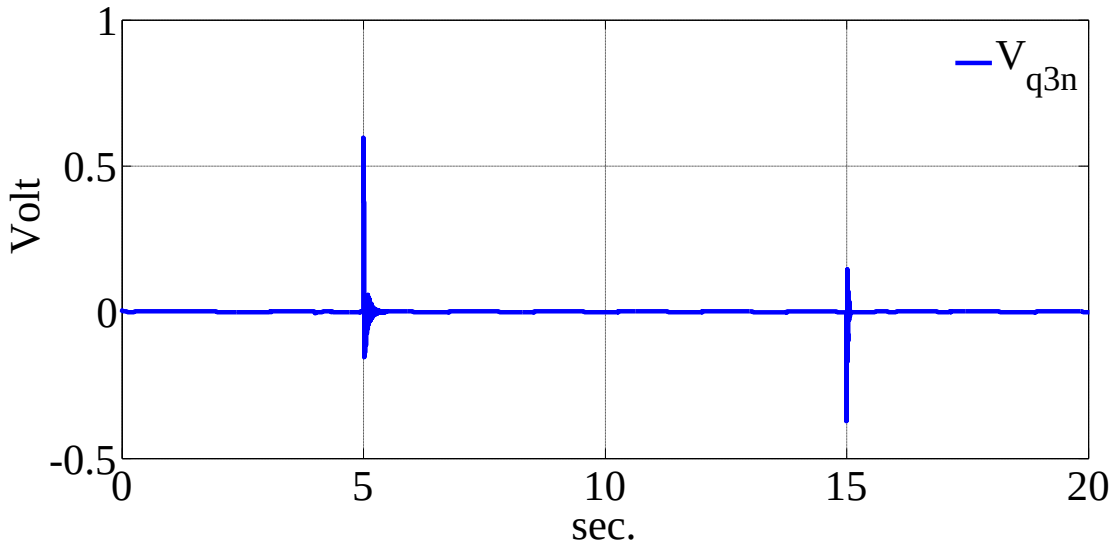

(a)

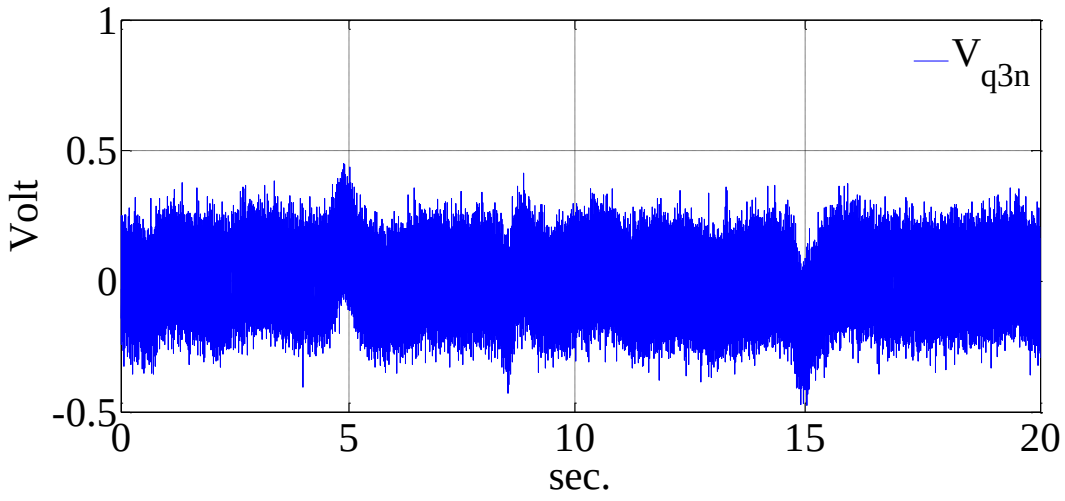

(b)

Figure 6.113: The voltages generated by the current regulators in q_{3n} axis for, (a) Simulation results, (b) Experimental results.

The voltages of the machine stator in the rotor reference frame are shown in Figures 6.114 to 6.117 for simulation and experimental results respectively. From these figures the effect of the load can be seen in the voltages.

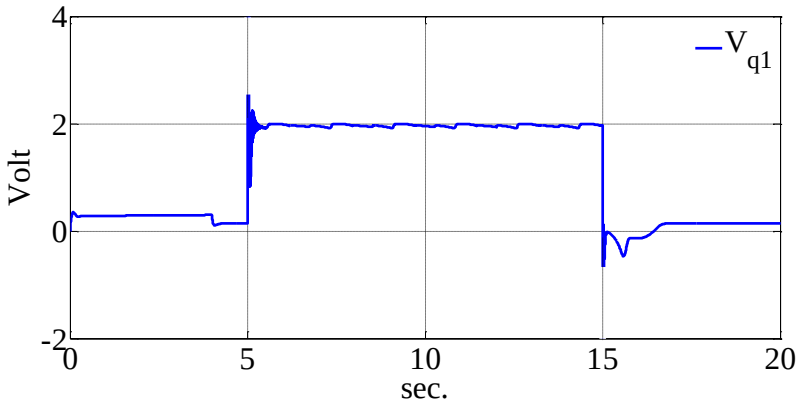

(a)

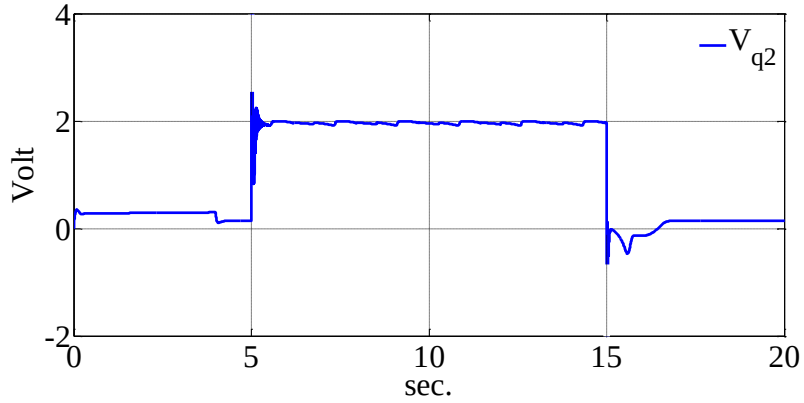

(b)

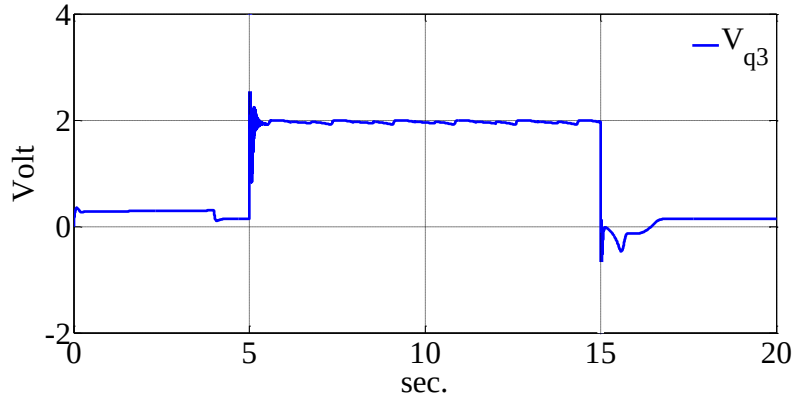

(c)

Figure 6.114: The voltages generated by the current regulators in the q axis of rotor reference frame for, (a) Machine '1', (b) Machine '2', (c) Machine '3' (simulation result).

By increasing the load torque the q and d axis voltages increase to let corresponding current also increase and generate more electromagnetic torque to keep the rotor speed constant.

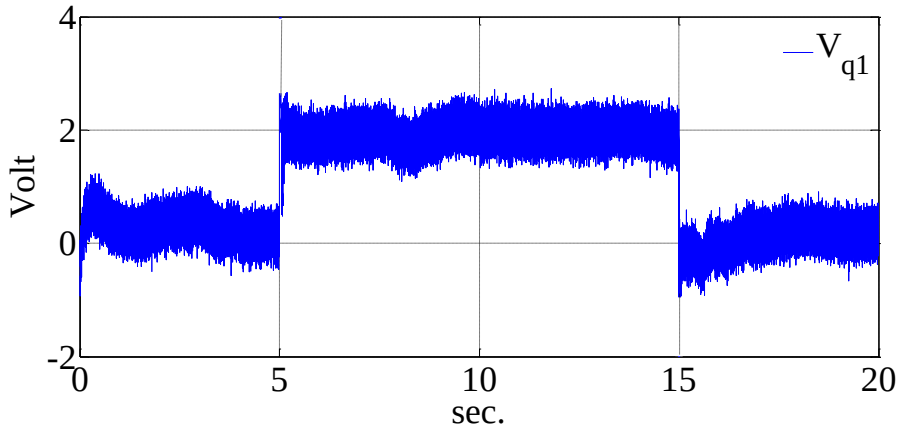

(a)

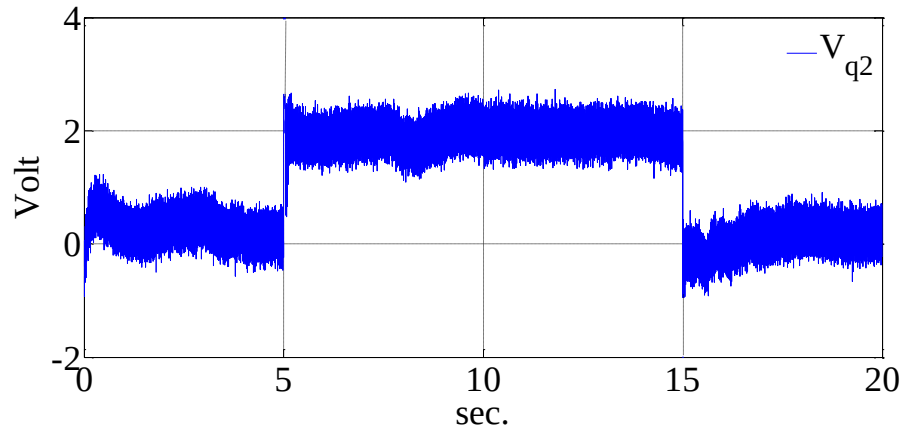

(b)

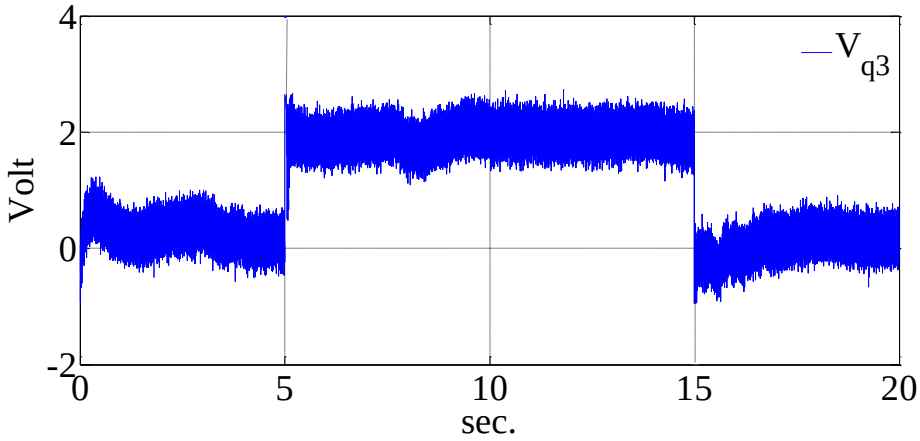

(c)

Figure 6.115: The voltages generated by the current regulators in the q axis of rotor reference frame for, (a) Machine '1', (b) Machine '2', (c) Machine '3' (experimental result).

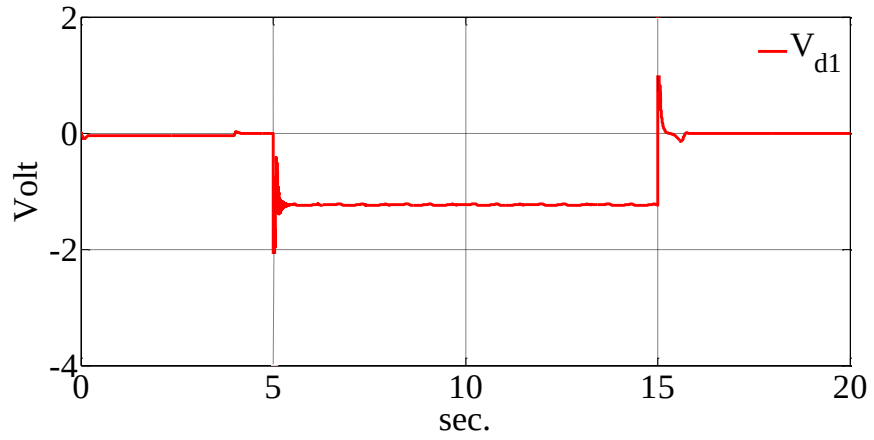

(a)

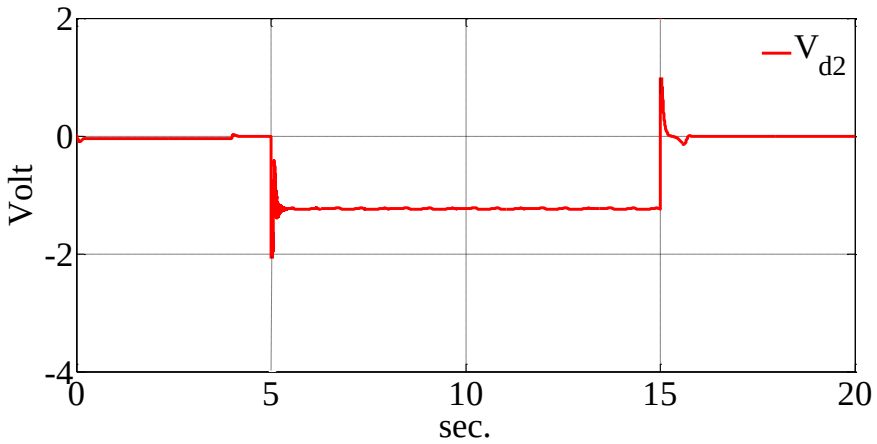

(b)

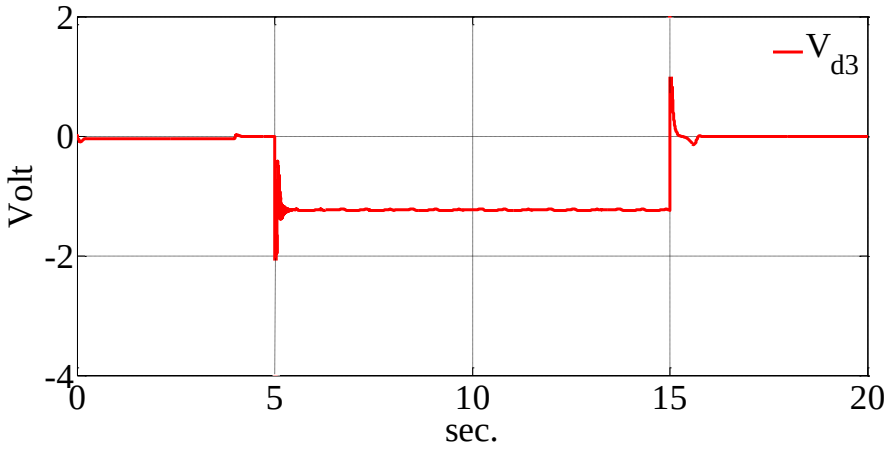

(c)

Figure 6.116: The voltages generated by the current regulators in the d axis of rotor reference frame for, (a) Machine '1', (b) Machine '2', (c) Machine '3' (simulation result).

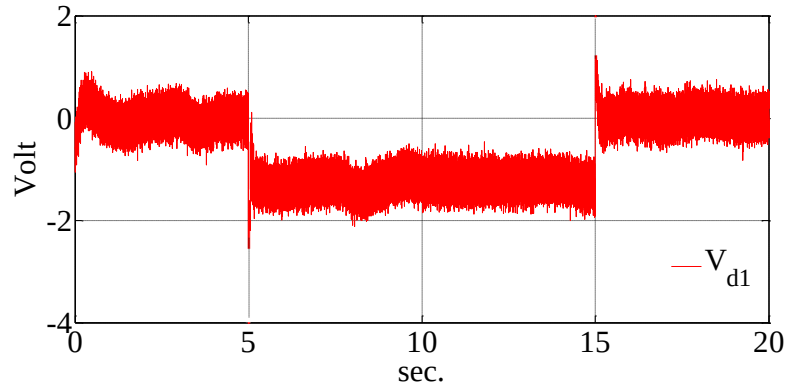

(a)

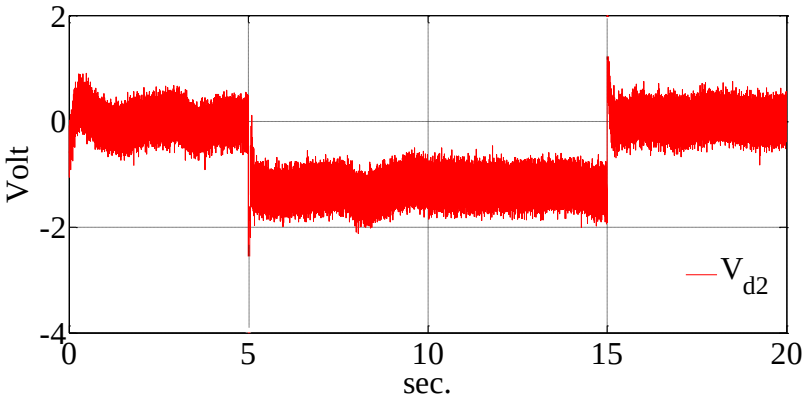

(b)

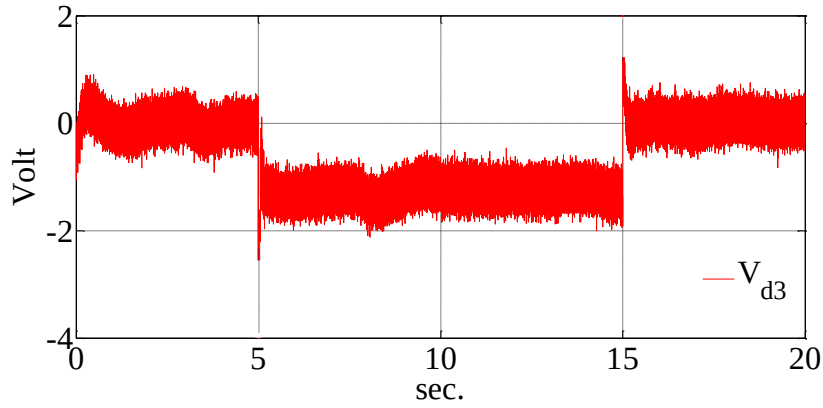

(c)

Figure 6.117: The voltages generated by the current regulators in the d axis of rotor reference frame for, (a) Machine '1', (b) Machine '2', (c) Machine '3' (experimental result).

The q axis currents in rotor reference frame are shown in Figures 6.118 and 6.119 for simulation and experimental results respectively. The effect of the load application also can be seen on these currents.

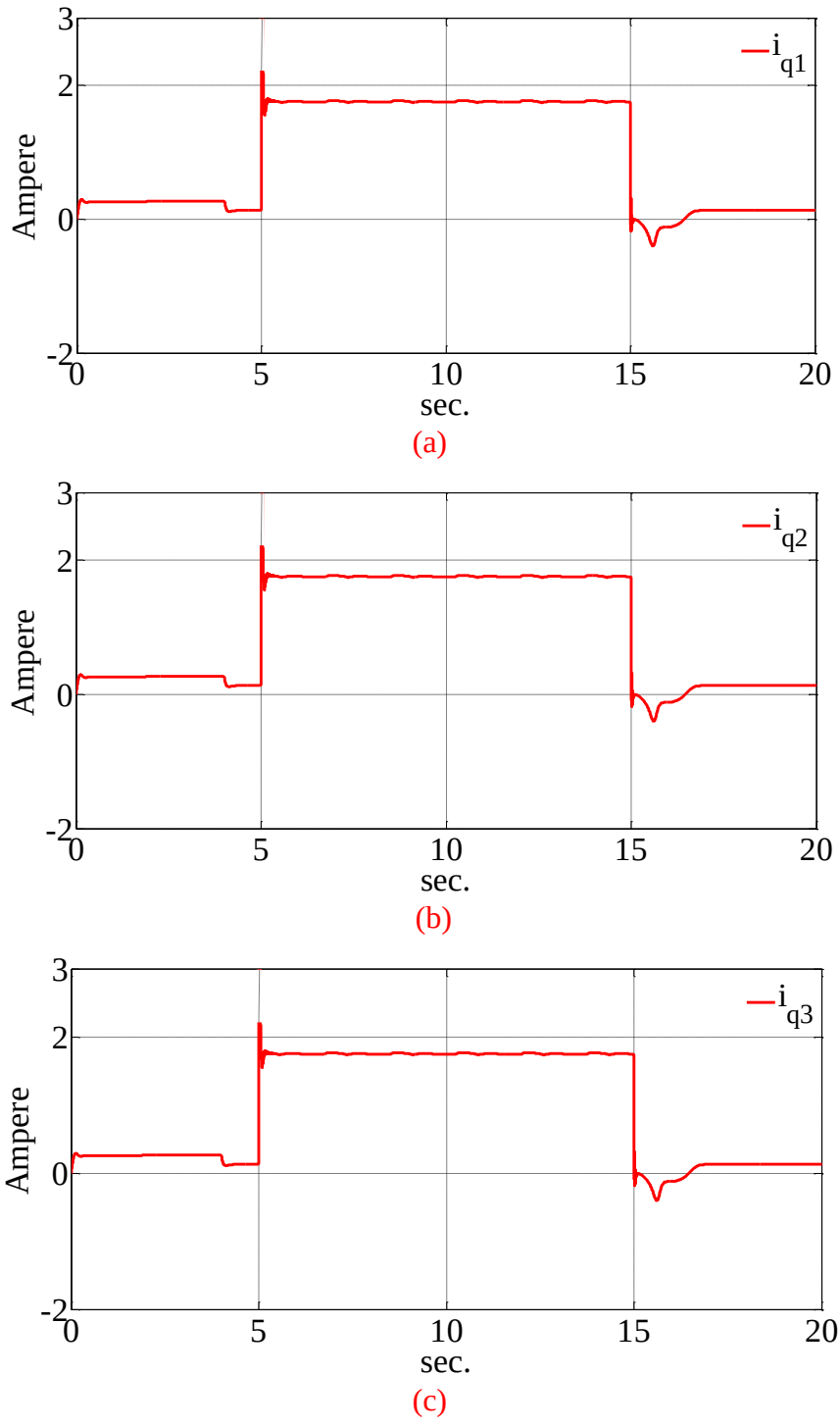

Figure 6.118: The currents generated by the current regulators in the q axis of rotor reference frame for, (a) Machine '1', (b) Machine '2', (c) Machine '3' (simulation result).

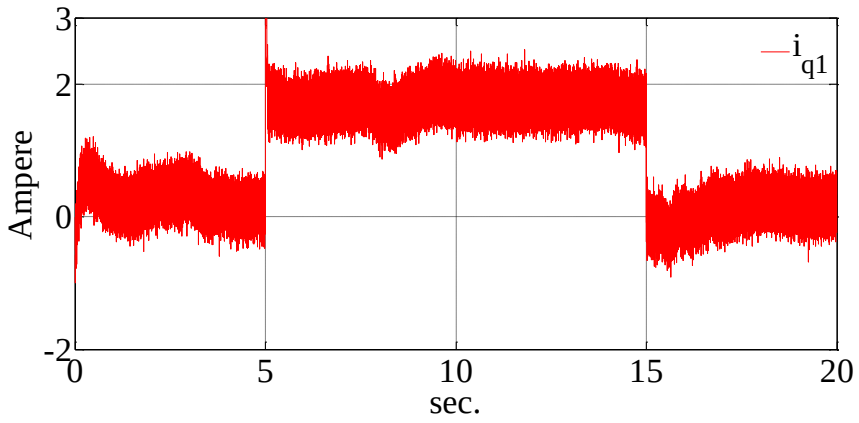

(a)

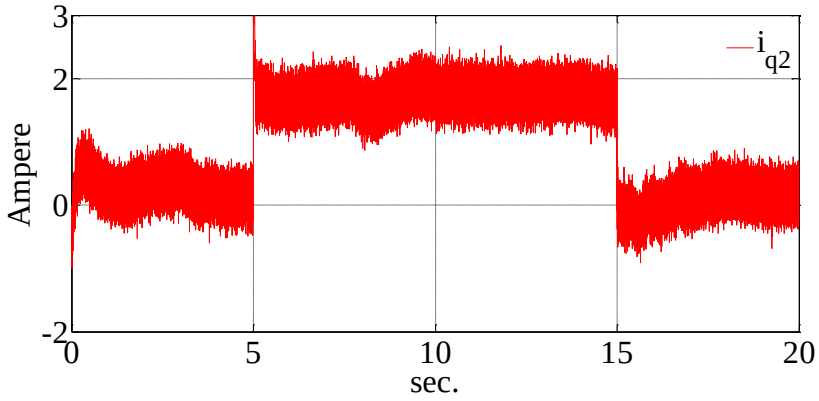

(b)

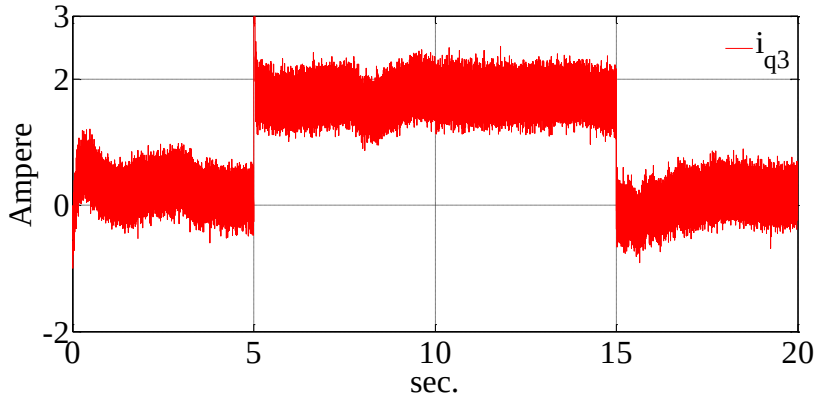

(c)

Figure 6.119: The currents generated by the current regulators in the q axis of rotor reference frame for, (a) Machine '1', (b) Machine '2', (c) Machine '3' (experimental result).

The d axis currents in rotor reference frame are shown in Figures 6.120 and 6.121 for simulation and experimental results respectively. The effect of the load application also can be seen on these currents.

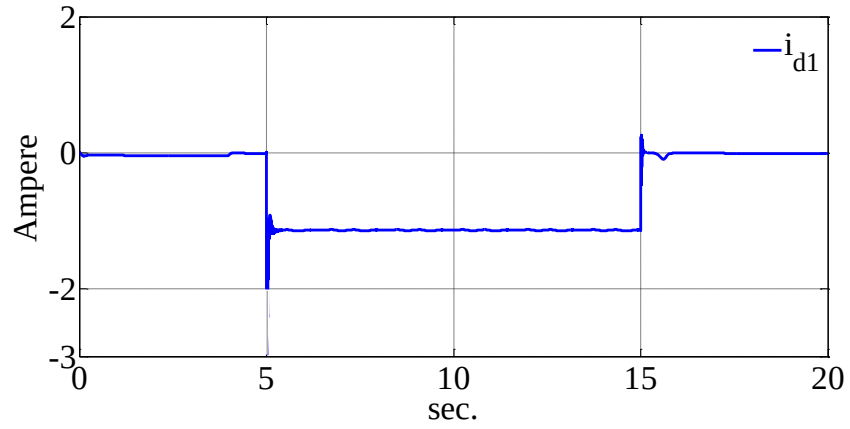

(a)

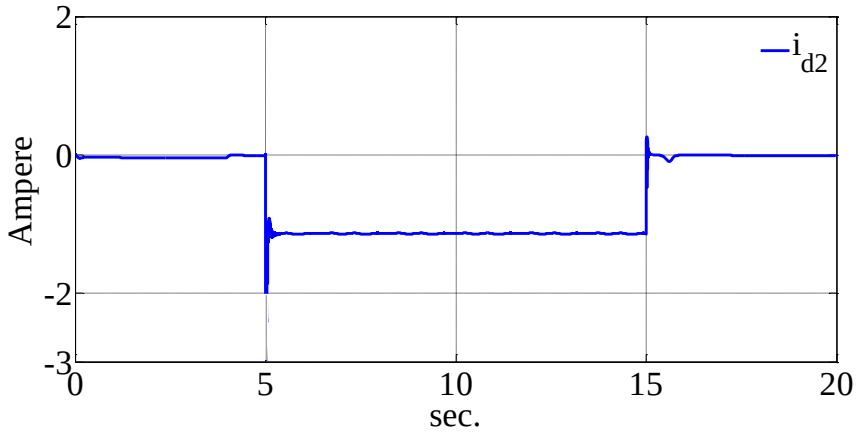

(b)

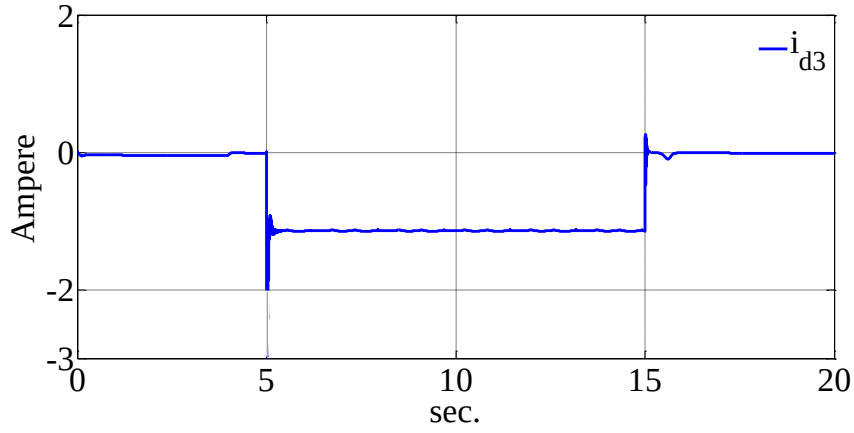

(c)

Figure 6.120: The currents generated by the current regulators in the d axis of rotor reference frame for, (a) Machine '1', (b) Machine '2', (c) Machine '3' (simulation result).

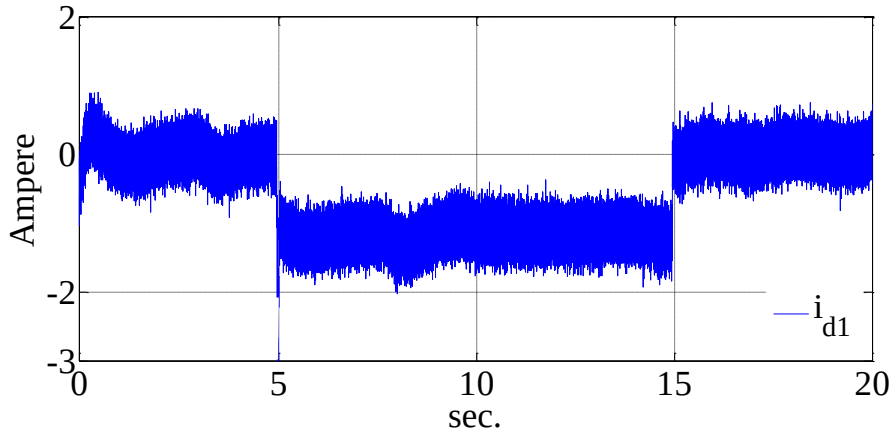

(a)

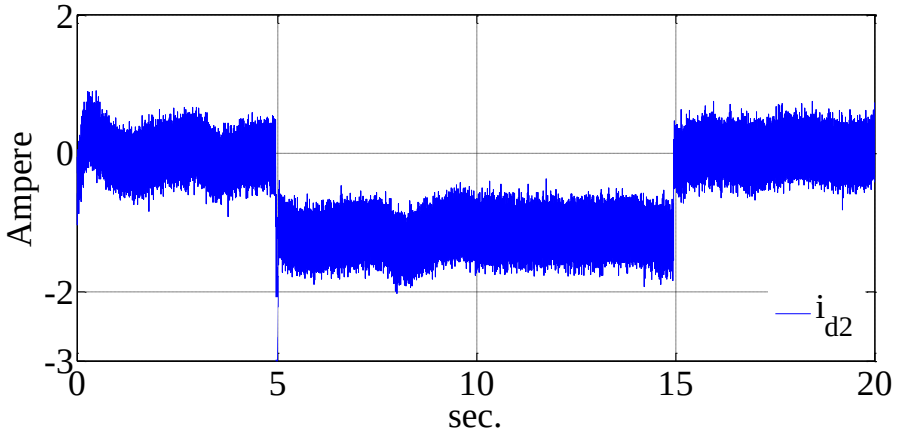

(b)

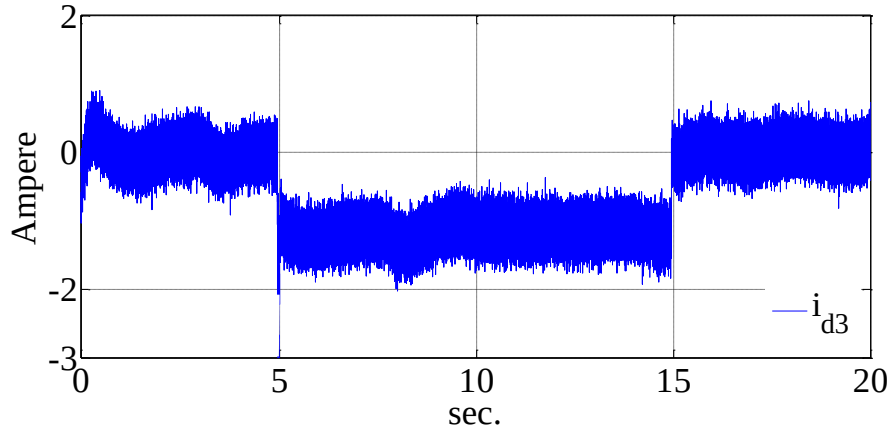

(c)

Figure 6.121: The currents generated by the current regulators in the d axis of rotor reference frame for, (a) Machine '1', (b) Machine '2', (c) Machine '3' (experimental result).

The same currents and voltages in the natural variables are shown in Figures 6.122 and 6.123 respectively.

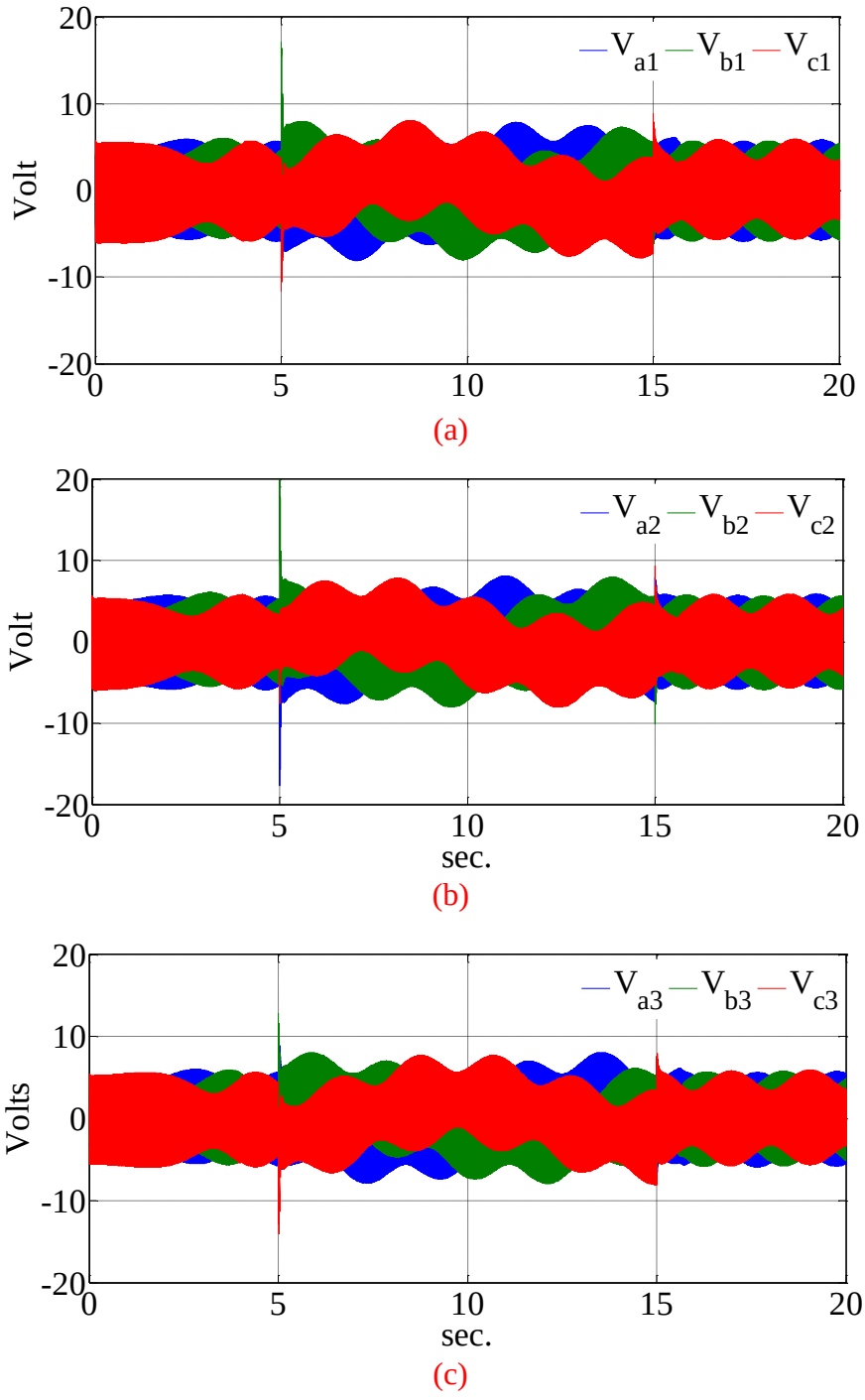

Figure 6.122: The voltages generated by the current regulators in natural variables, (a) Machine 1, (b) Machine 2, (c) Machine 3 (simulation results).

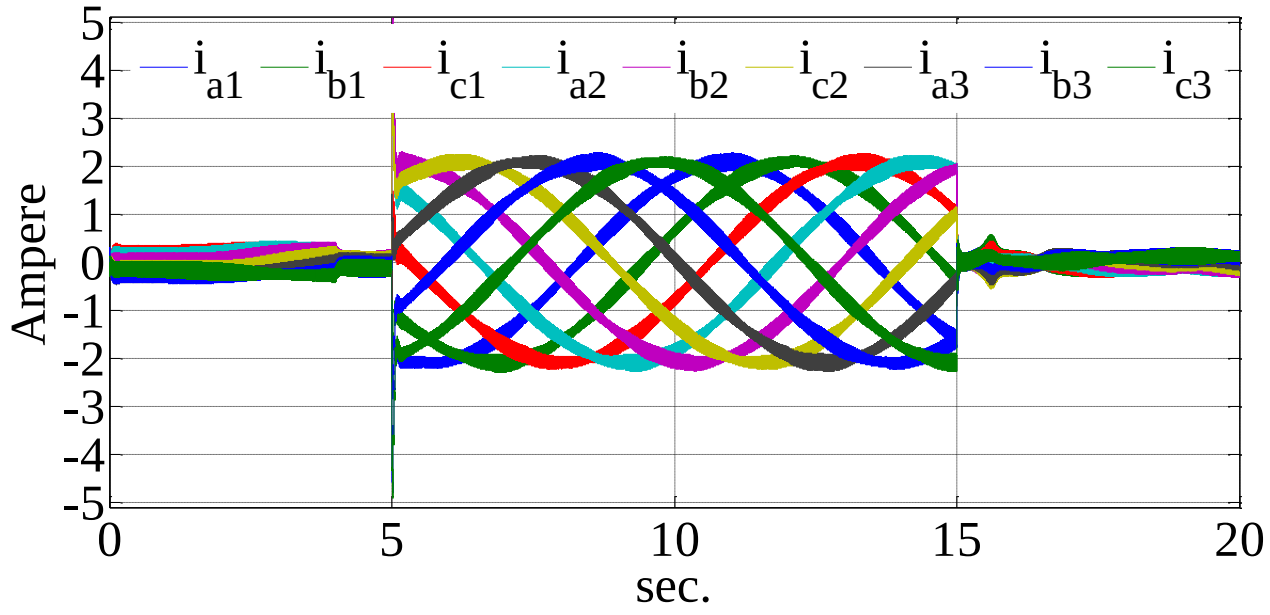

Figure 6.123: The stator currents generated by the current regulators in the natural variables (simulation results).

Figures 6.124 shows the phase currents of each machine separately for simulation results. The stator currents of the experimental results are shown in Figures 6.125 and 6.126 for the moments after and before applying load torque. The low frequency ripples on the experimental results are due to the non-linear effect of the magnetic saturation of the machine. Figures 6.127 and 6.128 show the currents of the fifth sequence for simulation and experimental results respectively. These currents are used for position estimation.

The currents in Figures 6.127 and 6.128 pass through a heterodyning block then through a low pass filter to remove their redundant high frequency parts. Figures 6.129 and 6.130 show the resulting currents after heterodyning and filtering for simulation and experimental results respectively.

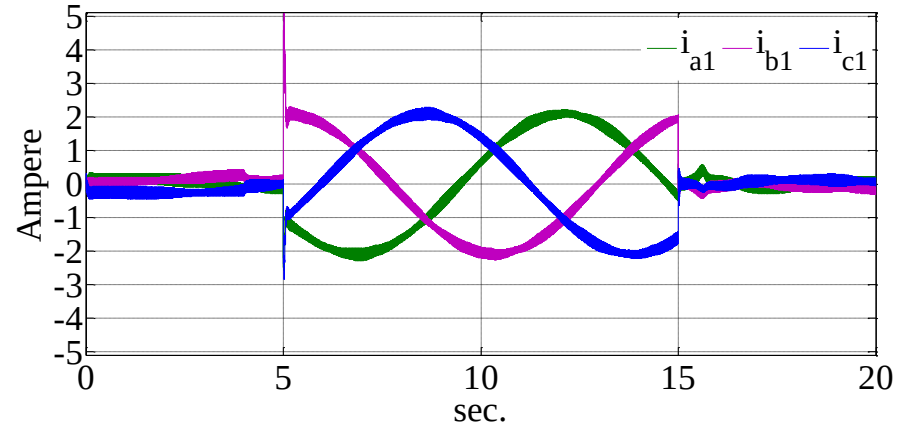

(a)

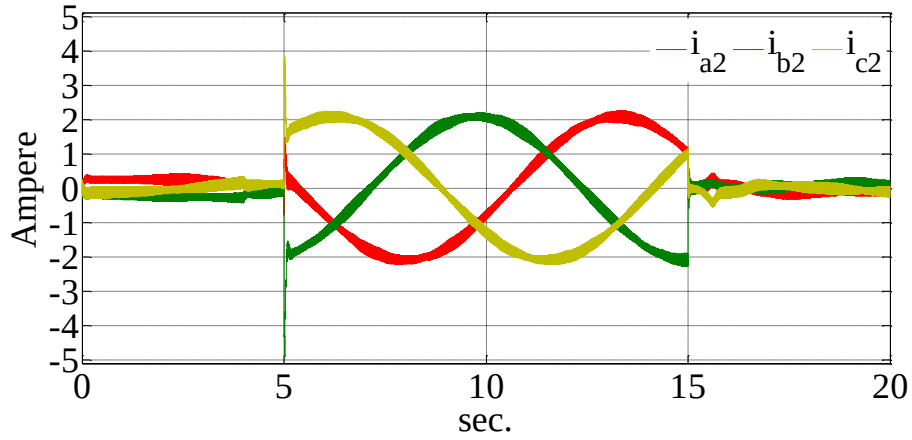

(b)

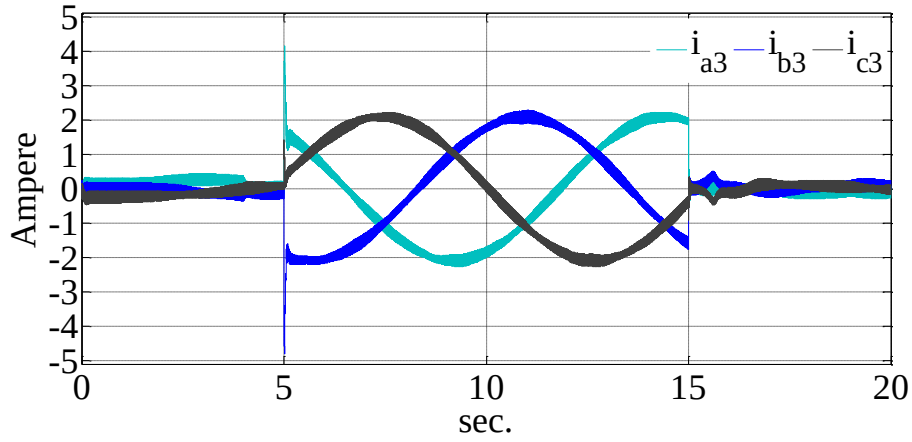

(c)

Figure 6.124: The current generated by the current regulators in natural variables, (a) Machine 1, (b) Machine 2, (c) Machine 3 (simulation results).

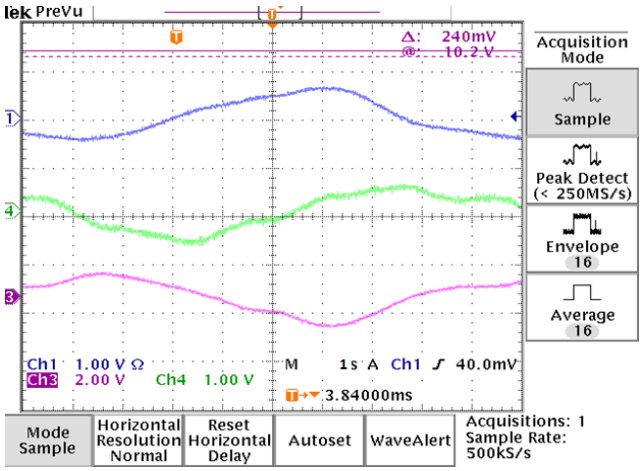

(a)

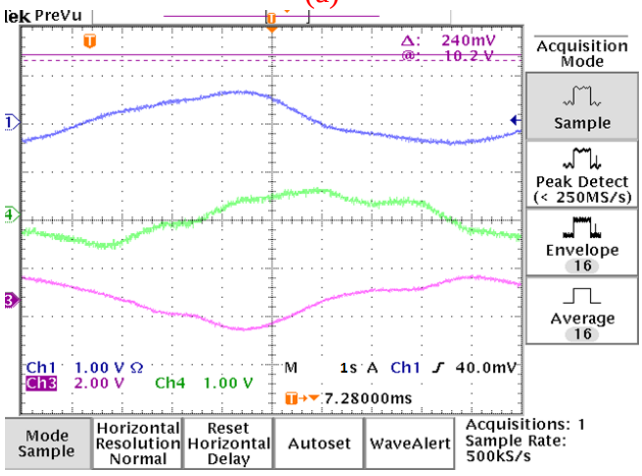

(b)

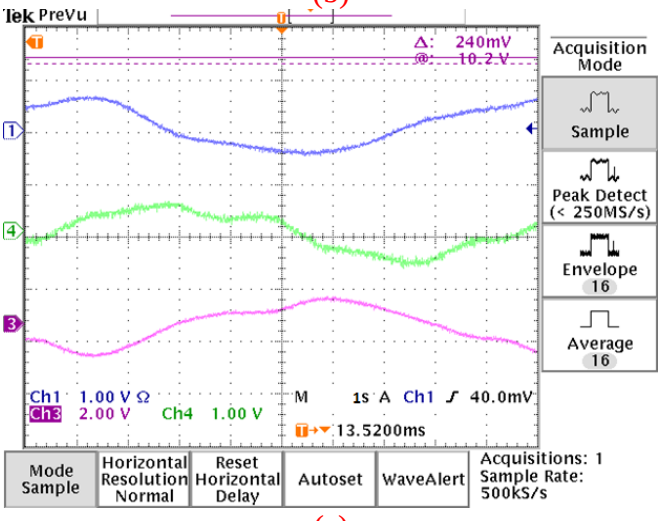

(c)

Figure 6.125: The current generated by the current regulators in natural variables, (a) Machine 1, (b) Machine 2, (c) Machine 3 after load application (experimental results 4 A/ scale).

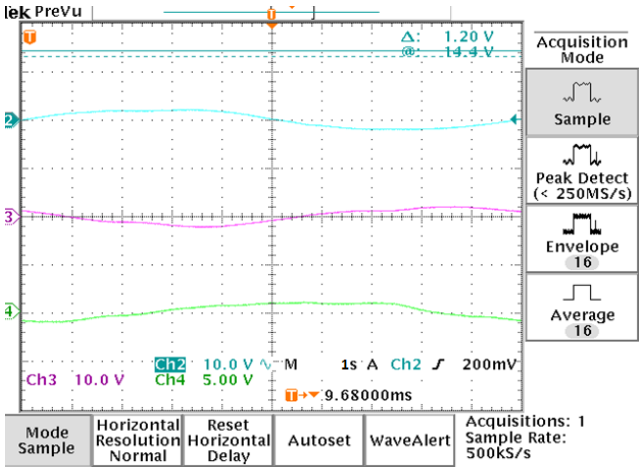

(a)

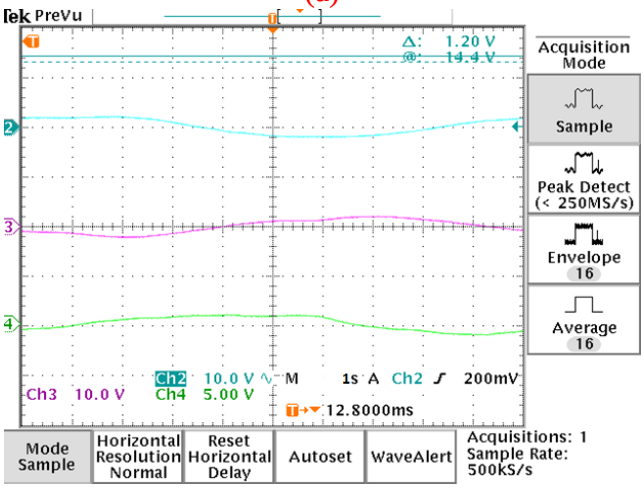

(b)

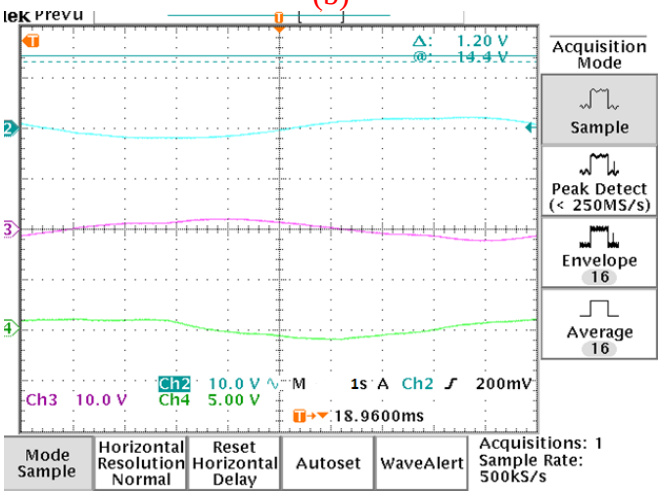

(c)

Figure 6.126: The current generated by the current regulators in natural variables, (a) Machine 1, (b) Machine 2, (c) Machine 3 before load application (experimental results 4 A/ scale).

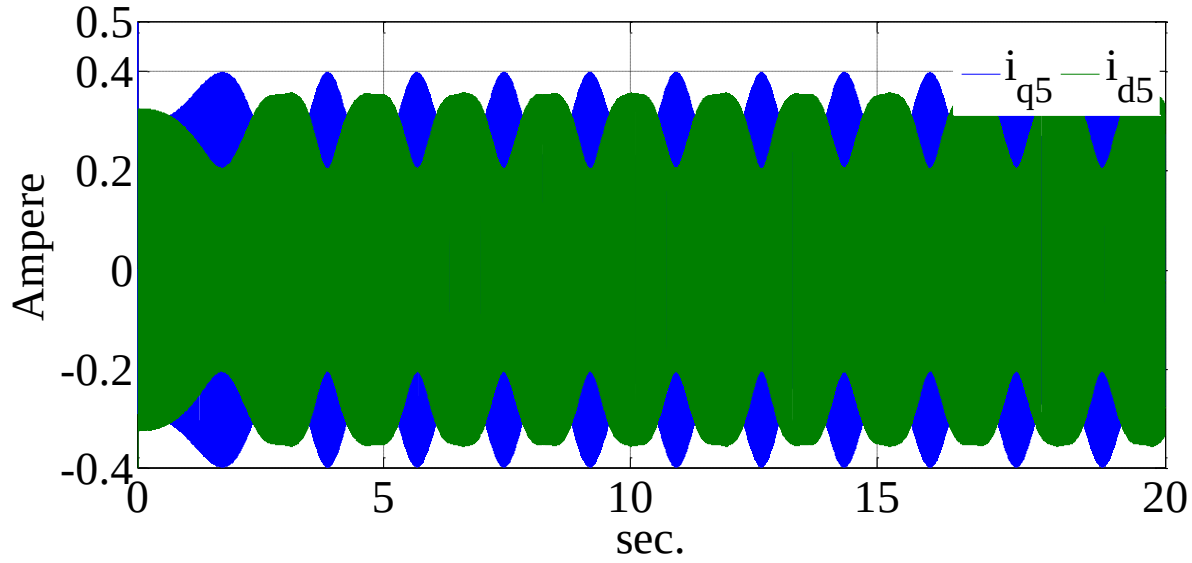

Figure 6.127: The fifth sequence of the stator current in the stationary reference frame (simulation results).

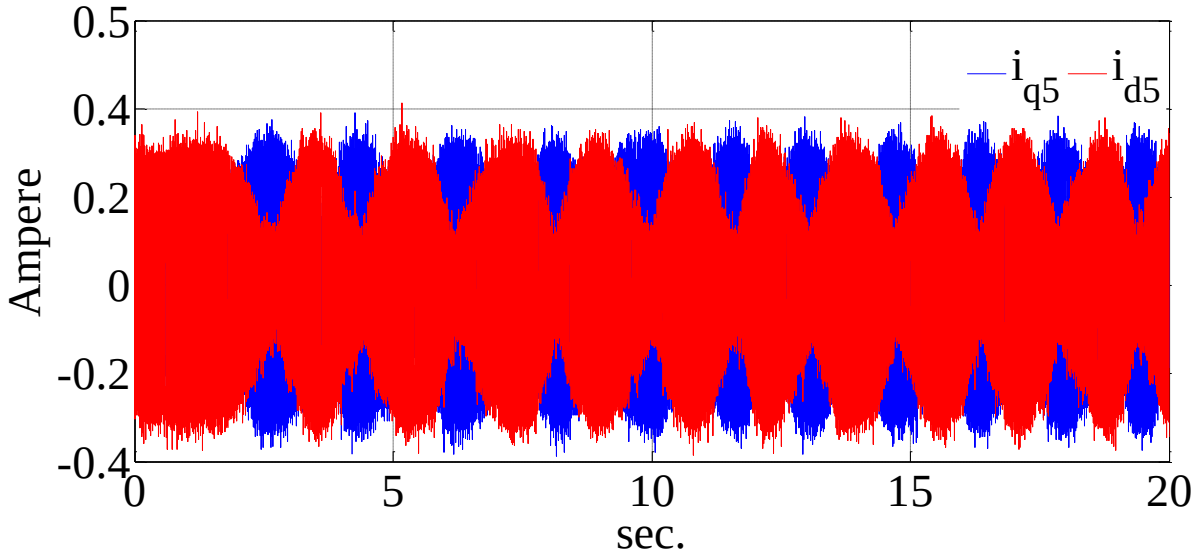

Figure 6.128: The fifth sequence of the stator current in the stationary reference frame (experimental results).

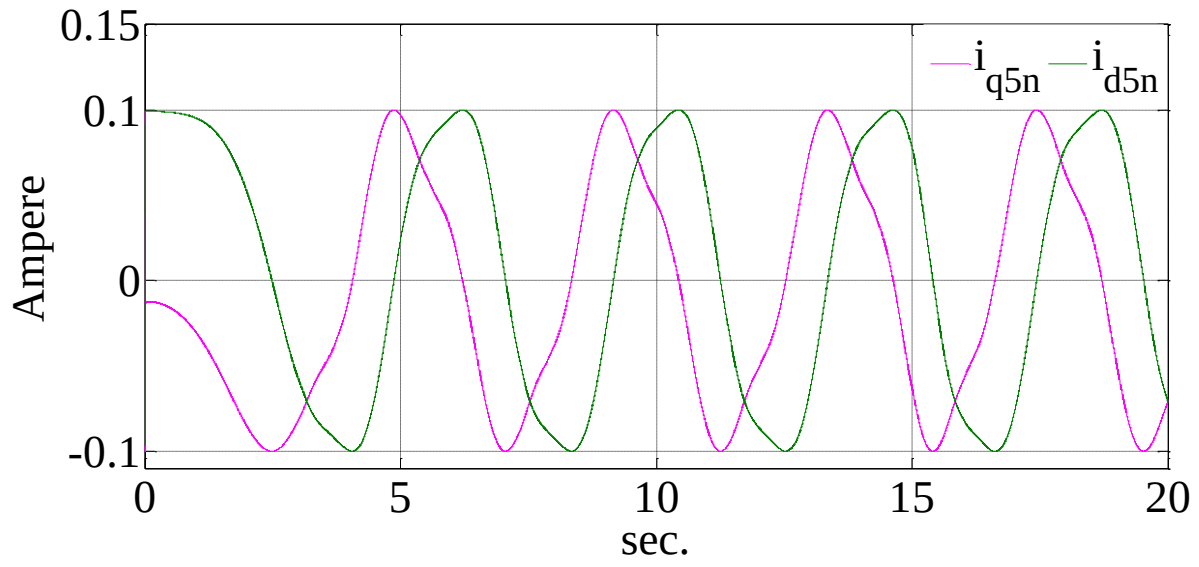

Figure 6.129: The fifth sequence of the stator current in the stationary reference frame after heterodyning and filtering (simulation results).

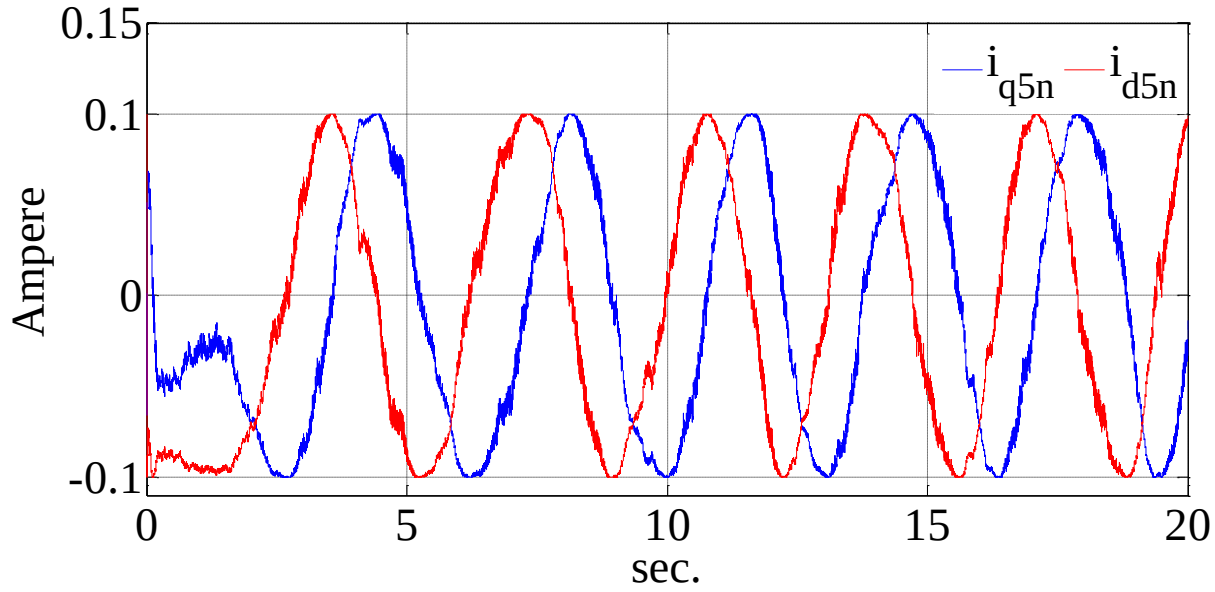

Figure 6.130: The fifth sequence of the stator current in the stationary reference frame after heterodyning and filtering (experimental results).

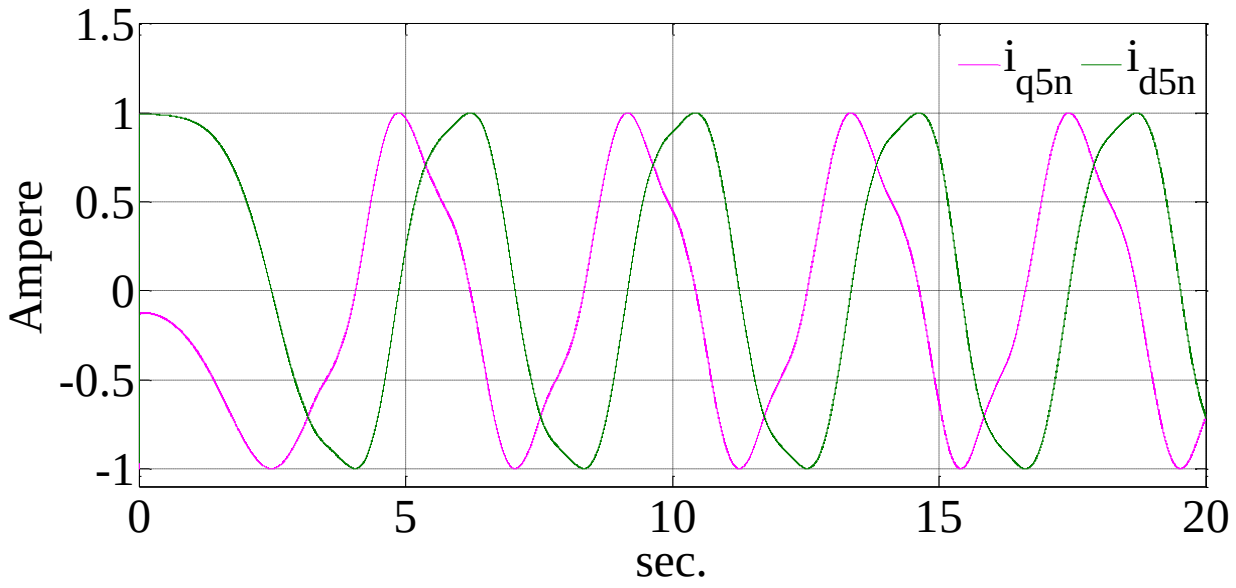

Figure 6.131: The normalize currents of the fifth sequence (simulation results).

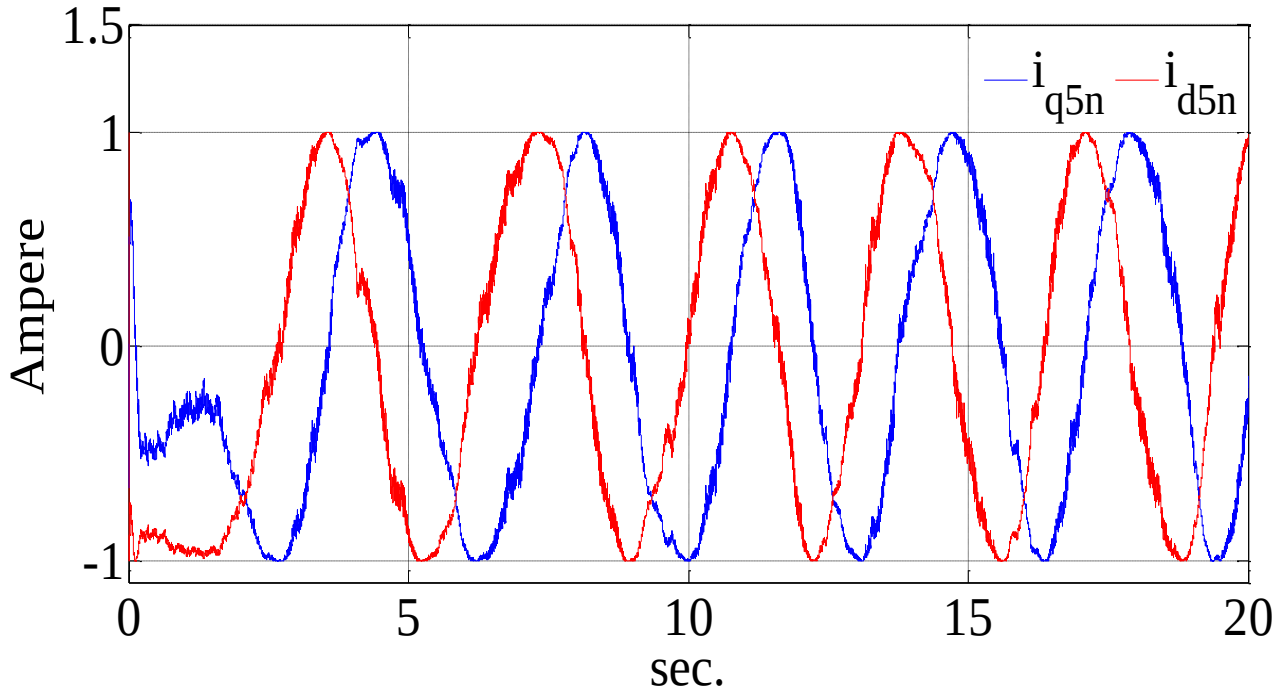

Figure 6.132: The normalize currents of the fifth sequence (experimental results).

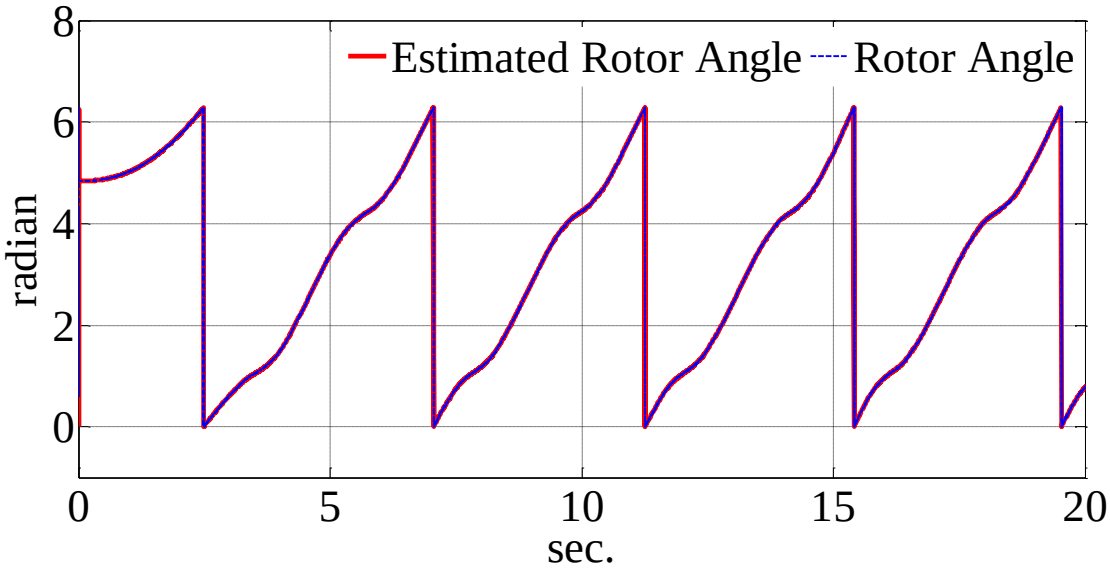

(a)

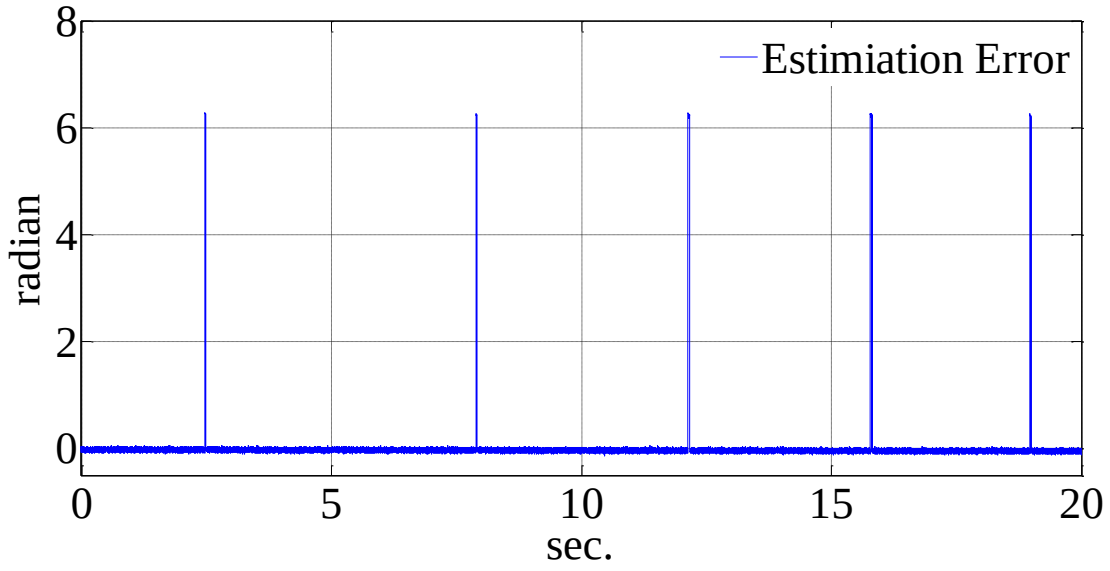

(b)

Figure 6.133: (a) The simulated and estimated rotor angle, (b) Estimation error (simulation results).

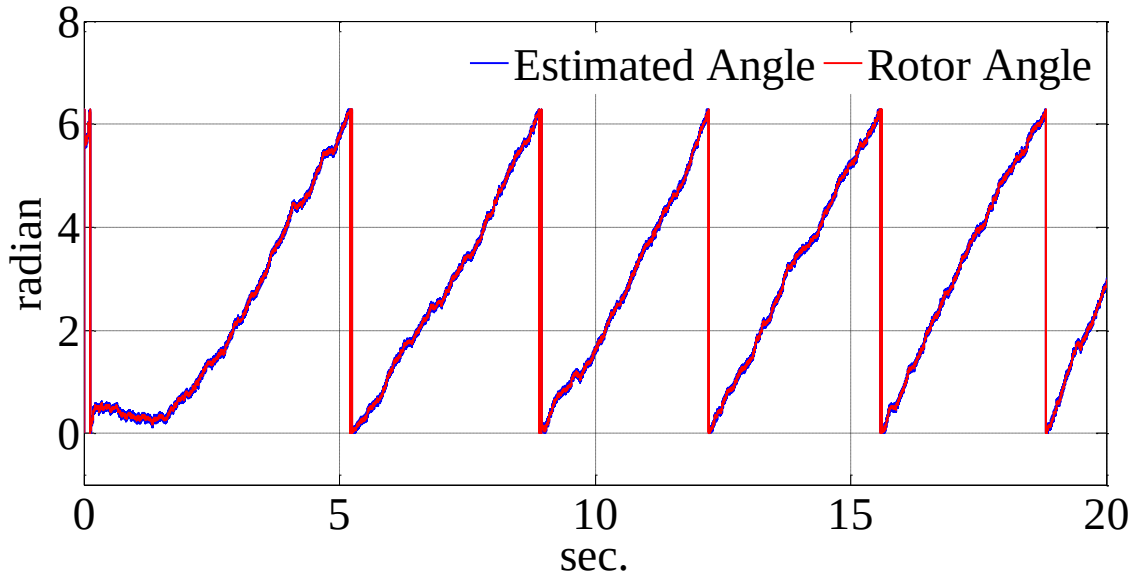

(a)

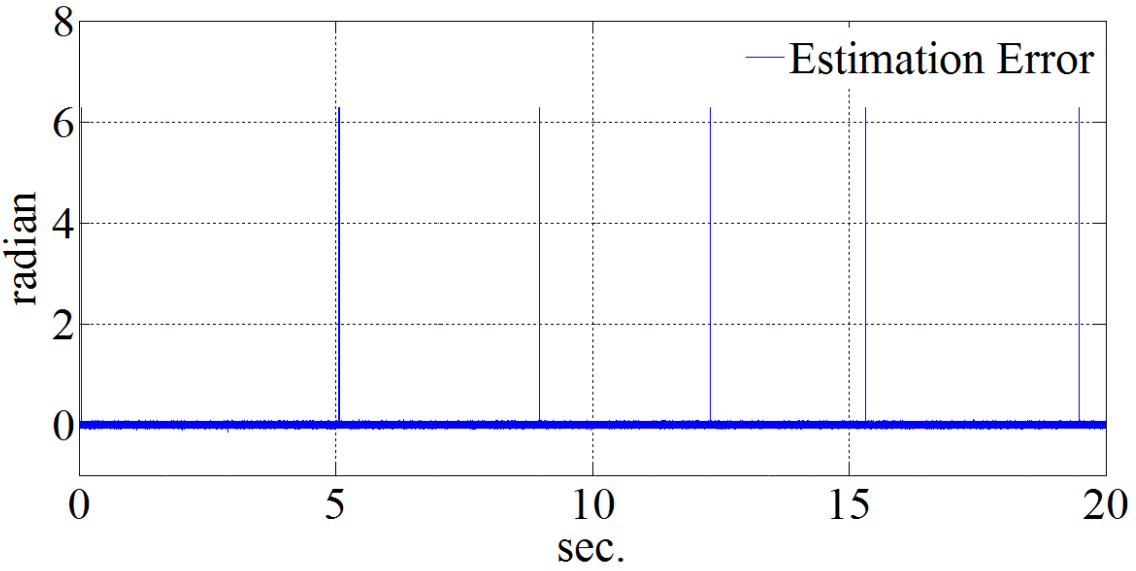

(b)

Figure 6.134: (a)The actual and estimated rotor angle, (b) Estimation error (experimental results).

After normalizing, the currents of the Figures 6.129 and 6.130 are used as the input signals of the observer. Figures 6.131 and 6.132 show the normalized currents for simulation and experimental results respectively. The signals of Figures 6.131 and 6.132 can be used as the input signals of Luenberger observer to estimate the rotor position. Figures 6.133 and 6.134 show the rotor angle and estimated angle along with the estimation error for simulation and experimental results respectively. It can be seen that the estimator can track the rotor position presicly.

6.7 Conclusion

In this chapter a speed controller for a triple-star nine-phase IPM is presented. The controller is designed based on the decoupled model of the machine. The controller uses minimum copper loss strategy in which the torque producing currents are obtained from the Lagrange method to minimize the copper loss while the machine still supports the load. Due to the coupling between the different three phase set machines, the controller design can be complicated. To remove the complexity raised by the couplings between the machine sets, controller is designed using the decoupled model of the machine. The rotor position needed for the controller is estimated using high frequency injection in the fifth sequence of the stationary reference frame. The equation for currents due to the high frequency injection were derived and the essential signal processing method for extracting the rotor position from the high frequency currents was presented. Finally, the controller is simulated with the full order coupled model of the triple-star machine using MATLAB/SIMULINK and the simulation results are presented. The simulation results are also verified with experimental results.